



University of Maribor

Faculty of Mechanical Engineering

FT2017

ISBN 978-961-286-086-8



9 789612 860868

international conference

FT 2017

conference proceedings

dr. Darko Lovrec
dr. Vito Tič



University of Maribor Press

Fluidna Tehnika 2017

Fluid Power 2017
Fluidna Tehnika 2017

MARIBOR, 14.-15. SEPTEMBER 2017



University of Maribor Press



University of Maribor Press

International conference Fluid Power 2017

(September 14TH – 15TH, 2017, Maribor, Slovenia)

(Conference Proceedings)

Editors:

Darko Lovrec, Ph.D.

Vito Tič, Ph.D.

September 2017

- Title:** International conference Fluid Power 2017
- Subtitle:** (September 14TH – 15TH, 2017, Maribor, Slovenia) (Conference Proceedings)
- Editors:** assoc. prof. Darko Lovrec, Ph.D., (University of Maribor, Faculty of Mechanical Engineering)
assist. prof. Vito Tič, Ph.D., (University of Maribor, Faculty of Mechanical Engineering)
- Review:** Darko Lovrec (University of Maribor, Faculty of Mechanical Engineering, Slovenia), Vito Tič (University of Maribor, Faculty of Mechanical Engineering, Slovenia), Niko Herakovič (University of Ljubljana, Faculty of Mechanical Engineering, Slovenia), Željko Šitum (University of Zagreb, Faculty of Mechanical Engineering and Naval Architecture, Croatia), Milan Kambič (OLMA d.o.o., Ljubljana, Slovenia), Franc Majdič (University of Ljubljana, Faculty of Mechanical Engineering, Slovenia), Edvard Detiček (University of Maribor, Faculty of Mechanical Engineering, Slovenia).
- Technical editors:** Jan Perša (University of Maribor Press)
- Design and layout:** University of Maribor Press
- Cover design:** assist. prof. Vito Tič, Ph.D., (University of Maribor, Faculty of Mechanical Engineering)
- Conference:** International Conference Fluid Power 2017
- Organizing Committee:** Vito Tič (University of Maribor, Faculty of Mechanical Engineering, Slovenia), Darko Lovrec (University of Maribor, Faculty of Mechanical Engineering, Slovenia), Tatjana Zabavnik (University of Maribor, Faculty of Mechanical Engineering, Slovenia), Mitja Kastrevc (University of Maribor, Faculty of Mechanical Engineering, Slovenia), Luka Jerebic (University of Maribor, Faculty of Mechanical Engineering, Slovenia), Aljaž Čakš (University of Maribor, Faculty of Mechanical Engineering, Slovenia), Klemen Pušnik (University of Maribor, Faculty of Mechanical Engineering, Slovenia), Aleš Krošel (University of Maribor, Faculty of Mechanical Engineering, Slovenia).
- Scientific Committee:** Darko Lovrec (University of Maribor, Faculty of Mechanical Engineering, Slovenia), Niko Herakovič (University of Ljubljana, Faculty of Mechanical Engineering, Slovenia), Heinrich G. Hochleitner (Technische Universität Graz, Austria), Željko Šitum (University of Zagreb, Faculty of Mechanical Engineering and Naval Architecture, Croatia), Vladimir Savić (University of Novi Sad, Faculty of Technical Sciences, Serbia), Radovan Petrovič (University of Kragujevac, Faculty of Mechanical Engineering, Serbia), Franc Majdič (University of Ljubljana, Faculty of Mechanical Engineering, Slovenia), Joerg Edler (Technische Universität Graz, Austria), Aleš Bizjak (Poclain Hydraulics, Slovenia), Milan Kambič (Olma d.o.o., Slovenia), Edvard Detiček (University of Maribor, Faculty of Mechanical Engineering, Slovenia).
- Program Committee:** Darko Lovrec (University of Maribor, Faculty of Mechanical Engineering, Slovenia), Vito Tič (University of Maribor, Faculty of Mechanical Engineering, Slovenia), Niko Herakovič (University of Ljubljana, Faculty of Mechanical Engineering, Slovenia), Željko Šitum (University of Zagreb, Faculty of Mechanical Engineering and Naval Architecture, Croatia), Milan Kambič (OLMA d.o.o., Ljubljana, Slovenia), Franc Majdič (University of Ljubljana, Faculty of Mechanical Engineering, Slovenia), Edvard Detiček (University of Maribor, Faculty of Mechanical Engineering, Slovenia).

Co-published by / Izdajateljica

University of Maribor
Slomškov trg 15, 2000 Maribor, Slovenia
tel. +386 2 23 55 280
<https://www.um.si>, rektorat@um.si

First published in 2017 by / Založnik

University of Maribor Press
Slomškov trg 15, 2000 Maribor, Slovenia
tel. +386 2 250 42 42, faks +386 2 252 32 45
<http://press.um.si>, zalozba@um.si

Edition: 1st
Available at: <http://press.um.si/index.php/ump/catalog/book/266>
Printed by: Demago d.o.o., Maribor
No. of Copies 120
Published in: September 2017

© **University of Maribor Press**

All rights reserved. No part of this book may be reprinted or reproduced or utilized in any form or by any electronic, mechanical, or other means, now known or hereafter invented, including photocopying and recording, or in any information storage or retrieval system, without permission in writing from the publisher.

CIP - Kataložni zapis o publikaciji
Univerzitetna knjižnica Maribor

621.22(082)(0.034.2)

INTERNATIONAL Conference Fluid Power (2017 ; Maribor)

Conference proceedings [Elektronski vir] / International Conference Fluid Power 2017, September 14th - 15th, 2017, Maribor, Slovenia ; editors Darko Lovrec, Vito Tič. - 1st ed. - El. zbornik. - Maribor : University of Maribor Press, 2017

Način dostopa (URL): <http://press.um.si/index.php/ump/catalog/book/266>

ISBN 978-961-286-086-8 (pdf)

doi: 10.18690/978-961-286-086-8

1. Lovrec, Darko

COBISS.SI-ID [92963329](#)

ISBN: 978-961-286-086-8 (PDF)
978-961-286-085-1 (Softback)

DOI: <https://doi.org/10.18690/978-961-286-086-8>

Price: Free copy

For publisher: full prof. Igor Tičar, Ph.D., Rector (University of Maribor)

International conference Fluid Power 2017

Dear participants of the international conference Fluid Power 2017!

DARKO LOVREC & VITO TIČ

Abstract The International Fluid Power Conference is a two day event, intended for all those professionally-involved with hydraulic or pneumatic power devices and for all those, wishing to be informed about the ‘state of the art’, new discoveries and innovations within the field of hydraulics and pneumatics.

The gathering of experts at this conference in Maribor has been a tradition since 1995, and is organised by the Faculty of Mechanical Engineering at the University of Maribor, in Slovenia. Fluid Power conferences are organised every second year and cover those principal technical events within the field of fluid power technologies in Slovenia, and throughout this region of Europe. This year's conference is taking place on the 14th and 15th September in Maribor.

We wish all participants at the International Conference-Fluid Power 2017 continued successful professional work, and hope that we have yet again added another small piece within the mosaic of fluid power.

Keywords: • fluid power technology • components and systems • control systems • fluids • maintenance and monitoring •



CORRESPONDENCE ADDRESS: Darko Lovrec, Ph.D., Chairperson of the Fluid Power 2017 organising committee, Associate Professor, University of Maribor, Faculty of Mechanical Engineering, Smetanova ulica 17, 2000 Maribor, Slovenia, e-mail: darko.lovrec@um.si. Vito Tič, Ph.D., Assistant Professor, University of Maribor, Faculty of Mechanical Engineering, Smetanova ulica 17, 2000 Maribor, Slovenia, e-mail: vito.tic@um.si.

Table of Contents

CONFERENCE PROCEEDINGS

Digital pneumatics: App-driven pneumatics for Industry 4.0 Markus Miklas	1
Fluid power drives in robotic systems Željko Šitum	11
Voice of the Machine™: Parker's complete Internet of Things (IoT) platform Igor Magel & Miha Šteger	25
With HYDAC on the way to Industrie 4.0: Industrie 4.0 based predictive maintenance Dejan Glavač	31
Global Analysis of an RC-Filter for a Switched Hydraulic Drive Evgeny Lukachev & Rudolf Scheidl	41
Precise force control for hydraulic and pneumatic press system Juraj Benić, Nikola Rajčić & Željko Šitum	57
Nonlinear position control of electrohydraulic servo systems Edvard Detiček & Mitja Kastrevc	73
Modern control system for servo hydraulic linear drive Matevž Štefane & Darko Lovrec	85
Impact of hydraulic network on operation of linear servo axes Tadej Jurgec & Vito Tič	95
A selection of the latest specifications and performance requirements for environmentally considerate hydraulic fluids ASTM D8029-16, Bosch Rexroth RE 90235, EPA VG 2013 Martin Ruch & Patrick Laemmle	103
Application of hydraulic and gear oils in the food processing industry Mitar Jocanović, Velibor Karanović, Vito Tič, Marko Orošnjak & Dragan Selinić	111
Inspection of Technical Cleanliness Detlef Meurer & Amela Mrak	121
MPC-Test: An introduction and examples of test results Manja Moder & Urška Cafuta	131
Hydraulic pump pulsation using Ionic Liquid Bernhard Manhartsgruber & Vito Tič	135
Mathematical Modelling and Experimental Research of Characteristic Parameters of aviation hydraulic piston pump Radovan Petrović, Huayong Yang, Maja Andjelković & Radoje Cvejić	143

Mathematical Modelling and Experimental Research of Characteristic Parameters barrel-valve plate of aviation hydraulic piston pumps Radovan Petrović, Shaoping Wang, Maja Andjelković & Radoje Cvejić	155
The nonlinear mathematical model of electrohydraulic position servo system Mitja Kastrevc & Edvard Detiček	163
Verification of a simulation model to predict the transmission behavior of hydrostatic bearing on machine tools Jörg Edler & Matthias Steffan	175
Design challenges of modern hydraulic power packs Tadej Tašner, Peter Hace & Kristian Les	185
Hydrostatic Transmission Design – Closed-loop Trailer Assist Drive Luka Jelovčan & Aleš Novak	195
Piezo actuators for the use in hydraulic and pneumatic valves Marko Simic & Niko Herakovic	207
Development of the heavy-duty flow divider (FD-H2) for mobile applications Anže Čelik & Luka Peternel	219
Influence of the Hydrodynamic Bearing on the Flow Characteristics of a Dynamically Operated Displacement Meter Othmar Bernhard & Jörg Edler	241
Testing based analysis of the gerotor orbital hydraulic motor Ervin Strmčnik & Franc Majdič	249
Tribological research of different material pairs for water hydraulic seat type of valve Andreja Poljšak, Franc Majdič & Mitjan Kalin	259
Test stand for determining the performance characteristics of hydraulic directional control valves Rok Pahič, Vito Tič & Darko Lovrec	271
Problems of testing new hydraulic fluids Milan Kambič & Darko Lovrec	281

Digital pneumatics: App-driven pneumatics for Industry 4.0

MARKUS MIKLAS

Abstract Piezo technology, integrated sensors for stroke and pressure, combined with software modules, open new perspectives to the use of pneumatic technologies for machine building. In a Motion Terminal a so-called valve becomes a freely programmable pneumatic element with four channels. The flow can be regulated proportionally and dynamically using software modules. Via different Motion Apps one pneumatic element can replace more than 50 traditional ones. Fast switching times, and low energy consumption are just two of the many advantages compared to traditional pneumatics. This new technology will open completely new fields for pneumatic applications and might even revolutionise the way machines will be built in future.

Keywords: • pneumatics • digital systems • components • sensors
•software

CORRESPONDENCE ADDRESS: Markus Miklas, Festo Gesellschaft m.b.H, Linzer Straße 227, 1140 Wien, Austria, e-mail: markus.miklas@festo.com, Invited author.

<https://doi.org/978-961-286-086-8.1>
© 2017 University of Maribor Press
Available at: <http://press.um.si>.

ISBN 978-961-286-086-8

1 The role of pneumatics in digital systems

Industry 4.0 represents a future where intelligent machines are self-aware and automation challenges can be solved by the machinery itself. In the factory of tomorrow, cyber-physical systems will communicate with one another using the Internet of Things. Microsystems will make decisions autonomously and highly sensitive robots will support employees so that they can continue to work, even in their later years.

Pneumatic applications are sturdy and reliable, which from an Industry 4.0 perspective might also be interpreted as inflexible. For pneumatics, this concept seems to leave only peripheral tasks. Simple, repetitive tasks might remain under the control of some intelligent sub-system. The “natural” motion for intelligent cyberphysical systems seems to be driven electrically.

For machine builders and machine operators pneumatic controls come with some additional challenges, since every logical function comes encapsulated in a physical valve. Changing the functionality means exchanging the valve. This also means that potentially a lot of valves and other pneumatic function elements such as throttles are kept on stock resulting in costs. Pneumatic valve terminal with controller and multiple functions, where any combination of functions can be implemented, but changing functions requires physical changes is shown in Figure 1.

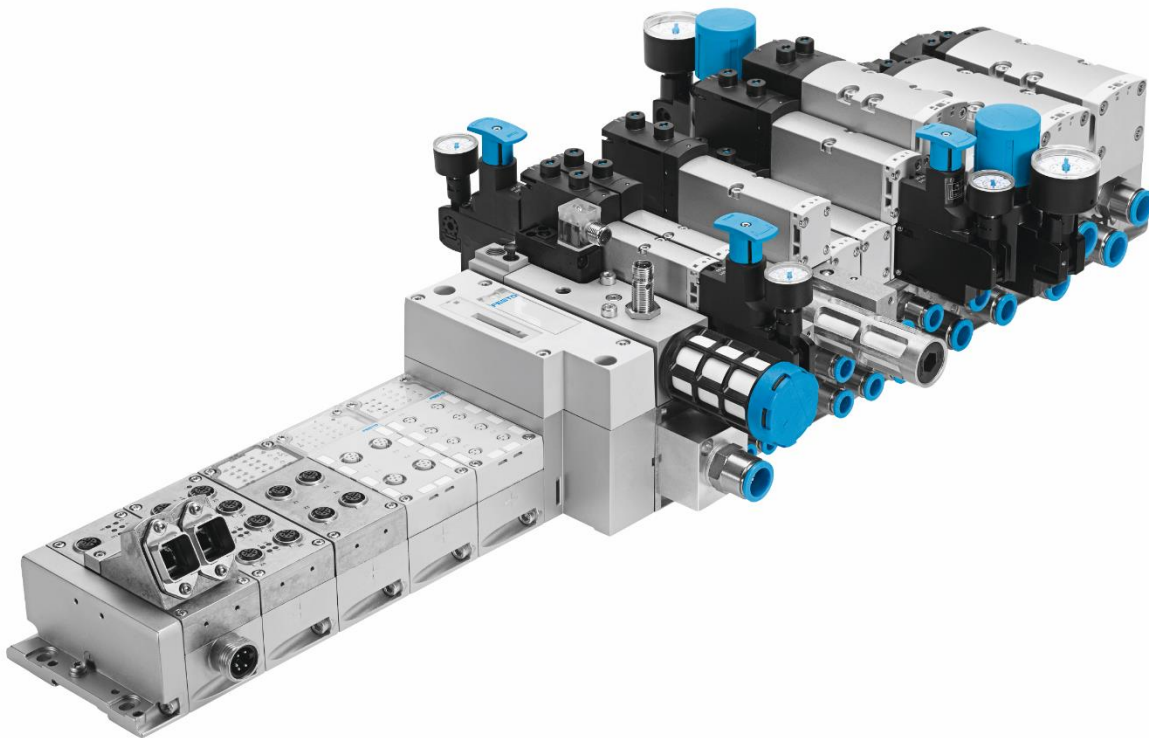


Figure 1: Pneumatic valve terminal with controller and multiple functions

2 Digital pneumatics

As a response to above mentioned challenges, Festo has developed the Festo Motion Terminal, the world's first standardised platform that will develop into a "cyber-physical system" thanks to its intelligent fusion of mechanics, electronics and software. This system is characterised by an extremely high level of adaptability and flexibility. It will enable you to build intelligent machines now for the world of tomorrow, and ensure your systems are truly ready for Industry 4.0, even in terms of pneumatics.

2.1 The Festo Motion Terminal as a cyber-physical system

Cyber-physical systems (CPS) provide the technical basis for the fourth industrial revolution. As communicative systems, they open the door to new types of functions, services and features as part of the "socio-technical" interaction between people and technology. They act as a bridge between the physical world that surrounds us and the digital world. Their flexibility and ability to adapt to modern production and machine development processes present new opportunities for standardisation, increased flexibility and profitability.

2.2 App-based function selection and decentralised intelligence

The Festo Motion Terminal implements functions using programs in the form of motion apps - functions and hardware are disconnected. This is done using integrated, flexible and programmable processors, as well as the smart actuator technology within the system. The decentralised intelligence and software-based function implementation make the system more flexible than "hardwired" components. Adaptations can now be carried out distributed within the system. This reduces both the bandwidth required for communication and the complexity of controlling and programming tasks for the entire system.

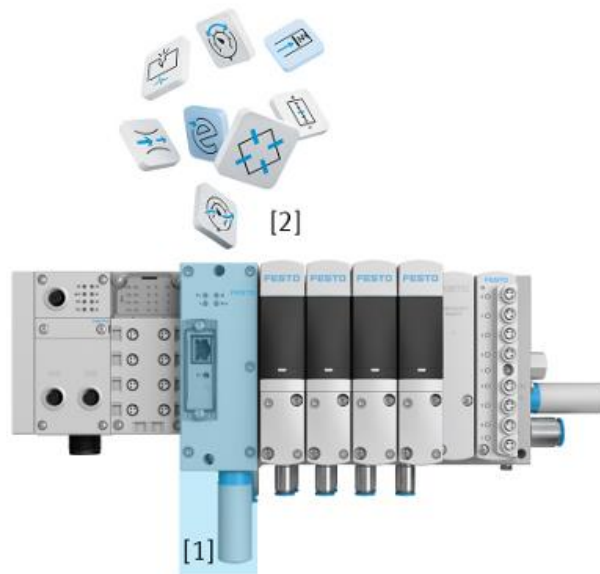


Figure 2: The Festo Motion Terminal

The Festo Motion Terminal has powerful on-board processors for decentralised intelligence in the integrated controller [1], plus function elements in the form of motion apps [2] – Figure 3. This means that pneumatic functions are no longer automatically connected to the mechanical hardware, and can simply be assigned using apps. As a result, one valve type is all you need to execute a wide range of pneumatic motions.

2.3 Smart actuator technology thanks to integrated sensors

An actuator is a component that influences the physical world, e.g. a valve. However, the sensors in a cyber-physical system turn it into much more than just a pneumatic actuator. Thanks to the new flexibility it offers, smart actuator technology enables components such as cylinders to perform new tasks.

This new valve technology can be used for a wide range of products, functions and complete solution packages. The only prerequisite is a valve design with multiple degrees of freedom for

actuation, as well as integrated data acquisition and processing suitable for a cyber-physical system. The overall economic advantages for both the machine builder and the operator as a result of the valve's variability are immense.

Composition of a digital valve [1] is shown in Figure 3. Four diaphragm poppet valves: actuating the poppet valves individually enables a high degree of flexibility. [2]. Four piezo pilot valves: the energy-saving piezo pilot valves control the diaphragm poppet valves precisely and proportionally. [3]. Valve electronics with sensors: the integrated stroke, pressure and temperature sensors provide optimal control and transparent condition monitoring.

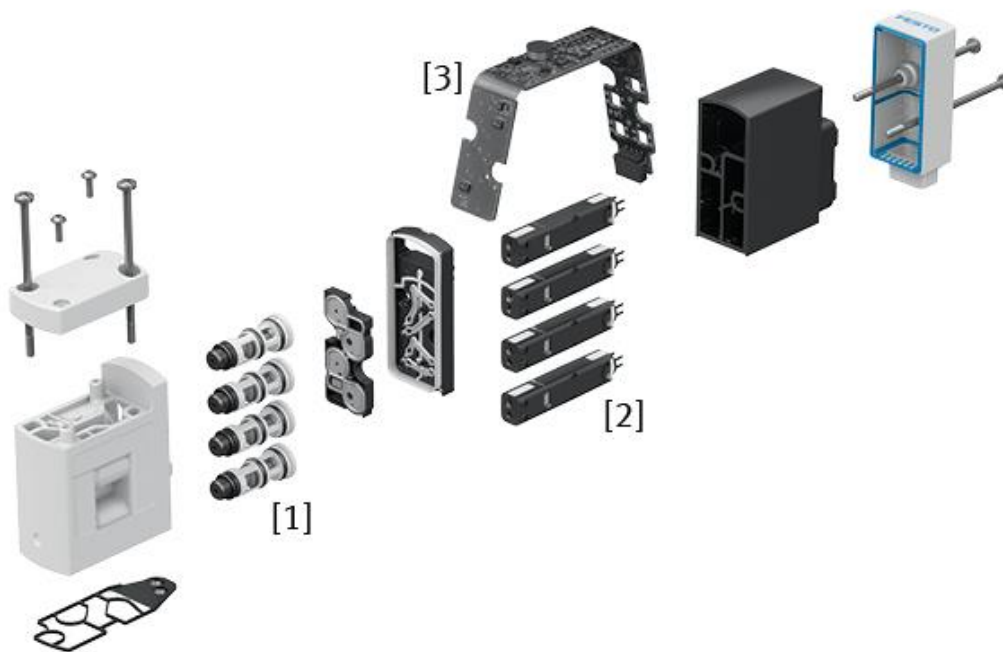


Figure 3: Composition of a digital valve

In the Festo Motion Terminal, this smart actuator technology is realised by a bridge circuit with integrated sensors that is made up of four 2/2-way valves in the form of piezo pilot and diaphragm poppet valves. The ability to pressurise and exhaust independently of one another is the key principle that allows the user to perform a wide range of conventional valve functions using a single valve. This valve technology can also be used to carry out proportional pressure regulation and complex control solutions, such as Soft Stop. The bridge circuit in the valve of the Festo Motion Terminal as an innovative valve system, is shown in Figure 4.

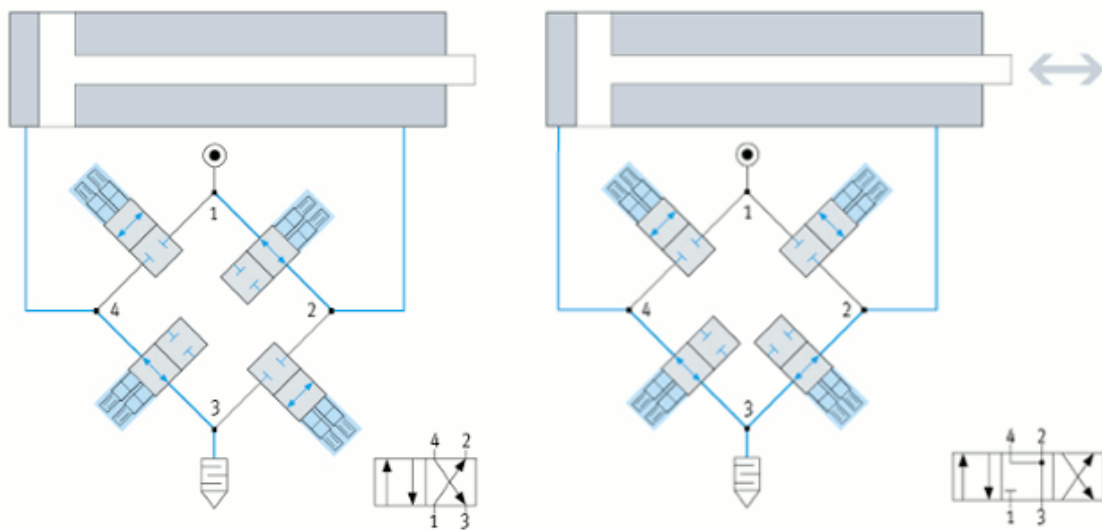


Figure 4: The bridge circuit in the valve of the Festo Motion Terminal

The bridge circuit in the valve of the Festo Motion Terminal is based on the basic elements of pneumatic valve functions. Four 2/2-way valves (diaphragm poppet valves) are connected in series to form a full bridge. Each diaphragm poppet valve (grey) is proportionally piloted and controlled by two piezo valves (blue). Sensors monitor the stroke of each poppet valve, while pressure sensors monitor the pressure at ports 2 and 4. All four pilot cartridges (blue) form a total of eight proportionally controlled 2/2-way valves. Thanks to the integrated sensors and proportional control, which allows the valves to be pressurised and exhausted independently, this single valve technology can now be used to execute a wide range of conventional valve functions and full system solutions, such as Soft Stop (end-position cushioning without a wear-prone shock absorber).

2.4 Integrated sensors with simulation comparison

Built-in sensors are essential in cyber-physical systems, whether they are used for adapting to changes in environmental conditions or for gathering all the necessary information for "big data" processes.

Simulation models enable the system to carry out evaluation and adaptation tasks independently. This means, for example, that external load cells are no longer needed for status monitoring during pressing procedures.

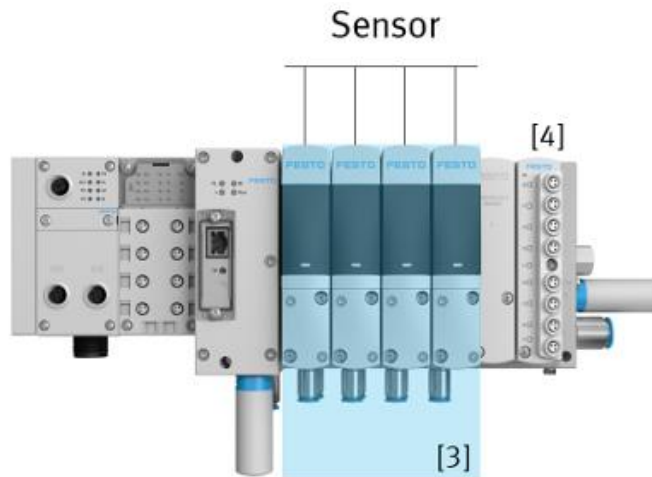


Figure 5: The combination of integrated sensors and software-based models

The combination of integrated sensors [3] (see Figure 5) and software-based models not only saves money, it also simplifies the system engineering, from design to modernisation. For certain tasks, the separately integrated inputs [4] can be used to process data from external sensors in real time for internal control. This opens the door to new types of pneumatic applications.

2.5 Intuitive user interfaces

Cyber-physical systems have a number of different user interfaces in order to ensure spatial flexibility. They prioritise simultaneous communication via multiple channels, also known as multi-modal communication. The essence of this type of communication is that data, functions and operation are easy to understand.

The Festo Motion Terminal offers you multiple human-machine interfaces. Adjustment is quick, easy and direct via the Ethernet connection, your web browser, the intuitive WebConfig interface or the process data of a conventional machine control system. The simple function integration offered by our motion apps will speed up commissioning, reconfiguration and system adaptations.

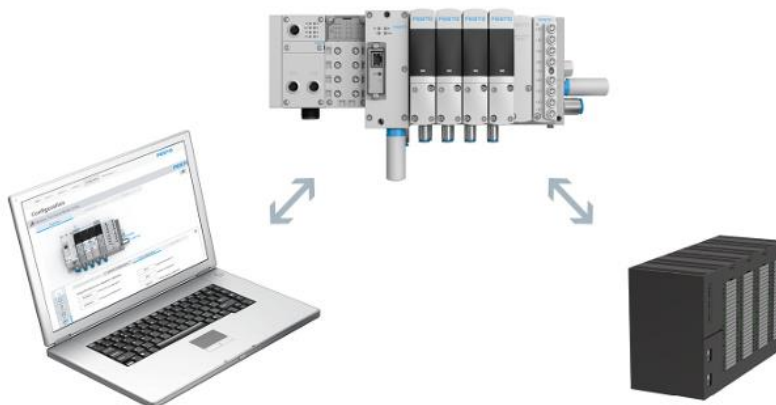


Figure 6: The Festo Motion Terminal offers a web interface and PLC connectivity

2.6 Adaptable communication interfaces

Cyber-physical systems (CPS) offer new networking capabilities in mechatronic systems. What's really new about this is CPS's standardised communication interfaces, which use open, global

standards to prepare the Festo Motion Terminal for future developments, such as software services and global networking.

The CPX bus nodes [5] on the Festo Motion Terminal and the multitude of available I/O modules provide a tried and tested standard for communication in machine and production networks – Figure 7. What's more, you can also use the OPC UA interface on the CPX-CEC to create a service-oriented architecture that is both platform and manufacturer-neutral – the ideal conditions for Industry 4.0.



Figure 7: The CPX bus nodes on the Festo Motion Terminal









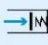

2.7 Motion apps - applications determine the pneumatic function

A wide range of products, functions and complete solution packages are integrated into the Festo Motion Terminal. One valve technology, a powerful controller and smart apps: this combination heralds a new era in terms of flexibility.

The apps are the key to almost limitless function integration in the area of valve terminals. This approach will:

- Reduce the system complexity,
- Speed up the engineering processes,
- Cut the time to market.

Table 1: Motion apps available at market start

	Directional control valve
	Valve functions of a piloted standard valve (e.g. 4/2, 3/2, 4/3...)
	Proportional directional control valve
	Proportional directional control valve for flow control (e.g. 2x3/3 or 5/3 like MPYE)
	Proportional-pressure regulation
	2x valve function for proportional pressure control (like VPPM)
	Model-based proportional-pressure regulation
	2x valve function for proportional pressure control with calculation model for improved and more accurate control for applications with long tubes (information about tube and cylinder needed)
	Supply and exhaust air flow control
	Cylinder movement with exhaust or supply air flow control (like GRLA)
	ECO drive
	Supply air flow control and instant stoppage of air supply as soon cylinder reaches end position (lower pressure level in cylinder chamber). Savings up to 70%!
	Presetting of travel time
	Selectable travel time for the movement of a specific cylinder (just with standard cylinder switches).
	Selectable pressure level (ECO)
	Selectable pressure level in cylinder end position and exhaust air flow control (like GRLA + LRP)
	Soft-Stop
	Cylinder movement with Soft Stop in end positions. This function increases cylinder dynamics and eliminates shock absorbers.
	Leakage diagnostics
	Leakage detection in the application (Preventive maintenance). Customer sees leakage level (red, orange, yellow, green).

2.8 Implementation and next steps

First machine builders use this new technology for completely new machine designs and new applications. The full scope of possibilities will show only over time. Festo itself also continues its research.

With its Bionic Learning Network it performs research on the future of motion and automation. A successful combination of the Festo Motion Terminal and Bionics is the BionicCobot first presented at Hannover fair in April 2017. This pneumatic lightweight robot is based on the human arm, is designed for save human-machine interaction and is fully controlled by the Festo Motion Terminal.

3 Conclusion

The Motion Terminal VTEM is opening up radical new dimensions in the world of automation, as it is the world's first valve to be controlled by apps. The first product to truly earn the label "digital pneumatics". For a multitude of functions that currently require you to order and install more than 50 separate products/positions. The key features comprise:

- Many functions in a single component – thanks to apps,
- Combines the advantages of electric and pneumatic technologies,
- Highest possible level of standardisation,

- Reduced complexity and time-to-market,
- Rising profitability and protection of intellectual property,
- Reduced installation expense,
- Increased energy efficiency.

References

- [1] N.N.: FESTO – internal sources

About the invited Author

Markus Miklas holds a degree in Precision Engineering from the Federal Technical College in Mödling, Austria. After technical college, he studied communication sciences at Vienna University. Most of his professional life he spend in technical communication, explaining and evangelising complex technologies to various audiences. After more than a decade in the IT industry he joined Festo in 2009. Since then he works in the regional sales management for Eastern Europe. In this role he also takes care of the roll out of the Festo Motion Terminal in the region.

Fluid power drives in robotic systems

ŽELJKO ŠITUM

Abstract Two main actuation technologies are used for stationary and mobile robotic systems. Electric actuators are commonly used to drive robots and manipulators, but tasks requiring highly dynamic actuation performance in terms of speed and torque cannot always provide satisfactory solutions unless they oversize them.

The other drive technique used for actuating robots and manipulators is based on fluid power technologies, that is, hydraulic drives for higher power and pneumatic drives for less power requirements.

This paper briefly reviews the history of robotic systems with fluid power drives, focusing on the development of several experimental robotic systems actuated by hydraulic and pneumatic drives, which have been designed as test models in the field of mobile robots, mechatronics, fluid power systems and feedback control education of mechanical engineering students.

Keywords: • robotics • fluid power • drive systems • actuators • control system •

CORRESPONDENCE ADDRESS: Željko Šitum, Ph.D., Assistant Professor, University of Zagreb, Faculty of Mechanical Engineering and Naval Architecture, Department of Robotics and Production System Automation, I. Lučića 5, Zagreb, Croatia, e-mail: zsitum@fsb.hr, Invited author.

1 Introduction

The majority of modern industrial robots and manipulators are successfully applied for repetitive and relatively simple manufacturing tasks that require organized work space and little interaction between robot and its environment. More recently, the scope of robots is rapidly expanding, and they are increasingly being applied in more complex cases, which generally require faster and more accurate motions and at a same time greater interaction with the environment in which they operate. Technological improvements and innovations within modern robotic systems as well as in artificial intelligence, communication and control techniques have made possible some new modalities in traditional robotic system applications [1]. Industrial robots may have three main types of actuators: hydraulic, pneumatic or electric drives. Owing to the fact that hydraulic drives provide high force multiplication they were preferred actuators for industrial robots during the *early stages of robotics development*. At that time, electric motors did not have satisfactory performance for practical use in many applications. But nowadays, electric drives are by far the most widely used actuators for industrial robots, because they are reliable and accurate and modern industrial robots with electric drives can lift really large loads (payloads over 2 tons), so they dominate in all segments of application [2].

The use of hydraulic systems in industrial applications has become widespread due to their advantages such as a high power density, good dynamic performance, high durability, high stiffness, etc. Example of state-of-the-art application of electro-hydraulic drives is remote handling of critical equipment in nuclear fusion reactor [3]. Reliable and robust control strategies are crucial for such applications. Electro-hydraulic servo systems have desirable features for application in highly automated production facilities as they are characterized with small size-to-power ratio, ability to produce large hydraulic power and large forces, all together in combination with simple processing/transmission of control signals in electrical components. However, precision motion and force control on high power levels are far from trivial. Significant nonlinearities of hydraulic components and complex phenomena of fluid dynamics make control of electro-hydraulic systems extremely challenging task, especially in cases of simultaneous motion of several controlled links of a robotic system. These difficulties are even more emphasized in plants with a large number of control variables and high performance requirements in terms of rapid responses and high accuracy in a wide range of working conditions, smooth and noiseless operation, all in conditions of dynamically changing structure of the robotic system [4].

Pneumatic drives, generally speaking, do not offer enough positional accuracy to be used to drive all robot joints, and pneumatics are mostly used only for grippers or to create a vacuum for robot end-effectors. Robotic manipulators with pneumatic drive are used mostly for pick and place operations such as loading machines, placing components on assembly lines, moving parts off conveyor belts, lifting or carrying a payload to a predetermined position, etc. [5]. Such drive units are fast, accurate and very cost effective.

One of the research directions in pneumatics relates to the area of pneumatic artificial muscle (PAM) actuators using biological principles for system design and control as an attempt to replicate natural human movement. Due to their adaptive compliance, elasticity, flexibility and lightweight, pneumatic muscles are suitable for use in bionic systems, i.e. biologically inspired designs of technical systems, where the applications of biological methods and processes found in nature are used to improve engineering systems and modern technological products [6].

Scientific and technical works in the past have shown that overall system performance can improve when some biological principles are incorporated within the designing of engineering solutions. Some new applications are also identified, particularly in the areas of bio-robotics and human-

friendly orthopaedic aid devices for the rehabilitations of polio patients. PAMs are progressively researched and used in modern human-like robotic systems, offering in many cases natural compliance properties. Fluidic muscles also have great potential within industrial applications for the actuation of new devices and manipulators. Their properties such as compactness, high strength, high power-to-weight ratio, inherent safety and simplicity are worthy features in advanced manipulating systems. Unfortunately, due to their highly nonlinear and time-varying nature pneumatic muscles are difficult to regulate regarding motion or force. Therefore, various control methodologies have been applied to control different robotic systems, manipulators and orthopaedic devices driven by PAMs [7] to [9].

This paper presents several self-made systems actuated by hydraulic and pneumatic drives, which have been designed and manufactured as test models within the fields of electro-hydraulic robotic systems, walking robots, mechatronics, fluid power systems and feedback control education.

2 Robotic manipulators actuated by hydraulic drive

2.1 A brief history of robotic manipulators

The idea of an automatic device to work for humans has long been in existence, but the prerequisite for the appearance of the first industrial robots have been achieved with the invention of the numerically controlled machines, the emergence of the first computers, and the integrated circuit. The first prototype of the industrial robot known as Unimate, created by American inventor George C. Devol, was produced in 1961 in the world's first robot manufacturing company Unimation founded by Joseph F. Engelberger. The Unimate was the hydraulically powered robot. The first robot was installed at a GM's plant and it was programmed to handle the hot metal parts used in die casting and for spot welding on auto bodies. It weighed two tons and was controlled by a program on a magnetic drum. The primary purpose of the first robots was to replace humans for the heavy, dangerous and monotonous tasks and they were mostly used for simple pick and place tasks.

Despite the fact that at the beginning the first industrial robots had a hydraulic or pneumatic drive, they have undergone a huge change since the first prototypes, so the robots with fluid power drives are rare today. The usage of industrial robots can be roughly divided into three main groups: material handling, process operations and assembly. Research on robotic applications for tasks on the assembly line showed that most of the manipulation items weighed only a couple of pounds, while pneumatic and hydraulic robots were intended for much larger loads and therefore not suitable for assembly works. At the same time robots with higher repeatability, acceleration and velocity were needed in order to respond to increased production demands. This leads to dominance of electric robots, which has continued to date.

The development of the microprocessor helped to create cost-effective control systems and modern industrial robot arms with electric drives continued to quickly evolve. The well-known Stanford Arm, invented by Victor Scheinman, was one of the first electronically powered, computer controlled, 6-dof electro-mechanical manipulator that performed small-parts assembly using feedback from touch and pressure sensors. By the middle of the 1970s, Unimation in collaboration with GM developed Scheinmans technology into a Programmable Universal Machine for Assembly (PUMA).

At that time the first anthropomorphic, completely electric driven, microprocessor-controlled industrial robot was IRB 6 developed by the Swedish manufacturer ASEA (now ABB). It was programmed to polish stainless steel pipes. Soon after German toolmaker KUKA introduced

Famulus, the first industrial robot with six axes which is nowadays the most commonly used kinematic for industrial robots.

The latest major step happened at the beginning of 1980, when researchers at Carnegie Mellon developed the Direct Drive Arm, where the motor is directly mounted in the joint, thus removing transmission mechanisms between the motors and loads. This results in a robot arm that can move smoothly, providing for high speed precision robots. The evolutionary development of industrial robots from their earliest beginnings to the present day is shown in Figure 1.



Unimate robot



Stanford Arm



Unimation PUMA



Anthropomorphic robot IRB 6
(ASEA-ABB)



Famulus robot
(KUKA)



Robot M-2000iA/2300
(FANUC)

Figure 1: Evolution of industrial robots

In the 1980s, enormous interest was focused on industrial robots. The automotive companies was, and still are, an important customer, but industrial robots are used in a wide variety of industries, including the mechanical, electronic and chemical industries among others. After having studied robot manipulators for decades, we are now witnessing a real interest in robotics and today there is a multitude of teams creating different robots worldwide for the applications such as: agricultural robots, hostile territory exploration, inspection robots, military robots, cleaning robots, service robots, robots for helping the handicapped, medical robots etc. We live in exciting times and the change in robotics technology has never been more rapid. Thus the question arises: are there niche applications for greater use of robots with fluid power drives?

2.2 Electro-hydraulic robotic manipulator (EHROM)

A prototype of the electro-hydraulic robotic manipulator (EHROM) was developed at the Faculty of Mechanical Engineering and Naval Architecture at the University of Zagreb, Croatia. Figure 2 shows the manipulator intended for manipulation of heavyweight objects in industrial applications,

e.g. in foundries to handle the heavyweight metal parts, assembly lines, CNC machines, welding operations, etc.

The manipulator was built in close cooperation with two Croatian companies. The robotic manipulator has three degrees-of-freedom (the spherical robots' structure RRT - two revolute joints and one prismatic joint for the telescopic extension arm) with a hydraulic gripper at the end of mechanical structure. The manipulator weights approximately 515 kg and when the telescopic extension arm is fully extended it measures an operating diameter of 3.8 m. This configuration allows the manipulator for reaching a wide working area, still being most affordable and flexible. The hydraulic power unit consists of a pump (axial piston pump Parker PV023), a tank containing 60 l oil, filters and proportional valve group (Danfoss PVG 32 with PVEH actuation modules). The oil pump is driven by a three-phase squirrel cage induction electric motor, 5.5 kW at 1410 rpm. The torque motor applies rotational power to the worm shaft causing the worm rotates against the wheel and allows rotary motion of the manipulator arm. Worm gears was used because large gear reduction was needed (worm gear reduction ratio $i=50:1$). Rotary motion of the telescope is realized using a double-acting cylinder, while the translational movement of the extension arm is achieved using a telescopic cylinder. Load-sensing technology is used for the manipulator operation, enabling simultaneous motion of all controlled axes. By using PVG proportional valves in combination with a variable displacement pump, it is possible to achieve a significant reduction in energy loss.

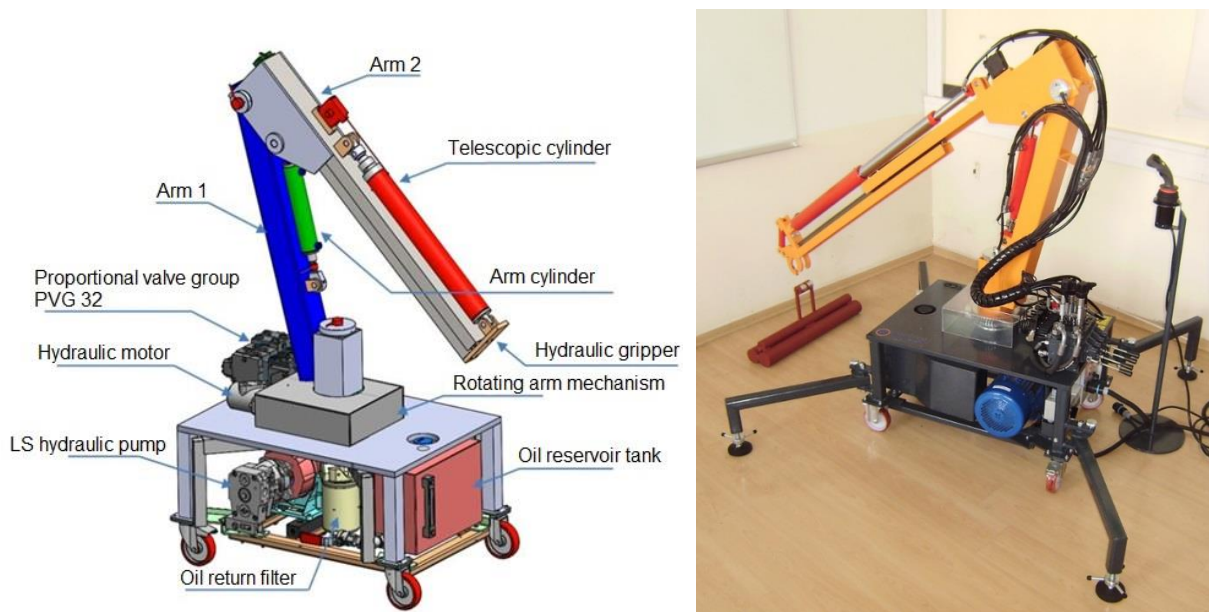


Figure 2: Prototype of the electro-hydraulic robotic manipulator (EHROM)

PVG valves also reduce heat generation, increase efficiency and power density. The manipulator can be controlled using levers on the proportional hydraulic valve or using a joystick, whereby the desired operation is commanded to the valve block for generating a suitable flow to the actuators that will move the mechanical arm. The operator easily control the valves using a joystick command input, which distributes the fluid on the principle of load-sensing hydraulic system. Recently, the wireless control of the proportional valve group has been realized via Bluetooth connection, using Arduino microcontroller and self-made control interface. [10]

In the future, the focus will be to build up a control for the end-effector's trajectory within the workspace. This will be achieved by using the inverse kinematics of the robot manipulator in order to determine the required joint angles that correspond to the desired position of the gripper. In the

context of this issue some solutions will be considered that improve better accuracy and repeatability of the manipulator, despite the non-linearity of the system, internal and external disturbances and complex phenomena of fluid dynamics. In order to achieve automatic control of the robotic manipulator and to carry out some advanced feedback control strategy, the system includes various sensors (two angular sensors, one displacement sensor, one force sensor and four pressure sensors).

The developed robotic manipulator prototype belongs to a group of complex, nonlinear multivariable systems with real industrial components, and performance characteristics which make it suitable for manipulating heavy weight objects in industrial applications. The robotic manipulator is totally open system and has an educational character. It will involve a variety of education activities such as explanation of the load-sensing systems operation, programming the desired trajectory of robots, etc. During the development of the prototype, a number of students had been involved in various stages of production of the necessary parts.

3 Robotic manipulators actuated by pneumatic drive

3.1 Pneumatics in robotic systems

Robotic manipulators with pneumatic drive are mainly used in smaller systems for pick and place operations with fast production cycles in manufacturing industries. The pneumatically actuated manipulation systems are widely used on the assembly line as automation systems which emphasize reliability, cost, cleanness, simplicity, easy maintenance and safety in operation. Robotic manipulators with pneumatic drive could be used for material handling in applications where electric or hydraulic robots are unsuitable due to fire hazard. Pneumatically driven robotic systems usually have a lower cost than hydraulic and electromechanical systems.

Although a pneumatic robot manipulator could be an inexpensive and simple solution for industrial applications, when compared to electro-mechanical actuators with identical power, it is still not competitive in those applications that demand accuracy, universality and flexibility. Namely, the nonlinear effects in pneumatic systems caused by the phenomena associated with air compressibility, significant friction effects, load variations, a wide range of air supply pressure, etc., make them difficult to control for variable set point applications. Therefore, pneumatic drives are traditionally used in manipulation tasks to quickly move loads between two positions using simple on-off valves. Development of proportional control valves has resulted in servo applications of pneumatic drives and pneumatic actuated drives are progressively used in modern automation systems, offering in many cases favorable cost / performance characteristics.

Figure 3 shows one of the first versions of a robot manipulator with pneumatic drives designed in 1970s at MIT.

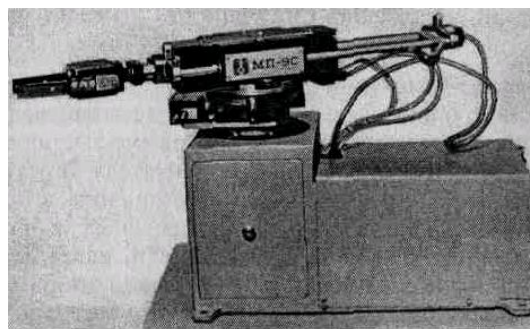


Figure 3: Pneumatically actuated industrial robot

3.2 Electro-pneumatic manipulator

A prototype of an electro-pneumatic manipulator, with three-degrees-of-freedom (one rotational and two translational degrees of freedom – type RTT) is shown in Figure 4. The manipulator was designed and manufactured in the Laboratory for automation and robotics to enable students to gain practical knowledge in the field of mechatronics, electro-pneumatics, industrial engineering, automated manufacturing systems, etc. The manipulator arm is connected by joints allowing either rotational motion or translational (linear) displacement.

Pneumatic cylinders are used as the main actuating system for the manipulator arm and are controlled by a solenoid valve manifold. The belt mechanism was used to convert linear actuation displacement of the pneumatic cylinder (SMC, type MGZ63TF-150) to angular displacement about the joint. One compact guide cylinder (SMC, type MGPM25R-100) and one standard double acting cylinder (SMC, type C95SB50-100) are used to achieve the translational movement of the manipulator. A pneumatic gripper (SMC, type MHC2-20D) was attached at the end of mechanical structure of the manipulator arm which is used as the end effector to grasp objects. This manipulator works as a pick and place robot, capable of picking objects from one location and drop them at another location.

A programmable logic controller (PLC) with relay outputs was used as a control device to energize solenoid valves module (SMC EX250) in order to control the movement of the pneumatic actuators. Ladder programming is used to execute the motion sequence of the robotic arm pick and place system. The supply of air pressure is given through an air supply unit, then through the compact manifold pressure regulator and directional control valves supplying the pressure individually to each cylinder connected to the valve block.

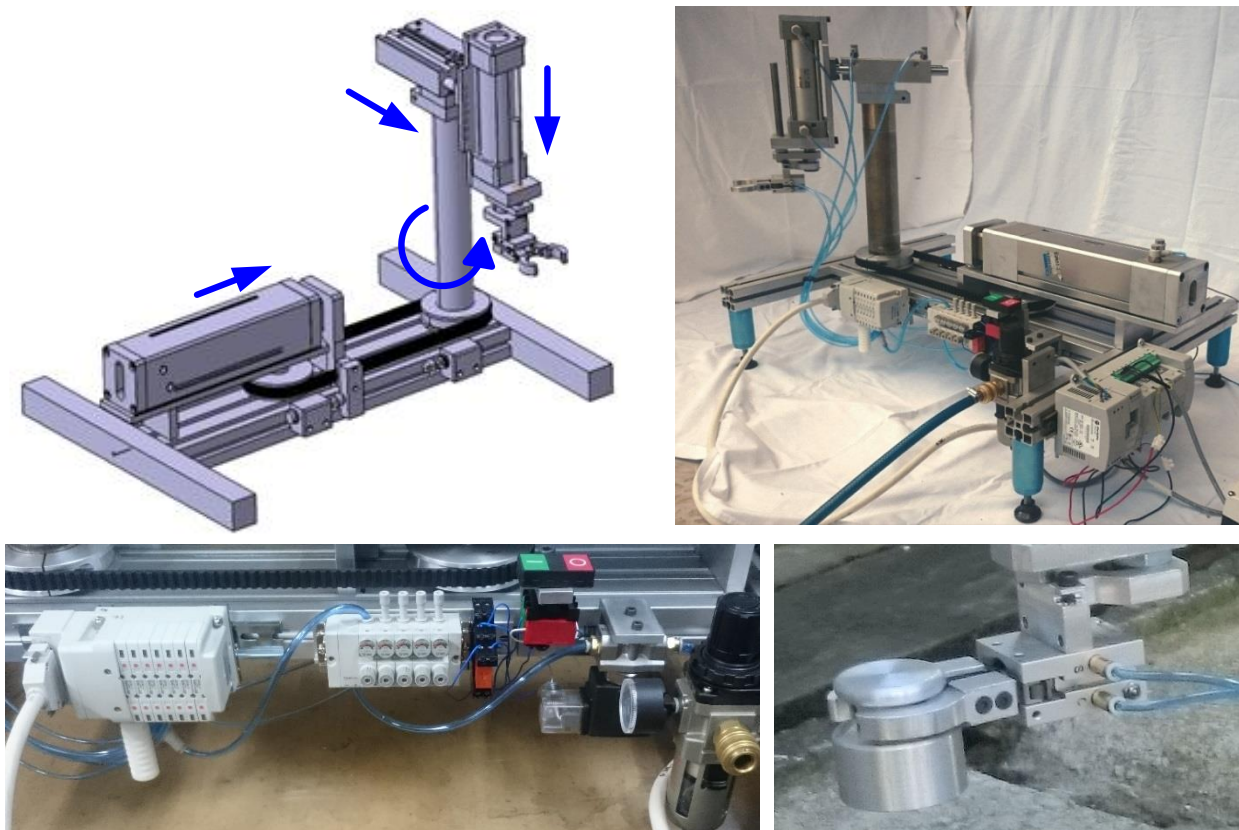


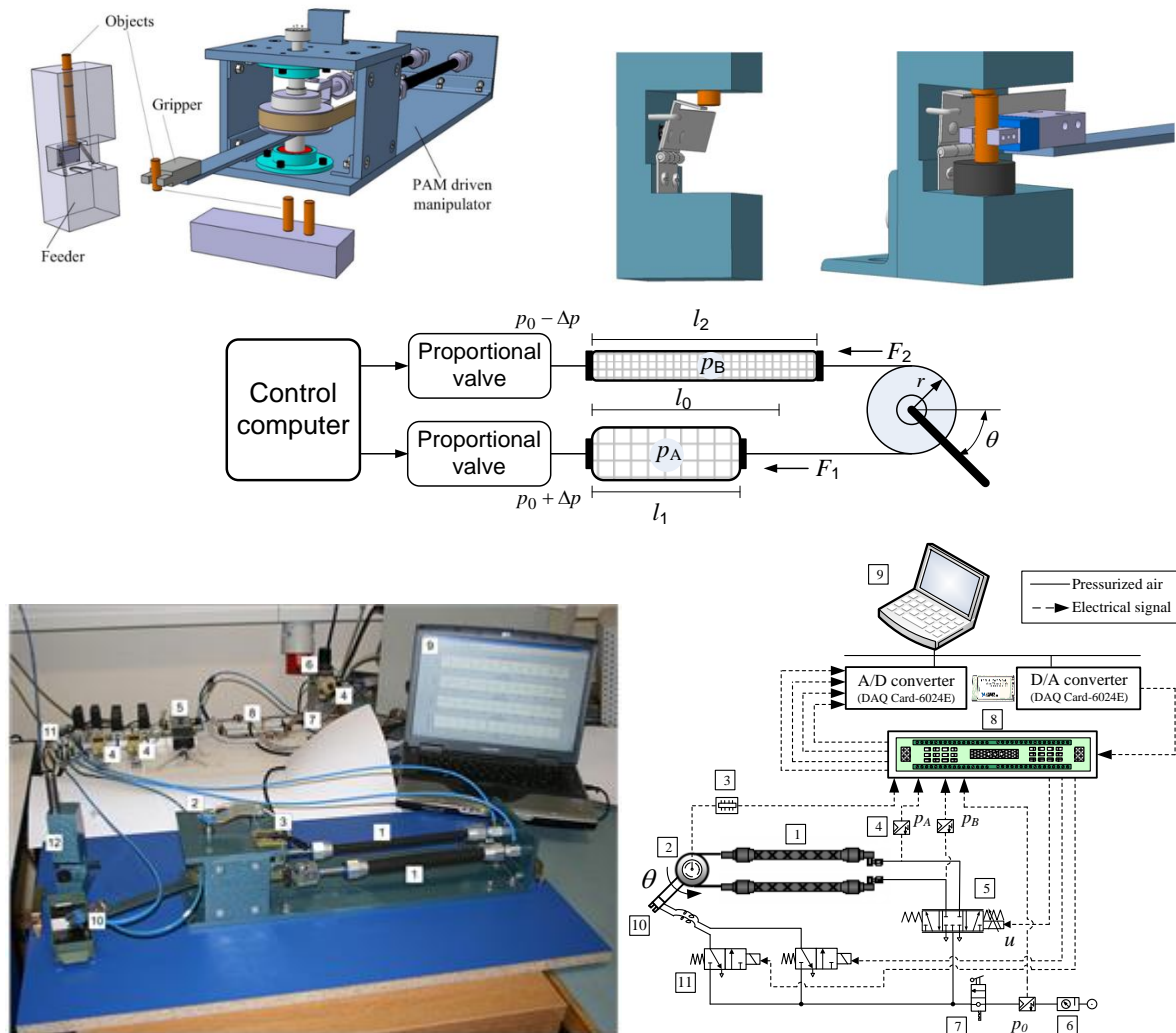
Figure 4: Robotic manipulator actuated by pneumatic cylindrical drives

3.3 Manipulator arm actuated by PAMs

Technological improvements and innovations in modern pneumatic components as well as in control strategies have made possible some new modalities in traditional pneumatic system applications. One of research directions is related to the area of pneumatic artificial muscle (PAM) actuators using biological principles for system design and control as an attempt to replicate natural human movement. Some new applications are also identified, particularly in the area of bio-robotics and human-friendly orthopaedic aid devices for rehabilitation of polio patients.

Fluidic muscles also have a great potential in modern manufacturing industries and assembly automation for the actuation of new types of robots and manipulators. Their properties such as compactness, high strength, high power-to-weight ratio, inherent safety and simplicity are worthy features in advanced manipulating systems. There exists several types of fluidic muscles that are based on the use of rubber or some similar elastic materials, such as the McKibben artificial muscle ([11], [12], [13]), the rubbertuator made by Bridgestone company ([14], [15]), the air muscle made by Shadow Robot Company [16], fluidic muscle made by Festo company ([17], [18]), the pleated PAM developed by Vrije University of Brussel [19], ROMAC (RObotic Muscle ACTuator), Yarlott and Kukolj PAM [20] and some others. The pneumatic muscle is a diaphragm contraction actuator, which shortens under pressure. It consists of an inflatable and flexible membrane (closed rubber tube) and two connection flanges along which they drive some mechanical load. Powered by compressed gas, the artificial muscle actuator contracts lengthwise when it expands radially, and converts the radial expansive force into axial contractile force and generate translational and unidirectional motion. We have used fluidic muscles in an antagonistic pair to provide powered torque required to move a planar manipulator arm. The pair of PAM actuators put into an antagonism configuration imitate a biceps-triceps system and emphasize the analogy between this artificial muscle and human skeletal muscle.

A single-joint manipulator arm driven by PAMs in an antagonistic coupling is illustrated in Figure 5. The pneumatic part includes PAM manipulator with pneumatic valve and measuring components, and the control part includes a control computer and data acquisition system.



Legend:

1: Pneumatic muscles; 2: Rotary potentiometer; 3: Voltage reference card; 4: Pressure sensors; 5: Proportional control valve; 6: Filter-regulator unit; 7: Manually operated valve; 8: Electronic interface; 9: Control computer with DAC card; 10: Gripper; 11: High-speed on/off solenoid valve ; 12: Feeder

Figure 5: Manipulator arm actuated by pneumatic artificial muscles

The pneumatic part is composed of an air supply with a filter/regulator unit, a directly actuated proportional control valve, and two pneumatic rubber muscles (Festo, MAS-10-220N-AA-MC-K), which are mounted antagonistically to actuate a revolute joint. The rotating torque is achieved by the pressure difference between the antagonistic muscles and the lever with a pneumatic gripper (Festo, HGP-06-A) is rotated as a result. For activation of the gripper a high-speed on/off valve (Matrix 758 series, 8 channel, 2-way) is used. Precision industrial single-turn potentiometer (made by Vishay Spectrol), which is attached to the revolute joint is used for measuring its angle θ . The measured signals from the process are fed back to the control computer equipped with a data acquisition card (NI DAQCard 6024E, 12-bit A/D and D/A converter).

4 Legged robots

Mobile robotics as a fast evolving engineering discipline is one of the more complex and most interesting research areas. People seem to have a fascination with human-looking robots and machines that mimicking existing biological systems. The field of robotics, and especially mobile

robotics, is a multidisciplinary research domain which includes mechanical, electronic and software engineering.

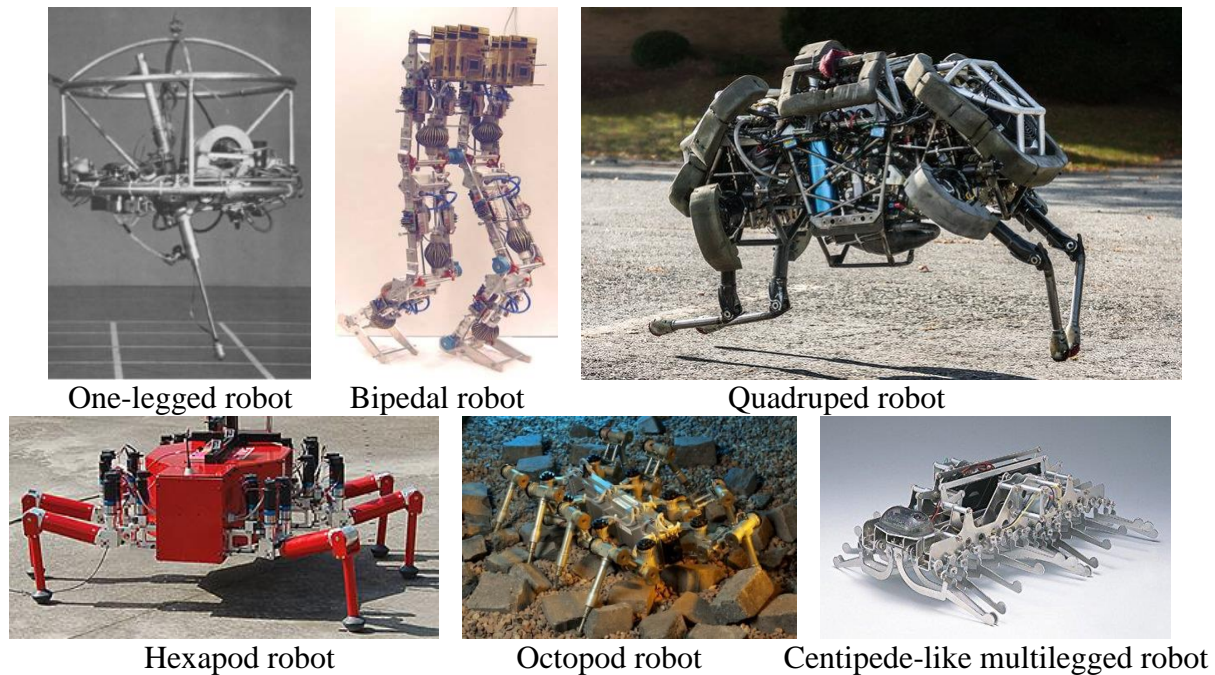


Figure 6: Legged robots

Legged robots over standard wheeled or tracked robots offer the potential to navigate highly challenging terrain. Walking robots can operate successfully within a complex, dynamic environment and recently the robotics community has attributed great potential to legged robots for acting within unstructured outdoor environments. Researchers inspired by the biomechanics of humans and animals (dogs, horses, insects, etc.) have developed a number of mono-pedal, bipedal, quadrupedal, hexapod, octopod and centipede-like multilegged robots driven by various types of actuators in order to create improved robotic systems [21] to [25].

Pneumatic muscles have performance characteristics very close to human muscles and due to similarities with biological muscles pneumatic actuation is a quite often used approach for actuating walking robots. Inspired by this trend and encouraged with the initiative of the Croatian Robotic Association we have started a project for developing a horse-inspired four-legged Walking Robot Actuated by Pneumatic Artificial Muscles (WRAPAM). This quadruped robot was designed with two degrees of freedom within each leg actuated by eight Festo air muscles and controlled by a modular valve terminal system which includes eight solenoid coils.

Two Festo fluidic muscles (model DMSP-20-150N-AM-CM) per leg are mounted for actuating the robotic joints. Each leg consists of two movable rotational segments and additionally incorporates a torsional spring which supports faster movement of the leg joint. The robot contains a small custom electronics module. The microcontroller ATmega2560 in a hardware interface Arduino Mega is used for controlling the movement of the robot. This microcontroller was chosen because of its accessibility, low cost and the large number of inputs/outputs that will be required in the future to upgrade the robot. In order to activate eight pneumatic valves the integrated chip ULN2803A is used which contains Darlington transistor drives for amplifying the electrical signals sent from the microcontroller to the level required by the valve block. The electronic circuit board includes a Bluetooth module which enables wireless communication between the controller and operator.



Figure 7: Construction process of WRAPAM and its final form

All components are mounted on the robot's frame in such a way that maintains the robot's centre of gravity. All components of the robot frame are hand-made using aluminium L-profiles or square tubing profiles. The power source for the compressed air supply and the control unit are housed on-the board. This pneumatically actuated quadrupedal robot, as shown in Figure 7, is a fully autonomous system, equipped with Bluetooth technology and USB connection for communication with a computer. It is controlled by a cell-phone or tablet computer. The robot's design includes an energy system that is used for supplying compressed air to pneumatic muscles, then valves for controlling the rate of airflow to the actuators as well as the control and electronic part of the system with proximity sensor.

5 Conclusion

The paper has presented a brief history and a quick survey of industrial and mobile/legged robotic systems with electric and fluid power drives, focusing on the development of several experimental systems actuated by hydraulic and pneumatic drives, which have been designed in the Laboratory for automation and robotics at the Faculty of Mechanical Engineering and Naval Architecture, University of Zagreb.

The article was first introduced the design and practical realization of a prototype of an electro-hydraulic robotic manipulator (EHROM) with three-degrees-of-freedom and a hydraulic gripper as the end effector. The robotic manipulator can be controlled using levers on the proportional hydraulic valve block, or using a profi-joystick. Also, the wireless control of the proportional valves has been realized via Bluetooth connection, applying a low-cost microcontroller and self-made control interface. The project EHROM is largely based on experiences from past activities in our Laboratory, which has resulted in several successfully implemented experimental systems in the field of electro-hydraulic controlled systems. The laboratory setups realized so far have the characteristics of real-life industrial systems. Then the paper has described the design and construction of a robotic manipulator with three-degrees-of-freedom actuated with pneumatic cylindrical drives and a pneumatic gripper as the end effector. The manipulator arm is controlled by the PLC device and could be used for simple pick-and-place applications. Then the article has presented the design and construction of a single-joint manipulator arm driven by a pair of pneumatic muscle actuators. PAMs are undoubtedly very suitable actuators for the actuation of new types of driving mechanisms and manipulators within the various manufacturing processes,

which have traditionally been dominated by pneumatic cylinders or motors. The final section describes the design and construction of a four legged walking robot actuated by pneumatic artificial muscles. The robot is a fully autonomous system with wireless application platform and its motion in all directions can be controlled by using a cell phone. By using realized robotic systems with fluid power drives through both theoretical and practical parts, students have the opportunity to learn about mechanical system construction, mathematical descriptions of practical systems, parameters identification of real processes, consideration of different control techniques and their experimental verifications. The complete educational experience involving practical applications and comparative analyzes of different system realization are recognized by educators in universities and control laboratories around the world.

Aknowledgements

The manipulator was built in close cooperation with two Croatian companies: Hidraulika Kutina – The factory of hydraulic and pneumatic equipment and components, Inc. from town Kutina and Rasco – The factory of communal equipment Ltd. from municipality Kalinovac.

References

- [1] Tennyson, S.J.: Advancements in Robotics and Its Future Uses; International Journal of Scientific & Engineering Research, 2011, 2, 8, ISSN 2229-5518, <http://www.ijser.org>
- [2] Brochures of Fanuc's product: Super Heavy Payload Robot, Fanuc M-2000iA/2300, <http://fanuc.co.jp>
- [3] Dubus, G., Davida, O., Nozais F., Meassona, Y., Friconneau, J.-P., Palmer, J.: Assessment of a water hydraulic joint for remote handling operations in the divertor region; Fusion Engineering and Design, 2008, 83, page 1845–1849
- [4] Sirouspour, M. R., Salcudean, S. E.: Nonlinear control of hydraulic robots; *IEEE Transactions on Robotics and Automation*, 2001, 17, 2, page 173-182
- [5] Hesse, S.: Modular Pick-and Place Devices; In: Blue Digest on Automation (Festo AG & Co.), Handling Pneumatics, 2000, Esslingen, Germany
- [6] Caldwell, D.G., Tsagarakis, N., Medrano-Cerda, G.A.: Bio-mimetic actuators: polymeric pseudo muscular actuators and pneumatic muscle actuators for biological emulation; *Mechatronics*, 2000, 10, page 499–530
- [7] Lilly, J.H.: Adaptive Tracking for Pneumatic Muscle Actuators in Bicep and Tricep Configurations; *IEEE Trans. on Neural Systems and Rehabilitation Engineering*, 2003, 11, page 333-339
- [8] Ahn, K.K., Nguyen, H.T.C.: Intelligent switching control of a pneumatic muscle robot arm using learning vector quantization neural network; *Mechatronics*, 2007, 17, page 255–262
- [9] Chang, M. K., Yen, P. L., Yuan, T. H.: Angle Control of a one-Dimension Pneumatic Muscle Arm using Self-Organizing Fuzzy Control; *IEEE Int. Conference on Systems, Man, and Cybernetics*, October 8-11, 2006, Taipei, Taiwan
- [10] Tašner, T., Les, K, Lovrec, D.: Bluetooth platform for wireless measurements using industrial sensors. *International journal of advanced robotic systems*, ISSN 1729-8806, 2013, vol. 10, pp. 1-9, doi: [10.5772/55478](https://doi.org/10.5772/55478).
- [11] Chou, C. P., Hannaford, B.: Measurement and modeling of McKibben pneumatic artificial muscles; *IEEE Trans. On Robotics and Automation*, 1996, 12, 1, page 90-102
- [12] Tondu, B., Lopez, P.: Modeling and control of McKibben artificial muscle robot actuators; *IEEE Control Systems Magazine*, 2000, 20, page 15-38
- [13] Caldwell, D. G., Medrano-Cerda, G. A., Goodwin, M.: Control of pneumatic muscle actuators; *IEEE Control Systems Magazine*, 1995, 15, page 40-48
- [14] Pack, R.T., Christopher J.L., Kawamura, K.: A Rubbertuator-Based Structure-Climbing Inspection Robot; *Proceedings of the IEEE Int. Conference on Robotics and Automation*, April 1997, Albuquerque, New Mexico.
- [15] Inoue, K.: Rubbertuators and applications for robotics; *Proceedings of the 4th Int. Symposium on Robotics Research*, 1987, page 57-63

- [16] Shadow Robot Company: Design of a Dextrous Hand for advanced CLAWAR applications; www.shadow.org.uk
- [17] Hildebrandt, A., Sawodny, O., Neumann, R., Hartmann, A.: A Flatness Based Design for Tracking Control of Pneumatic Muscle Actuators; 7th Int. Conference on Control, Automation, Robotics and Visions, ICARCV 2002, Vol. 3, page 1156-1161
- [18] Thanh, D. C., Ahn, K. K.: Nonlinear PID control to improve the control performance of 2 axes pneumatic artificial muscle manipulator using neural network; *Mechatronics*, 2006, 16, page 577–587
- [19] Daerden, F.: Conception and realization of Pleated Pneumatic Artificial Muscles and their use as compliant actuation elements; PhD Thesis, Vrije Universiteit Brussel, 1999
- [20] Daerden, F., Lefeber, D.: Pneumatic Artificial Muscles: actuators for robotics and automation; *European Journal of Mechanical and Environmental Engineering*, 2002, 47, page 10-21
- [21] Raibert, M.H., Brown, H.B., Jr., Chepponis, M.: Experiments in balance with a 3D one-legged hopping machine; *Int. Journal of Robotics Research*, 1984, 3, page 75-92.
- [22] Verrelst, B., Vanderborght, B., Vermeulen, J., Van Ham, R., Naudet, J., Lefeber, D.: Control Architecture for the Pneumatically Actuated Dynamic Walking Biped 'Lucy'; *Mechatronics*, 2005, 15, page 703-729
- [23] Raibert, M., Blankespoor, K., Nelson, G., Playter R., and the BigDog Team: BigDog, the Rough-Terrain Quadruped Robot; *Proceedings of the 17th World Congress The International Federation of Automatic Control Seoul, Korea, July 6-11, 2008*
- [24] Gonzalez de Santos, P., Cobano, J. A., Garcia, E., Estremera, J., Armada, M. A.: A six-legged robot-based system for humanitarian demining missions; *Mechatronics*, 2007, 17, page 417–430

About the invited author

Željko Šitum received the Ph.D. degree in 2001 in mechanical engineering from the University of Zagreb, Croatia. He is a Full Professor at the Department of Robotics and Production Systems Automation at the Faculty of Mechanical Engineering and Naval Architecture, University of Zagreb. His research interests include digital control of dynamic systems, fluid power systems control, mechatronics and computer simulations, while his current research interest is mainly in modelling and control of hydraulically actuated robotic systems.

Voice of the Machine™ Parker's complete Internet of Things (IoT) platform

IGOR MAGEL & MIHA ŠTEGER

Abstract When you hear, Voice of the Machine, you may imagine a robot from the movies warning of danger in a voice that can be easily understood by the people around it.

Today's IoT-empowered machines – machines with a voice – can warn you of danger, but not quite that dramatically.

By empowering machines to “speak,” valuable data is generated and captured as these machines perform their intended function, whether that function is delivering compressed air or transferring fluids. IoT enables those empowered machines to communicate with each other and with management systems that consolidate data to provide visibility into components and systems that have, until now, been “in the dark.”

The Voice of the Machine embodies Parker's approach to IoT, including the centralized initiative to standardize IoT technology and IoT-empowered products that result from that initiative.

Keywords: • machine • fluid power • electronic • software • IoT technology •

CORRESPONDENCE ADDRESS: Igor Magel, Parker Hannifin EMEA, Etoy, Switzerland - Office Germany, La Tuilière 6, 1163 Etoy, Switzerland, e-mail: igor.magel@parker.com. Miha Šteger, Parker Hannifin Ges.m.b.H., Wiener Neustadt - Branch Office Slovenia, Velika Bučna vas 7, 8000 Novo mesto, Slovenia, e-mail: miha.steger@parker.com.

1 Introduction

Much of the focus of IoT development has been on enterprise-level platforms that provide a top-down view of large systems. Yet, enterprise-level IoT, while indispensable to the future, captures only about 10 percent of the data available, limiting the ability to support predictive maintenance and performance optimization at the component level. Unless supported by discrete-level IoT systems to deliver the remaining 90 percent of data from critical components, enterprise-level systems are unable to tap their potential to transform the business. Fortunately, the reverse is not true: discrete IoT systems can deliver immediate value independent of the enterprise-level system while still supporting the long-term objectives of those systems.

To move forward with IoT, Parker believes an immediate opportunity exists in discrete application areas. Voice of the Machine was created to help capitalize on this opportunity. It is central to Parker's digital transformation and builds on a 100 years of application experience at the discrete component level. This paper outlines Parker's IoT approach delivered under the Voice of the Machine platform, and how the supporting technology allows industrial operators to begin leveraging the benefits of IoT today while maintaining future flexibility.

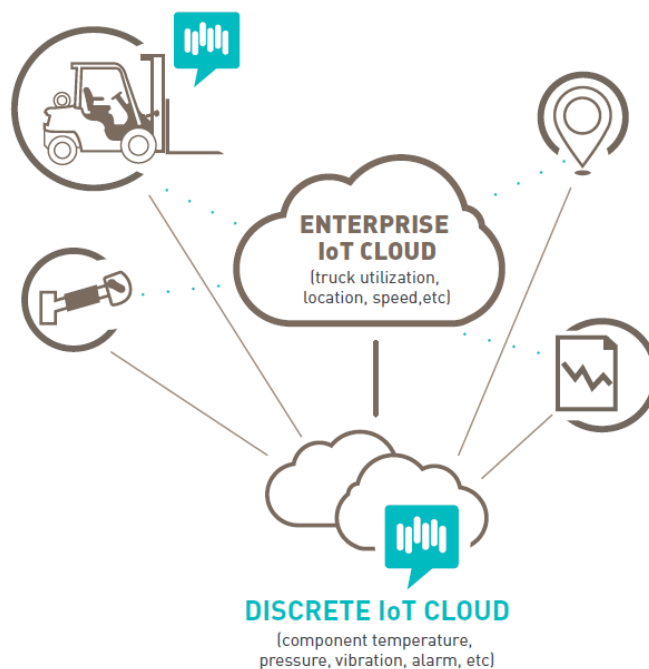


Figure 1: Voice of the Machine solutions take IoT to the last mile by providing visibility into critical components

2 Understanding the Voice of the Machine

Through Voice of the Machine, a common sets of standards, principles and best practices has been established across all Parker operating groups. As a result, all Parker products use the same communication standards, security architecture, and visualize data in the same way. This ensures a delivery of value through interoperability and creates a consistent user experience. From a technology perspective, the efforts are focused on minimizing the challenges that have prevented operators in critical industries from leveraging IoT to solve operating problems, such as downtime and maintenance costs. Considering this transformation for actual operations, there are of challenges like legacy devices that are not IoT-enabled, competing communication protocols used

by various suppliers, securing devices and data, and determining what data to collect and how to present it to the people who can use it to improve operations.



Figure 2: Voice of the Machine uses data encryption and device and user authentication to create a secure end-to-end ecosystem

3 Voice of the Machine in action

Voice of the Machine is being implemented across a broad range of Parker products. Here are three examples:

- a) Connected factory compressed air systems
- b) Electro-hydraulic control
- c) Asset management

a) Connected factory compressed air systems

In manufacturing, compressed air is critical to keeping lines operating. With IoT-empowered compressed air systems, a quick deployment of condition monitoring and predictive maintenance routines for factory compressed air piping systems is possible. The condition monitoring system uses advanced sensors, software and wireless or Bluetooth connectivity to provide a comprehensive picture of system performance through both real-time and historical data. By providing data on vital operating metrics, such as pressure, temperature, humidity, power and flow, through an easy-to-use interface, users can rapidly diagnose problems, such as leaks, and employ predictive maintenance routines that allow them to address seemingly minor issues before they snowball into serious problems.



Figure 3: Advanced compressed air system condition monitoring - Transair® powered by SCOUT™ Technology

b) Electro-hydraulic control

Parker's IQAN® Connect solution integrates intelligent hydraulic components with electronic control hardware and software to create a seamless digital ecosystem. With IQAN Connect, equipment performance is optimized and remote monitoring is simplified for OEMs and fleet managers. The system's building-block approach reduces development time and enables advanced functions to be added without custom programming. Because IQAN Connect stores data in the cloud, information can be accessed instantly, allowing adjustments to machine operation to be made in real time. Assets are managed with live diagnostics to help reduce downtime, maximize return on investment, and improve safety and productivity.

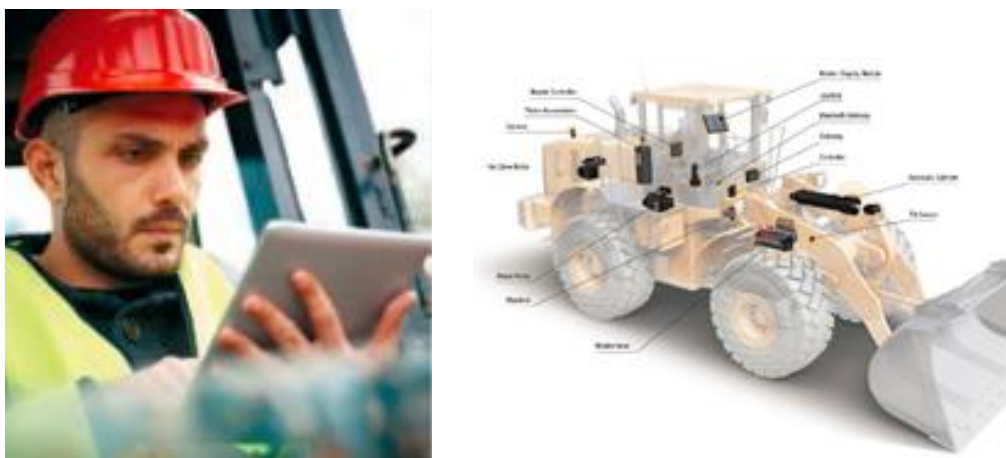


Figure 4: Parker IQAN® Connect – a totally electro-hydraulic approach that replaces traditional systems in mobile machines.

c) Asset management

The Parker Tracking System (PTS) is an innovative component-tagging and asset management solution that focuses on critical-wear components to drive new levels of productivity, efficiency, and reliability. Ideal for companies looking to plan for and perform asset management and replacement services for a wide variety of product types, PTS can establish detailed asset location data, create and deploy custom inspection templates, store and retrieve historical inspection results and schedule and personalize MRO alerts and notifications. PTS has been engineered with key industries and user profiles in mind. What makes PTS unique is the ability to move asset records between accounts or create “Affiliate” relationships between users.



Figure 5: The Parker Tracking System (PTS) innovative component-tagging and asset management solution

4 Conclusion

While IoT can be seen as early in its maturity, the technology has reached the point in its evolution where it can deliver significant value in industrial applications if the right partner and right approach are selected. Parker's Voice of the Machine initiative and solutions were created to enable a focused, cost-effective and secure approach to IoT. Through Voice of the Machine most critical assets for condition monitoring can be targeted, realizing immediate benefits while laying the foundation for expanded use of IoT in the future.

References

- [1] Listening to the Voice of the MachineTM: The Value of Discrete IoT White paper 2017, www.parker.com/IoT

With HYDAC on the way to Industrie 4.0: Industrie 4.0 based predictive maintenance

DEJAN GLAVAČ

Abstract Technology and ever shortening product life cycles, increased individualisation of customer wishes, resources becoming scarce and globalisation are bringing about enormous challenges for the manufacturing industry.

The resulting problems do, however, create a high potential for innovative solutions. For machinery and system builders, there are diverse opportunities to generate competitive advantages. Connectivity and digitalization will play a key role here.

HYDAC offers a wide range of products and services and possess in-depth application knowledge, making HYDAC a partner for all kinds of Industrie 4.0 developments. Furthermore, we work with our customers on future-focused products, digital services and new business models.

Keywords: • hydraulic • technology • Industrie 4.0 • predictive maintenance • sensors •

1 With HYDAC on the way to Industrie 4.0

Technology and ever-shortening product life cycles, increased individualization of customer wishes, resources becoming scarce and globalization are bringing about enormous challenges for the manufacturing industry.

The resulting problems do, however, create a high potential for innovative solutions. For machinery and system builders, there are diverse opportunities to generate competitive advantages. Connectivity and digitization will play a key role here.

On this basis, it will be possible to develop new business models as well as new product and service offers. The changes that industry is aiming for are deemed so extensive that in Germany there is talk of a fourth industrial revolution or, put simply, “Industrie 4.0”.

In other parts of the world, corresponding developments are being advanced under terms such as Smart Factory or Industrial Internet of Things (IIoT).



Figure 1: Industrie 4.0 concept: Smart Factory - Industrial Internet of Things (IIoT)

1.1 What is the best way to describe “Industrie 4.0”?

Many different definitions have been put forward. In brief, “Industrie 4.0” is often defined as “the merger of cutting-edge information and communication technology with the manufacturing industry” or as the “Internet of things and services” in the industrial sector. The very far-reaching vision and goals of Industrie 4.0 are illustrated by the in-depth definition of “Platform Industrie 4.0”: “Industrie 4.0” stands for a new level of organization and control of the entire value chain across the life cycle of products.

This cycle is orientated towards the ever increasing individualized customer requirements, encompassing the idea, the development, the assignment, the manufacturing, the delivery of the product to the end customer and the recycling, including the associated services. The basis is the

availability of all relevant information in real time by connectivity of all instances involved in value creation and the ability to derive the optimum value creation flow from the data at each point in time.

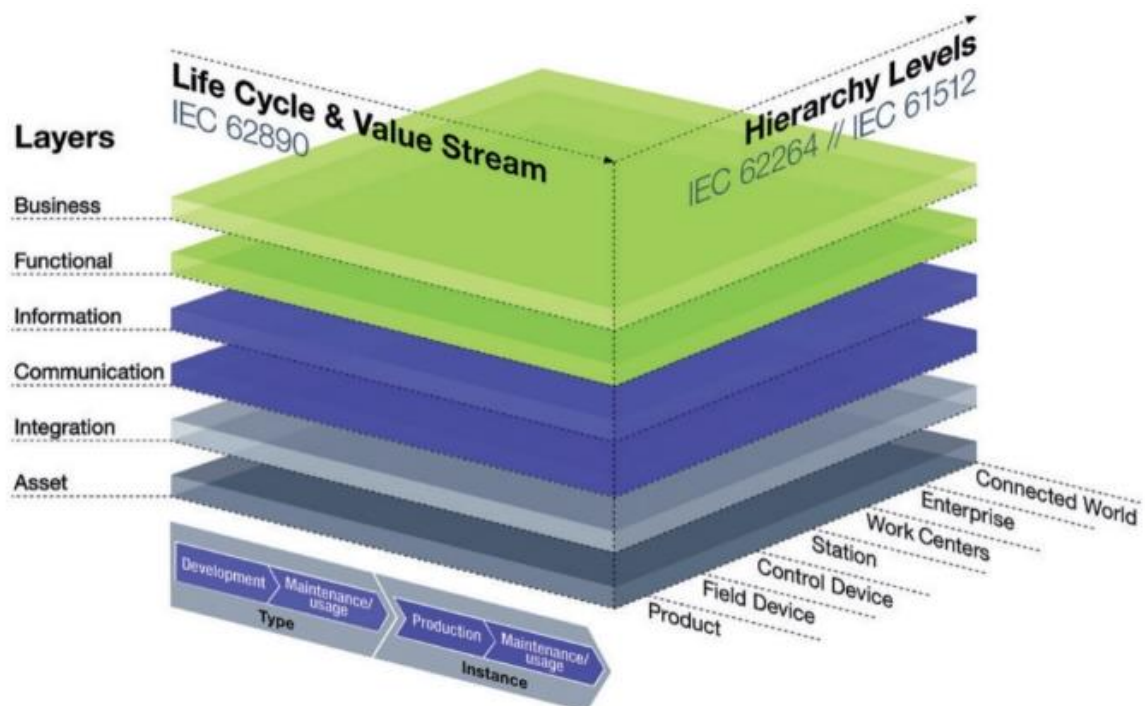
Linking people, objects and systems creates cross-company added value networks that are dynamic, real-time optimized and self-organizing and that can be optimized in accordance with criteria such as costs, availability and resource usage.

1.2 Targets Industrie 4.0

- More extensive digitalization and automation of value chains/ networks,
- New business models and new forms of added value,
- Efficient production of customized products “batch size of one”,
- Flexibilization ,
- Further increase in efficiency (in terms of productivity and resource efficiency),
- Improved information and transparency as a basis for optimizing decisions and processes,
- New design for work - thus overall increase in competitiveness in global competition.

To allow the far-reaching vision of I 4.0 to be realized, comprehensive foundations must be laid, particularly in relation to the security of networked systems, legal frameworks, standardization and research & development. The industry is currently at the beginning of this development and is first of all pursuing a migration strategy towards I 4.0.

The I 4.0 solutions currently offered are often isolated solutions, such as distinct production units or assistance systems, that use available solutions directed towards I 4.0.



Source: Plattform Industrie 4.0

Figure 2: Reference architecture model Industrie 4.0 (RAMI 4.0)

At the same time, existing components and systems are naturally also used, if their characteristics meet the current requirements for the development towards to I 4.0 or can be adapted to do so.

2 HYDAC capability regarding Industrie 4.0

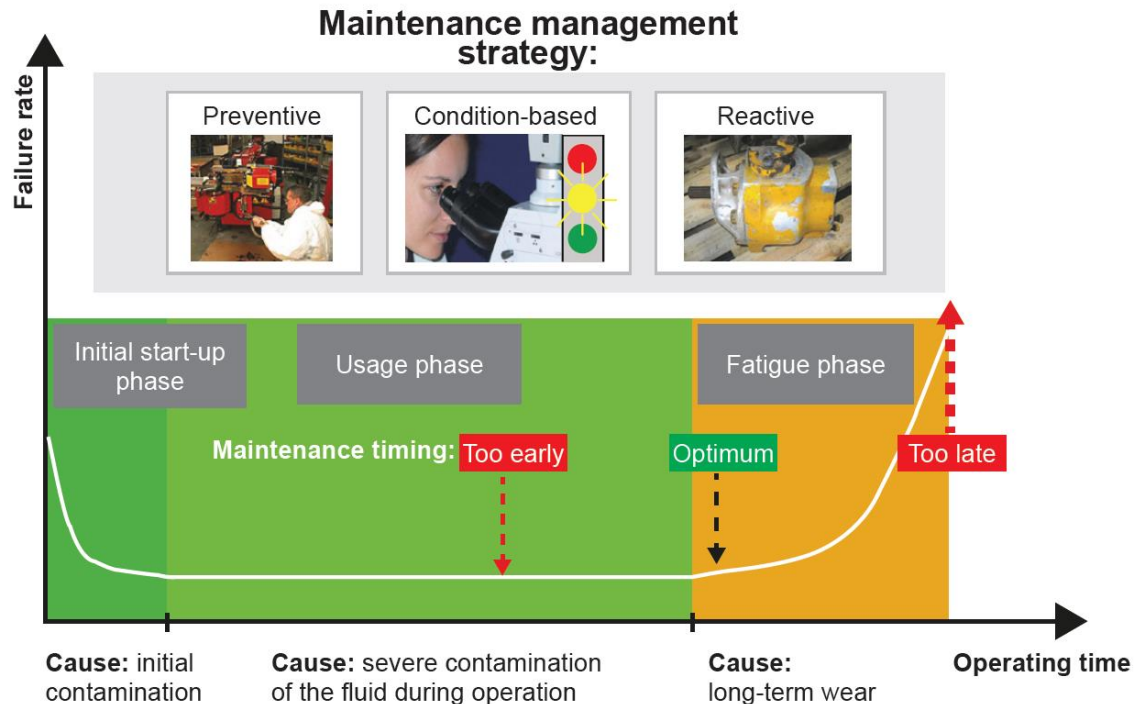
HYDAC offers a wide range of products and services and possess in-depth application knowledge, making HYDAC a partner for all kinds of I 4.0 developments. Furthermore, we work with our customers on future-focused products, digital services and new business models.

Being very strongly integrated in industrial manufacturing processes, hydraulic is predestined to be highly involved in the fourth industrial revolution. Hydraulic power units and lubrication systems often play a key role in industrial manufacturing of goods, mobility, production of power and ores. A chance for Industrie 4.0 is that it enables the operator of the machines to know the state of the machine through 4.0 sensors which give current data about the process. The operator is thus in the position to see correlations in the collected data and can optimize the production process.



Figure 3: Sensors and signals – prerequisite for implementing of Industrie 4.0 concept

Since very widely used and trusted in by the operators, hydraulics is ideal for the mid-term implementation of Industrie 4.0 principals, especially in the field of maintenance so called predictive maintenance 4.0 which can be seen as integral part of Industrie 4.0.



2.1 Predictive maintenance - the strategy that predicts when machinery will require maintenance

In hydraulic and lubrication oil systems, friction, wear, leakage and excess temperatures can contribute to the operating fluid becoming contaminated, with solid particle contamination or water, for example. This contamination then goes on to cause errors in components and subsystems and ultimately in the system as a whole. Furthermore, the normal ageing process of the fluid causes performance losses that often result in system downtime.

In order to prevent these time-consuming and costly consequences, monitoring the condition of the operating fluid is of major significance. The condition of the operating fluid is comparable to a “fingerprint” of the overall condition of the system.

Implementing a predictive maintenance strategy allows the service life of all critical machine elements to be fully utilized, by detecting a variation from the fluid’s normal condition early on.

This is the basis for a significant reduction in operating costs resulting from costly unplanned system downtime being eliminated or minimized. As soon as the beginnings of a variation are detected, the remaining service life of the corresponding parameter or component can be estimated and used for ongoing production in a controlled manner. Meanwhile, spare parts can be procured and maintenance with minimal costs can be scheduled.

A predictive maintenance strategy thus allows available resources to be utilised optimally, reducing the total costs for the machinery throughout its service life (life cycle cost - LCC).

2.2 Achieving Condition-based, predictive maintenance strategy

The predictive concept, which is the only one that allows the service life of all critical machine parts to be fully utilized, by detecting a “rise” in levels which indicates the start of a (fluid) deviation from the normal condition. This is the basis of a substantial reduction in operating costs by cutting out or minimizing expensive and unplanned maintenance and stoppages. As soon as the beginnings of a variation are detected, it is possible to estimate how much service life remains for the corresponding parameter or component and to use this service life in a controlled manner for ongoing production. Meanwhile, spare parts can be procured and maintenance with minimal costs can be scheduled. To clarify this point further, the advantages and disadvantages of different maintenance management concepts can be differentiated as follows:

- In the reactive model, the biggest cost factors are unplanned maintenance and production stoppage.
- In the preventive model, the biggest cost factor is the high proportion of planned maintenance. Moreover, components are rejected which could continue to be used.
- In the predictive model, there are some small additional costs initially for the Fluid Condition Monitoring System, but the total operating costs and therefore the LCC are the lowest. The typical cost distributions of the three maintenance management strategies are compared in the Figure 5.

A suitable Fluid Condition Monitoring (FCM) System always forms the maintenance management. In practice, two types of FCM can be implemented, as shown in Figure 5.

	Periodic / offline	Continuous / online
Implementation	Service crew with portable equipment	Integration of sensors
Features	<ul style="list-style-type: none"> • Oil sampling, measurements using particle counters • Monitoring the measurements over longer time periods • Variations result in specific measures 	<ul style="list-style-type: none"> • Permanent sensor installation • Definition of limits/alarm thresholds • Remote data transmission to monitoring centres or control rooms via intranet/Internet/GSM/satellite • Variations result in immediate specific service measures
Examples		

Figure 5: A suitable Fluid Condition Monitoring (FCM) System

A further cost advantage of Fluid Condition Monitoring is obtained right from the design stage because of the possibility of improving the sizing of the components:

- Components no longer need to be over-sized and therefore more expensive,
- The risk of components being operated at the limit is eliminated,
- The system has a higher efficiency as a result.

The greatest benefit of permanently installed fluid condition sensors and subsystems is the facility to monitor the fluid condition:

- on a continuous basis,
- practically in real-time.

The key system characteristics to be monitored and the appropriate sensors (to complement the conventional sensors for pressure, temperature, flow rate etc.) are listed in order of priority in Table 1 and Figure 6.

Table 1: The key system characteristics to be monitored

System characteristic	Fluid condition sensor
Wear	1. Solid particle sensor
Fluid cross-contamination after addition of incorrect fluid or leakage	2. Differential pressure sensor for filters
Water ingress through condensation or leakage	3. Sensor for free or dissolved water
Fluid ageing condition on basis of hydrolysis or oxidation	4. AN (acid number) sensor 5. Differential pressure sensor for filters



Figure 6: The appropriate sensors for monitoring of system characteristics

For implementation in a predictive maintenance concept, the electrical sensor outputs must be configured according to the following guidelines:

- Essentially, the output signals must enable the system or the operator to estimate the remaining service life of a component or a process to carry out planned maintenance.
- Switch outputs alone are usually adequate for slow processes.
- Analogue or digital bus outputs should ideally be used for highly transient processes.

3 Predictive maintenance in practice

3.1 Wind energy – turbine gearbox

The task was to monitor the gearbox lubrication system online in order to prevent secondary damage and also production stoppages (electricity generation). The solution was found through installation of a Metallic Contamination Sensor (MCS) for full-flow monitoring of the lubrication circuit. As the image on Figure 7 shows, a Metallic Contamination Sensor (MCS) was used to detect a bearing failure. The curve shows the number of accumulated particles, i.e. the amount of metal detached from the driving gear. Each jump corresponds to one or more detected metal particles. The first warning was confirmed by a visual inspection because the main bearing showed slight damage but this was classed as non-critical. Consistent with this, a repair was planned and until then the wind turbine could continue to be operated at 80% capacity (the lower curve in the graph shows the power generated).

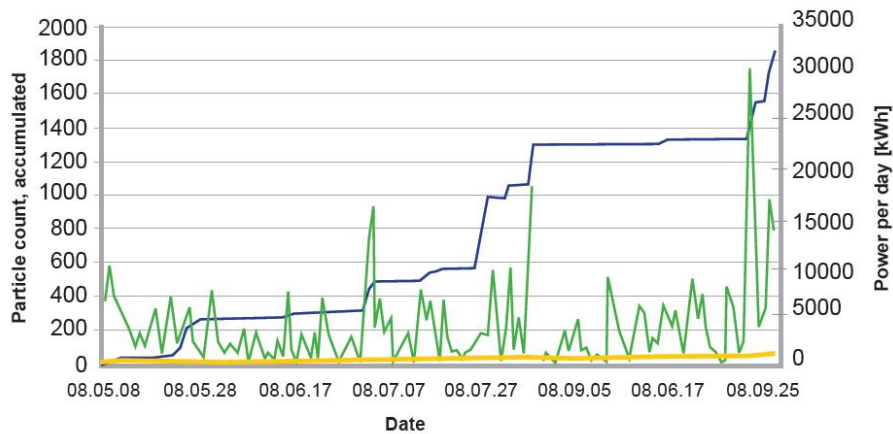


Figure 7: Preventive maintenance of wind turbine gear box and MCS

The progress of the damage was monitored until the bearing repair was performed and no unplanned maintenance or downtime was required and the costs for a new gearbox (roughly €360,000) could be avoided.

3.2 Steel industry – rolling mills

In rolling mills the operating fluid for controlling the rolls is exposed to very high rates of solid-particle and water ingress. This is inherent to the conditions of hot/cold rolling processes. The task was to reduce unplanned maintenance and downtime costs by installing fluid sensors. The solution was found with standardization of a Fluid Condition Monitoring subsystem and its integration in the hydraulic circuit. The subsystem consists of a visual particle sensor, a water sensor and a data-logging device with display. The maintenance and downtime costs could be significantly reduced, as seen of Figure 8.

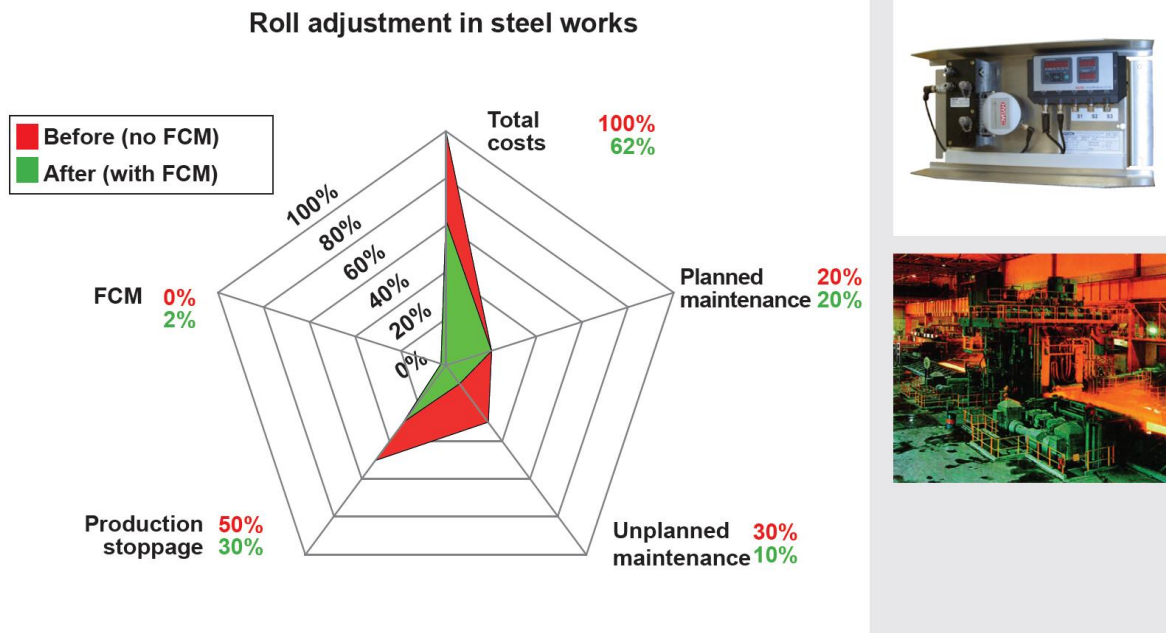


Figure 8: Benefits of using FCM on rolling mills

4 Conclusion

The examples listed clearly show that using Fluid Condition Monitoring in combination with a predictive condition-based maintenance system and appropriate measures can help to considerably reduce the maintenance and the corresponding life cycle cost of production machines.

Further additional benefits are:

- Rapid notification when fatal errors occur
- Opportunities for optimising component and system service life

Fluid Condition Monitoring is therefore an efficient system design element for reducing the life cycle cost of modern production machines, predestined for the design of predictive maintenance strategies.

References

- [1] Hydac International internal material

Global Analysis of an RC-Filter for a Switched Hydraulic Drive

EVGENY LUKACHEV & RUDOLF SCHEIDL

Abstract In switched hydraulic systems control is done by fast on-off valves which are operated at high frequencies. Such operation is likely to excite unwanted oscillatory response in the multi-modal combined hydro-mechanical system.

This paper presents a detailed analysis for a system comprising a hydraulic cylinder, which is connected to the on-off valves by a long transmission line and a hydraulic RC-filter placed right after the valves. The problem of an optimal tuning of this filter for quite different system configurations is treated in a comprehensive way to allow a full global understanding of the system and filter parameter influences on the main oscillation effects.

Keywords: • switched hydraulic drive • oscillation • analysis • RC-filter • tuning

CORRESPONDENCE ADDRESS: Evgeny Lukachev, Johannes Kepler University Linz, Institute of Machine Design and Hydraulic Drives, Altenberger Straße 69, 4040 Linz, Austria, e-mail: evgeny.lukachev@jku.at.
Rudolf Scheidl, Evgeny Lukachev, Johannes Kepler University Linz, Institute of Machine Design and Hydraulic Drives, Altenberger Straße 69, 4040 Linz, Austria, e-mail: rudolf.scheidl@jku.at.

1 Introduction

Switched hydraulic drives represent a direction in the Digital Fluid Power (see e.g. [1] for definition) in which actuators are controlled by fast switching on-off valves. The flow is defined by the ratio of opened and closed states duration. In comparison to another digital approach – parallel connection – switched systems benefit from the reduced number of valves per metering edge and generally finer resolution, but at the same time suffer from pulsations caused by continuous valve switching, intrinsic to this type of control.

The problem arises particularly strongly in the schemes with a single valve per metering edge if it has to manage in the same application fast motion and precise position tracking. The latter requires extremely short pulses that have very large excitation bandwidth. The situation can be worsened by long transmission lines, which are inevitable if the valve cannot be placed directly at the actuator. The hydraulic system in this case exhibits a complex multimodal oscillatory behavior defined by a large number of parameters describing the cylinder, the transmission line and the switching pulse shape. Resulting oscillations of the actuator output as well as pulsations of pressure and flow impair significantly the system performance in terms of position/speed/force tracking, increase noise and reduce reliability.

Despite the fact that noise filtering in hydraulics is studied for decades, the problem of pulsations arising between the control unit and the actuator was not addressed before long as they are normally not excited by servo valves. Considering nature of these pulsations and system requirements, the attenuator device must provide good damping in a broad band and at the same time pass the signal in the demanded drive frequency range. Thus, most of the existing techniques are not applicable for switched hydraulics due to different disadvantages and limitations described, e.g., in [2], [3].

The growing popularity of digital fluid power increased the researchers' interest in the solutions for attenuation of pulsations caused by valve switching. The proposed methods can be divided into two groups: intelligent switching and implementation of filters. Methods of the first group are presented in [4] and [5]. An example of a filtering device – hydraulic RC-filter – designed for switched control applications is proposed by the authors in [6] for the case of a hydraulic cylinder and a transmission line (Figure 2). A comprehensive analysis of this filter with derived basic design rules is given in [7], which also presents measurement results verifying the analytical model and proving the filter effectiveness.

However, different parameter cases studied in [7] showed qualitatively different performance of the filter-switched control drive system, especially in terms of cylinder natural frequency damping. The relatively large parameter space of the problem was the main obstacle for building a general theory of such filter for any reasonable combination of the system and filter parameters.

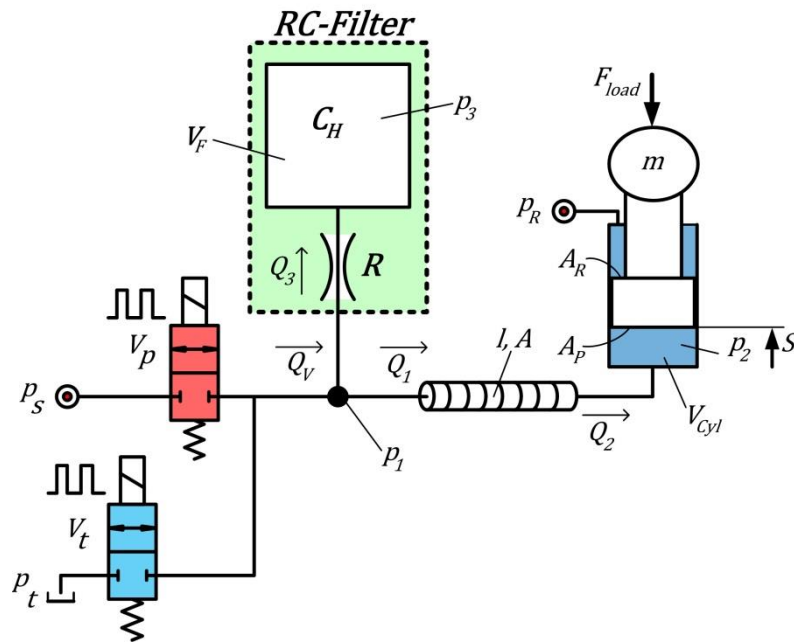


Figure 2: Schematic of a hydraulic switched control drive with a transmission line between valves and actuator and an RC-Filter for oscillation dampening

The main goal of this paper is an attempt to further decrease the number of variables by the proper nondimensionalization and by means of multi parameter optimization. The resulting model must provide a global view of filter capabilities and limitations for a certain class of hydraulic drives and also a simple guidance for the filter parameter choice in a given hydraulic system.

2 System model

2.1 Linear mathematical description

The system model is based on the drive schematic from Figure 2. In order to apply linear analysis methods the following assumptions and simplifications are introduced:

- The switching valves are considered as the system boundary and their effect is replaced by an input flow Q_v .
- Filter elements are described by linear equations with constant R and C parameters.
- Fluid friction in the pipeline is neglected.
- The cylinder capacity variation due to change of cylinder position is negligible within a few switching pulses.
- Cylinder friction is neglected.
- Rod side pressure is considered constant in the relevant frequency range, thus its influence on system dynamics can be omitted.

The system of equations is formulated in frequency domain employing the Fourier Transform and reads:

$$\begin{aligned}
-\omega^2 m \hat{S} &= \hat{p}_2 A_P - \hat{F} \\
\hat{Q}_1 &= \hat{Q}_V - \hat{Q}_3; \quad \hat{Q}_3 = \frac{\hat{p}_1 - \hat{p}_3}{R}; \quad j\omega \hat{p}_3 = \frac{\hat{Q}_3}{C_H} \\
j\omega \hat{p}_2 &= \frac{\hat{Q}_2 - j\omega \hat{S} A_P}{C_{Cyl}} \\
\hat{Q}_1 &= j \frac{\hat{p}_2 - \hat{p}_1 \cdot \cos\left(\frac{\omega L}{c}\right)}{Z_H \cdot \sin\left(\frac{\omega L}{c}\right)} \\
\hat{Q}_2 &= j \frac{\hat{p}_2 \cdot \cos\left(\frac{\omega L}{c}\right) - \hat{p}_1}{Z_H \cdot \sin\left(\frac{\omega L}{c}\right)} \\
\hat{u}(\omega) &= \int_{-\infty}^{\infty} u(t) e^{-j\omega t} dt \\
Z_H &= \frac{\sqrt{E\rho}}{A}; \quad c = \sqrt{\frac{E}{\rho}}; \quad j^2 = -1; \quad C_{Cyl} = \frac{A_P S_0}{E}; \quad C_H = \frac{V_F}{E}
\end{aligned} \tag{1}$$

Transmission line equations employ the model of D'Souza and Oldenburger [8] for the case of zero viscosity. L and A are the pipeline dimensions and Z_H is its hydraulic impedance. c is the wave propagation speed in the fluid, ρ and E – its density and bulk modulus. S_0 is the initial cylinder position, A_P – area of the piston, m – the moving mass. The meaning of other letters is clear from Figure 2.

Equation (1) can be solved for the system state vector $\hat{\mathbf{x}} = [\hat{S}, \hat{p}_1, \hat{p}_2, \hat{p}_3, \hat{Q}_1, \hat{Q}_2, \hat{Q}_3]$ as a function of a linear combination of components of the input vector $\hat{\mathbf{u}} = [\hat{Q}_V, \hat{F}]$. At this point the part of the solution dependent on \hat{F} is omitted from further investigation. This decision is motivated by the following reasons:

- The main interest of the research is the hydraulic drive subsystem and its eigen dynamics.
- Operation without load is often the most critical mode for hydraulic drives in terms of oscillation problem as the load normally increases overall system damping.
- Investigation of the whole variety of different load types currently lies outside the scope of the research.

Of all state variables the cylinder position \hat{S} represents the highest interest. From the solution of (1) the transfer function for \hat{S} over the input valve flow \hat{Q}_V is obtained:

$$\frac{\hat{S}}{\hat{Q}_V} = - \frac{j A_P Z_H (-j + \omega C_H R)}{\omega \left(\begin{aligned} &\left(\begin{aligned} &jm\omega - m\omega^2 C_H R - \\ &jm\omega^3 Z_H^2 C_H C_{Cyl} + j\omega Z_H^2 A_P^2 \end{aligned} \right) \sin(\Omega) + \\ &\left(\begin{aligned} &jm\omega^2 (C_H + C_{Cyl}) Z_H - m\omega^3 Z_H C_H C_{Cyl} R \\ &-j Z_H A_P^2 + \omega Z_H C_H R A_P^2 \end{aligned} \right) \cos(\Omega) \end{aligned} \right)} \tag{2}$$

2.2 Nondimensionalization

Expression (2) can be used for building the frequency response characteristic for a given parameter set, which gives comprehensive information about filter efficiency in damping of different oscillation modes. Examples are depicted in Figure 3 for two different drive types and different values of R .

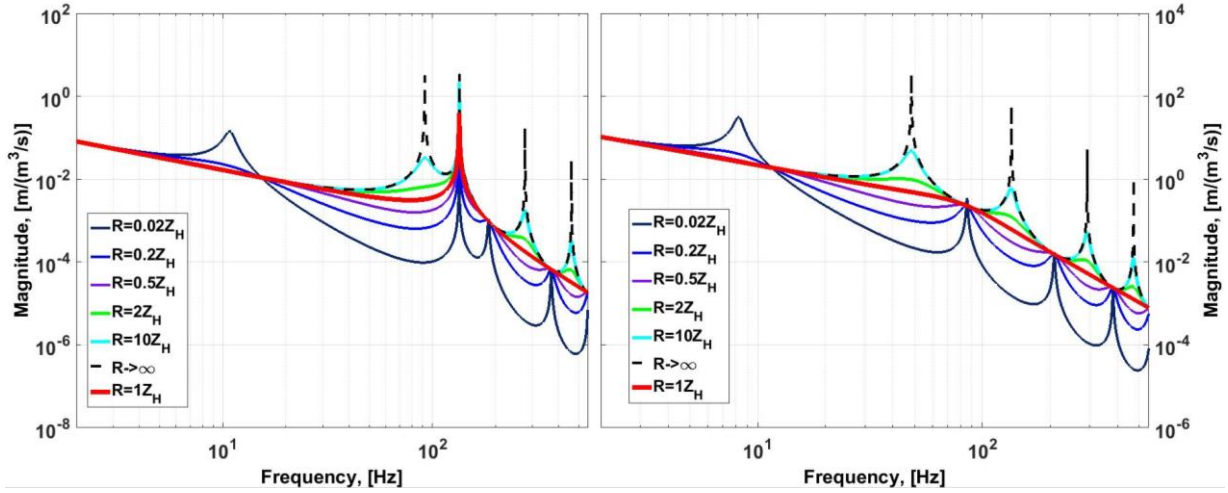


Figure 3: Examples of amplitude frequency characteristics according to (2)

However, the number of variables and the complexity of the transfer function make it of little use for sound understanding of parameter influence and interaction in the whole space of drive dimensions. In order to reduce the number of variables, the set of non-dimensional parameters (3) was proposed in [7], resulting in the transfer function (4).

$$\Omega = \frac{\omega L}{c}; \quad a = \frac{A}{A_p}; \quad \lambda = \frac{S_0}{L}; \quad \mu = \frac{\rho AL}{m}; \quad \gamma = \frac{C_H}{C_{Cyl}}; \quad \tau_{CR} = C_H R \frac{c}{L} \quad (3)$$

$$\frac{\hat{S}cA_p}{\hat{Q}_v L} = \frac{1 + j\Omega\tau_{CR}}{\Omega \left(-\Omega\tau_{CR} \left(\cos(\Omega) \left(1 - \frac{a\Omega^2\lambda}{\mu} \right) - \sin(\Omega) \frac{\Omega a^2}{\mu} \right) - j \left(\cos(\Omega) \left(\frac{a\Omega^2\lambda(1+\gamma)}{\mu} - 1 \right) + \sin(\Omega) \left(\frac{a^2\Omega - \Omega^3\lambda^2\gamma}{\mu} + \frac{\Omega\lambda\gamma}{a} \right) \right) \right)} \quad (4)$$

This expression still contains 3 drive (a, λ, μ) and 2 filter (τ_{CR}, γ) parameters and does not provide a direct insight. A further analysis of (4) lead to a drive component description by only 2 non-dimensional parameters by the following relations:

$$\tilde{a} = \frac{a}{\sqrt{\mu}}; \quad \tilde{\lambda} = \frac{\lambda}{\sqrt{\mu}} \quad \text{or} \quad \tilde{a} = \frac{A\sqrt{m}}{A_p\sqrt{\rho AL}}; \quad \tilde{\lambda} = \frac{S_0\sqrt{m}}{L\sqrt{\rho AL}} \quad (5)$$

This means that in the scope of the derived model any combination of the cylinder and the transmission line can be uniquely defined in a 2 dimensional variable space $(\tilde{a}, \tilde{\lambda})$ which is a significant reduction of the initial parameter number. Two additional variables are needed to describe the filter.

Relations (5), although not obvious from first sight, have a certain physical meaning. If the cylinder and the transmission line model is transformed into a simple lumped parameter mechanical equivalent (see Figure 4), the value of \tilde{a}^2 would mean the ratio of the cylinder mass and the effective fluid mass, the latter is calculated on the basis of kinetic energies equality:

$$\tilde{a}^2 = \frac{m_Z}{m_{F_{EFF}}} \quad (6)$$

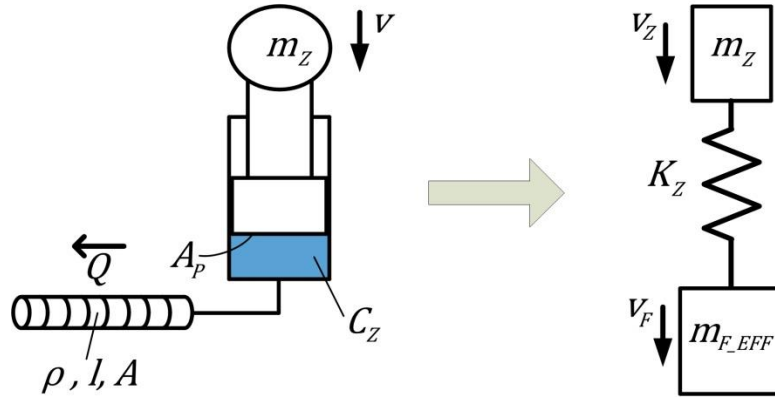


Figure 4: Mechanical equivalent model

$\tilde{\lambda}$ -value represents the ratio of fluid volumes in the cylinder V_Z chamber and in the pipeline V_R multiplied by \tilde{a} :

$$\tilde{\lambda} = \tilde{a} \frac{V_Z}{V_R} \quad (7)$$

3 Global analysis by multicriteria optimization

3.1 Multicriteria optimization and methods

Multicriteria optimization problem (also called multi objective or Pareto optimization) is the problem of finding a set of optimal solutions for multiple optimization criteria. In mathematical terms it can be formulated as:

$$\begin{aligned} \min(f_1(\bar{x}), f_2(\bar{x}), \dots, f_n(\bar{x})); \quad \bar{x} \in X \\ \bar{x} = (x_1, x_2, \dots, x_k) \end{aligned} \quad (8)$$

where $f_1(\bar{x}), f_2(\bar{x}), \dots, f_n(\bar{x})$ are the objective functions ($n > 1$), x_1, x_2, \dots, x_k – the parameters for optimization, X – the set of possible solutions. Criteria in real engineering problems are often conflicting, so it is normally not possible to find the \bar{x} minimizing all objectives. In this case Pareto optimal solutions are of interest. The solution is called Pareto optimal if it cannot be improved in any of the objectives without degrading at least one of the other objectives. The results of the optimization present a Pareto front – a set of Pareto optimal solutions (Figure 5). When a Pareto front is obtained, still a decision on the final choice has to be made. If there is a solution that minimizes all objective functions, the Pareto front collapses into a single point, corresponding to this solution.

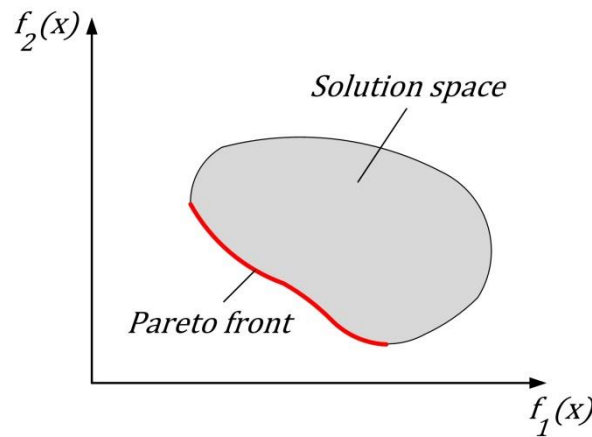


Figure 5: Example of a Pareto front for 2 objectives.

There are plenty of algorithms developed for solving the multi-criteria optimization task. An overview is given for instance in [9]. In brief, all methods are divided into gradient based and non-gradient based. The latter are preferable if the derivative of the objectives cannot be explicitly calculated and the objective functions are not smooth or have local minima.

3.2 Parameters, constraints and criteria for optimization

In terms of control theory the cylinder with the transmission line represents the so called plant. Its parameters ($\tilde{\alpha}$ and $\tilde{\lambda}$) are normally fixed in the process of the control scheme design. The filter (described by τ_{CR} and γ) is a compensator; its task is to change the drive response in a favorable way. Compensator parameters can be chosen from a wide range of values, limited only by practical aspects. The choice of these parameters is a common engineering problem and is often solved by optimization.

Employing this approach to the filter-drive system the filter parameters are found as optimization results calculated for a mesh of points on the $\tilde{\alpha}$ - $\tilde{\lambda}$ plane, which represents the variety of hydraulic drives. Thus, τ_{CR} and γ form the parameter vector for the optimization problem.

There are some considerations for the range of possible parameter values based on practical issues and due to some results of previous research. They are added as optimization constraints to narrow the problem.

It was shown in [7] that the ratio R/Z_H equal to 1 is a reasonable upper boundary value of R . Filter resistances higher than the pipeline hydraulic impedance are not particularly useful. For the lower boundary no certain value exists, yet it makes sense to omit near zero values representing no local resistance. The second filter parameter, γ , is defined for a given drive by the filter capacity C_H . It is important to define its upper limit. First, higher values require more space. This can be solved by implementation of gas spring hydraulic accumulator, but the latter has nonlinear characteristic and negative effect on the reliability. Second, higher volumes make the drive softer. It cannot be observed from the transfer functions (2) or (4), because the load term is omitted. Therefore, it should be taken into consideration by constraint definition. An initial guess for the feasible upper limit is 20 volumes of the pipeline fluid. The lower limit is taken as 1/10 of the pipeline fluid thus practically representing the system without filter. Transforming this limits into system parameters results in the following expression for γ :

$$0.1 \cdot \tilde{\alpha}/\tilde{\lambda} \leq \gamma \leq 20 \cdot \tilde{\alpha}/\tilde{\lambda} \quad (9)$$

If the \tilde{a}^2 term is large enough, the cylinder inertia would add some significant contribution to the fluid inductance. To consider this effect, multiplier $(\tilde{a}^2 + 1)$ is introduced into (10):

$$0.1 \cdot \tilde{a}/\tilde{\lambda} (\tilde{a}^2 + 1) \leq \gamma \leq 20 \cdot \tilde{a}/\tilde{\lambda} (\tilde{a}^2 + 1) \quad (10)$$

Criteria for optimization are based on the system frequency response – the main indicator of the filter efficiency in damping of different oscillation modes. Frequency range is divided into two domains by the value corresponding to 80% of the cylinder resonance. The first criterion is the deviation of the system from the ideal response as given by an incompressible, inviscid, zero density fluid in the first frequency domain. The deviation is estimated as the mean ratio of the actual and ideal responses or its opposite if the actual response is lower. This criterion is dominated by transmission line modes. The second criterion evaluates how much the actual amplitude exceeds the linear approximation of the critically damped cylinder frequency response in the second domain, consisting of cylinder resonance frequency range and beyond. The second criterion is also based on the ratio of amplitudes.

Frequency response for evaluation is constructed numerically in a user defined Matlab function. Ω is defined as a linearly spaced vector. The correspondent value of amplitude is calculated according to (4). Mathematical expressions for objective functions read:

$$I_1 = \left[\sum_i \max \left(\left(\frac{A_{act}}{A_{id}} \right)_i, \left(\frac{A_{id}}{A_{act}} \right)_i \right) / \Omega_i - \sum_i \frac{1}{\Omega_i} \right] \cdot \frac{\Omega_Z}{\max(i)}; \quad \Omega \leq 0.8\Omega_Z$$

$$I_2 = \max \left(\left(\frac{A_{act}}{A_{id}} \right)_i, 1 \right) - 1; \quad \Omega > 0.8\Omega_Z$$
(11)

where A_{act} is the frequency response calculated according to (4), A_{id} – ideal response, Ω_Z – the cylinder resonance frequency, i – index of the frequency vector used in the calculation. The term $1/\Omega_i$ in the I_1 definition is needed to increase the error weight on lower frequencies. Terms after the minus sign in both expressions are introduced in order to make the ideal response objectives equal zero: $I_1^{id}, I_2^{id} = 0$.

A graphical representation of both criteria for the arbitrary frequency response (red line) is depicted in Figure 6. The black line corresponds to the ideal response.

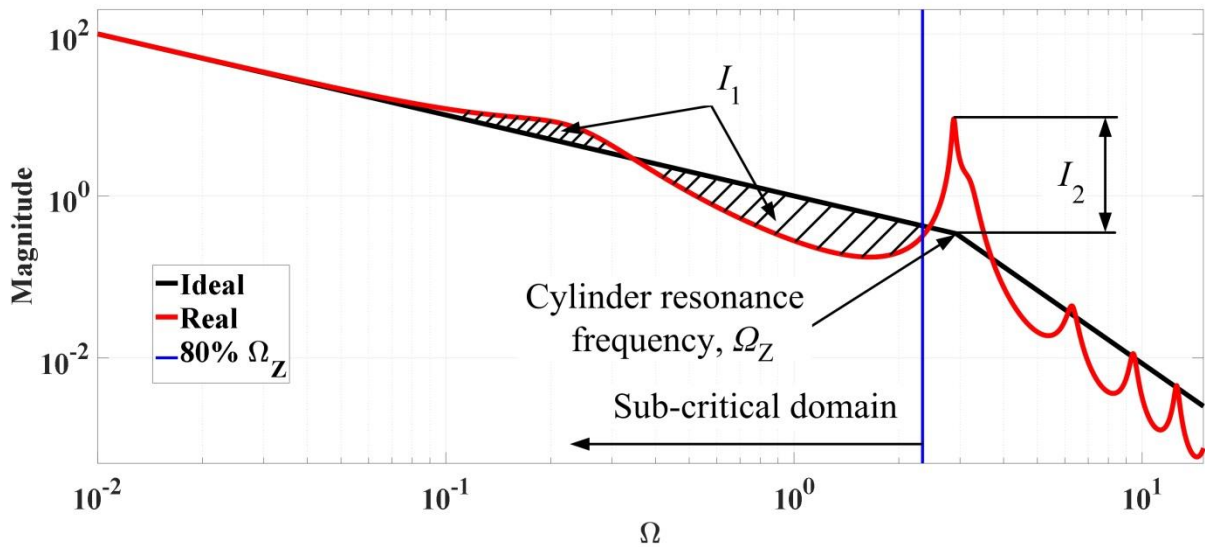


Figure 6: Visualization of criteria

From the previous experience, two objectives describing the system performance are conflicting at least for some of the drive dimensions. This suggests that the result of the optimization in an arbitrary point $(\tilde{a}_i, \tilde{\lambda}_i)$ is expected to be a Pareto front, although a collapse of this front into a single point for some of the areas on \tilde{a} - $\tilde{\lambda}$ plane is not excluded.

Considering that no derivatives with regard to optimization parameters are available, non-gradient optimization method, namely, genetic algorithm is employed. For the search of optimal solution (Pareto front) the multi objective Genetic Algorithm for Optimization developed by Popov [10] was implemented.

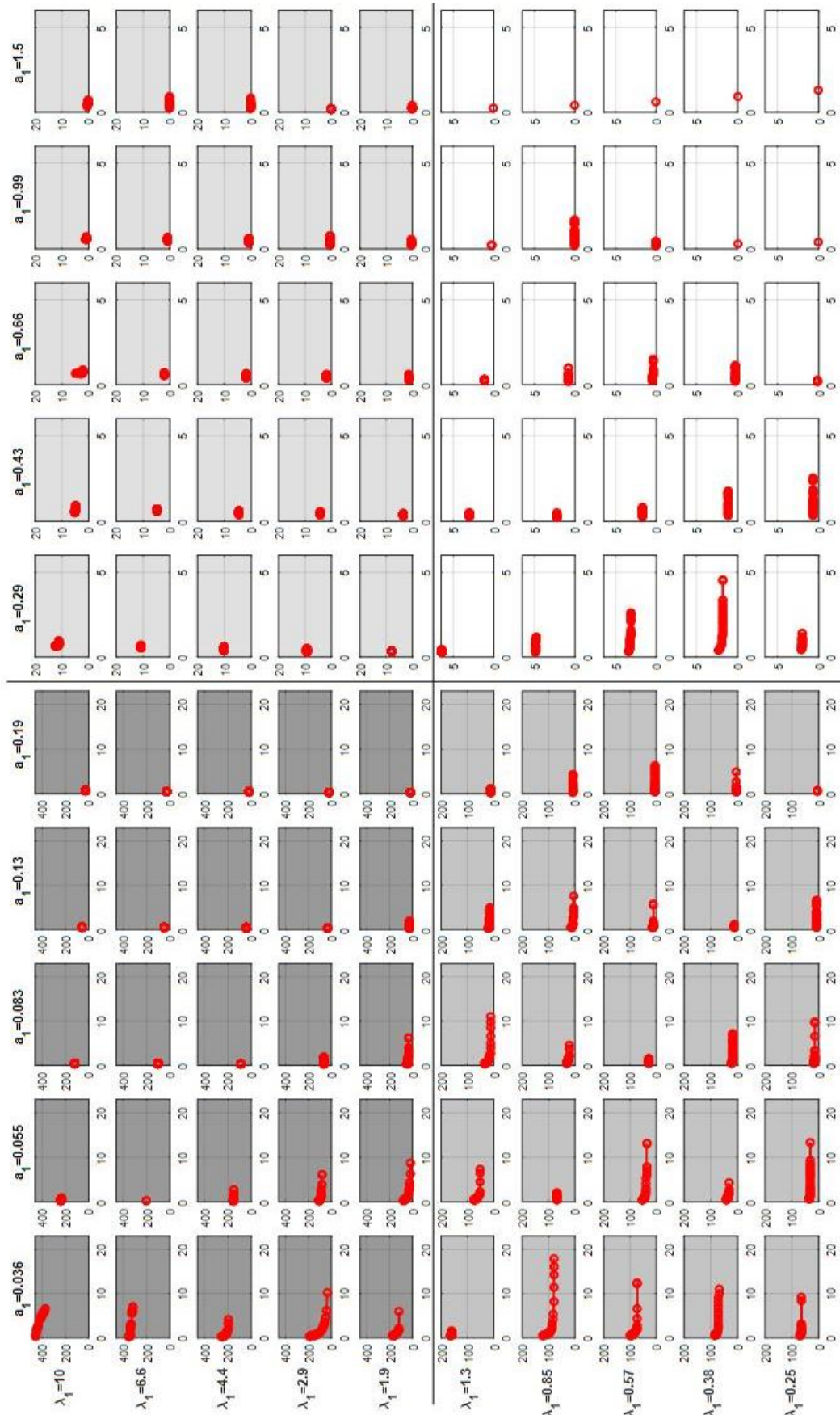


Figure 7: Atlas of Pareto fronts on the \tilde{a} - $\tilde{\lambda}$ plane (hint: $\tilde{a}=a_1$, $\tilde{\lambda}=\lambda_1$ in the diagrams)

4 Results and interpretation

4.1 Pareto front atlas

This research was conducted in the framework of an investigation of the possibility to replace servo valves in the control of hydraulic drives with digital valves for a variety of drives in industrial plants. Therefore, the choice of values for $\tilde{\alpha}$ and $\tilde{\lambda}$ for the Pareto front atlas was based on the variety of the hydraulic drives typically used in such plants.

The results for the 10x10 logarithmically spaced mesh of plant parameters are presented in Figure 7. The $\tilde{\alpha}$ - $\tilde{\lambda}$ plane is divided into 4 quadrants with different scales of axes and I_2 . The right and the left halves have also different scale of I_1 objective. This scaling allows for easier visualization of trends.

It is possible to achieve good values of I_1 for the whole atlas, which was expected since this criterion is dominated by transmission line and the RC-filter is effective in damping of the corresponding oscillation modes. More interesting is the possibility to dampen oscillations of cylinder natural frequency, indicated by I_2 . This possibility depends strongly on the parameters of the plant. I_2 is in direct relationship with the $\tilde{\alpha}$ parameter and is inverse to $\tilde{\lambda}$.

By the high values of $\tilde{\alpha}$ the cylinder caused pulsations can be effectively dampened by the filter. Explanation lies in the physical meaning of $\tilde{\alpha}^2$ – the ratio of the cylinder mass to the effective mass of the fluid (6). Small values of $\tilde{\alpha}$ mean that the cylinder oscillations do not excite significant flow of the fluid in the pipeline. This flow is crucial for the filter operation.

Influence of $\tilde{\lambda}$ is related to its proportional dependency on the initial cylinder position. Higher values of $\tilde{\lambda}$ mean softer piston chamber fluid (due to larger values of cylinder position S_0). This is equal to a softer spring in the mechanical model of Figure 4, which also worsens transmission of the cylinder oscillations to the filter attachment point.

The next step consists of analyzing the shape of Pareto fronts at different atlas domains. First, there are regions where the Pareto front collapses into a point (Figure 8a), which generally means that the objectives are not conflicting. This happens at high $\tilde{\alpha}$ values. Second, regions exist where the second criterion cannot be reasonably improved. The Pareto front in this case is the line, horizontal to the I_1 -axis (Figure 8b). Finally, in some regions optimization results present a classical type of Pareto front for two conflicting objectives (Figure 8c). In the systems with correspondent parameter values it is possible to improve one of the criteria at the expense of the other.

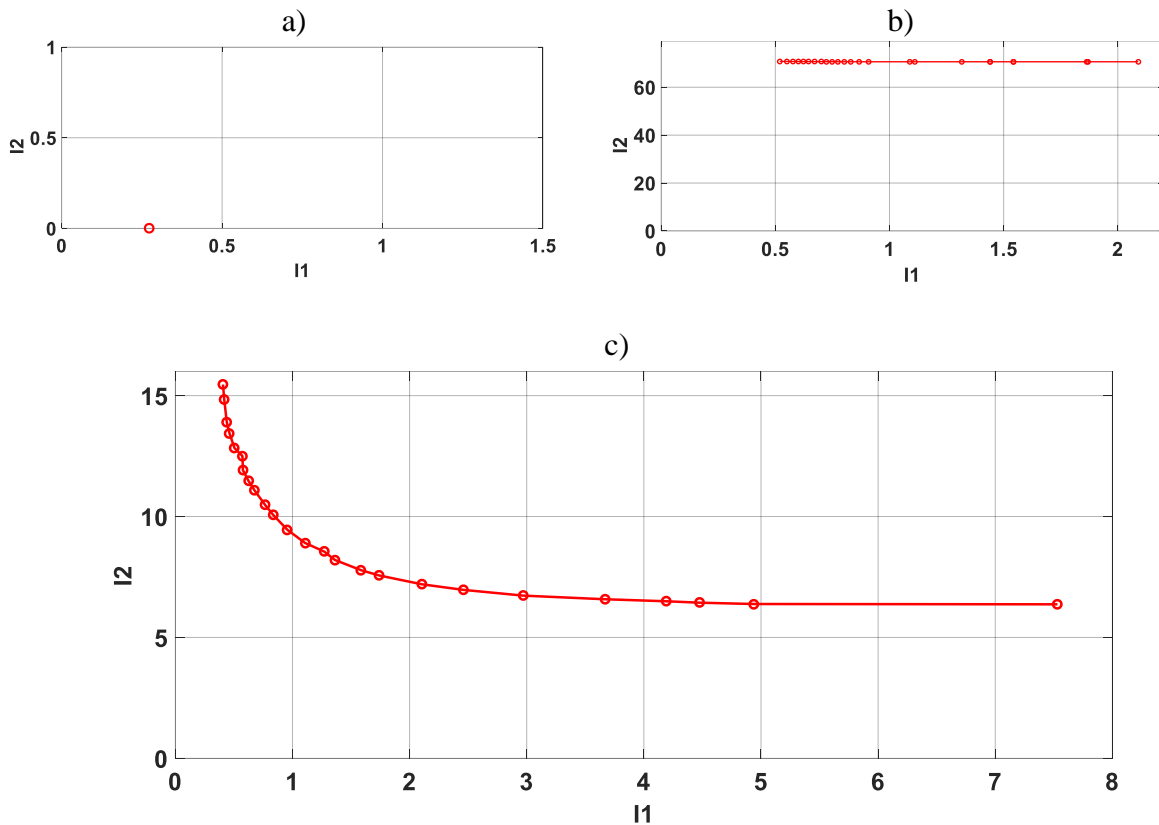


Figure 8: Pareto front shapes

4.2 Matlab GUI tool for result evaluation

For easier and faster evaluation of the optimization results a simple tool with graphic user interface was created in the Matlab GUI module. At the script launch, the atlas of Pareto fronts is plotted in the figure window on the basis of the optimization results. Right mouse click on chosen axes creates the magnified plot of the Pareto front for the correspondent parameters (Figure 9). Left mouse click above axes – creates the plot of amplitude characteristics for end points of the Pareto front (minimal I_1 and I_2). The plot contains also ideal characteristic (used for evaluation of the objectives) and the characteristic with resistance equal to the pipeline impedance (capacity is the same as in the minimal I_1 case). An example is depicted in Figure 10. If the mouse click is done directly above the Pareto front, the amplitude characteristic for the solution, closest to the pointer is also depicted (Figure 11).

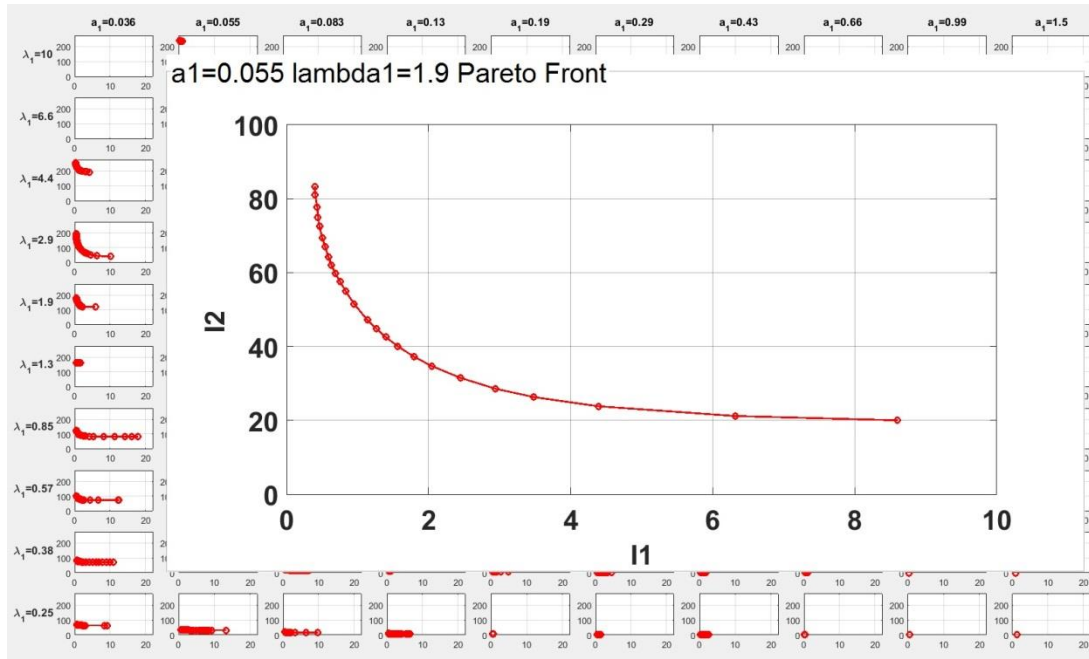


Figure 9: Pareto front, magnified with the right click

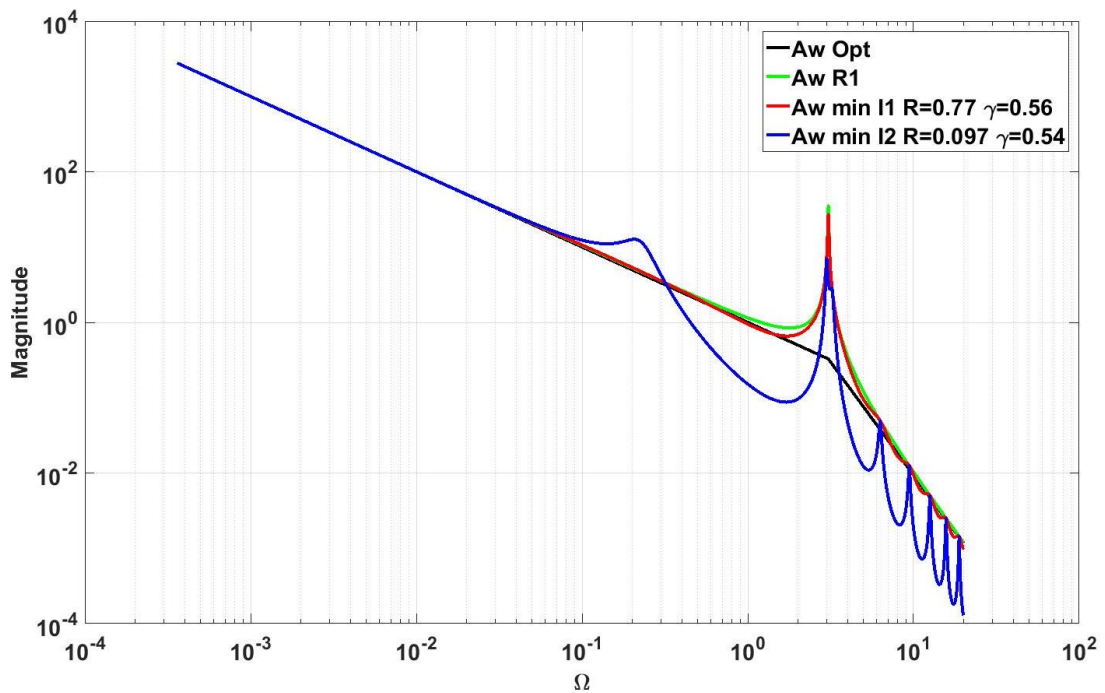


Figure 10: Plot of the correspondent amplitude characteristics

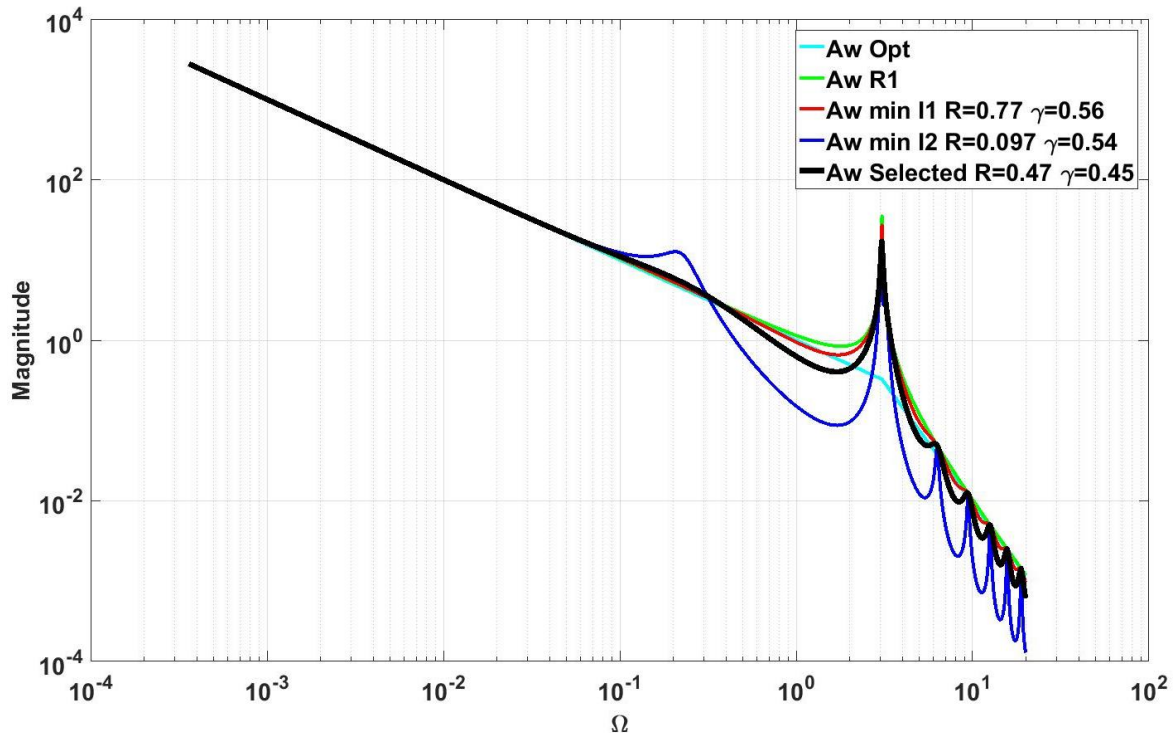


Figure 11: Plot of the amplitude characteristics including selected solution point

5 Conclusion

In this paper the global analysis of the hydraulic RC-filter for switched control drives is presented. A modified nondimensionalization of an existing analytical model resulted in a reduced plant parameter space with only to 2 variables. The space of the filter parameters was reduced by multi objective optimization. These lead to an atlas of Pareto fronts for different points on the plant parameter plane. The atlas gives a comprehensive overview about the filter performance for the whole variety of feasible drive dimensions. The new approach to the filter investigation has significantly improved understanding of the RC-filter's ability to dampen transmission line and cylinder oscillations and how this depends on the plant parameters.

In addition, a simple tool based on the Matlab GUI module was created providing easier evaluation of the optimization results. The tool can be utilized in the filter design for the forthcoming digital hydraulic applications, which require pulsation damping.

A next step of the research is an investigation of the filter influence on the system response to the external load by considering the cylinder force dependent part of the transfer function.

Acknowledgment

This work has been carried out at LCM GmbH as part of a K2 project. K2 projects are financed using funding from the Austrian COMET-K2 programme. The COMET K2 projects at LCM are supported by the Austrian federal government, the federal state of Upper Austria, the Johannes Kepler University and all of the scientific partners which form part of the K2-COMET Consortium.

References

- [1] M. Linjama: Digital Fluid Power - State of the Art; The Twelfth Scandinavian International Conference on Fluid Power, SICFP'11, proceedings; Tampere, Finland, 2011
- [2] J. Mikota: Contributions to the development of compact and tuneable vibration compensators for hydraulic systems. PhD Thesis, Johannes Kepler University, Linz, 2002
- [3] M. Ijas: Damping of Low Frequency Pressure Oscillation. PhD Thesis, Tampere University of Technology, Tampere, 2007.
- [4] C. Gradl and R. Scheidl: A basic study on the response dynamics of pulse-frequency controlled digital hydraulic drives; Bath/ASME Symposium on Fluid Power & Motion Control, FPMC 2013, proceedings; Sarasota, Florida, USA, 2013
- [5] R. Haas and E. Lukachev: Optimal feedforward control of a digital hydraulic drive; Workshop on Digital Fluid Power DFP 2015, proceedings; Linz, Austria, 2015
- [6] E. Lukachev, R. Haas and R. Scheidl: A Hydraulic Switching Control Concept Exploiting a Hydraulic Low Pass Filter; The 14th Mechatronics Forum International Conference, Mechatronics 2014, proceedings; Karlstad, Sweden, 2014
- [7] R. Haas, E. Lukachev and R. Scheidl: An RC Filter for Hydraulic Switching Control with a Transmission Line Between Valves and Actuator. International Journal of Fluid Power 15(3); July 2014; pages 139-151
- [8] A. F. D'Souza and R. Oldenburger: Dynamic response of fluid lines. ASME, Journal of Basic Engineering, 86, pp. 589-598, 1964.
- [9] M. Pettersson: Design Optimization in Industrial Robotics. Methods and Algorithms for Drive Train Design. PhD Thesis, Linköping University, Institute of Technology, 2008
- [10] A. Popov: Genetic Algorithms for Optimization; User manual, Hamburg, 2005.

Precise force control for hydraulic and pneumatic press system

JURAJ BENIĆ, NIKOLA RAJČIĆ & ŽELJKO ŠITUM

Abstract This paper presents the force control methods for a pneumatic and a hydraulic press. Both systems have been made for educational purposes as well as for experimental testing and verification of different control techniques.

The pneumatic press contains a proportional pressure valve which is used for pressure regulation in a cylinder chamber and has direct impact on controlled force. The hydraulic press contains a servo-solenoid pressure-control valve for regulating the cylinder pressure. The pressing force can also be indirectly measured by a pressure transducer which is installed in the cylinder chamber.

Experimental tests have shown that electrically actuated control components supported by the appropriate measuring devices and computer programs make it possible to improve the characteristics of the hydraulic and pneumatic systems required in modern industrial plants.

Keywords: • press • hydraulic and pneumatic • force control • pressure sensor • force sensor • simulation •

CORRESPONDENCE ADDRESS: Juraj Benić, University of Zagreb, Faculty of Mechanical Engineering and Naval Architecture, I. Lučića 5, Zagreb, Croatia, e-mail: juraj.benic@fsb.hr. Nikola Rajčić, University of Zagreb, Faculty of Mechanical Engineering and Naval Architecture, I. Lučića 5, Zagreb, Croatia, e-mail: stuslu@fsb.hr. Željko Šitum, Ph.D., Assistant Professor, University of Zagreb, Faculty of Mechanical Engineering and Naval Architecture, Department of Robotics and Production System Automation, I. Lučića 5, Zagreb, Croatia, e-mail: zeljko.situm@fsb.hr.

1 Introduction

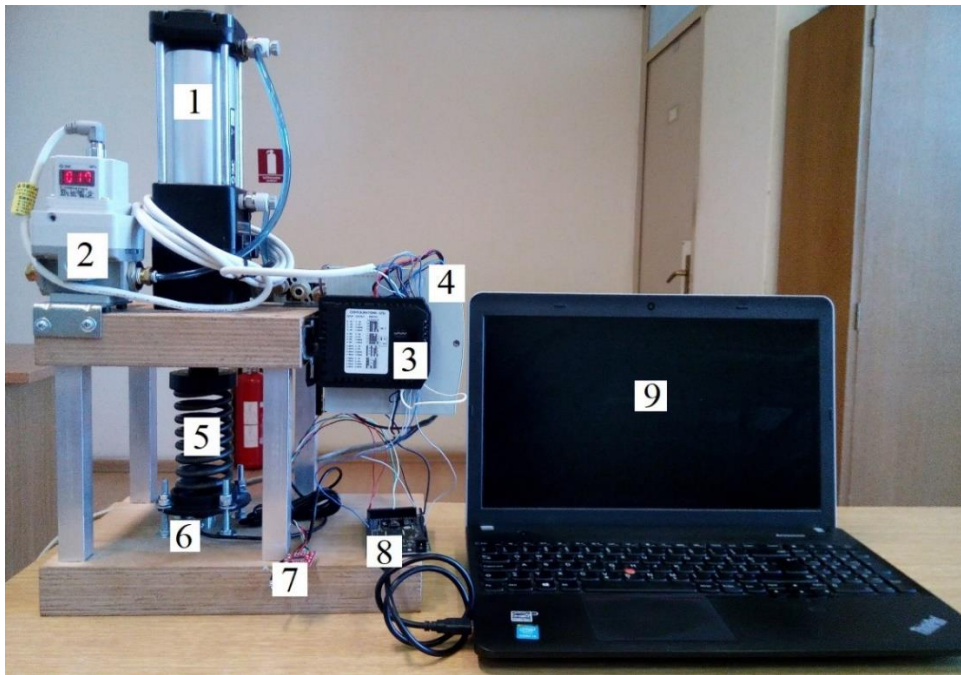
Presses are one of the most used machine tools in industry for different materials forming. In the past, for pressing tasks in industry, mechanical presses were more frequently used, but nowadays, especially for large pressing force, hydraulic presses take precedence due to their numerous advantages, such as full force through the stroke, the moving parts operate with good lubrication, the force can be programmed, the stroke can be fully adjustable which contributes to the flexibility of application. Also, hydraulic presses can be made for huge force capacities. On the other hand, hydraulic presses are generally slower than mechanical presses, which is overcome with the development of new valves with higher flow capacities, smaller response time and improved control capabilities. Pneumatic presses can be used for less force capabilities, but they can move several times faster than hydraulic presses. Pneumatic presses are extremely adaptable to different process requirements and they are very low-maintenance. Most hydraulic and pneumatic presses used in industry are working in an open-loop and are usually operated manually or using a control device such as programmable logic controller (PLC), where the end positions of the ram are set via dead stops or limit switches. Today's industry is looking for flexible solutions that will be able to achieve some new characteristics of hydraulic and pneumatic systems, such as the ability of controlled motion, the possibility of continuous control of the required values, a simple data transfer and signal processing, the possibility of monitoring and process visualization etc. The increase of micro-electronics in recent years has reduced the cost of computer equipment to a level acceptable for industrial applications which has enabled the implementation of sophisticated control strategies in practice. Therefore, modern hydraulic and pneumatic systems suffered a great evolution towards electronics and microprocessor controlled electro-hydraulic components in order to achieve new control possibilities [1]. Commonly, due to its complexity, almost every advanced controller must be implemented on a digital computer. Such control systems, that have electrically-actuated valves, can respond to complex demands posed by today's technology. The ability of force control or positioning control systems to follow-up varying reference signals is often required for proper operation of the technological process [2], [3]. Therefore, a new quality and significant improvement in the functioning of presses are obtained by applying the force feedback, where the force output is measured by a load cell and the cylinder movement is controlled via proportional or servo valve [4], [5], [6].

This paper presents basic construction of a pneumatic and a hydraulic press and the implementation of force control algorithms. Control algorithms and data monitoring are implemented on a real-time hardware board. The control algorithms are tested via numerical simulations, as well as experimentally to verify their practical use and effectiveness.

2 Experimental setup

A photo of the pneumatic press on which experiment is carried out is shown in Figure 12. A pneumatic double acting cylinder (1) with 100 mm stroke and 50 mm bore is used as actuator to convert compressed air into mechanical power. An electro-pneumatic regulator (2), SMC ITV3050, is used for controlling the pressing force. It has current type input signal in the range 4÷20 mA for the pressure output range of 0÷9 bar and gives an analogue (monitor) output signal in the range of 1÷5 V proportional to the pressure output. The force acting on the spring (5) is directly measured by a disc load cell (6), type TAS606. Rated load of the load cell is 200 kg, while the maximum output is 7.5 mV when the sensor is connected to 5 V power supply from Arduino board (8). The load cell analogue to digital converter with amplifier (7), type HX711, is used to amplify the load cell output signal. The Arduino Mega 2560 board (8) is used for data acquisition which offers 16 analogue inputs with 10-bit resolution, 54 digital input/output pins (of which 15

provides PWM output) and USB connection to the control computer (9). A signal converter (3) is used to convert Arduino 0÷5 V voltage output to 4÷20 mA current input signal for the proportional pressure-control valve. Both the signal converter and the proportional pressure-control valve are powered by 24 V power supply (4). The control algorithm is implemented in Matlab/Simulink software, which allows executing the simulation program in external mode, similar to the Real-Time Workshop tool.



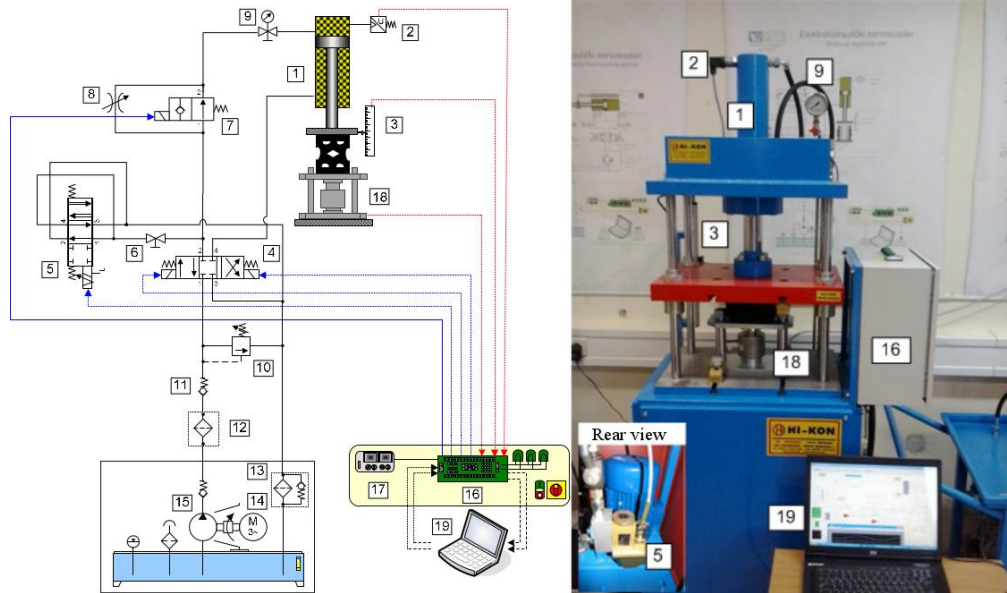
1-Pneumatic cylinder, 2-Proportional pressure-control valve, 3-Signal converter, 4-Power supply, 5-Spring, 6-Load cell, 7-A/D converter, 8-Arduino board, 9-Control computer

Figure 12: Pneumatic press

A schematic diagram and a photo of the hydraulic press on which experiments have been carried out are shown in Figure 13. The hydraulic cylinder (1) which is used to actuate the press is a double acting 300 mm stroke cylinder with 80 mm bore and 60 mm diameter rod. The control of the pressing force is accomplished using an electro-hydraulic servo valve (5) with a box chopper amplifier and ± 10 V analogue input signal. Maximum pressure in the system is limited by a pressure relief valve (10). The force acting on the rubber bumper is directly measured by the force sensor (18), which is a compression load cell. The pressure inside the cylinder chamber is measured by a pressure transducer (2), with a measuring range 0 to 250 bar and an output signal 0 to 10 V. In this system it is also possible to measure displacement of the press by using a micro-pulse linear transducer (3). Since the servo valve is installed in the system, particular attention should be given to ensure the cleanliness of oil, so a high pressure filter (12) and a return flow filter (13) are set in the hydraulic circuit. The hydraulic power is provided by a hydraulic gear pump (15), with a volumetric displacement of the pump of $2.6 \text{ cm}^3/\text{rev}$ and the maximum nominal pressure of 25 MPa. Data acquisition in the system is handled by a National Instruments DAQCard-6024E (for PCMCIA), which offers both 12-bit analogue input and analogue output. Control algorithms were developed in the Matlab/Simulink environment supported by Real-Time Workshop (RTW) program. Detailed description of the system can be found in [5].

The considered experimental electro-hydraulic and electro-pneumatic systems have been made in the Laboratory for automation and robotics at the Faculty of Mechanical Engineering and Naval

Architecture. The modules are used for research purposes in the field of hydraulic and pneumatic systems control, as well as for training students.



1-Hydraulic cylinder, 2-Pressure transducer, 3-Micro-pulse linear transducer, 4-Solenoid 4/3 valve, 5-Servo valve, 6-Shut-off valve, 7-Solenoid 2/2 valve, 8-Throttling valve, 9-Manometer, 10-System pressure relief valve, 11-Ball check valve, 12-Pressure filter, 13-Return flow filter, 14-Three-phase electric motor, 15-Hydraulic pump, 16-Electronic interface, 17-Electric rectifier, 18-Force sensor (load cell), 19-Control computer

Figure 13: Hydraulic press, a) schematic diagram, b) photo

3 System modelling

3.1 Pneumatic press system modelling

The problem under consideration is shown in Figure 14. The goal is to make the actuator compress an object with a desired force. The force producing element is a double-acting pneumatic cylinder driven by a proportional pressure-control valve. The mathematical model of the pneumatic actuator interaction with its environment is given bellow. The force balance equation for the mechanical part of the system can be written as follows:

$$m \ddot{x} = F_p - b \dot{x} - k_e x \quad (1)$$

where m , b , x represent the mass, damping and displacement of the actuator, while k_e represent spring stiffness. The actuator force F_p allows interaction between the cylinder piston and its environment and its given by:

$$F_p = A(p - p_a) \quad (2)$$

where A is piston area, p is inlet pressure and p_a is atmospheric pressure.

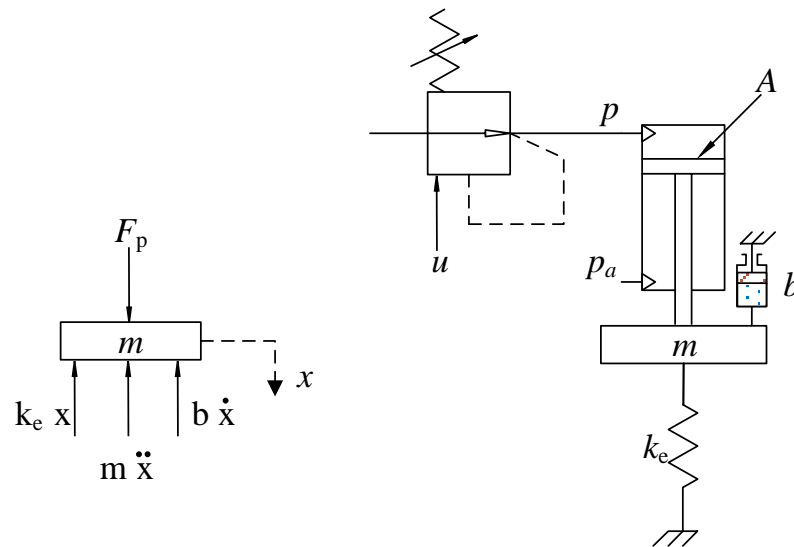


Figure 14: Schematic model of the pneumatic press

The output of interest on the experimental test system is the force F of the pneumatic press and that force is equal to the compression of a spring x multiplied by its stiffness k_e :

$$F = k_e x \quad (3)$$

From (3) the velocity and acceleration are given by:

$$\dot{x} = \frac{\dot{F}}{k_e} \quad \text{and} \quad \ddot{x} = \frac{\ddot{F}}{k_e} \quad (4)$$

Substituting equations (2), (3) and (4) into equation (1) gives the force balance equation for the pneumatic actuator and it can be written as follows:

$$\begin{aligned} \frac{m}{k_e} \ddot{F} &= F_p - \frac{b}{k_e} \dot{F} - F \\ \ddot{F} &= \frac{k_e}{m} A(p - p_a) - \frac{b}{m} \dot{F} - \frac{k_e}{m} F \end{aligned} \quad (5)$$

The mathematical model of the proportional pressure control valve is obtained from experimentally measured pressure response on a step command input. The pressure responses for step input signals with amplitudes of 1 V, 2 V and 5 V are shown in Figure 4. The pressure transient-response of the valve has an aperiodic form, and can be approximated by a first-order lag term as follows:

$$T_v \frac{dp(t)}{dt} + p(t) = K_v u(t) \quad (6)$$

where T_v is a time constant and K_v is the gain of the proportional pressure-control valve.

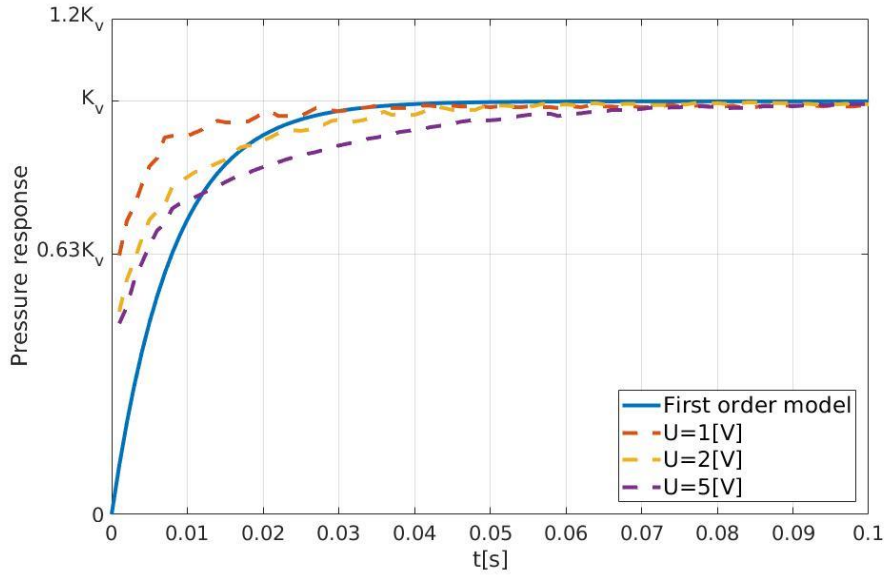


Figure 15: Step response of the proportional valve

The force control loop uses a PID controller given by the following expression:

$$u(t) = K_p e(t) + K_i \int e(t) dt + K_d \dot{e}(t) \quad (7)$$

where K_p , K_i , K_d represents proportional, integral and derivate gain and $e(t)$ represents the control error between the measured force and the desired force trajectory given by:

$$e(t) = F_r(t) - F(t) \quad (8)$$

The mathematical model of the system can be written in the standard state-space form as $\dot{\mathbf{x}} = \mathbf{f}(\mathbf{x}(t), \mathbf{u}(t))$ where state variables $\mathbf{x} = [x_1 \ x_2 \ x_3 \ x_4]^T$ are chosen as: $x_1 = p$, $x_2 = F$, $x_3 = \dot{F}$ and $x_4 = \int e(t)$, then the simplified representation of the actual system dynamics which includes the controller can be written in the state-space form as follows:

$$\begin{aligned} \dot{x}_1 &= \frac{K_v}{T_v} u(t) - \frac{1}{T_v} x_1 \\ \dot{x}_2 &= x_3 \\ \dot{x}_3 &= \frac{k_e}{m} A(x_1 - p_a) - \frac{b}{m} x_3 - \frac{k_e}{m} x_2 \\ \dot{x}_4 &= e(t) = F_r(t) - F(t) \end{aligned} \quad (9)$$

The state-space model is given in general nonlinear form and it is used for numerical simulation of the pneumatic press. The desired output of the system is the force F (variable x_2).

3.2 Hydraulic press system modelling

For the hydraulic press system, the considered model and the obtained solution are similar to the previously presented model for the pneumatic press, as shown in Figure 16. The force producing element, similar to the pneumatic press, is a double acting hydraulic cylinder controlled by a

pressure type servo valve. The simplified nonlinear mathematical problem describing the hydraulic actuator interacting with its environment is derived below and the complete mathematical model is given in [7].

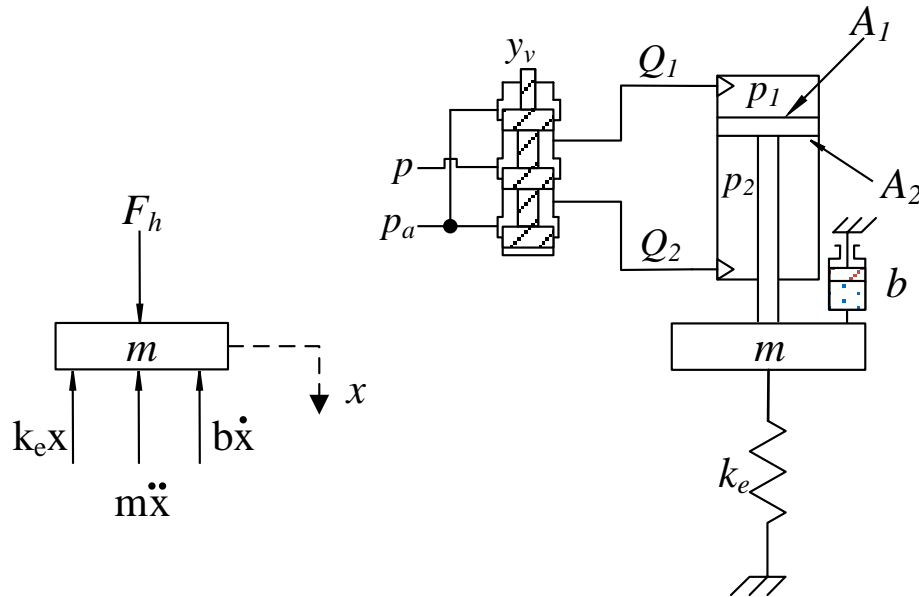


Figure 16: Schematic model of the hydraulic press

The force balance equations for the mechanical part of the system can be written as follows:

$$m \ddot{x} = F_h - b \dot{x} - k_e x - F_{fc}(\dot{x}) \quad (10)$$

where, similar to the pneumatic press model, m , b , x represent the mass, damping and displacement of the actuator, while k_e represents the spring stiffness. Here we assume a classical friction model that includes the viscous and Coulomb friction, F_v and F_{fc} respectively, and is given by:

$$F_{\text{friction}}(\dot{x}) = F_v + F_{fc}(\dot{x}) = b \dot{x} + f_c \text{sgn}(\dot{x}) \quad (11)$$

The actuator force F_h allows interaction between the piston and its environment and is given by:

$$F_h = p_1 A_1 - p_2 A_2 \quad (12)$$

where A_1 and A_2 are the cross sectional piston areas, p_1 is the inlet pressure and p_2 is the outlet pressure. The output of interest is similar to the case of the pneumatic press and it's actually the force F of the hydraulic press. It is supposed that the force is equal to the compression of the rubber spring x multiplied by its stiffness k_e :

$$F = k_e x \quad (13)$$

From (13) the velocity and acceleration are as follows:

$$\dot{x} = \frac{\dot{F}}{k_e} \quad \text{and} \quad \ddot{x} = \frac{\ddot{F}}{k_e} \quad (14)$$

Substituting equations (12), (13) and (14) into equation (10) gives the force balance equation for the hydraulic actuator and it can be written in following form:

$$\begin{aligned} \frac{m}{k_e} \ddot{F} &= F_h - \frac{b}{k_e} \dot{F} - F - F_{fc}(\dot{x}) \\ \ddot{F} &= \frac{k_e}{m} (p_1 A_1 - p_2 A_2) - \frac{b}{m} \dot{F} - \frac{k_e}{m} F - \frac{k_e}{m} F_{fc}(\dot{x}) \end{aligned} \quad (15)$$

From [7] the expression for the piston and rod side actuator pressures may be written as follows:

$$\dot{p}_1 = \frac{\beta}{V_1} (Q_1 - \dot{V}_1) = \frac{\beta}{V_0 + A_1 x} (Q_1 - A_1 \dot{x}) \quad (16)$$

$$\dot{p}_2 = \frac{\beta}{V_2} (Q_2 - \dot{V}_2) = \frac{\beta}{V_0 - A_2 x} (-Q_2 + A_2 \dot{x}) \quad (17)$$

where V_1 and V_2 are total fluid volumes in the two cylinder chambers, V_0 is the half-volume, A_1 and A_2 are the annulus area of the piston and rod side of the cylinder.

If we suppose that the bandwidth of the servo valve is much higher than the dynamics of the control system, then the valve dynamics can be neglected and the flow is taken as a linear function of the control signal u :

$$Q(y_v, p) = K u \quad (18)$$

where K is the flow/signal gain of the valve and its value is estimated from the flow/signal characteristic curve.

If we derive the expression for F_h and substitute equations (16), (17) and (18) into equation (12) then the acting force derivate is given by:

$$\begin{aligned} \dot{F}_h &= \dot{p}_1 A_1 - \dot{p}_2 A_2 = \frac{A_1 \beta}{V_0 + A_1 x} (K u - A_1 \dot{x}) - \frac{A_2 \beta}{V_0 - A_2 x} \left(-\frac{K}{\varphi} u + A_2 \dot{x}\right) = \\ &= \left(\frac{\beta A_1 K}{V_0 + A_1 \frac{F}{k_e}} + \frac{\beta A_2 \frac{K}{\varphi}}{V_0 - A_2 \frac{F}{k_e}} \right) u - \left(\frac{\beta A_1^2}{k_e V_0 + A_1 F} + \frac{\beta A_2^2}{k_e V_0 - A_2 F} \right) \dot{F} \end{aligned} \quad (19)$$

If we choose PI controller, then the control signal will be equal:

$$u(t) = K_p e(t) + K_i \int e(t) dt \quad (20)$$

where K_p , K_i , represent proportional and integral gain of the controller and $e(t)$ represents the error between the measured force and the desired force trajectory given by the following expression:

$$e(t) = F_r(t) - F(t) \quad (21)$$

Similar to the case of pneumatic press, the state-space model can be written as $\dot{\mathbf{x}} = \mathbf{f}(\mathbf{x}(t), \mathbf{u}(t))$ where state variables $\mathbf{x} = [x_1 \ x_2 \ x_3 \ x_4]^T$ are chosen as: $x_1 = F$, $x_2 = \dot{F}$, $x_3 = F_h$ and $x_4 = \int e(t)$, then the simplified representation of the actual system dynamics, which includes the controller, can be written in the state-space form as follows:

$$\begin{aligned} \dot{x}_1 &= x_2 \\ \dot{x}_2 &= \frac{k_e}{m} x_3 - \frac{b}{m} x_2 - \frac{k_e}{m} x_1 - \frac{k_e}{m} F_{fc}(x_2) \\ \dot{x}_3 &= -\left(\frac{\beta A_1^2}{k_e V_0 + A_1 x_1} + \frac{\beta A_2^2}{k_e V_0 - A_2 x_1} \right) x_2 + \left(\frac{\beta A_1 K k_e}{k_e V_0 + A_1 x_1} + \frac{\beta A_2 K k_e}{(k_e V_0 - A_2 x_1)\varphi} \right) u \\ \dot{x}_4 &= e(t) = F_r(t) - F(t) \end{aligned} \quad (22)$$

The state-space model is given in a general nonlinear form and it is used for numerical simulation of the hydraulic press. The desired output of the system is the force F (variable x_1).

4 Simulation model and numerical results

The numerical simulations are carried out in Matlab/Simulink program to verify the stability of the process for proposed controllers, both for pneumatic and hydraulic press. The simulations were performed using the Matlab ODE solver. In these examples, the relative and absolute tolerance for the ODE routine was set to 10^{-6} . The developed controllers were tested for a sinusoidal and square wave reference signal.

4.1 Pneumatic press simulation model and numerical results

The simulation was performed using parameters listed in Table 1, which were obtained from manufacture's data sheets and measurements, while corresponding results are shown in Figure 17. During simulation it was found that the values greater than 1 for proportional gain K_p and values greater than 2 for integral gain K_i of PI controller have resulted in a significant oscillatory response of the cylinder pressure. The simulation showed that the control algorithm could achieve good abilities for tracking square wave reference forces with fast response to changes in reference trajectory.

Table 1: Parameters for pneumatic press system

Parameter	Value	Parameter	Value
m	1 kg	T_v	0.008 s
A	$1.963 \cdot 10^{-3} \text{ m}^2$	K_v	0.18 MPa/V
k_e	80 N/mm	K_p	0.5
b	80 N/(m/s)	K_i	2
p_a	101 kPa	K_d	0.01

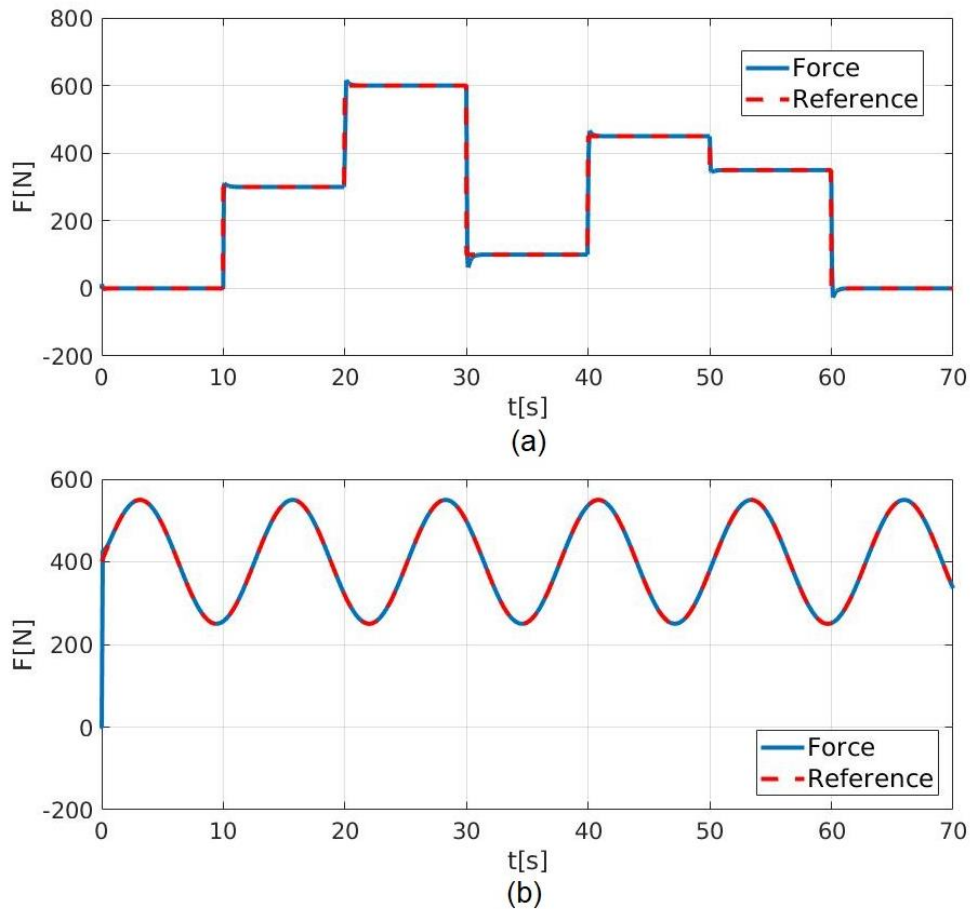


Figure 17: Pneumatic press simulation results, (a) square wave force tracking, (b) sine wave force tracking

4.2 Hydraulic press simulation model and numerical results

The numerical simulations for the hydraulic press were carried out with parameters listed in Table 2, which were obtained from manufacture's data sheets and measurements.

The results obtained through numerical simulations are shown in Figure 18. These results confirm that the PI controller couldn't follow square wave reference signal without tracking error and also unwanted high frequency oscillations occurred in the control variable.

Table 2: Parameters for hydraulic press system

Parameter	Value	Parameter	Value	Parameter	Value
β	$1.4 \cdot 10^7 \text{ N/m}^2$	V_0	$7.5398 \cdot 10^{-4} \text{ m}^3$	b_a	520 N s/m
A_1	$50.26 \cdot 10^{-4} \text{ m}^2$	m	50 kg	f_c	120 N
A_2	$28.27 \cdot 10^{-4} \text{ m}^2$	k_e	$5.46 \cdot 10^{-5} \text{ N/m}$	K_p	6
φ	1.7778	K	$8.33 \cdot 10^{-6} \text{ m}^3/\text{V s}$	K_i	2

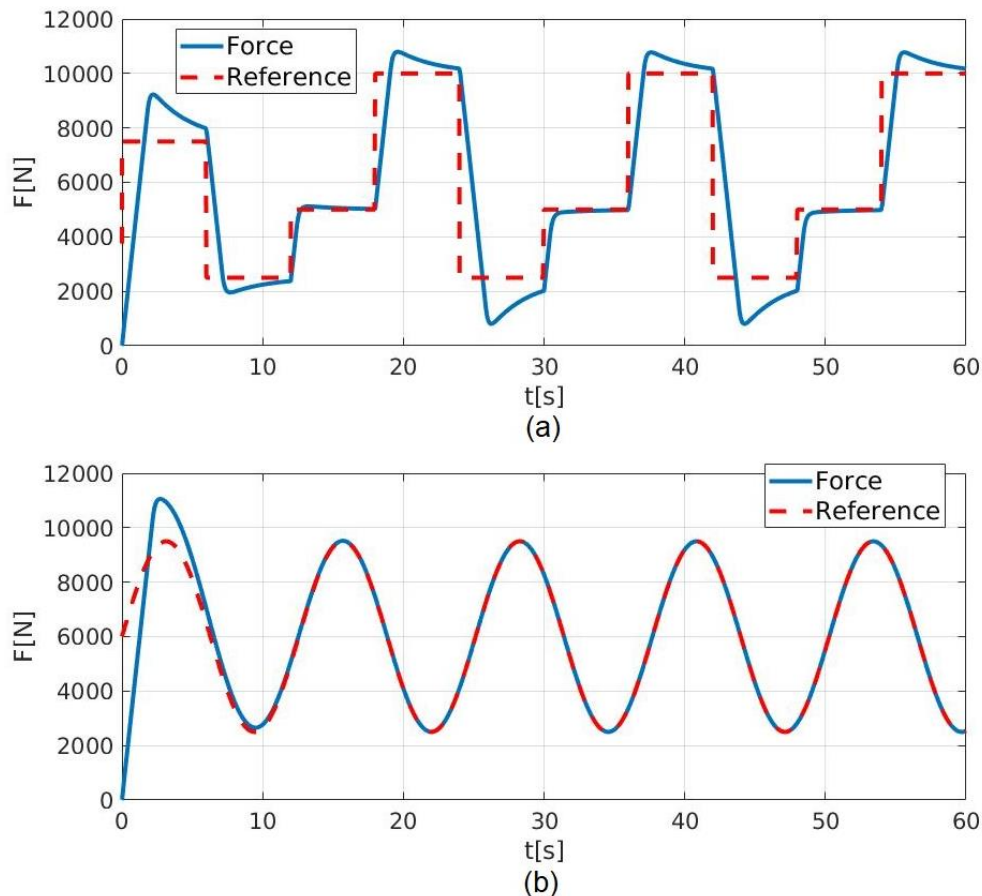


Figure 18: Hydraulic press simulation results, (a) square wave force tracking, (b) sine wave force tracking

5 Experimental results

The control algorithms are implemented in Matlab/Simulink environment, which allows executing the simulation program in real time. Such implementation of control algorithms allows real time data monitoring and online tuning of controller parameters. Block diagrams are used for the controller design procedure which gives simple data flow representation. The experimental results obtained for both systems are compared with those obtained from simulations

5.1 Pneumatic press experimental results

Implementation of a PID controller for the pneumatic press system is given in Figure 20. By activating the switch in controller model it is possible to choose between sine and square wave input signal. The controller is implemented on a standard laptop PC with a sampling rate of 20Hz. During experiments, signals that were recorded are the pressing force, the error between the reference force and the pressing force, the control signal on the proportional pressure-control valve and the pressure from the pneumatic actuator inlet.

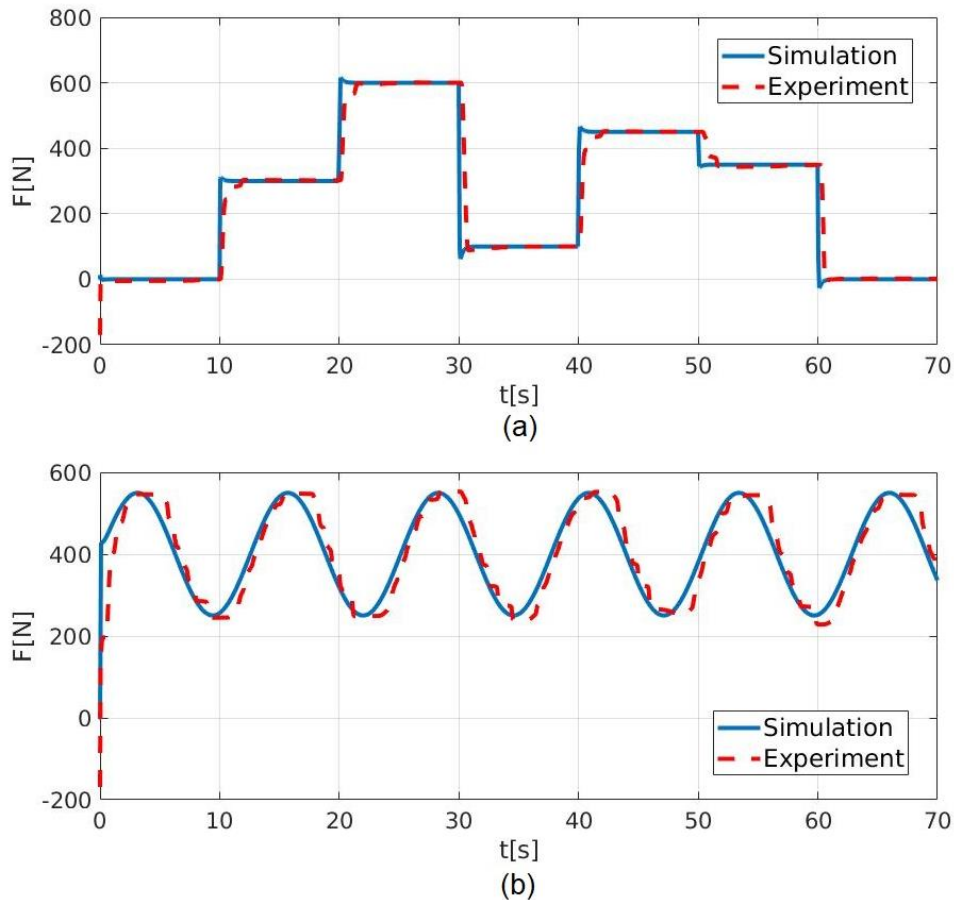


Figure 19: Pneumatic press experimental results, (a) square wave force tracking, (b) sine wave force tracking

The first experimental test was carried out for the square wave input signal and the results are shown in Figure 19. The measured results exhibit an aperiodic response, without overshoot and with small output error. The second experiment was carried out for the sinusoidal signal of frequency 0.08 Hz. The force response is shown in Figure 19. The experiment demonstrates that the PID controller follows the reference sinusoidal input signal with significant control error. Both experiments were carried out with PID gains obtained from numerical simulations.

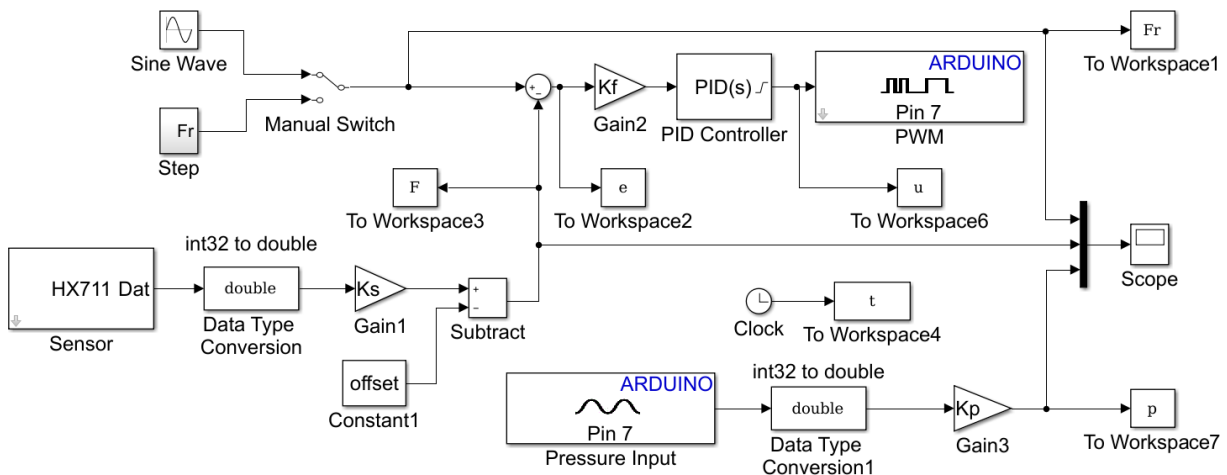


Figure 20: Simulink model used for experimental testing of the pneumatic press

5.2 Hydraulic press experimental results

The model using PI controller for the hydraulic press force control is shown in Figure 21. The switch shown on the Simulink model is used for choosing between square and sine wave input. The controller is implemented on a standard laptop PC with sampling rate of 100Hz. Signals that are being acquired are the pressing force, the control signal for the servo valve, and the pressure from the hydraulic cylinder inlet.

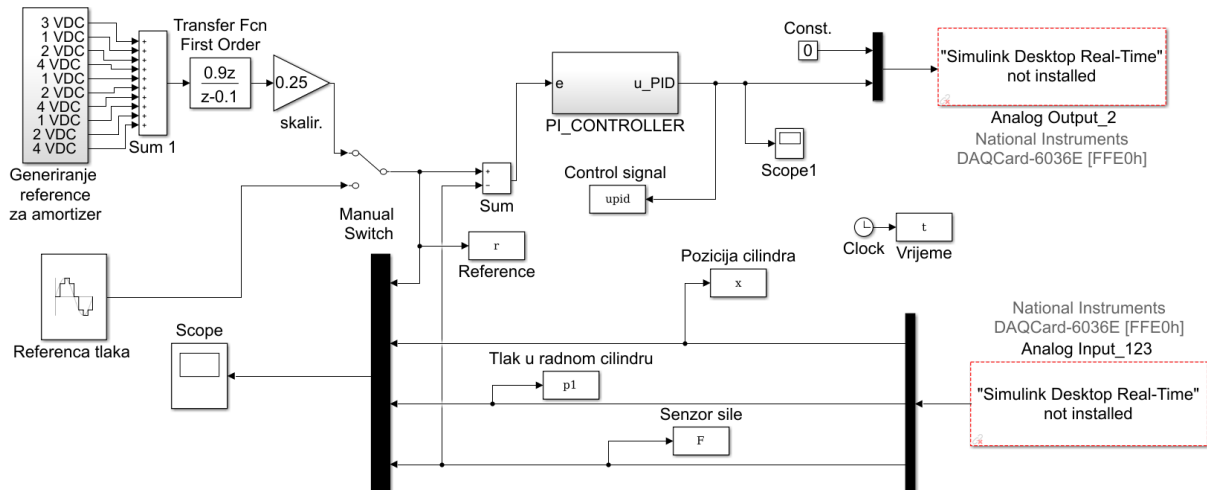


Figure 21: Simulink model used for experimental testing of the hydraulic press

Experimental results for the hydraulic press are shown in Figure 22. PI regulator gains, used for experimental test, are the same gains used in numerical simulation test. The value for proportional (K_p) gain was set at 6, and value for integral (K_i) gain was set at 2. The first test was carried out for the square wave reference signal. Results showed similar trend as the results from numerical simulation. Therefore, the linear PI regulator follows the reference square wave input signal with significant control error because of many nonlinearities of the hydraulic systems. The second test was performed with the sinusoidal wave signal with the frequency of 0.08 Hz. From observed experimental results it can be concluded that PI controller shows inferior results for the sinusoidal wave than for the square wave input signal, which was expected.

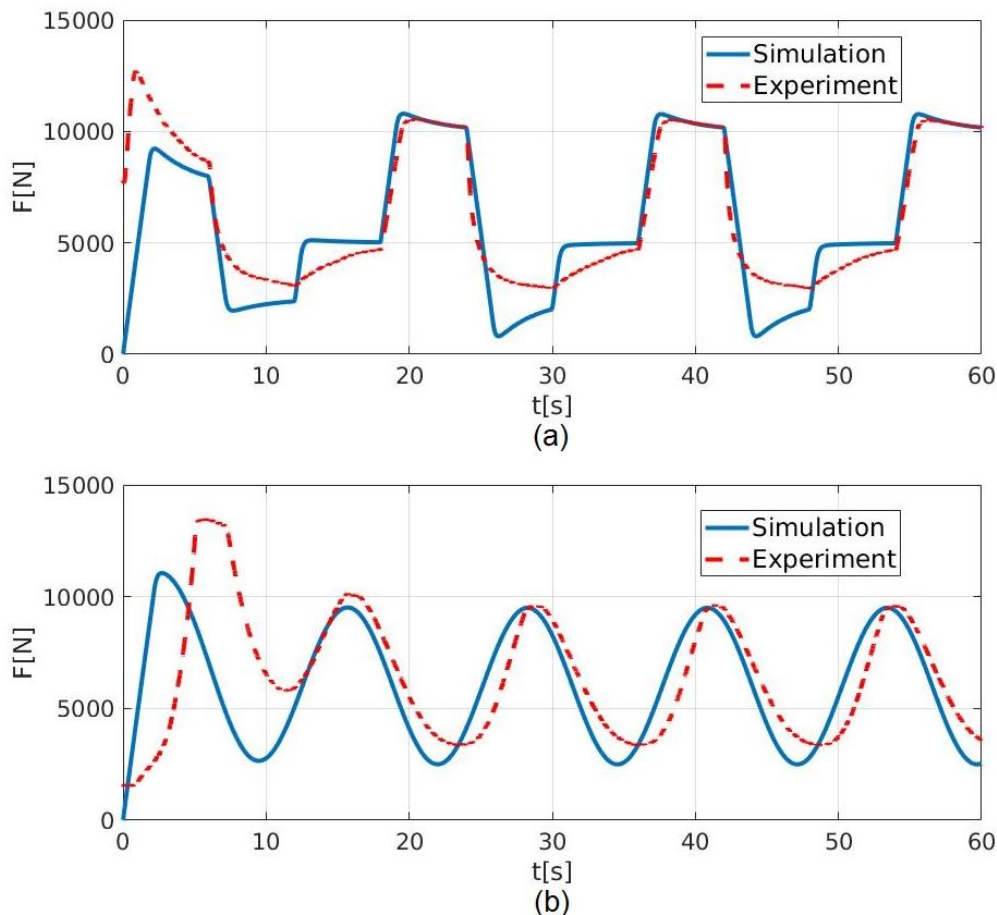


Figure 22: Hydraulic press experimental results, (a) square wave force tracking, (b) sine wave force tracking

6 Conclusion

According to the experimental results, it can be concluded that in the case of PID controlled force of the pneumatic press, valid results can be obtained only for square wave input signal. Moreover, numerical simulations didn't present the same results as the experimental tests, because of many simplifications in the mathematical model. For the hydraulic press system PI controller could only be used for tracking desired constant input force. For the square and the sinusoidal wave input signal it is needed to consider new ways of the system control. The experimental results show that there are no high frequency oscillations in the control signal, unlike the oscillations which have appeared in numerical simulations. For better systems control, new control algorithms should be considered, such as sliding mode control, back stepping control or fuzzy control. Mentioned control algorithms could probably give better results than PID controller.

References

- [1] Murrenhoff, H.: Trends in Valve Development, O+P Ölhydraulik und Pneumatik, Vol. 46, Nr. 4., pp. 1-36, 2003
- [2] Detiček, E., Kastrevc, M.: Design of Lyapunov based nonlinear position control of electrohydraulic servo systems, Strojniški vestnik, Vol. 62, Nr. 3, pp. 163-170, 2016
- [3] Detiček, E., Gubljak, N., Kastrevc, M.: Design of Lyapunov based nonlinear velocity control of electrohydraulic velocity servo systems, Tehnički vjesnik, Vol. 24, No. 3, pp. 745-751, 2017

- [4] Chen, H., Yang, G., Liao, C.: Precision Force Control for an Electro-Hydraulic Press Machine, *Smart Science*, Vol 2, pp. 132-138, 2014
- [5] Falcão Carneiro, J., Gomes de Almeida, F.: Using two servovalves to improve pneumatic force control in industrial cylinders, *The International Journal of Advanced Manufacturing Technology* Vol. 66, pp. 283-301, 2013
- [6] Ledezma, J. A., Negri, V. J. D., Pieri, E. R. D.: New approach for hydraulic force control based on hydraulic compliance, *Int. Conf. Fluid Power Mechatronics 2015*, proceedings; Harbin; pp. 454–459
- [7] Šitum, Ž., Žilic, T., Milic, V.: Improving performance of a hydraulic press with real-time nonlinear control; *The 9th International Fluid Power Conference*, 9. IFK, 2014, Aachen, Germany, 2014

Nonlinear position control of electrohydraulic servo systems

EDVARD DETIČEK & MITJA KASTREVC

Abstract This paper studies the nonlinear closed loop control of an electrohydraulic servo system with use of Lyapunov theory of nonlinear systems using integrator backstepping. Because of highly nonlinear nature of electrohydraulic servo system, the conventional control strategies mostly cannot reach desired control objectives. Nonlinear mathematical model of the system contains many nonlinear terms, which influence also the dynamic errors of the control system. Modern control strategy should be able to cope with these nonlinearities.

Two different nonlinear design procedures are employed here, feedback linearization and integrator backstepping. Backstepping is used because it is a powerful and robust nonlinear strategy.

The research studies represented in the paper shows big potential of Lyapunov based nonlinear controller design procedures, to obtain desired control objectives.

Keywords: • electrohydraulic servo system • nonlinear control • Lyapunov theory • integrator backstepping • computer simulation •

CORRESPONDENCE ADDRESS: Edvard Detiček, Ph.D., Assistant Professor, University of Maribor, Faculty of Mechanical Engineering, Smetanova ulica 17, 2000 Maribor, Slovenia, e-mail: edvard.deticek@um.si.
Mitja Kastrevc, Ph.D., Assistant Professor, University of Maribor, Faculty of Mechanical Engineering, Smetanova ulica 17, 2000 Maribor, Slovenia, e-mail: mitja.kastrevc@um.si

1 Introduction

Electrohydraulic servo systems take important place in modern industrial automation. It has been used in many kinds of mechanizations, including robots, computer numerical control (CNC) press brakes, computer controlled testing machines, etc.

Electro hydraulic actuator system has become one of the most important actuators in the recent decades. It offers many advantages such as good capability in positioning, fast and smooth response characteristics and high power density. Due to its capability in positioning, it has given a significant impact in modern equipment for position control applications [1] and [2]. The applications in position control can be found in production assembly lines, robotics, aircrafts and testing equipment. However, excellent positioning in these applications requires an accurate electro hydraulic actuator. Therefore, the development of suitable controller which could reflect such characteristics is very significant, although the dynamics of electro hydraulic servo system is highly nonlinear [3], as well as pneumatic systems [4].

In ordinary feedback systems the method of feedback linearization is used to eliminate nonlinearities. Feedback linearization employs changes of coordinates to transform a given nonlinear system into equivalent linear one. A major advantage of feedback linearization approach is related to the cancelations of systems nonlinear dynamics that are introduced in design process. On the other hand some kinds of nonlinearities can have positive effects on system stability, therefore their cancellation can lead to instability in the presence of modelling uncertainties. As a solution to this problem the integrator backstepping approach is proposed. The fundamental concept of backstepping method is introduced by Krstic et.al. in their book [5].

The approach focusing on the stabilization problem in stochastic nonlinear systems is developed in the extension of this book. The backstepping control method is also presented in [6], [7] and [8] where this technique is explained in detail for regulating and tracking problem.

There are numerous of applications in industry, where the backstepping approach was used to obtain successful control of electric machines, wind turbines, based power production, robotic production systems and flight trajectory control.

Integrator backstepping control method allows also finding a solution for optimal control problems [9], estimating parameters and adaptive control design, as well as, development of robust nonlinear controllers. The observer based backstepping technique has been designed for force control of electrohydraulic actuator system [10]. The developed control system combine backstepping observer with adaptive and sliding mode controller. Electrohydraulic active suspension control system is also designed by backstepping approach [11]. To obtain best value for its tuning parameters the particle swarm optimization tool is proposed in [12].

It is proved that the technique improve the transient stability and damping presented in the system. The performance of backstepping controller also depends on its gains or controller parameters. In this paper, the controller is developed on the basis of simplified mathematical model, while the parameters are tuned manually to prevent the control signal chattering.

2 Simplified model of the system

For the purpose of design of a closed loop controller the complete mathematical model of the system which consists of the hydraulic actuator dynamics, including the load and SV dynamics can be simplified according to manufacturers data of real system components. Usually a

simplification can be obtain when the dynamic of the servo valve with control electronics is much higher than the dynamic of the cylinder and load.

For hydraulic system with $A_p=6.4 \cdot 10^{-4} \text{ m}^2$, $V_t=131.85 \cdot 10^{-6} \text{ m}^3$ and $m=200 \text{ kg}$ the minimum natural frequency is:

$$\omega_{H \min} = \sqrt{\frac{4\beta \cdot A_p^2}{m \cdot V_t}} = 310,052 \left[\frac{\text{rad}}{\text{s}} \right] \Rightarrow 49,35 [\text{Hz}] \quad (1)$$

Natural frequency can be read out, from the manufacturers data sheet for SV MOOG 769 [13] we can read out $f_{Hsv}=325\text{Hz}$.

Because of very high natural frequency of servo valve with comparison to hydraulic cylinder ($\omega_{Hsv} \gg \omega_{Hmin}$), taking in to account also dynamic effect of manifold which decreases hydraulic natural frequency, the dynamic of SV can be neglected. The servo valve can be described only by static relationship between spool position and the valve current input. Moreover the combined assembly of servovalve and electronic amplifier can be described by the equation:

$$x_v = k_v \cdot u \quad (2)$$

where k_v [mV^{-1}] is combined SV and electronic amplifier gain. Therefore the simplified system equations have the following form:

$$\begin{aligned} \dot{x}_p &= v_p \\ \dot{v}_p &= \frac{A_p}{m} p_L - \frac{1}{m} \left[\sigma_{vf} \cdot \dot{x}_p + F_{co} \cdot \text{sgn}(\dot{x}_p) + \text{sgn}(\dot{x}_p) \cdot F_{so} \cdot e^{\frac{|\dot{x}_p|}{c_s}} \right] - \frac{F_{ext}}{m} \\ \dot{p}_L &= \frac{4\beta}{V_t} \cdot C_d \cdot k_v \sqrt{\frac{p_s - \text{sgn}(u) p_L}{\rho}} \cdot u - \frac{4\beta}{V_t} \cdot A_p \cdot \dot{x}_p - \frac{4\beta}{V_t} \cdot k_L \cdot p_L \end{aligned} \quad (3)$$

where x_p is actual piston position, v_p piston velocity and p_L load pressure.

3 Controller design

For a spatial class of nonlinear dynamical systems, the backstepping control has emerged us successful control strategy. Some of nonlinear systems can be observed as a systems constructed from subsystems. The number of subsystems depends of dynamic model order. Because of this recursive structure, the designer can start the design process at the known-stable system and design, "back out", new controllers that progressively stabilize each outer subsystem. The process is finished when the final external control is reached.

The mathematical description of nonlinear system in new set of coordinates allows us to use the backstepping approach to force it to behave like a linear one [5]. Backstepping has the availability to avoid cancellations of useful nonlinearities and pursue the objectives of stabilization and tracking rather than that of linearization method. Besides, backstepping approaches relaxes the matching conditions on perturbations which means that the perturbation doesn't have to appear in the equation that contains the input of the system. This controller can be used for tracking and

regulation problem. For tracking problem, backstepping always use the error between the actual and desired input in order to start the design process.

The system state equations can be represented in “strict feedback form”:

$$\begin{aligned}\dot{x}_1 &= x_2 \\ \dot{x}_2 &= a_1 x_3 - a_2 x_2 - a_3 \operatorname{sgn}(x_2) - a_4 \\ \dot{x}_3 &= a_5 \sqrt{p_s - \operatorname{sgn}(u) x_3 u} - a_6 x_2 - a_7 x_3\end{aligned}\quad (4)$$

where $x_1=x_p$, $x_2=v_p$ and $x_3=p_L$, with:

$$a_1 = \frac{A_p}{m} \quad a_2 = \frac{\sigma_{vf}}{m} \quad a_3 = \frac{F_{co}}{m} \quad a_4 = \frac{F_{ext}}{m} \quad a_5 = \frac{4\beta}{V_t \sqrt{\rho}} \cdot C_d \cdot k_v \quad a_6 = \frac{4\beta}{V_t} \cdot A_p \quad a_7 = \frac{4\beta}{V_t} \cdot k_L$$

In the procedure of design a backstepping controller it is preferable to replace nonlinear terms with differentiable mathematical functions. An essential factor of its validity is the continuous dependence of its solutions on the data of the problem that can be stated by the Lipschitz inequality given by:

$$\|f(x) - f(y)\| \leq L \|x - y\| \quad (5)$$

To satisfy condition in Eq. (5) we estimated the “*sgn*” function with continuously differentiable function “*tanh = th*” (hyperbolic tangent) except in last equation.

$$\dot{x}_1 = x_2 \quad (6a)$$

$$\dot{x}_2 = a_1 x_3 - a_2 x_2 - a_3 \operatorname{th}(\lambda x_2) - a_4 \quad (6b)$$

$$\dot{x}_3 = a_5 \sqrt{p_s - \operatorname{sgn}(u) x_3 u} - a_6 x_2 - a_7 x_3 \quad (6c)$$

λ – free coefficient ($\lambda=2$)

The control objectives were to stabilize the plant and to track the given reference signal asymptotically. The detailed derivations of finding backstepping control input are covered in next three steps [10].

Step1

We want the x_1 – position variable to track a reference signal, say, $r(t)$. So we have the first error variable:

$$z_1 = x_1 - r \quad (7)$$

and its derivative:

$$\dot{z}_1 = \dot{x}_1 - \dot{r} \quad (8)$$

where $r(t)$ is the reference input.

For equation (6a) we can define a virtual control α_1 . Virtual state variable z_2 represents the difference between the actual and virtual control of (6a), i.e.

$$z_2 = x_2 - \alpha_1 \quad \rightarrow \quad x_2 = z_2 + \alpha_1 \quad (9)$$

Define a candidate control Lyapunov functional for this equation:

$$V_1 = \frac{z_1^2}{2} \quad (10)$$

The derivative of V yields:

$$\dot{V}_1 = (x_1 - r) \cdot z_2 + (x_1 - r)(\alpha_1 - \dot{r}) \quad (11)$$

Select a virtual control for the first order system:

$$\alpha_1 = \dot{r} - K_1 z_1 = -K_1 x_1 + K_1 r + \dot{r} \quad (12)$$

where $K_1 > 0$. Hence, \dot{V} can be rewritten as:

$$\dot{V}_1 = -K_1 z_1^2 + z_1 z_2 \quad (13)$$

Step2

Define a second virtual state

$$z_3 = x_3 - \alpha_2 \quad \rightarrow \quad x_3 = z_3 + \alpha_2 \quad (14)$$

Thus:

$$\dot{z}_2 = \dot{x}_2 - \dot{\alpha}_1 \quad (15)$$

Define a candidate control Lyapunov functional for this equation:

$$V_2 = V_1 + \frac{z_2^2}{2} \quad (16)$$

The derivative of V_2 is:

$$\dot{V}_2 = \dot{V}_1 + z_2 \cdot \dot{z}_2 \quad (17)$$

Select a virtual control for this system to remove any potentially undesired z_2 , x_1 and x_2 terms:

$$\alpha_2 = \frac{1}{a_1} (a_2 x_2 + a_3 \tanh(\lambda x_2) + a_4 + \dot{\alpha}_1 - z_1 - K_2 z_2) \quad (18)$$

where $K_2 > 0$, therefore:

$$\dot{V}_2 = -K_1 \cdot z_1^2 - K_2 \cdot z_2^2 + a_1 \cdot z_2 \cdot z_3 \quad (19)$$

Step 3

Let's recall $z_3 = x_3 - \alpha_2$. The derivative of z_3 is:

$$\dot{z}_3 = \dot{x}_3 - \dot{\alpha}_2 \quad (20)$$

With augmentation of the initial control Lyapunov functional to reflect the presence of the new state variable:

$$V_3 = V_2 + \frac{z_3^2}{2} \quad (21)$$

The derivative yields

$$\dot{V}_3 = \dot{V}_2 + z_3 \cdot \dot{z}_3 \quad (22)$$

Select an actual control for this system

$$u = \frac{1}{a_5} \frac{1}{\sqrt{p_s - x_3}} [-a_1 z_2 + a_6 x_2 + a_7 x_3 + \dot{\alpha}_2 - K_3 z_3] \quad (23)$$

where $K_3 > 0$. Then we get:

$$\dot{V}_3 = -K_1 \cdot z_1^2 - K_2 \cdot z_2^2 - K_3 z_3^2 \quad (24)$$

where $K_1, K_2, K_3 > 0$. Note that Equation (16) is the Lyapunov function of the system defined by Equations (18a) to (18c) and that the control law given by Equations (12), (18) and (23) renders its derivative negative semidefinite.

4 Results

In order to verify the effectiveness of the proposed backstepping control algorithm, simulation experiments have been done on the electrohydraulic servo system. Main parameters of the system are given in table 1.

Computer simulation scheme i.e. Simulink model represents Figure 1.

For position control systems dynamically aperiodic response is demanded. The final position accuracy is tested at small steps of reference value.

Table 1: Main parameters of the EHS system

Par.	Value	Par.	Value	Par.	Value	Par.	Value
A_p	$6.4 \cdot 10^{-4} \text{ m}^2$	m	200 kg	F_{ext}	[N]	p_s	210 bar
σ_{yf}	70 Ns/m	V_t	$131.85 \cdot 10^{-6} \text{ m}^3$	k_L	$3 \cdot 10^{-13} \text{ m}^5/\text{Ns}$	ρ	850 kg/m^3
F_{co}	19.62 N	β	$1.5 \cdot 10^9 \text{ Pa}$	C_d	0.63	k_v	$5.53 \cdot 10^{-7} \text{ m}^2/\text{V}$

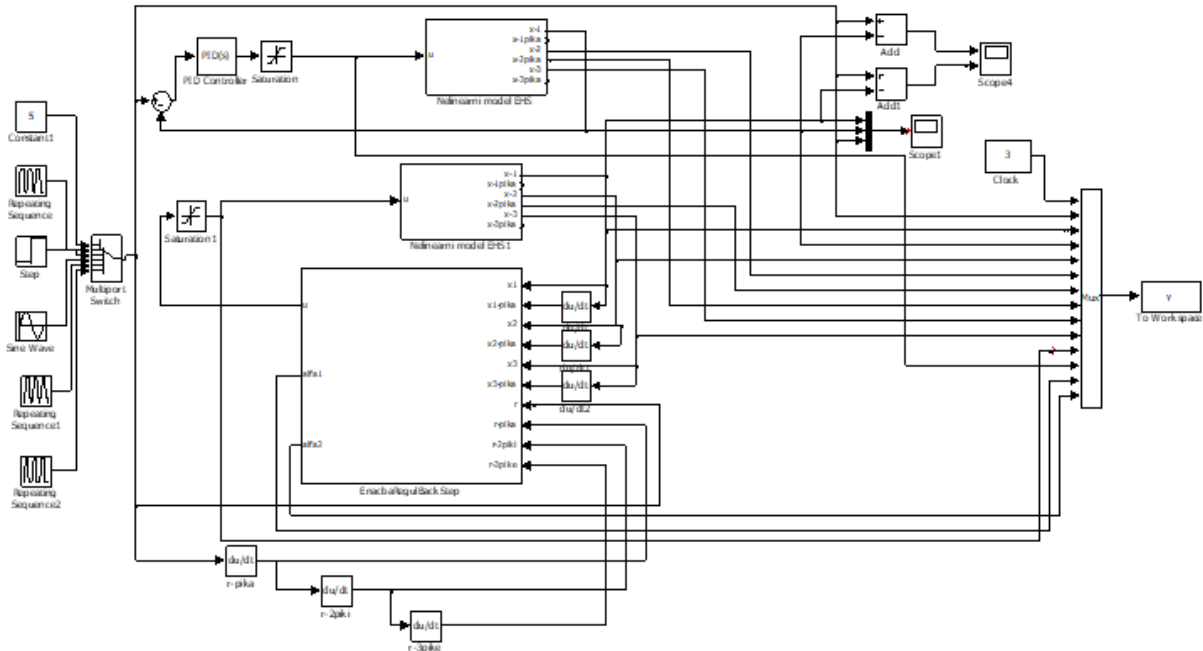


Figure 1: Simulink scheme used for simulation

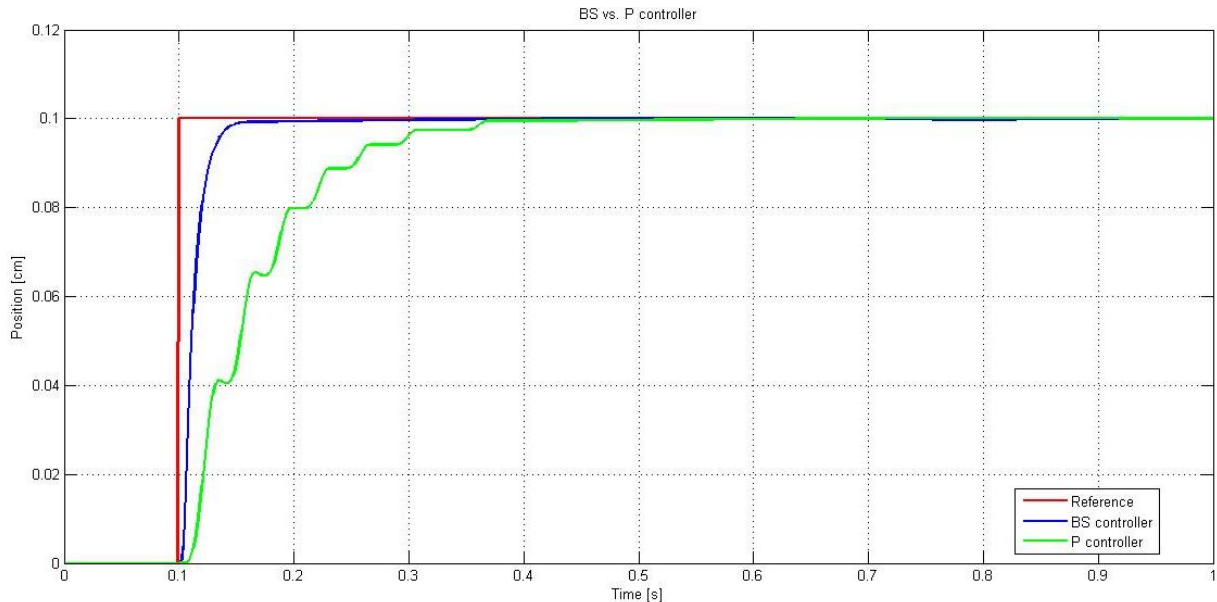


Figure 2: Simulation results of the system step response

In Figure 2 the comparison of systems dynamic response between P-controller and backstepping controller to 1mm desired position step is shown.

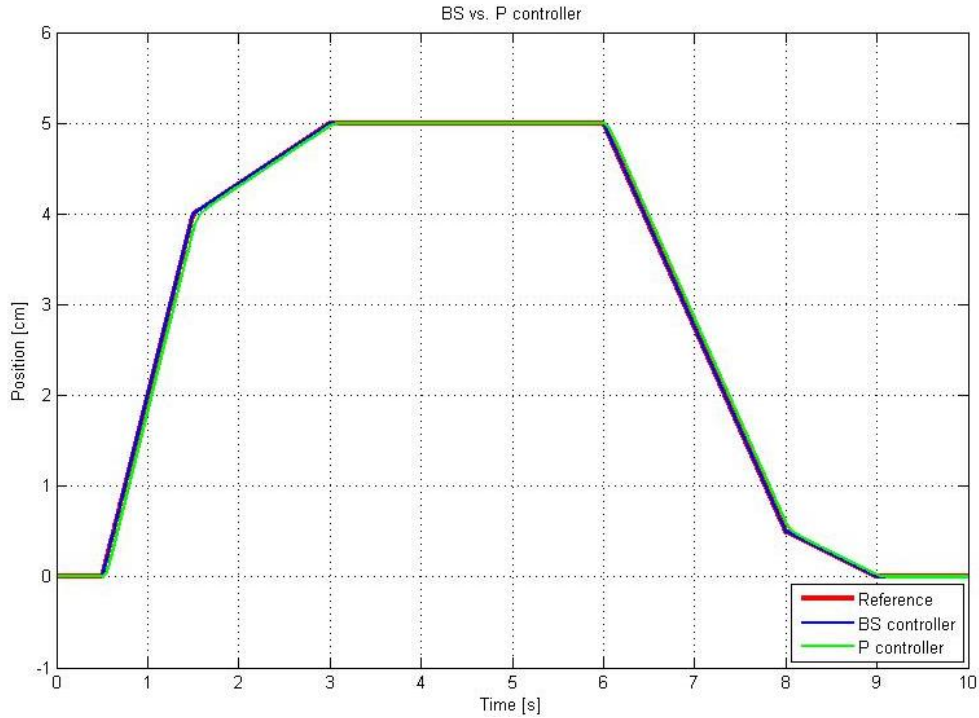


Figure 3: Dynamic response on ramp reference

In Figure 3, the comparison of systems dynamic response to ramp reference input is shown. The corresponding details are shown on Figures 4, 5, 6 and 7.

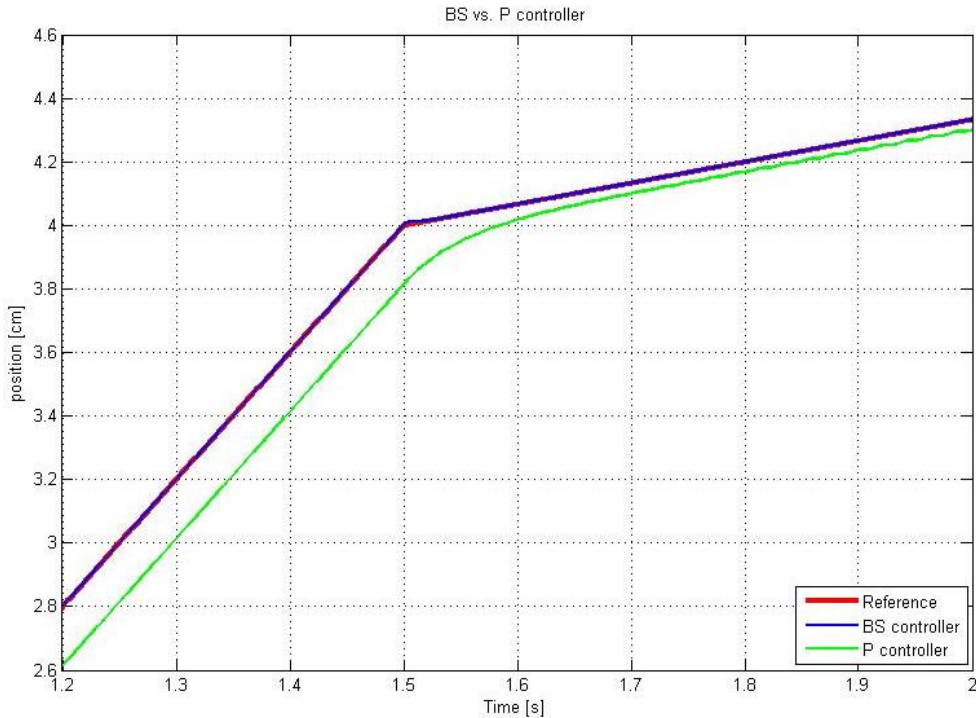


Figure 4: Detail "a"

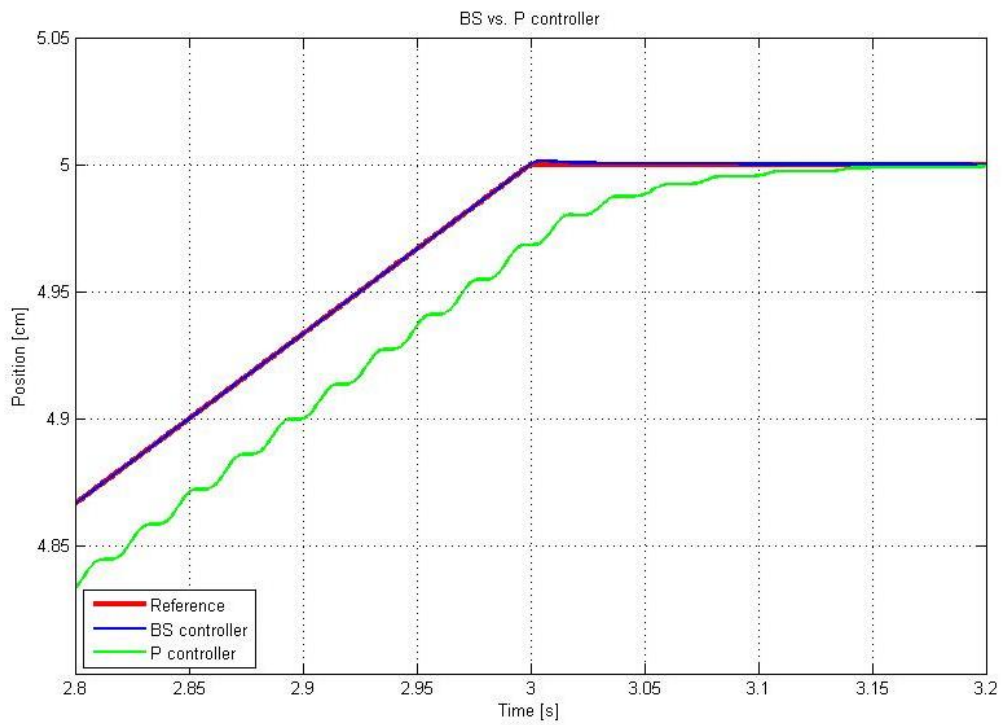


Figure 5: Detail "b"

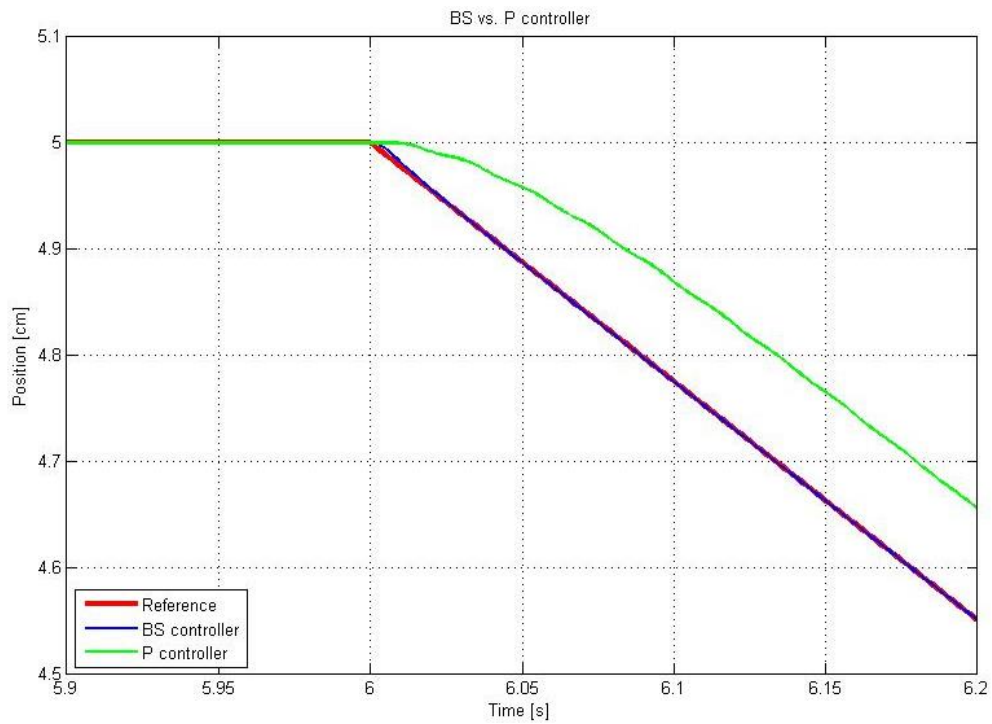


Figure 6: Detail "c"

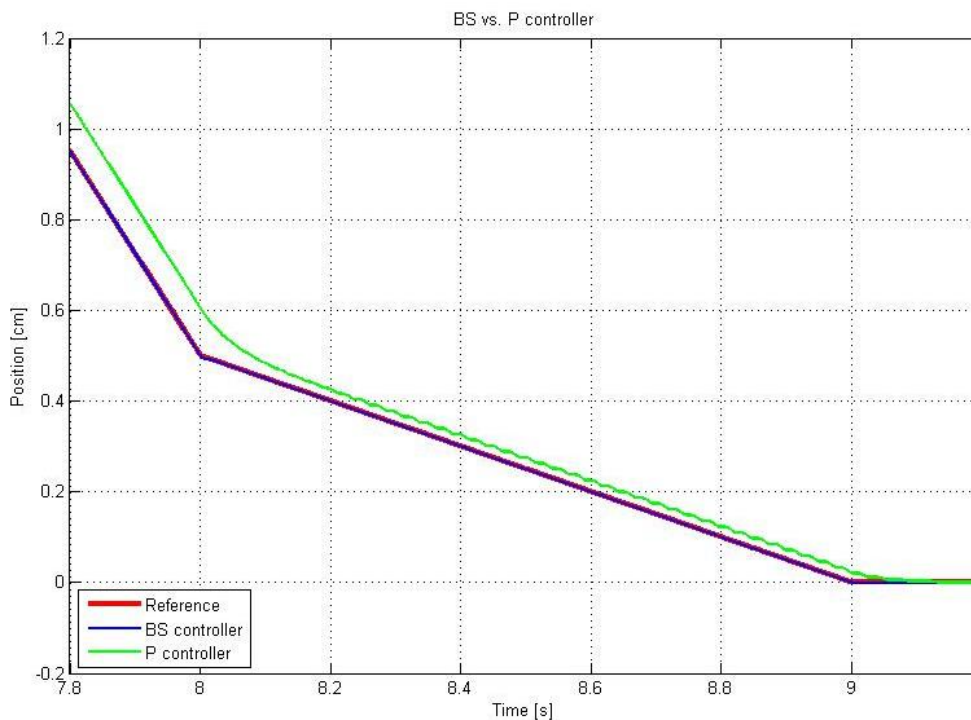


Figure 7: Detail “d”

The results are obtained with P-controller gain $K_P=2.5$, while the backstepping controller parameters are $K_1=110$, $K_2=1100$, $K_3=440$.

5 Conclusions

In this paper, a controller design procedure is presented in order to control the position of the electro-hydraulic servo system. Comprehensive investigation was carried out on the mathematical modelling and computer simulation of dynamic behaviour of whole system, based on real laboratory experimental data.

Because of very fast SV in combination with large moving mass and relatively long hydraulic cylinder, the mathematical model was reduced to third order, neglecting SV first stage dynamics. Such simplified mathematical model was used as a basis to design the closed loop controller. The developed control strategy is based on Lyapunov stability theory of nonlinear systems. We proposed a robust nonlinear controller, using integrator backstepping approach.

The validity of the proposed new feedback law has been tested and compared with P-controller in various computer simulations. In all cases the nonlinear controller shows best tracking performance, with very small position tracking error. Excellent tracking capability of the proposed new controller is also recognized by ramp reference input. Furthermore the tracking errors converge to zero quickly in contrast to the non-zero tracking error of the P-controller. The new controller also shows a certain measure of robustness to small parameter changes. Finally, the controller guaranties a prescribed transient performance and final tracking accuracy. Our future work will look towards the development of nonlinear adaptive controller which would be able to work in the presence of parametric uncertainties and environmental changes.

References

- [1] Khalil, H. K.: Interactive analysis of closed loop electro-hydraulic control systems, 13th International Conference on Aerospace Sciences & Aviation Technology, ASAT-13-HC-0, 2009

- [2] Kovari, A.: Effect of Leakage i Electrohydraulic Servo Systems Based on Complex Nonlinear Mathematical Model and Experimental Results, Acta Polytechnica Hungarica, vol. 12, no. 3, p. 129-146, DOI:10.12700/APH.12.3.2015.3.8, 2015
- [3] Merritt, H. E.: Hydraulic Control Systems. Wiley, NewYork, 1967
- [4] Šitum, Ž., Pavković, D., Novaković, B.: Servo Pneumatic Position Control Using Fuzzy PID Gain Scheduling, Journal of Dynamic Systems, Measurement and Control-Trans. Of tge ASME 126, 2004
- [5] Kritic, M., Kanellakopouls, I., Kokotovic, P. V.: Nonlinear and Adaptive Control Design, John Wiley and Sons Hoboken, 1995
- [6] Khalil, H. K. : *Nonlinear Systems*, 3rd ed., Prentice Hall, Upper Saddle River, 2002
- [7] Lee, S. J., Tsao, T.-C.: Nonlinear backstepping control of an electrohydraulic material testing system, Proceedings of the American Control Conference, vol 6. p. 4852-4830, DOI:10.1109/ACC.2002.1025422, 2002
- [8] Ursu, I., Ursu, F., Popescu, F.: Backstepping design for controlling electrohydraulic servos, Journal of the Franklin Institute, vol. 343, no. 1, p. 94-110, DOI:10.1016/j.jfranklin.2005.09.003, 2006
- [9] Bonchis, A., Corke, P.I., Rye, D.C., Ha, Q.P.: Variable structure methods in hydraulic servo systems control. Automatica; vol.37, no. 4, p. 589–95, DOI:10.1016/S0005-1098(00)00192-8, 2001
- [10] Nakkarat, P., Kuntanapreeda, S.: Observer-based backstepping force control of an electrohydraulic actuator, Control Engineering Practice, vol. 17, no. 8, p. 895-902, DOI:10.1016/j.conengprac.2009.02.011, 2009
- [11] Sun, W., Gao, H., Kaynak, O.: Adaptive Backstepping Control for Active Suspension Systems With Hard Constraints, IEEE/ASME Transactions on Mechatronics, vol. 18, no. 3, p. 1072-1079, DOI:10.1109/TMECH.2012.2204765, 2013
- [12] Wonohadidjojo, D.M., Kothapalli, G., Hassan, M.Y.: Position Control of Electro-hydraulic Actuator System Using Fuzzy Logic Controller Optimized by Particle Swarm Optimization, International Journal of Automation and Computing, vol. 10, no. 3, p.181-193, DOI:10.1007/s11633-013-0711-3, 2013
- [13] MOOG. Servovalves with Integrated Electronics D769 Series. Rapport technique, MOOG Inc.

Modern control system for servo hydraulic linear drive

MATEVŽ ŠTEFANE & DARKO LOVREC

Abstract This paper presents an approach to a customised servo hydraulic linear drive design, together with a user-friendly control concept, that offers a tailor-made control of the whole system - from modelling of the cylinders to the programming of the complete system. The emphasis is on the modern control system approach.

The system is designed as a testing device for testing of different control algorithms, which can be transferred to real life industry applications with focus on applications, which require precise dynamic positioning, e.g. testing devices. With the upgrading of the system, it is also possible, besides the position control, to use the force control concept.

A brief overview of the components used in the system and programming of the control system allows the end user not only to test different control algorithms on a real system, but also to record, export and analyse data from the performed tests.

Keywords: • servo hydraulic • linear drive • design • control • TwinCat •

CORRESPONDENCE ADDRESS: Matevž Štefane, La&Co d.o.o., Limbuška cesta 2, 2341 Limbuš, Slovenia, e-mail: matevz.stefane@la-co.si. Darko Lovrec, Ph.D., Chairperson of the Fluid Power 2017 organising committee, Associate Professor, University of Maribor, Faculty of Mechanical Engineering, Smetanova ulica 17, 2000 Maribor, Slovenia, e-mail: darko.lovrec@um.si.

1 Introduction

Nowadays, electrohydraulic linear servo actuators (linear servo drives, or, briefly servo cylinders), are present in almost all ranges of applications that include the automotive industry, robotics, mining, material fatigue-testing systems, special purpose machines, metal processing, machining plants, motion simulators, oil exploration, aerospace, etc.

Servo cylinders are used wherever there are requirements for:

- Fast and stiff response for resisting loads (motion simulators, rolling mills, machine tool drives, etc...),
- Bigger forces (lifting platforms, digging machines, presses, etc...),
- Precision and accurate response control (machine tools, testing devices, robotics, landing gears, etc...),
- Manual control of motion involving considerable forces (power steering, aircraft controls, heavy machinery),
- Complex automatically controlled motions (4D-cinema theatres, flight and driving simulators, robots, fatigue-testing of materials, etc.).

The performance of hydraulic servo cylinders is relatively high compared to conventional ones. They are able to handle big inertia and torque loads with high accuracy and fast response time. They are extremely stiff and use special seals with a low friction coefficient. The basic concept consists of a power supply, control unit, electronic interface, servo valve, actuator and feedback transducer (Figure 1). ([1] to [4])

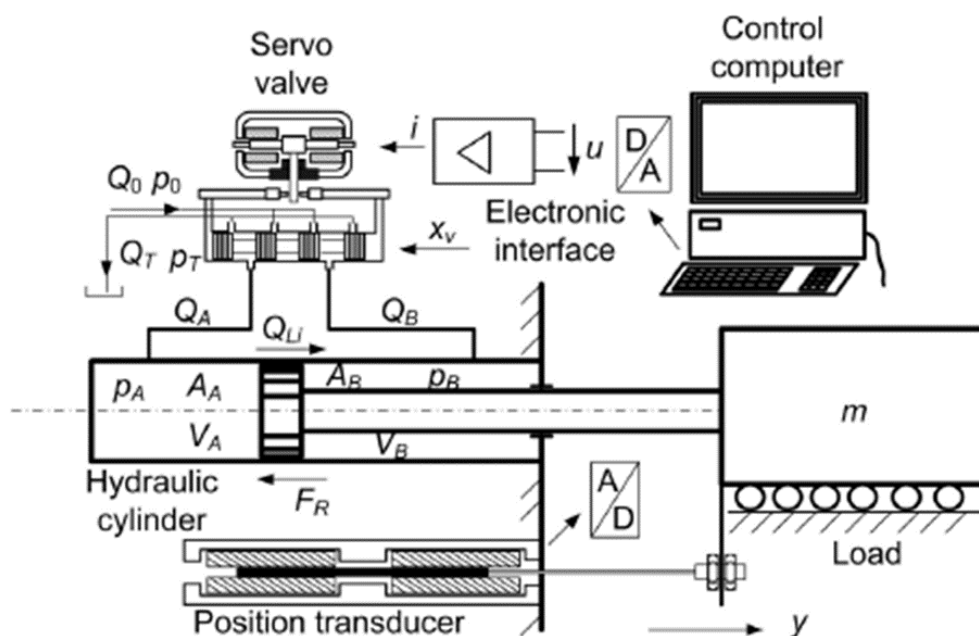


Figure 23: Schematic of a hydraulic linear servo cylinder drive [2]

2 Customised hydraulic linear servo axis

The elementary function of each hydraulic cylinder, as well as of the servo hydraulic cylinder, is to convert hydrostatic energy into mechanical energy, into linear motion.

The design of a servo hydraulic cylinder depends on its application. In our case, cylinders are used within a purposely-built testing station, which is used for testing of different control algorithms; later, they can be used for durability testing of different materials or machinery assemblies as an actuator of the multi axis fatigue-testing device. The cylinder is of double-rod cylinder design form, with the same effective area on both sides of the piston. This means that the piston rod extends and retracts with the same speed and force at constant flow and pressure settings.

The cylinders used are customised, double-ended with low friction sealing. They are robust and fatigue rated, with dynamic force of 40 kN and stroke of 110 mm (in this, the presented case). Working pressure is rated at 210 bar, testing pressure is rated at 310 bar.

2.1 Structure design and mounting options

On the top and bottom of the cylinder there are connections for manifolds, on which servo valves are installed. So, there is the possibility of using two servo valves on the same cylinder. This results in increased dynamic of the cylinder. In this configuration, trunnion mounting or back flange mounting of the cylinder is used. Another possible configuration is to use one manifold and servo valve per cylinder at closing the other ports. Because of the design of the testing bench, we used the second option, as it gave us the possibility to mount the cylinder on a flat surface via the custom built mounting plate (Figure 2, right).

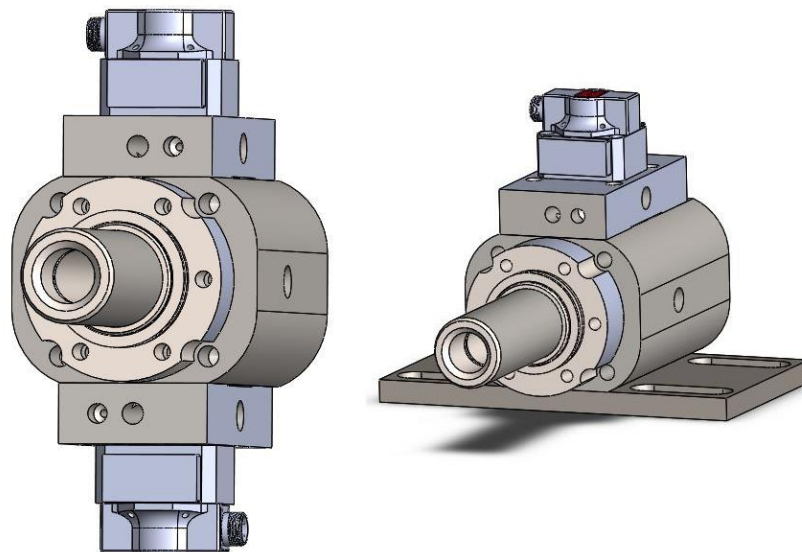


Figure 24: Configuration with two (left) and one (right) servo valves

The cylinder is double acting with a rod extending on both sides of the cylinder. A cross-section schematic of the cylinder is shown in Figure 3. The position measurement sensor 2* (see Figure 3) is secured in the sensor housing 3* inside the cover-end base 1*. The piston area amounts to 1241 mm² and a heavy front flange 9* is mounted to prevent misalignment, sagging or bending of the piston under load. The piston rod 7* is hollow and hard-chromed. It is housed in cylinder 8* made of high grade alloy steel material (42CrMo4). On the cylinder is an attached manifold block 10*. The tapped hole inside the manifold block allows the hydraulic oil to flow between the cylinder and servo valve.

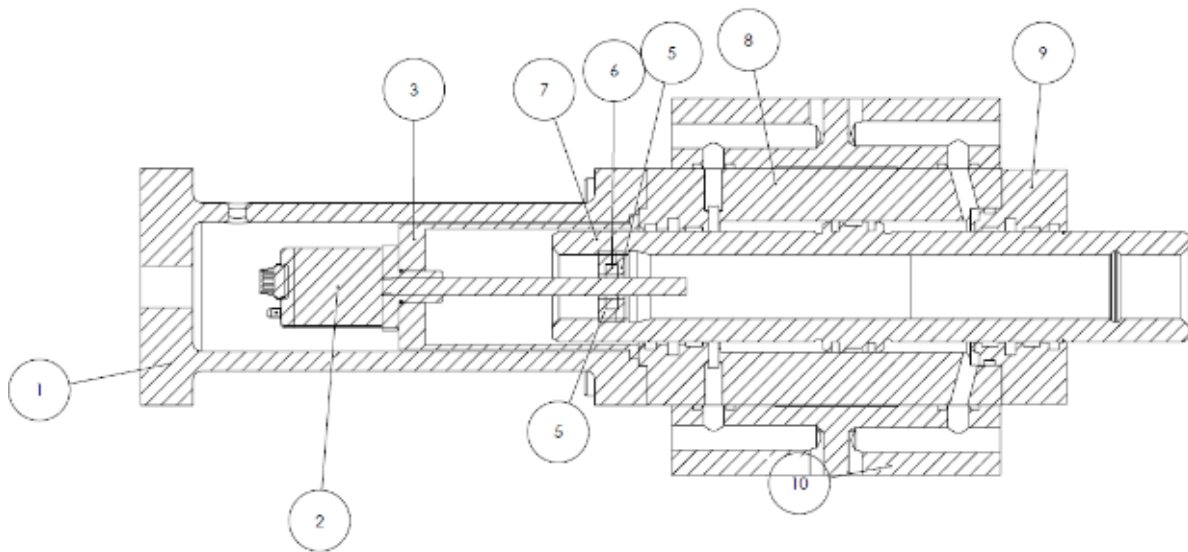


Figure 25: Cross-section of servo cylinder

3 Static analysis of servo cylinder

The hydraulic cylinder and piston rod are modelled with a computer aided static and modal analysis tool, performed by using finite element methods. Analyses were made using Solidworks software. With static analysis of these elements, we can obtain information about static stresses and deformation of the cylinder under pressure with respect to boundary conditions. So, it can be determined if components would withstand maximal stress during operation. [5]

3.1 Stress test of the cylinder

A stress test was carried out with load equivalent to 30 MPa (300 bar). Results are shown in Figure 4. It results in a safety factor of 1.00746. A safety factor of 1.0 at a location indicates that the material at that location has just started to fail. This determines maximal pressure allowed in the system. Selecting a smaller value of pressure increases the life cycle of the hydraulic cylinder. [5]

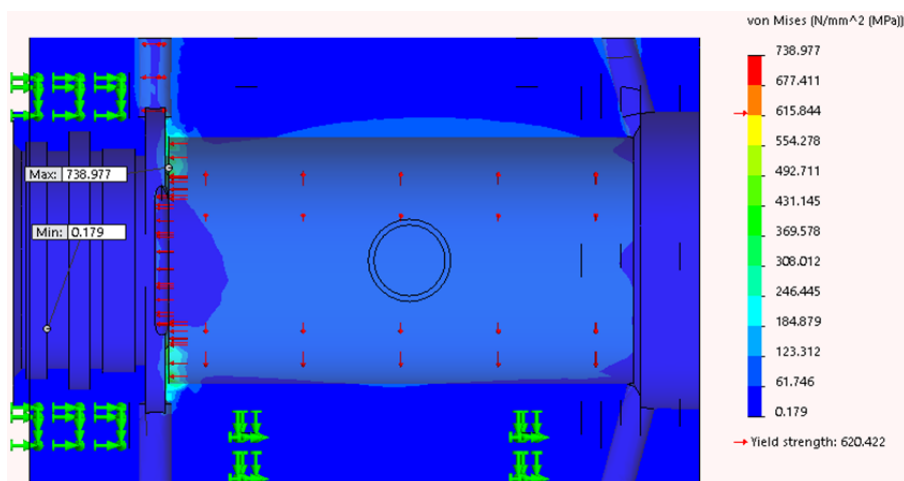


Figure 4: Stress test of the cylinder filled with 30 MPa of pressure [5]

3.2 Stress test of the piston rod

The piston rod is made from the same material as the cylinder itself. Pressure applied on the piston rod affects more the back lateral face, where grooves with two different radius chamfers are

designed (Figure 5). Assuming that the fluid flow in the cylinder is laminar, this design with two different chamfers enables larger pressure distribution, which results in rapid movement of the actuator. [5]

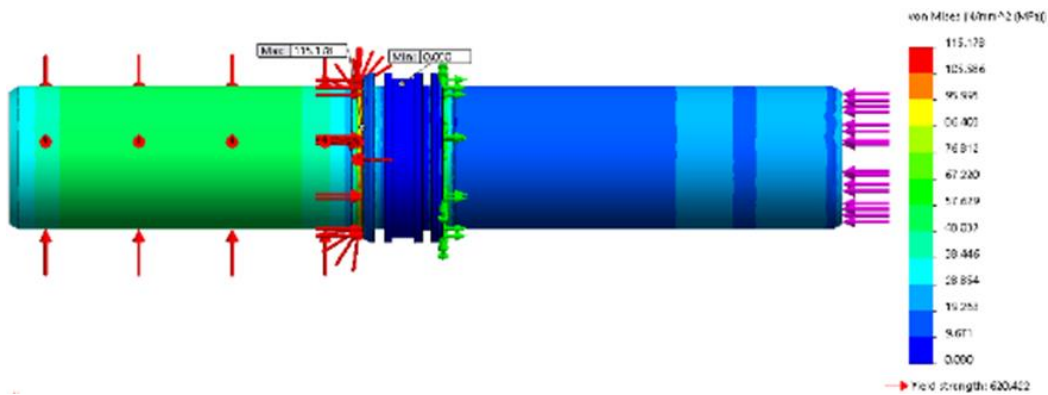


Figure 5: Static nodal stress of the piston rod with applied pressure of 30 MPa [5]

4 Control components of the linear drive

The most important component within a servo hydraulic drive is the servo valve. There are two Moog G-761 valves in this application set [6]. These are 2-stage valves with spool and bushing and dry torque motor. Maximum operating pressure is 315 bar and maximum flow through the valves is rated at 63 L/min. To improve the dynamic of the system, four bladder accumulators with nominal volume 0,75 litres are mounted on the hydraulic cylinders (two on each cylinder). For the setting of operating pressure and for the pressure relief of the hydraulic system, a proportional pressure relief valve is used DBEM (Bosch-Rexroth). For the supply, an axial piston pump Parker PAV32 is used with variable displacement. The hydraulic circuit of the whole system is shown in Figure 6.

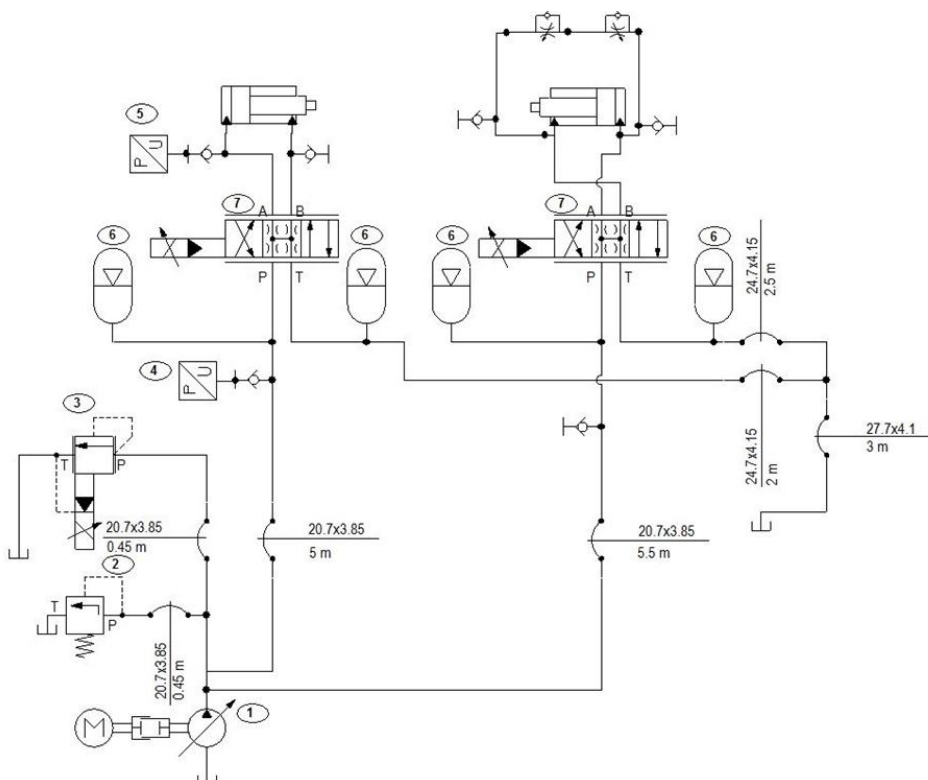


Figure 6: Hydraulic circuit of the system

For the control and monitoring of the entire system, as well for the control of the two servo axis, an open high-performance quad-core CPU controller Beckhoff CX5140-0125 is used, with embedded OS PC. The command signal for servo valves is converted with servo amplifier-control cards. The feedback loop is realised through MTS sensors in the cylinders. An embedded PC also controls the pump and its settings, and the DBEM valve. Additionally, two pressure sensors can measure pressure at different measuring ports (Figure 6).

5 System control

The system is designed as a testing bench for different testing algorithms. Figure 7 shows the possibilities of positioning the cylinders on the testing table.

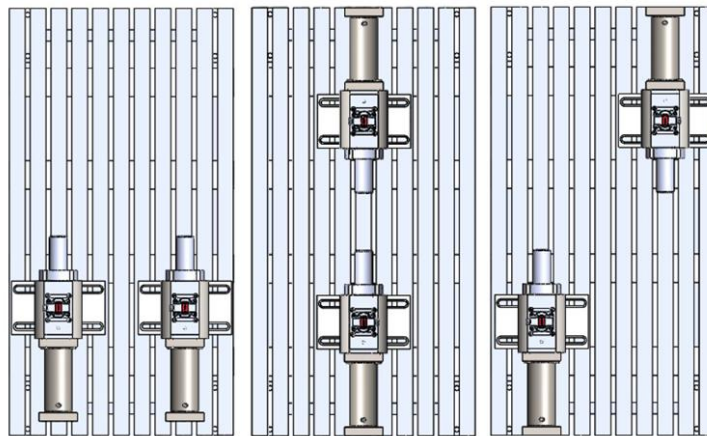


Figure 7: Plausible cylinders' arrangement

On left side of Figure 7, the cylinders are positioned parallel to one another. This position is used for study of problematic parallel movement. In the middle of the figure, the cylinders are positioned opposite one another. This configuration enables connection of the cylinders with load cell, and testing of force control algorithms and/or contra-load profile. On the right of Figure 7, the cylinders enable generation of bending load on the testing element. Different cylinder layouts are also possible, in view of the requirements of testing the object.

As already mentioned, system control runs on a Beckhoff embedded PC. The programme is divided into two separate programmes that communicate with each other. The first programme is a PLC programme, programmed in TwinCAT3, and controls all modules connected to the embedded PC. This programme processes all input, and sends all output signals. It also contains all regulators, and all calculations are done here.

Other programme is used for user interface and analysis of recorded data. It is programmed in a Visual studio in C# language. The benefit of this approach is that, in C#, there are more possibilities for signal processing than in the visualization package included in TwinCAT3. Command values typed in the visualization programme are sent to the PLC programme, values from different sensors and variables on the PLC programme are read by the visualization programme, and their value is represented accordingly.

5.1 PLC programme

The PLC programme receives process input signals and generates output signals. There are different programming languages supported in TwinCat 3. For this programme, a combination of Ladder Logic Diagram (LD) and Structured Text (ST) are used. The programme is divided into

several subprogrammes. They are controlled by a programme called Main. Figure 8 shows a list of all programmes and code of the programme Main.

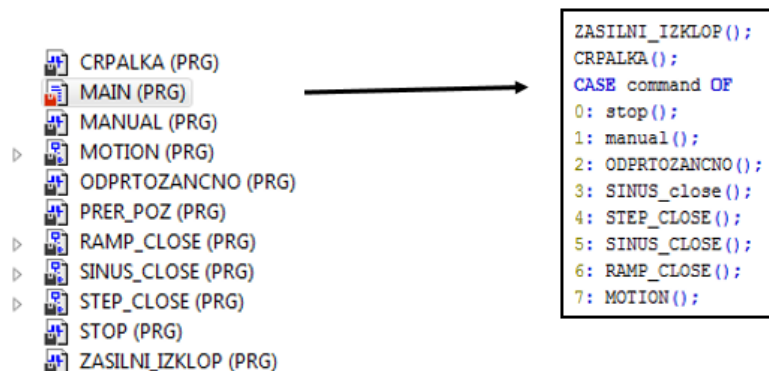


Figure 8: List of all programmes and code of the programme Main

Programmes enable testing the response of the system to step signal, sinus signal, ramp signal, S-profile signal, and it is also possible to drive cylinders manually. Controllers and signal generators are available in TwinCat3 and they are included in the programmes. It is possible to change controller parameters with a user interface.

5.2 User interface

By using the user interface, which can be adapted to the requirements of an individual user, the user can control the whole system and system's parameters. The programme is divided to a series of subprogrammes, used to set parameters and test different control algorithms. The layout of the user interface window for the pump control is shown in Figure 9. It is possible to set different system pressure levels and pump flow via a simple entering of appropriate numerical values for the pressure or flow rate. For reference, there are two graphs. The first graph shows the relation between command signal and set-pressure, and the second graph shows flow in relation to set time of the swashplate.

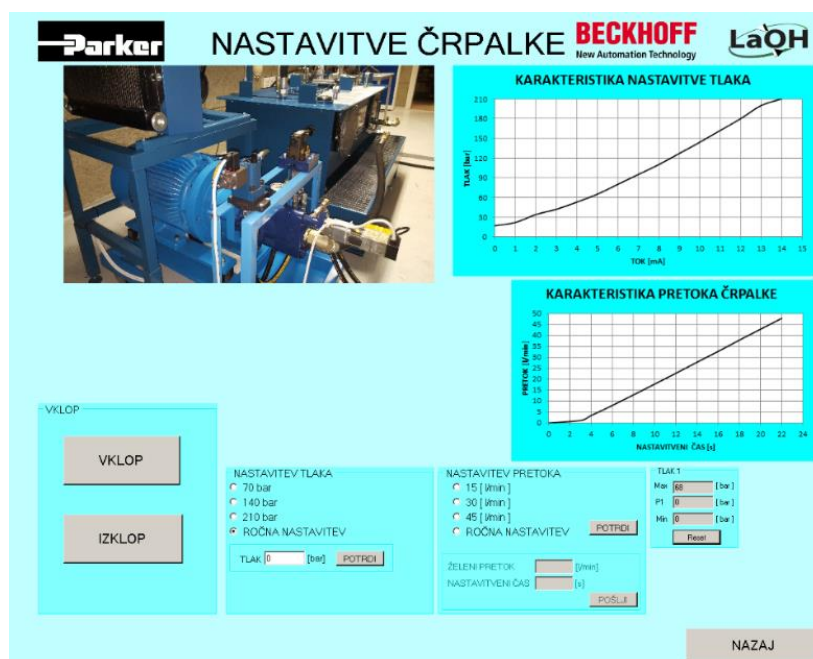


Figure 9: Setting the operating parameters

Data analysis can be performed with the help of a visualization programme and with the use of cursors, which are used to read data on graphs accurately. Another option is that the user exports the recorded graph to Excel. Besides the reference graph plots, the actual position can be shown simultaneously and, in the case of S-profile-control, the speed and acceleration signals as well. Values from pressure sensors are plotted on a different graph. The programme also displays maximal, minimal and current pressure values of the system automatically. The layout of the user-interface window for S-profile control is shown in Figure 10.

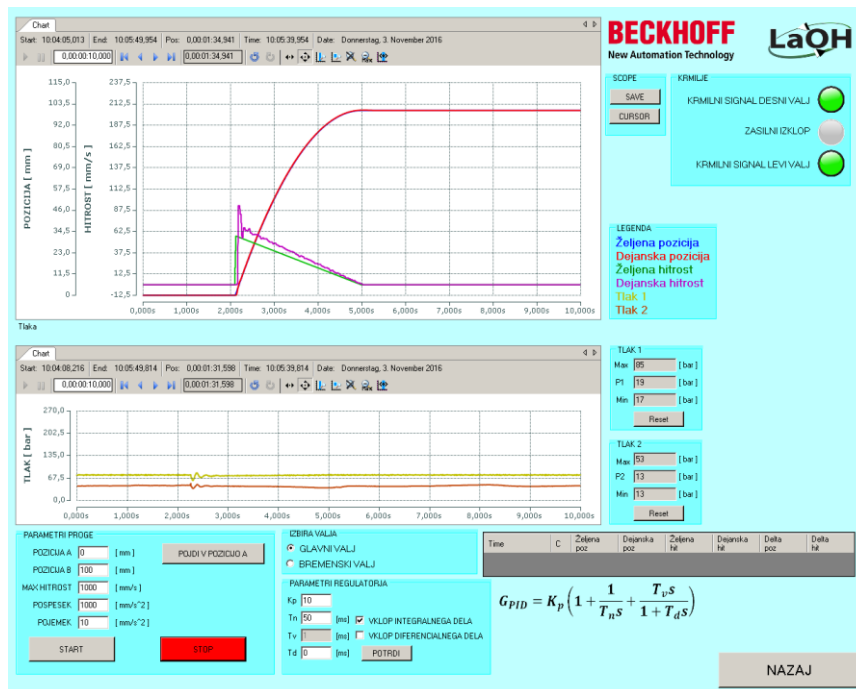


Figure 10: S-profile-control

6 Control example

Figure 11 shows, as an example, step responses of the system before and after the parameter optimization in the case of a classical PID-controller. At this point, we must mention that the parameters of the controller are dependent on the system set up. This means e.g., that if the controller is set for flow in the amount of 15 L/min and 140 bar, it won't work optimally when flow and pressure of the system are changed.

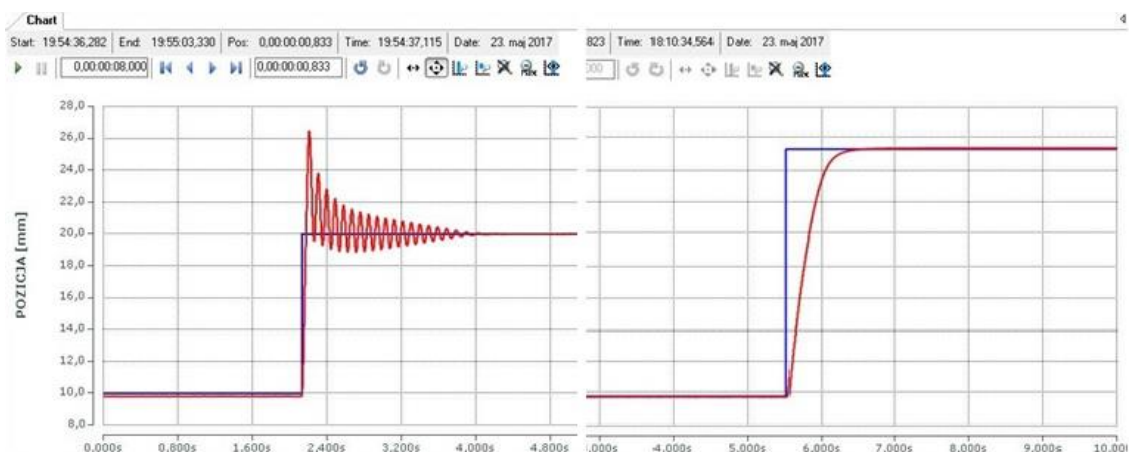


Figure 26: System step response with 25 % overshoot (left), and with fine-tuned controller parameter (right)

In the shown case, the stroke of the rod amounts to 10 mm (change in position from 10 to 20 mm). On the left side of Figure 11 is shown the step response with 25 % overshoot and long settling time. In this case, the integral and differential parameters of the PID-controller were set to 0. On the right side of Figure 11, the integral and differential values were set in such a manner, that the desired position was achieved without overshoot.

7 Conclusion

The main purpose of the project was to design a servo multifunctional hydraulic linear drive system that is suitable for developing and testing of different control algorithms, and for durability tests of different materials, various forms of simple products and complete machinery sets. In order to meet these requirements, the servo cylinders are designed in such a way that they allow the fulfillment of different requirements, both in terms of assembly, and in terms of system dynamics.

From the point of view of the control of a single cylinder, both position control and force control are enabled. In this regard, it is possible to use, and test, various control concepts, from the classical one, to the modern, adaptive non-linear concepts. When designing the individual control concept, and monitoring concept for individual components and the entire system as well, setting of operating parameters, control and visualization of individual quantities, and data archiving ..., such an interface design was taken into account, allowing user-friendly input of data and adapting the appearance of the interface to their needs and desires.

In order to meet all these requirements and options, only "open" control systems for the control electronics and the entire control, monitoring and data management system, together with the appropriate, compatible software, must be used as in the presented case.

References

- [1] Murrenhoff, H.: Servohydraulik, Umdruck zur Vorlesung, IFAS-RWTH Aachen, Shaker Verlag, 2002.
- [2] Jelali, M., Agazarian, Y. M., Kroll, A.: Hydraulic Servo-Systems: Modelling, Identification and Control, Springer, London, 2nd edition, 2002
- [3] Nazir, M. B.: Electrohydraulic servosystem, A practical guideline for control and optimisation, VDM Verlag Dr. Mueller e.J., 2010
- [4] Detiček, E., Župerl, U.: An Intelligent Electro-Hydraulic Servo Drive Positioning, Journal of Mechanical engineering, 57, (2011), 10, pp. 394-404, 2011
- [5] Fanomezantsoa, T.: Designing a servo hydraulic cylinder for test applications, Maribor, Master's thesis, Univerza v Mariboru, Fakulteta za Strojništvo, 2016
- [6] G761 Series Servo Valves. Accessible at WWW:
http://www.moog.com/literature/ICD/Moog-ServoValves-G761_761Series-Catalog-en.pdf, [04.08.2017]

Impact of hydraulic network on operation of linear servo axes

TADEJ JURGEC & VITO TIČ

Abstract The paper presents the impact of a hydraulic network on the operation of hydraulic actuators and an entire hydraulic system. We were particularly interested in the influence of hydraulic accumulators at various pre-charge pressures and the influence of a hydraulic pipeline of different dimensions. The tests were performed using an open-loop controlled servo-valve with sinus signal at various frequencies and amplitudes. One of the aims of the research was to verify experimentally the recommendations on pre-charge pressures of hydraulic accumulators given by manufacturers that are often only defined roughly.

Keywords: • hydraulic • network • accumulator • pre-charge pressure • pressure oscillation •

CORRESPONDENCE ADDRESS: Tadej Jurgec, University of Maribor, Maribor Faculty of Electrical Engineering and Computer Science, Koroška cesta 46, 2000 Maribor, Slovenia, e-mail: tadej.jurjec@gmail.com. Vito Tič, Ph.D., Assistant Professor, University of Maribor, Faculty of Mechanical Engineering, Smetanova ulica 17, 2000 Maribor, Slovenia, e-mail: vito.tic@um.si.

1 Introduction

Choosing the proper hydraulic accumulator size and its pre-charge pressure are essential for the optimal operation and dynamic response of a hydraulic system, especially when operating linear hydraulic servo axes. The hydraulic accumulators can store compressed hydraulic fluid (energy) and discharge it when the pressure drops. Since servovalves and cylinders operate at high speeds and frequencies, they can require a considerable volume (flow) of hydraulic fluid instantly. These accumulators are often placed closed to the servovalves to help overcome restrictions and drag from a long pipeline [1].

The presented research was focused on gas-charged diaphragm accumulators that are placed near servovalves to increase the response time of the servocylinders.

2 Hydraulic system setup

The hydraulic system operating a servoaxis is powered by a Parker PAV 32 axial piston pump driven by an 18,5 kW asynchronous motor capable of delivering around 45 L/min at maximum pressure of 315 bar. An electrically controlled pilot operated proportional pressure relief valve (Bosch Rexroth DBEM 10) is placed near the pump to control the fluid pressure in the pressure line. Figure 1 shows the actual hydraulic system used in the research, whereas Figure 2 presents the corresponding hydraulic plan of the system. Only one servoaxis was used in the research, while the other was disconnected from the hydraulic system.

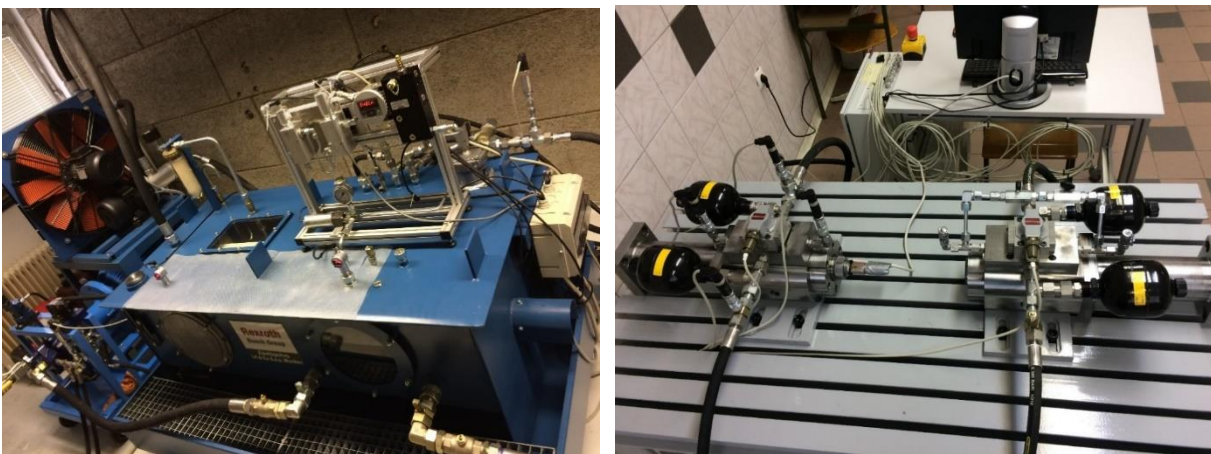
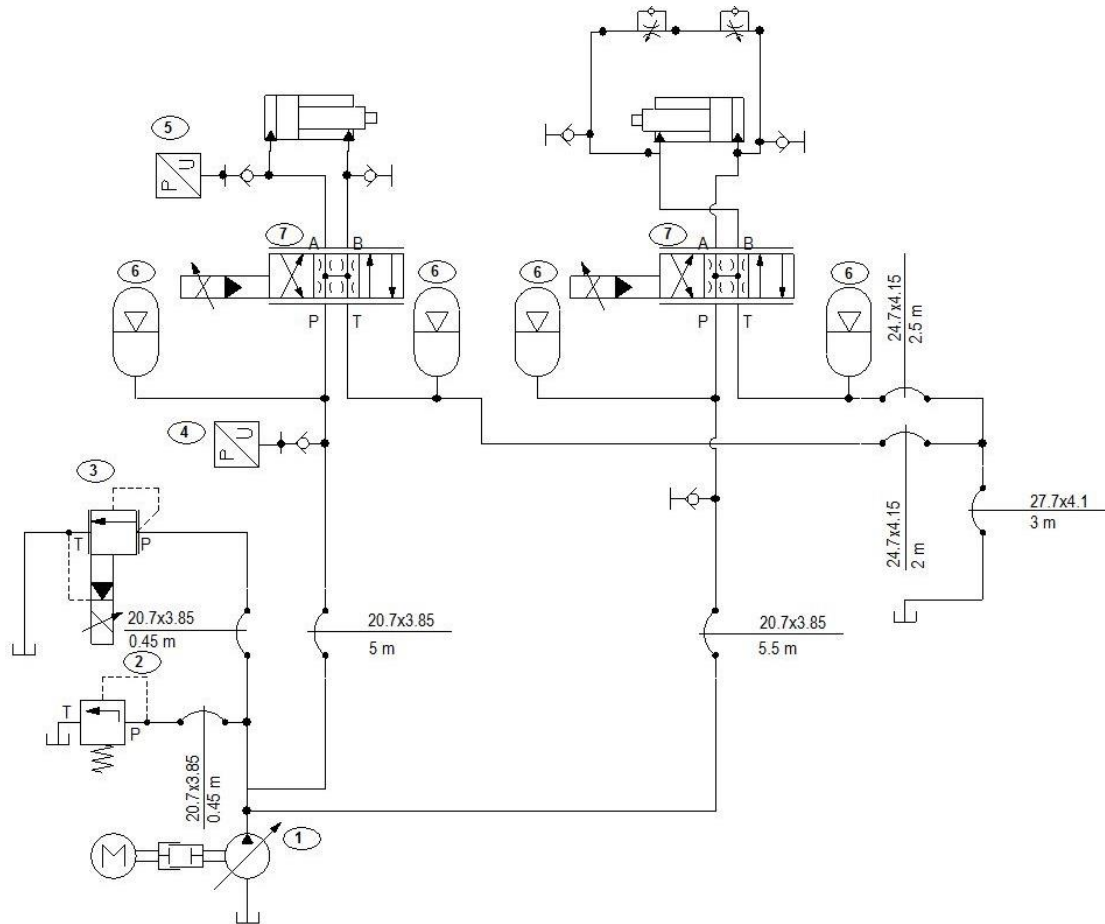


Figure 1: Hydraulic power unit (left) and servoaxes (right)



ID	Component	Manufacturer	Model	Qty.
1	Hydraulic pump	Parker	PAV 32	1
2	Pressure relief valve	Kladivar	VV-6-A	1
3	Proportional pressure relief valve	Rexroth	DBEM 10/51	1
4	Pressure transducer	Hawe	DT 2-4 (0-400 bar)	1
5	Pressure transducer	Hawe	DT 2-4 (0-400 bar)	1
6	Hydraulic accumulator	Hydac	Diaphragm 0,75 L	4
7	Servo_valve	Moog	G-761	2

Figure 2: Hydraulic plan [2]

2.2 Linear servo axis

The linear hydraulic servo system under investigation includes a 74,5 / 63 x 100 mm cylinder driven by a Moog G-761 servovalve, which is a two-stage servovalve with torque motor used in the pilot stage. The valve is equipped with two 0,75 L diaphragm type hydraulic accumulators: One on the P and one at the T line. During the test, the pre-charge pressure of the T accumulator was not under investigation, and was set to a constant pressure of 3 bar.

Experimental measurements, which were taken at 1 kHz, were made at various working points, altering:

- Working pressure – 70, 140 and 210 bar,
- Amplitudes of sinus signal fed to the servovalve – 25, 50 and 75 %,
- Frequency of sinus signal fed to the servovalve – from 0,5 to 20 Hz,
- Accumulator gas pre-charge pressure – from 40 to 110 % of working pressure.

There were 6 pressure transducers placed in the system (not all are shown in Figure 2):

- Right after the pump,
- At the P, T, A and B lines of the servovalve (Figure 3 left),
- Just before the return filter at the tank.

Although this paper only focuses on pressure oscillation in the P line near the servovalve, the other measurements can be used to investigate the pressure and flow conditions in the observed hydraulic network further.



Figure 3: Servocylinder with servovalves and accumulators on P and T (left)
Gas-charge diaphragm type hydraulic accumulator [3]

3 Results

The results of measured pressure oscillation (at the P line near the servovalve) at different working conditions are shown in the following Figures 4 to 7. The results are presented as the RMS value of the pressure oscillation: Average working pressure was subtracted from the measured signal, then the RMS was calculated.

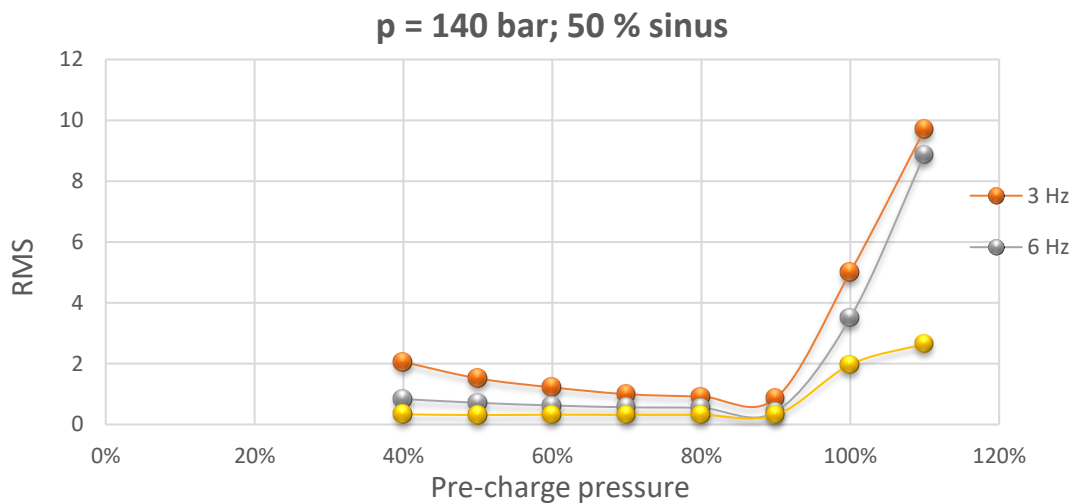


Figure 4: Pressure oscillation at 140 bar, 50 % amplitude of sinus signal to valve

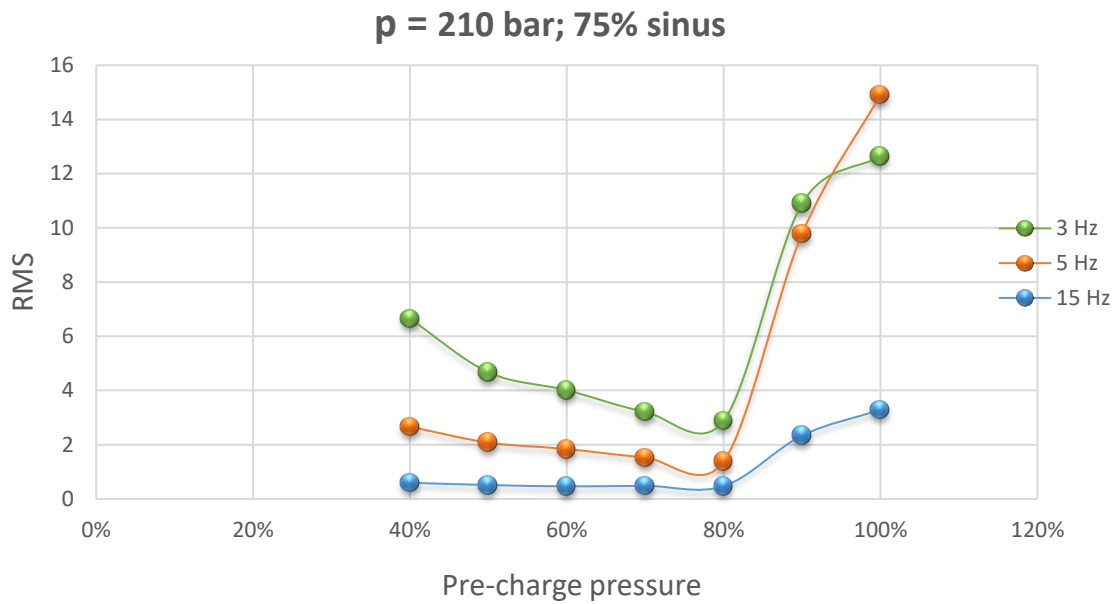


Figure 5: Pressure oscillation at 210 bar, 75 % amplitude of sinus signal to valve

The first phenomena we can notice from the figures are that the pressure oscillation is most severe at frequency of 3 Hz due to the natural frequency of the hydraulic cylinder, especially in the region of the overcharged accumulator, which corresponds to the hydraulic network without an accumulator.

Figures 4 and 6 show two working points where the minimum pressure pulsation was recorded at 90 % of accumulator pre-charge, whereas Figures 5 and 7 show two working points where the minimum pressure pulsation was recorded at 80 % of accumulator pre-charge. In the latter two cases, the pressure pulsation at 90 % precharge is much greater than in the first two cases at 80 % pre-charge. Thus, if we would like to pre-charge an accumulator to cover various working points of the linear servo axis, we recommend pre-charging it to 80 % of working pressure.

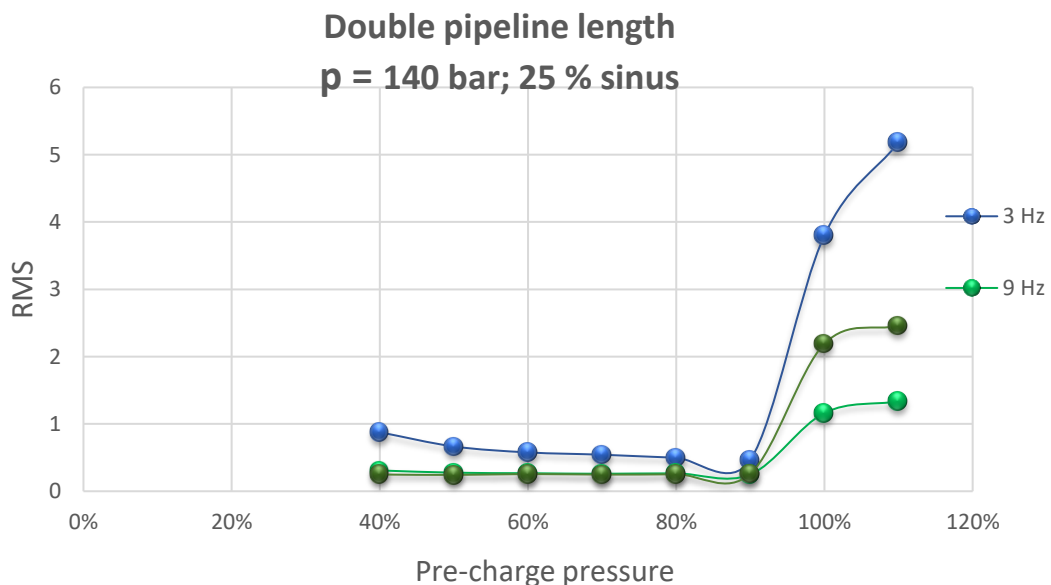


Figure 6: Pressure oscillation at 140 bar, 25 % amplitude of sinus signal to valve, double pipeline length

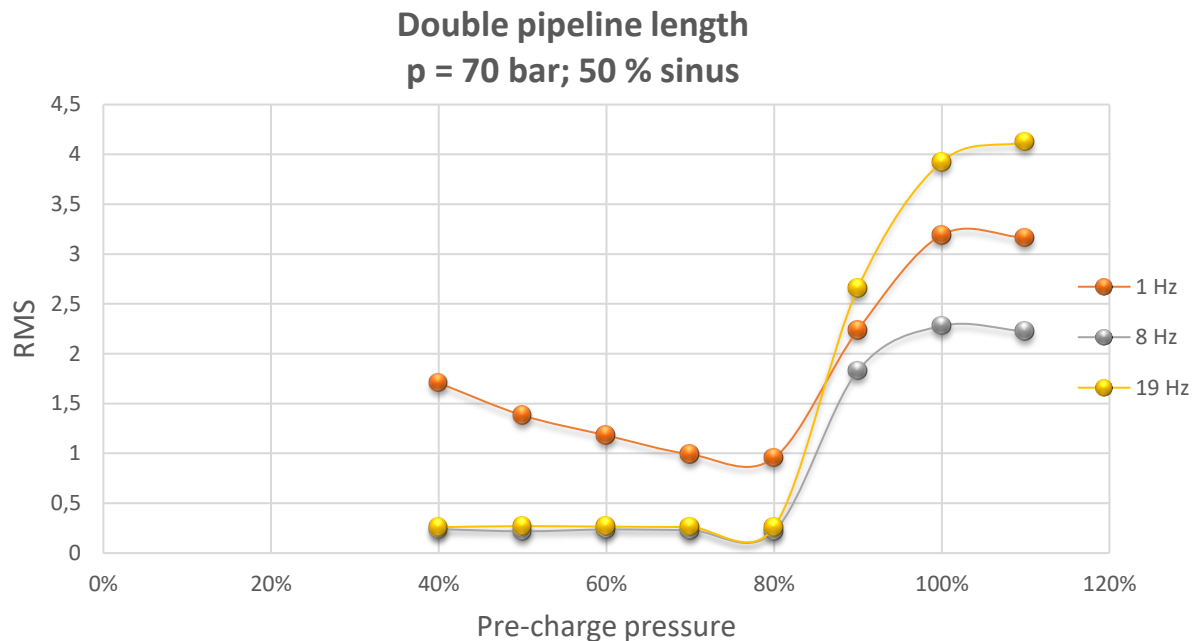


Figure 7: Pressure oscillation at 70 bar, 50 % amplitude of sinus signal to valve, double pipeline length

Comparing the measurements at nominal pipeline length (cca. 5 m) and extended pipeline length at P and T to double their length (cca. 10 m), we can also conclude that such extension has no significant influence on the pressure oscillation at line P.

4 Conclusion

The experiments conducted in the scope of this research allowed us to find optimal pre-charge pressures for the hydraulic accumulators used on the servo axes to improve dynamic behaviour of the hydraulic cylinders.

The paper presents only the first findings in the scope of this extensive research, where pressure oscillations were recorded at six different points in the servo hydraulic network. In the future, we are planning to conduct more complex data analysis and compare it to the corresponding simulation model.

References

- [1] Savić, V., Knežević, D., Lovrec, D., Jocanović, M., Karanović, V.: Determination of pressure losses in hydraulic pipeline systems by considering temperature and pressure. *Strojniški vestnik*, ISSN 0039-2480, 2009, Vol. 55, No. 4, str. 237-243, ilustr. http://www.sv-jme.eu/scripts/download.php?file=/data/upload/2009/SV-4-09/Delovna/4_Savic.pdf, 2009
- [2] Štefane, M.: Implementation and first start of linear electrohydraulic servo axis. Univerza v Mariboru, Fakulteta za elektrotehniko, računalništvo in informatiko, Master thesis, 2017
- [3] N.N.: Freudenberg hydraulic accumulators. Available at WWW: <https://www.fst.com/products/hydraulic-accumulators-and-suspension-systems/hydraulic-accumulators?UserSource=Tobul> [12. 12. 2016]

A selection of the latest specifications and performance requirements for environmentally considerate hydraulic fluids ASTM D8029-16, Bosch Rexroth RE 90235, EPA VG 2013

MARTIN RUCH & PATRICK LAEMMLE

Abstract Since 2002, introducing ISO 15380 specifying minimum requirements for readily biodegradable hydraulic fluids classified HETG, HEPG, HEES or HEPR, a few important specifications were launched recently.

We would like to shortly highlight the following selection of important and latest regulations and standards for environmentally considerate hydraulic fluids: ASTM D8029-16; Standard Specification for Biodegradable, Low Aquatic Toxicity Hydraulic Fluids.

Bosch Rexroth RE 90235; Rating of hydraulic fluids for Rexroth hydraulic components (pumps and motors). PANOLIN HLP SYNTH 32 is the first and still only readily biodegradable hydraulic fluid successfully passed Bosch Rexroth RE 90235 and being published on the Bosch Rexroth Fluid Rating List RDE 90245.

EPA Vessel General Permit 2013 (VGP); EPA test requirements state, all vessels must use an EAL in all oil to sea interfaces. “Environmentally Acceptable Lubricants” means lubricants that are biodegradable and minimally-toxic and are not bioaccumulative.

Keywords: • hydraulic fluids • biodegradable • specification • low aquatic toxicity • Bosch Rexroth test

CORRESPONDENCE ADDRESS: Martin Ruch, PANOLIN International Inc, Bläsिमühle 2 – 6, 8322 Madetswil, Switzerland, e-mail: martin.ruch@panolin.com. Patrick Laemmle, PANOLIN International Inc, Bläsिमühle 2 – 6, 8322 Madetswil, Switzerland, e-mail: patrick.laemmle@panolin.com.

<https://doi.org/978-961-286-086-8.10>

ISBN 978-961-286-086-8

© 2017 University of Maribor Press

Available at: <http://press.um.si>.

1 Introduction

Since 2002, introducing ISO 15380 specifying minimum requirements for readily biodegradable hydraulic fluids classified HETG, HEPG, HEES or HEPR, a few important specifications were launched recently.

Minimum requirements as well as ratings help equipment manufacturers and endusers to easily select the correct hydraulic fluid for the specific application. Within readily biodegradable hydraulic fluids not only technical parameters and performance are important. Also the eco-tox profile has to be respected.

Especially within the eco-tox profile of a readily biodegradable hydraulic fluid it is important to specify the relevant test methods to avoid misinterpretation respectively force all fluid manufacturers to apply to the relevant minimum requirements.

2 ASTM D8029-16

2.1 Standard Specification for Biodegradable, Low Aquatic Toxicity Hydraulic Fluids

This specification covers performance requirements for biodegradable hydraulic fluids with low aquatic toxicity used in industrial/mobile hydraulic applications. There are some cases where biodegradable fluids have been found to perform differently than traditional mineral oils, which makes separate performance requirements desirable.

Also included in this specification are requirements for environmental behavior and physical properties as well as compatibility of mixtures of hydraulic fluids. [1]

2.2 Technical Parameters

ASTM D8029-16 was approved January 01, 2016 and published in February 2016. Under the direct responsibility of subcommittee D02.N0, involving different parties from the lubricants and additive industry, the latest standard for readily biodegradable hydraulic fluids was successfully developed.

The following parameters within ASTM D8029-16 are remarkable or even unique:

- This specification assumes that all biodegradable hydraulic fluids shall have a minimum impact on human health, which is documented in the safety data sheet of offering a labeling-free product in accordance with globally harmonized system (GHS) regulation.
- ISO VG 15 is included (important within steel-water works or hydro power installations).
- ASTM D665B is subject to report.
- ASTM D2070 Standard Test Method for Thermal Stability of Hydraulic Oils.

2.3 Eco-Tox Profile

The eco-tox profile of an environmental considerate hydraulic fluid is defined within table on Figure 1. It is remarkable that the *ultimate* biodegradability according to OECD 301 B, respectively comparable methods like ASTM D5864 or ISO 9439, is requested within an international standard again. Both major standardization bodies, ASTM and ISO, refer to the

ultimate biodegradability which leads to the conclusion that all other method (e.g. primary biodegradation etc.) are no longer a topic to be discussed and argued at the moment.

Characteristics of Tests	Units	Requirements	EPA Standard
Ultimate Biodegradability, min ^A	%	60	Test Method D5864 ^B /OPPTS 835.3110 [former 712-C-98-076]
	%	67	Test Method D6731 ^B /OPPTS 835.3110 [former 712-C-98-076]
Bioaccumulation ^F		Log K _{ow} <3 or >7	OECD Test No. 117 ^G
		BCF ≤ 100 L/kg	OECD Test No. 305 ^G
Acute Aquatic Toxicity			
Acute fish toxicity, 96 h, LC50, min ^A	mg/L	100	OPPTS 850.1075 ^C [former 712-C-96-118]
Acute Daphnia toxicity, 48 h, EC50, min ^A	mg/L	100	OPPTS 850.1010 ^D [former 712-C-96-114]
Acute Algae toxicity, 72 h, EC50, min ^A	mg/L	100	OPPTS 850.5400 ^E [former 712-C-96-164]
Renewability	%	Report	Test Methods D6866

Figure 1: Environmental Behaviour Requirements; excerpt from ASTM D8029-16

2.4 Conclusion regarding ASTM D 8029-16

ASTM D 8029-16 represents the latest independent standard for biodegradable hydraulic fluids and incorporates a complete eco-tox profile including bioaccumulation as well as a certain technical performance. Thermal stability evaluated by ASTM D2070 will lead to a discrimination of performance. Oxidation stability testing by ASTM D943 (modified; no water) remains integral part; unfortunately only very long test duration would lead to any discrimination. The setup of a suitable oxidation test for EALs (based on esters) would be desirable.

3 Bosch Rexroth RE 90235

3.1 Rating of hydraulic fluids for Rexroth hydraulic components

Rexroth fluid test RFT-APU-CL (Rexroth Fluid Test Axial Piston Unit Closed Loop). Fluid test for closed loop applications using a combination of units consisting of a hydraulic pump A4VG045EP and a hydraulic motor A6VM060EP.

The safe and reliable operation of industrial and mobile equipment is only possible if the hydraulic fluid used is selected with respect to the application. The main tasks of the hydraulic fluid are e.g. transmission of power, lubricate the components, reduction of friction, corrosion prevention and heat dissipation. Unfortunately the common element “hydraulic fluid” is often disregarded during conceptual design. Increased requirements on machines and equipment constantly raise the quality requirements on the hydraulic fluid. For choosing a suitable hydraulic fluid, adequate knowledge and experience are needed. Therefore Bosch Rexroth offers the rating of hydraulic fluids for Rexroth hydraulic components as a service. [2]

3.2 Technical Parameters

Bosch Rexroth does define the technical parameters and minimum requirements for “environmentally acceptable hydraulic fluids” as follows; *ISO 15380 and additional Bosch Rexroth requirements including pump test RFT-APU-CL.*

The following technical parameters are remarkable or outstanding within this specification:

- elastomer compatibility 72 NBR 902 after 1008 hours at 100 °C,
- elastomer compatibility 75 FKM 595 after 1008 hours at 130 °C,
- ASTM D2070 Standard Test Method for Thermal Stability of Hydraulic Oils,
- pump test RFT-APU-CL.

3.3 Pump Test RFT-APU-CL

Fluid test for closed loop applications using a combination of units consisting of a hydraulic pump A4VG045EP and a hydraulic motor A6VM060EP. This fluid test represents the requirements on a hydrostatic transmission. [2]

The RFT-APU-CL is splitted into three test cycles; break-in test followed by a swivel cycle test and a final corner power test. The operating data age given in Figure 2.

Operating data		
1. Break-in test	A4VG045 EP	A6VM060 EP
Speed	2000 min ⁻¹	2000 min ⁻¹
Operating pressure	250 bar	250 bar
Leakage temperature Hydraulic motor		60 °C at port T
Operating time	10 h	10 h
2. Swivel cycle test	A4VG045 EP	A6VM060 EP
Speed	4000 min ⁻¹	4000 min ⁻¹
Operating pressure	450 bar	450 bar
Leakage temperature Hydraulic motor		100 °C at port T
Operating time	300 h	300 h
3. Corner power test	A4VG045 EP	A6VM060 EP
Speed	4000 min ⁻¹	4000 min ⁻¹
Operating pressure	500 bar	500 bar
Leakage temperature Hydraulic motor		100 °C at port T
Operating time	200 h	200 h

Figure 2: Operating data; excerpt from RE 90235; RFT-APU-CL

These demanding test conditions in combination with the before mentioned technical parameters lead to an OEM specification representing the latest state-of-the-art and most complete fluid rating at the moment.

PANOLIN HLP SYNTH 32 is the first and until today only readily biodegradable hydraulic fluid fulfilling all criteria according to Bosch Rexroth RE 90235 and therefore it is listed within Bosch Rexroth Fluid Rating List RDE 90245 [3].

M. Ruch & P. Laemmle: A selection of the latest specifications and performance requirements for environmentally considerate hydraulic fluids ASTM D8029-16, Bosch Rexroth RE 90235, EPA VG 2013



Figure 3: Test bench RFT-APU-CL and awarding dot for PANOLIN HLP SYNTH 32

To demonstrate the outstanding performance of PANOLIN HLP SYNTH 32 and the demanding parameters by Bosch Rexroth RFT-APU-CL please find below a selection of the components at initial stage, after the test passed with PANOLIN HLP SYNTH 32 and examples of failed parts.



Figure 4: Components out of RFT-APU-CL; pictures by Bosch Rexroth AG

3.4 Eco-Tox Profile

Within RE 90235 the minimum requirements towards eco-tox profile refer to ISO 15380.

Characteristic of test	Unit	Requirement	Test method or applicable standard
Biodegradability, min.	%	60	ISO 14593 or ISO 9439
Toxicity ^a			
Acute fish toxicity, 96 h, LC50, min.	mg/l	100	ISO 7346-2
Acute Daphnia toxicity, 48 h, EC50, min.	mg/l	100	ISO 6341
Bacterial inhibition, 3 h, EC50, min.	mg/l	100	ISO 8192
^a Water-soluble fluids shall be tested according to the test method cited. Fluids with low water solubility shall be tested using water-accommodated fractions, prepared according to ASTM D6081.			

Figure 5: Environmental behaviour requirements for categories HETG, HEPG, HEES and HEPR; excerpt from ISO 15380

3.5 Conclusion regarding RE 90235

Bosch Rexroth RE 90235 represents one of the most demanding and complete minimum requirements for environmental considerate hydraulic fluids. A positive aspect is the inclusion of “real life” elastomers instead of Standard Reference Elastomers (SREs).

4 EPA Vessel General Permit 2013

4.1 Scope

This permit became effective on December 19, 2013 and will be renewed in 2018. VGP is an extension of the US EPA clean water act and a detailed review of;

- environmental protection procedures,
- vessel inspection schedules,
- manning levels,
- crew training and qualification,
- recording and documentation.

EPA Vessel General Permit 2013 represents a collection of mandatory management practices under which vessels are authorized to discharge and is a permit, authorizing effluent discharges incidental to normal vessel operation. It applies to all commercial vessels (> 24 meters in length and > 8 m³ ballast capacities) in US waters (3 nm of US Coast; can be up to 12 nm). The VGP deals with 27 waste streams for discharges, such as fuel bunkering, ballast water, bilge water and many more as well as oil-to-sea interfaces where the use of environmental acceptable lubricants is a must. [4]

4.2 Key Strands

The EPA Vessel General Permit 2013 adopts best management practice for;

- self inspection,
- rectification,

M. Ruch & P. Laemmler: A selection of the latest specifications and performance requirements for environmentally considerate hydraulic fluids ASTM D8029-16, Bosch Rexroth RE 90235, EPA VG 2013

- documentation,
- self reporting.

Failure to report, record or rectify causes of pollution can incur heavy penalties including fines, black-listing and imprisonment.

4.3 Oil-to-sea interfaces / Technical Parameters

There are no technical parameters specified but the use of environmental acceptable lubricants is a must at all oil-to-sea interfaces. The technical parameters are defined by the component manufacturers of stern tubes, propulsions, hydraulic systems and all other installations used on a vessel.

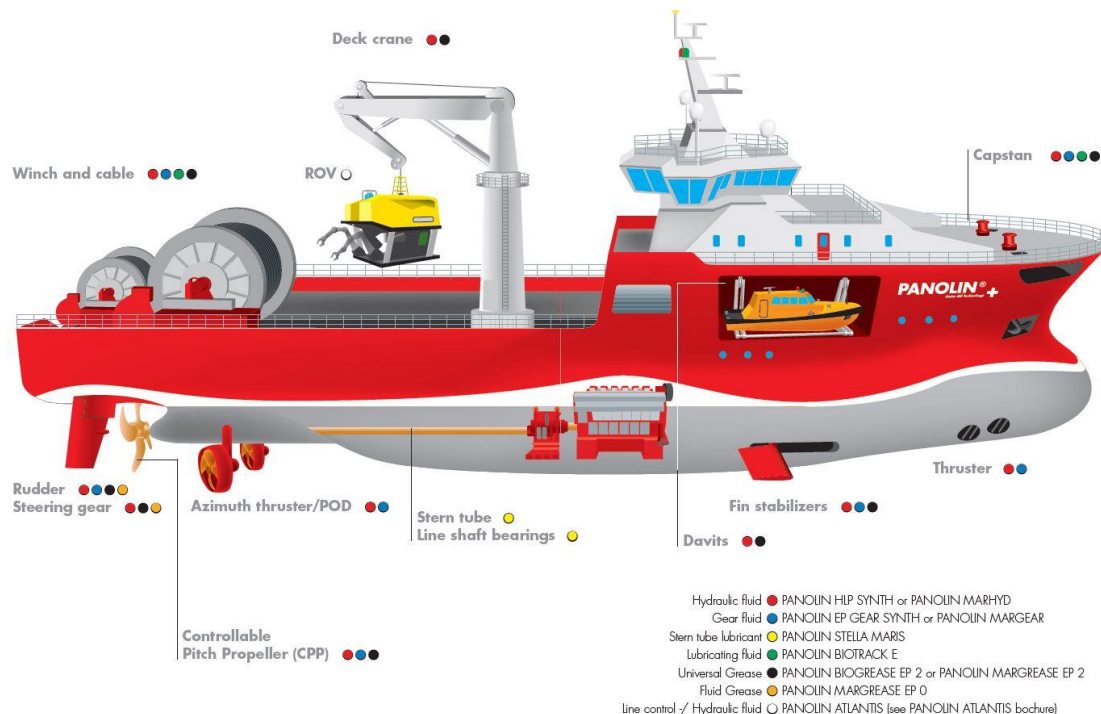


Figure 6: PANOLIN ECLs application guide

4.4 Exo-Tox Profile for Lubricants

“Environmentally Acceptable Lubricants” means lubricants that are “biodegradable” and “minimally-toxic,” and are “not bioaccumulative” as defined in this permit. For purposes of the VGP, products meeting the permit’s definitions of being an “Environmentally Acceptable Lubricant” include those labelled by the following labelling programs: Blue Angel, European Ecolabel, Nordic Swan, the Swedish Standards SS 155434 and 155470, Convention for the Protection of the Marine Environment of the North-East Atlantic (OSPAR) requirements, and EPA’s Design for the Environment (DfE).

Compliance with EPA Vessel General Permit 2013

Assessment in accordance to requirements of Vessel General Permit 2013

- a VGP accepts result based on formulation and main constituents
– see Appendix A, VGP 2013 final version
- b VGP accepts testing of formulation – see Appendix A, VGP 2013 final version
- c OECD test method valid for single substances testing only;
data reported should be seen as a summary of all single
> 1 % components in stated formulation
- d Report

PANOLIN HLP SYNTH, ISO VG 15/22/32/46/68/100				
Characteristics of test	Units	Specification	Result	Method
Biodegradability ^a	% ThOD	>60	>60	OECD 301, 306
Toxicity ^b				
Algae	LC ₅₀	>100 mg/l	>100	OECD 201
Daphnia	EC ₅₀	>100 mg/l	>100	OECD 202
Fish	LC ₅₀	>100 mg/l	>100	OECD 203
Bioaccumulation ^c	Log K _{ow}	<3 or >7	pass	OECD 107, 117
Visible sheen	Gloss, visual color etc.	– ^d	no visual color	58 FR 12507

Figure 7: Compliance with EPA Vessel General Permit 2013

5 Summary**5.1 Minimum requirements and specifications ... where does it lead to**

The use and purpose of minimum requirements, specifications and ratings by authorities, standardization committees, OEMs and equipment manufacturers are important and simplify the process to do the right choice. They will lead to a differentiation of performance and eco-tox profile for readily biodegradable hydraulic fluids on the market and demonstrate the need and increasing demand for sustainable and environmentally considerate lubricants.

Nevertheless, we want to point out that all these new requirements and fluid tests are expensive and sometimes limit the reconcilability of different requirements on one fluid. It is important to carefully select the need and necessity of further standardization procedures and to involve all parties to create relevant criteria which lead to successful and recognizable market implementation.

References

- [1] ASTM International: ASTM D8029-16 Standard Specification for Biodegradable, Low Aquatic Toxicity Hydraulic Fluids
- [2] Bosch Rexroth AG: RE 90235/02.2015 Rating of hydraulic fluids for Rexroth hydraulic components (pumps and motors)
- [3] Bosch Rexroth AG: RDE 90245/03.2017 Bosch Rexroth Fluid Rating List
- [4] EPA: Vessel General Permit for discharges incidental to the normal operation of Vessels (Final 2013 VGP)

Application of hydraulic and gear oils in the food processing industry

MITAR JOCANOVIĆ, VELIBOR KARANOVIĆ, VITO TIČ, MARKO OROŠNJAK & DRAGAN SELINIĆ

Abstract Technological production systems of food processing industry use machines that have specific requirements such as safe interaction of machine elements with raw processing material. To satisfy stringent requirements, different types of lubricants are developed. This paper gives an example of synthetic ester based hydraulic and gear oil use, in the food processing industry.

Keywords: • food processing industry • hydraulic oil • gear oil • lubrication • tribology •

CORRESPONDENCE ADDRESS: Mitar Jocanović, Ph.D., Senior Professor, University of Novi Sad, Faculty of Technical Sciences, Trg Dositeja Obradovića 6, Novi Sad 106314, Serbia, e-mail: mitarj@uns.ac.rs. Velibor Karanović, Ph.D., Assistant Professor, University of Novi Sad, Faculty of Technical Sciences, Trg Dositeja Obradovića 6, Novi Sad 106314, Serbia, e-mail: velja_82@uns.ac.rs. Vito Tič, Ph.D., Assistant Professor, University of Maribor, Faculty of Mechanical Engineering, Smetanova ulica 17, 2000 Maribor, Slovenia, e-mail: vito.tic@um.si. Marko Orošnjak, Assistant, University of Novi Sad, Faculty of Technical Sciences, Trg Dositeja Obradovića 6, Novi Sad 106314, Serbia, e-mail: orosnjak@uns.ac.rs. Dragan Selinić, OLMA d.o.o, Beograd, Bulevar Mihajla Pupina 10D/III, 11070 Novi Beograd, Serbia, dragan.selinic@olma-lubricants.com.

1 Introduction

Application of food-grade lubricants in food processing industry demands special types of base oils and additives, which must meet stringent requirements, set by the NSF (National Sanitation Foundation) Class H1 standard. The H1 specification refers to the food-grade lubricants used in food, feed and pharmaceutical processing industry, and packaging equipment environments where exist the possibility of incidental food and drug contact [1]. NSF was established in the 1940's as the national foundation for standardization, setting special requirements for lubricants used in food industry on American market.

In addition to the discussed criteria, food-grade lubricants meet other international standards in food-processing industry, such as:

- Halal,
- Kosher,
- ISO 22000 – food-safety standards, and
- GMP - manufacturers of drugs, blood and medical devices.

Depending on the mode of application (liquid, semi-liquid, solid or aerosol), food-grade lubricants must often meet stringent requirements of machine exploitation, while remaining safe in contact with processed food [2].

Hydraulic and gear H1 oils can be used in the lubrication of all types of compressor applications including some types of refrigeration compressors, vacuum pumps, air lines, chains, bearings, generally speaking in all lubrication and heat transfer applications where there is a chance of incidental contact with food, food stuffs, drinking water, potable water, or ground water may occur.

Typically, these applications can be found in the following industries: Meat and Poultry Processing Plants, Egg Processing Plants, Fish and Seafood Processing Plants, Breweries and Wineries, Soft Drink and Bottling Plants, Vegetable and Fruit Processors, Cheese and Cheese Product Producers, Bakeries, Snack Food Manufacturers, Pasta Manufacturers, Pet Food and Animal Feed Producers, Oil Mills and Seed Cake Processors, Pharmaceutical and Drug Manufacturers, Cosmetic Manufacturers, Food and Beverage Container Manufacturers, Paper and Paperboard Manufacturers, Water Well Drillers, Drinking and Potable Water Treatment Plants.

This paper reviews two examples: gear reducer oil usage in a lubrication system of a cigarette-making machine, and a hydraulic oil used for Blow/Fill/Seal hydraulic machine systems.

2 Physical-chemical characteristics of hydraulic and gear oil in for use in the food industry

Just as with other types of standard industrial lubricating oils, all other physical/chemical properties food-grade lubricants must match the quality of conventional mineral oils.

The base oils which are contained in food-grade hydraulic and gear reducer oils are manufactured according to H1 and are predominantly of ester type [3]. The majority of synthetic esters (among various types) are quickly biologically degradable, almost matching vegetable oils in that respect, as proven by numerous experiments [2, 3, 4]. However, the advantage of synthetic esters lies in their better oil oxidation stability and pour point at low temperatures. Another advantage is their ability to mix with mineral oils.

Synthetic ester based oils are used for manufacture of various types of products, including: hydraulic oils, oils for two-stroke gasoline engines, oil mixtures for Diesel engines used in ecologically sensitive environments (forestry, river and lake shipping, etc.), gear reducer oils and all other industrial oils which must meet ecological and food-safety requirements [5, 6].

Generally, the synthetic ester based oils perform exquisitely in comparison with their mineral base counterparts, regarding:

- thermal stability,
- oxidation stability,
- low volatility – this results in less make-up requirements due to evaporation loss,
- replacement intervals (longer, compared to mineral oils)
- viscosity index (VI) – temperature properties,
- flow properties at low temperatures,
- operating temperature limitations,
- resistance to radiation,
- resistance to flame.

As regards chemical characteristics, hydraulic and gear reducer oils used in food processing industry must meet following requirements:

- Good corrosion properties - according to ASTM D-130 copper corrosion test, allowed limits are 1a to 1b [7];
- Lower values of total acidity number –TAN, approximately 1 (0.9 – 1.1), as opposed to conventional hydraulic and gear reducer oils which feature 2 and 3 mgKOH/g and higher. Tests are performed according to ASTM D-974 standard [8];
- Resistance to demulsification of food-grade hydraulic and gear reducer oils should also meet high standards. According to ASTM D 1401 10-minute test, mixture of 40ml oil and 40 ml water in a test tube must not result in a visible emulsion. The result is expressed as 40/40/0 (oil/water/emulsion) [9];
- Foaming of hydraulic and gear reducer oils should also be minimized to meet stringent requirements. During first stage of test, oil sample is tested at 24°C for 10 minutes, followed by the second 10-minute stage at 94°C, and the third 10 minute stage at 24°C. This experiment simulates real operating conditions of oil at various temperatures and loads, allowing the foaming to be monitored. The test result should equal zero. One of the most widely accepted specifications for such testing is ASTM D-892 [10];
- Corrosion protection test also shows that this types of oils must meet stringent exploitation requirements. According to ASTM D-665 A&B specification, the result of test should be - *pass* [11];
- Lubricating characteristics of food-grade hydraulic and gear reducer oils are tested according to various specifications, of which the most widely used are:
 - Four Ball test – a test with four balls where the oil sample is tested for a period of one hour at 75°C, under the 40 kg load and 1200 rpm. The result is a wear trace on the test ball which must not exceed 0.4 mm (ASTM D – 4172) [12];
 - Shell Four Ball EP test (ASTM D-2783) - gear reducer oils [13];
 - Timken OK wear test (ASTM D-2782) [14];
 - Vickers Pump Wear test (ASTM D-2882) - hydraulic oils [15];

- FZG test (DIN 14635-1 or ASTM D-5182), which uses various loads to monitor the intensity of wear between a meshed pair of gears. Test result values depend on the meshed pair used - class 10 corresponds to light loads, while class 12 corresponds to heavy loads [16, 17];
- Oxidation stability test by a rotating bomb, according to ASTM D-2272, tested oil should be stable after a 250-minute test interval [18].

The discussed physical/chemical properties are common to all types of hydraulic and gear reducer oils, from conventional to the specific ones. However, they differ with respect to boundary values, which are more stringent for food-grade lubricant oils.

3 H1 gear reducer oil for lubrication of cigarette filter making machine in tobacco industry

Machines used for processing and packaging in tobacco industry are specific both design and application-wise. The problem of lubricating components and assemblies in these machines lies in the fact that the lubricant must possess qualities, which allow it to be exposed to tobacco without compromising its safety.

The cigarette filter-making machine is specific in terms of operating at very high speeds, which range between 8.000 and 20.000 cpm (cigarettes per minute). During operation, a compact circulation system for lubrication, with a 40-liter tank and lubrication pump capacity of 5.8 l/min, performs the task of lubricating all critical points. Shown in Figure 1 is a photo image of the machine, while Figure 2 shows the head, which rotates at high speed and attaches, filters to cigarette paper (position 3, Figure 3).



Figure 1: Filter Maker machine [19]



Figure 2: Rotating wheel, which attaches filters to cigarette papers [19]

Figure 3 illustrates the lubrication circulating system and the cross-sections of all lubrication points.

The Filter Maker machine has six lubrication points, which are vital to machine operation:

- Worm/worm wheel pair (Position 1) teeth contact is maintained over a point;
- Gear reducer with conical gears (Position 2) – teeth contact is maintained across a line;
- Main axle bearing the rotating head (Position 3);
- Roller bearing DIN 628 (Position 4) – the ball and cage maintain a point contact;
- Roller bearing DIN 625 (Position 5) – the ball and cage maintain a point contact;
- Gear reducer with conical gears (Position 6) – teeth contact is maintained across a line.

Due to specific contacts, the worm/worm wheel pair is the most critical component (Position 1), together with the roller bearings (Positions 4 and 5) which maintain a point contact between working elements. In order to reduce wear, gear reducer oil used in the circulation system should, in addition to other properties, possess good EP (extreme pressure) and AW (anti wear) characteristics, i.e., good lubrication properties which are maintained under high load pressures, and friction reduction under high rpm's. The compact circulation system provides just the adequate lubrication with a quick circulation of lubricant fluid, which takes 8 minutes to pass through the pump and the entire circulation system.

The manufacturer recommends oil change at every 4000 hours of machine operation. However, within the discussed system, this oil retains its lubricating characteristics even after 8000 hours of machine operation. Considering its characteristics, this type of gear reducer oil allows very long exploitation providing regular maintenance (absence of water and solid particles, and stable operating temperature - as provided by the discussed system).

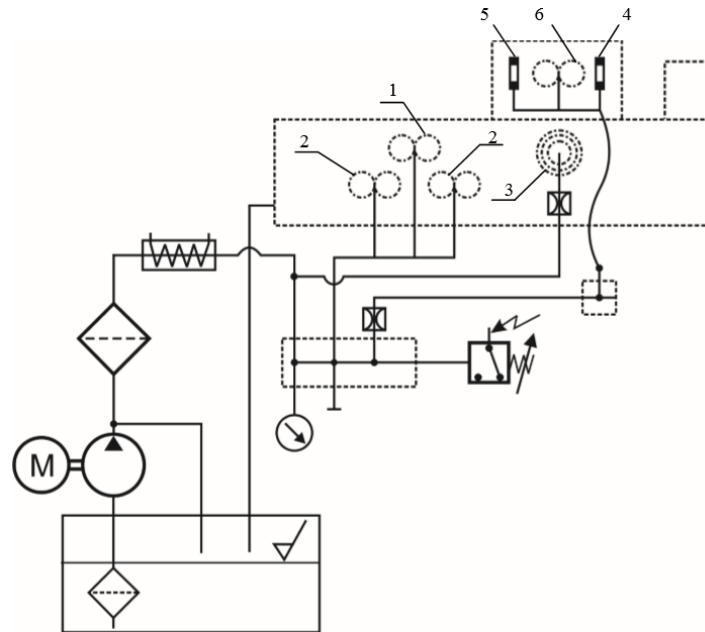


Figure 3: Circulation system for lubrication on the Filter Maker machine [19]

4 H1 hydraulic oil for lubrication Blow/Fill/Seal machine in pharmaceutical process and package equipment in food/drug industry

Machines that are used for production and packaging of liquid solutions in pharmaceutical industry are also specific by construction and by application itself. Specific requirement of Blow/Fill/Seal (B/F/S) machines is that they need reliable work of hydraulic servo system during production/injection of polymer container, later filling with solution and welding, with usage of H1 hydraulic safety oil for pharmaceutical industry applications. B/F/S Packaging Machines are distinguished by high performance output during their exploitation. According to construction of tool and size or type, machines in process of blow-molding/filling/sealing produce high amount of series in numbers presented in a Table 1.

Table 1: Quantities of made solutions by unit of time in accordance with number of cavities and container size [20]

Number of Cavities	Container Size (mL)	Containers/Hour
12	500	2550
14	500	2700
14	250	3150
16	100	4000
20	50	5150
30	20	7700
36	20	9250
40	5	10250
48	5	12500
50	2	13100
60	0.2 ÷ 3	15700

It can be seen from looking at the table that B/S/F Packaging Machine must achieve 261 cycle per hour in order to produce 15700 bottles of solution size range from 0.2 – 3 ml. Only the cycle of

injection/filling/welding takes about 13,79 sec, after which 60 finished doses are removed from the tool.

The process itself is intense and requires high quality oil for hydraulic system of B/S/F packaging machine able to withstand a large number of load cycles, resistant to oxidation and thermal stress. Likewise, systems that are using vane pumps, oil needs to have good EP and AW properties, because of the high-pressure loads to which operating elements of the pump are exposed. B/S/F Packaging machine are shown in Figure 4.

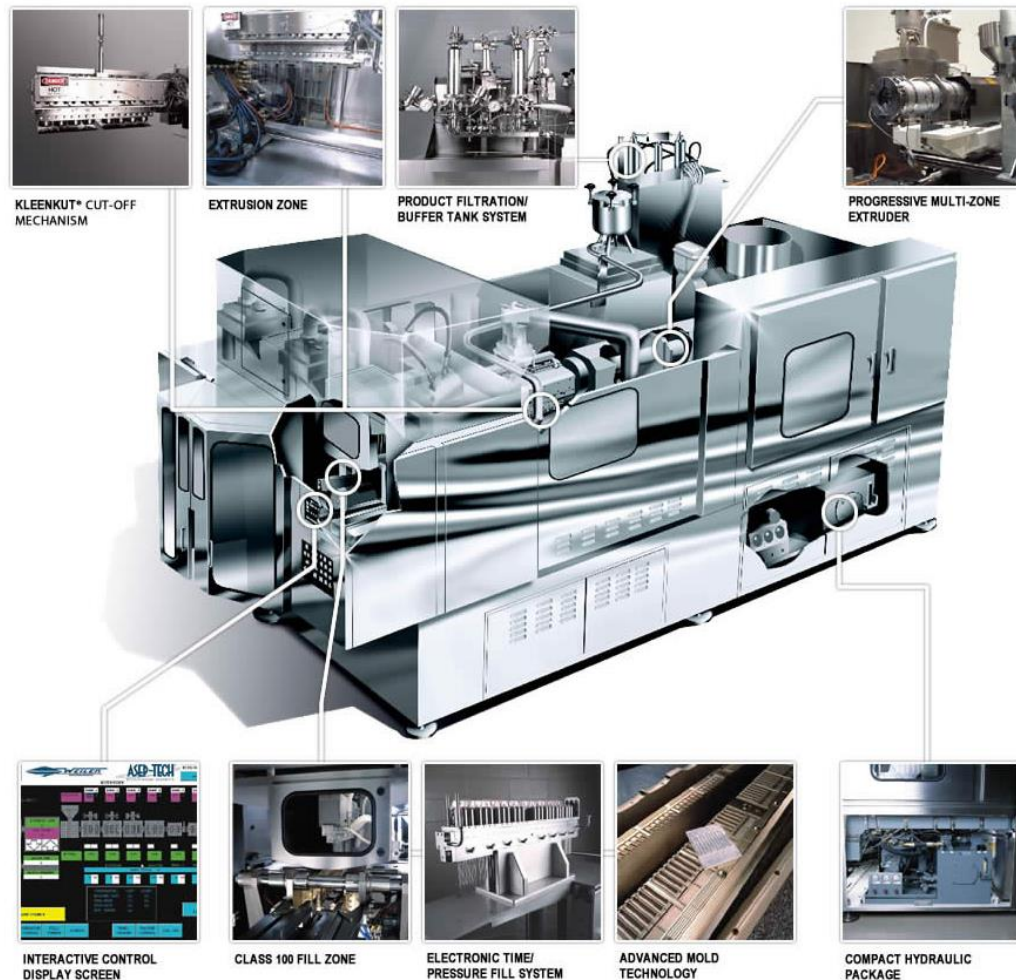


Figure 4: B/S/F Packaging Machines

From the Figure 4, it can be seen that progressive multi-zone extruder is driven by a hydraulic system. Likewise, locking system of the plastic casting tool is powered by the hydraulic system. Due to the need for a product to be packed in an aseptic zone, where because of these conditions great attention is paid to the cleanliness of all elements involved in the production (solutions, liquids, air), hydraulic system is avoided due to the possibility of contamination during the production process. Therefore, these types of machines have three a-septicity zones that guarantee that the end product meets strict standards related to products obtained in pharmacology. In addition to the above characteristics, hydraulic fluids used in this type of machines must satisfy long lifetime of exploitation, which should be in range from 8.000 to 10.000 work-hours. Considering its characteristics, this type of hydraulic oil allows very long exploitation providing regular maintenance (absence of water and solid particles, and stable operating temperature).

Naturally, in order to keep its properties within the required limits throughout exploitation period, the oil is sampled and tested for physical and chemical characteristics in certified laboratories, on a regular basis.

5 Conclusion

From example of usage of gear and hydraulic oils, the following conclusion is posed: in order to get high quality ester oils that will be applied in food processing and pharmaceutical industry high-quality base oil with high-quality additives must be secured. High-quality oil means high-quality ester oil that guarantees long-lasting exploitation, while additives must secure improvements of certain physical and chemical properties meeting strictly specified standard requirements that are used in food processing and pharmaceutical industry.

Usage of ester hydraulic and gear oils are shown on adequate examples, which with adequate maintenance secure long lifespan of machines, thus (depending on the maintenance commitment) can experience even up to 20.000 lifetime work-hours. It only indicates the following: ester oil in the future will be leading oil in food processing and pharmaceutical industry usage. In food processing industry, conventional-mineral oils are still in use, thus it needs to be replaced with ester oils. Another favourable feature of ester oil is that the price gradually equates with the price of mineral oils. Consequently, besides good properties that ester oil poses, the price will also influence on suppression of mineral oil usage, primarily in food processing industry.

References

- [1] NSF International standards, from <http://www.nsf.org/consumer/>, 2004.
- [2] Savić, V., Jocanović, M.: Characteristics and Degradation of Lubricating Oil, (2004), IKOS, Novi Sad
- [3] Keit, P., Hodge, B.: Hydraulic Fluids, (1996), Arnold, New York, USA
- [4] Totten, E. G.(2000). Handbokk of hydraulic fluid technology, Marcel Dekker, Inc; New York.
- [5] FUCHS LUBRICANTS (UK) PLC, CASSIDA FLUID GL - Gear lubricants for use in food manufacturing equipment, 2010.
- [6] FUCHS LUBRICANTS (UK) PLC, CASSIDA FLUID HFS –Hydraulic lubricants for use in food manufacturing equipment, 2017, <https://www.fuchs.com/us/en/brands/a-k/cassida/>
- [7] ASTM D-130, Standard Test Method for Corrosiveness to Copper from Petroleum Products by Copper Strip Test, American Society for Testing and Materials
- [8] ASTM D-974, Standard Test Method for Acid and Base Number by Color-Indicator Titration, American Society for Testing and Materials, International
- [9] ASTM D 1401, Standard Test Method for Water Separability of Petroleum Oils and Synthetic Fluid, American Society for Testing and Materials, International
- [10] ASTM D-892, Standard Test Method for Foaming Characteristics of Lubricating Oils, American Society for Testing and Materials, International
- [11] ASTM D-665 A&B, Standard Test Method for Rust-Preventing Characteristics of Inhibited Mineral Oil in the Presence of Water, American Society for Testing and Materials, International.
- [12] ASTM D – 4172, Standard Test Method for Wear Preventive Characteristics of Lubricating Fluid (Four-Ball Method), American Society for Testing and Materials
- [13] ASTM D-2783, Standard Test Method for Measurement of Extreme-Pressure Properties of Lubricating Fluids (Four-Ball Method), American Society for Testing and Materials, International.
- [14] ASTM D-2782, Standard Test Method for Measurement of Extreme-Pressure Properties of Lubricating Fluids (Timken Method), American Society for Testing and Materials, International
- [15] ASTM D-2882, Standard Test Method for Indicating the Wear Characteristics of Petroleum and Non-Petroleum Hydraulic Fluids in Constant Volume Vane Pump, American Society for Testing and Materials, International

- [16] DIN ISO 14635-1 “Zahnräder - FZG-Prüfverfahren - Teil 1: FZG-Prüfverfahren A/8,3/90 zur Bestimmung der relative Fresstragfähigkeit von Schmierölen”
- [17] ASTM D-5182, Standard Test Method for Evaluating the Scuffing Load Capacity of Oils (FZG Visual Method), American Society for Testing and Materials International
- [18] ASTM D-2272, Standard Test Method for Oxidation Stability of Steam Turbine Oils by Rotating Pressure Vessel, American Society for Testing and Materials International
- [19] HAUNI PRIMARY GmbH, <https://www.hauni.com/en/nc/products/secondary/cigarette-making/filter-cigarette-maker/detail/product/protos-m5.html>, 2017
- [20] Weiler Engineering, Inc., <http://www.weilerengineering.com/asep-tech/model-640>

Inspection of Technical Cleanliness

DETLEF MEURER & AMELA MRAK

Abstract The technical cleanliness of surfaces which are relevant to function has become increasingly important over the last 25 years. The background is the growing demands on components, their service life, the technical design, the permissible tolerances and the resulting sensitivity to solid contamination.

This paper considers the air extraction (air exhaust) and the rinsing extraction by means of high volumetric flows to obtain the solid contamination present on the functional surface without its analysis. The basis for the extraction performance are the standards and regulations: TECSA, VDA19-1 (revision 2015) and ISO 16232.

In essence, two types of extraction are distinguished

A) Wet extraction using the following procedures: syringes, ultrasound, rinsing and shaking

B) Dry extraction using the following methods: blow-off and flow-through

Keywords: • Technical Cleanliness • TECSA • VDA19-1 • ISO 16232 • extraction methods • surface cleanliness control •

CORRESPONDENCE ADDRESS: Detlef Meurer, HYDAC Filter Systems GmbH, Sulzbach/Saar, Postfach 12 51, D-66273 Sulzbach/Saar, Germany, e-mail: detlef.meurer@hydac.com. Amela Mrak, HYDAC d.o.o., Tržaška cesta 39, 2000 Maribor, Slovenia, e-mail: amela.mrak@hydac.si.

1 Introduction

In the past years, the requirements for cleanliness of components, assemblies and finished products in optics, precision mechanics, electromechanics and, above all, the automotive industry and suppliers have increased considerably. Continuous improvement of characteristics and miniaturization of assemblies resulted in increased sensitivity of these to impurities with which they come into contact in the process of production, assembly, packaging, storage, etc.

Purity of the surface is becoming one of the major sources of production costs, but it can also have a significant impact on the quality characteristics and reliability of the product. For this reason, the control of the cleanliness of the area has become an important topic for all the winners who want to improve product characteristics, reduce feces and increase the productivity and competitiveness of the company.

The expectations and requirements of manufacturers and customers in respect of finished components and production machinery are growing steadily. The power densities are increasing; the tolerances are shrinking. In the pursuit of energy and cost efficiency, as well as environmental protection, weights in vehicles and machines are being drastically reduced. In addition, there is a switch to lead-free materials, for example, which means more exacting requirements in terms of the surface quality. Whereas in the past hard particles merely dented materials containing lead, today with modern new materials they cause immediate damage, leading to stoppages. The tolerance to solid contamination is constantly shrinking. Parallel to this, the manufacturer has to guarantee his customers an ever higher level of availability. So more and more companies are monitoring and optimizing the technical cleanliness in production processes. Production stage breakdowns are reduced, quality and availability of machines and components are increased and rectifications can be significantly reduced. This saves on costs and there are fewer warranty claims which in turn boosts customer satisfaction. This further strengthens customer confidence and market acceptance. "The term "technical cleanliness" refers to minimizing contamination so that particles will not constrain or interfere with the subsequent function of the technical component." (Source: Wikipedia).

2 Technical cleanliness - legal basis and testing methods

Damage caused by particles was recognized as being a problem at the beginning of the 1990s because of failures in the field. Specialists from different sectors of the automotive industry were called together to devise a standard, in collaboration with the Fraunhofer Institute, which would deal exclusively with technical cleanliness. This saw the formation of "TecSa"(industrial association for technical cleanliness) in 2001. As a member of TecSa, HYDAC played a leading role in developing the guidelines for cleanliness testing in the automotive industry.

As part of TecSa, the VDA Volume 19, Part 1, was compiled: "Technical cleanliness - Inspection of particle contamination of function-related automotive parts / 1st edition 2004". In 2010, the second volume of this study appeared, Volume 19 Part 2: "Technical cleanliness in installation - environment, logistics, personnel and installation equipment" which deals with technical cleanliness throughout the process chain. As an international standard, ISO 16232 was developed in 2007: »Road vehicles - Cleanliness of components of fluid circuits«. It is the international equivalent of VDA Volume 19. Both standards are fully compatible. The above standards are the guidelines by which technical cleanliness is tested today.

2.1 VDA 19-1 (Revision: 2015)

The development of VDA 19 and ISO 16232 lies in the years 2001-2003 and is due to the TECSA regulations of an industrial association under the direction of Fraunhofer IPA Stuttgart. In the revision, topics were reintroduced, existing explanations were further expanded taking into account the developments and knowledge of the past 12 years.

Chapter 11 has been supplemented, which relates to work safety and the environment. These issues are relevant because hazardous substances can be used as test and analysis fluids. In this chapter, distinctions are made regarding the technical structure of the extraction equipment open systems and closed systems (Figure 1).

Anhang 11 Arbeitssicherheit und Umwelt

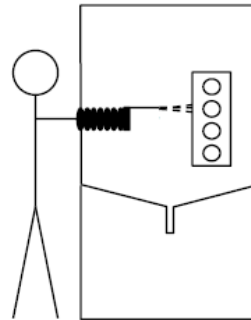
A 11.1 Mögliche Gefährdungen bei der Extraktion mit Lösemit- teln (Beispiele)

**A) vollständig geschlossene
Spritzkammer:**

Beim Öffnen nach der Extraktion

- Aerosolexposition
- Arbeitsplatzgrenzwerte
- Explosionsgefahr

bewerten.

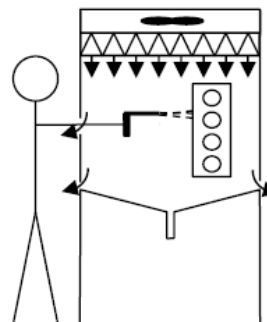


**B) geschlossene Spritzkammer mit
Luftversorgung und Leckagen:**

Bei der Extraktion (und danach)

- Arbeitsplatzgrenzwerte
- Explosionsgefahr

bewerten.



**C) geschlossene Spritzkammer mit
Luftversorgung, Leckagen und
Absaugung:**

- Explosionsgefahr in der Absaugung

bewerten.

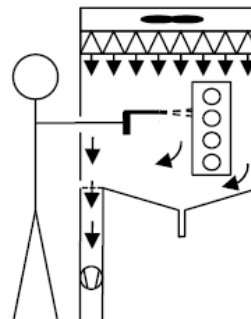


Figure 1: Chapter 11 - Work safety and the environment (source VDA 19-1; Revision: 2015)

Aerosols: The formation of aerosols is present during the test procedures. Therefore, the following table has been created (Figure 2). If a test is carried out above 0.7 pressure (above the described field), a closed system is indispensable. The value for nozzle cross-section and flow rate used for

the start parameters is marked with an X and is within a range in which there is no danger of aerosol.

A 6.4.2.4 Informationen zu Düsendurchmesser und Volumenstrom

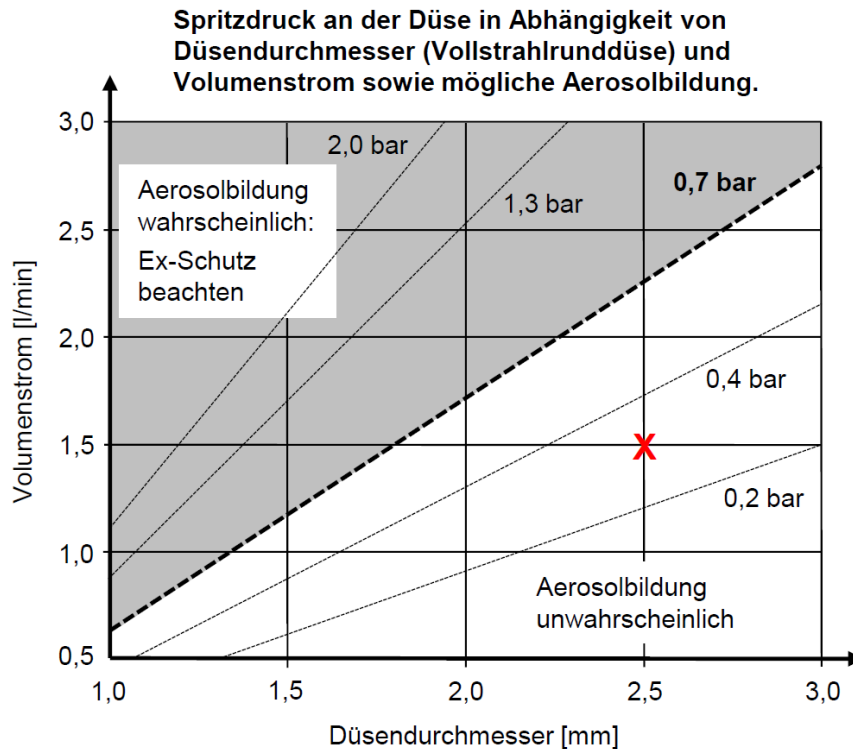


Figure 2: Formation of aerosols in relation to the ratio Volume - Nozzle diameter (source VDA 19-1; Revision: 2015)

2.2 Testing methods

The VDA Volume 19.1 and ISO 18413 provides conditions for the use and documentation of methods for determining the contamination of surfaces of components and systems with solid contamination. The procedures for preparing the test sample, the methods for separating particles from the sample with fluid, measuring particle analysis, evaluating the results and documenting - all of them are described in details (Figure 3).

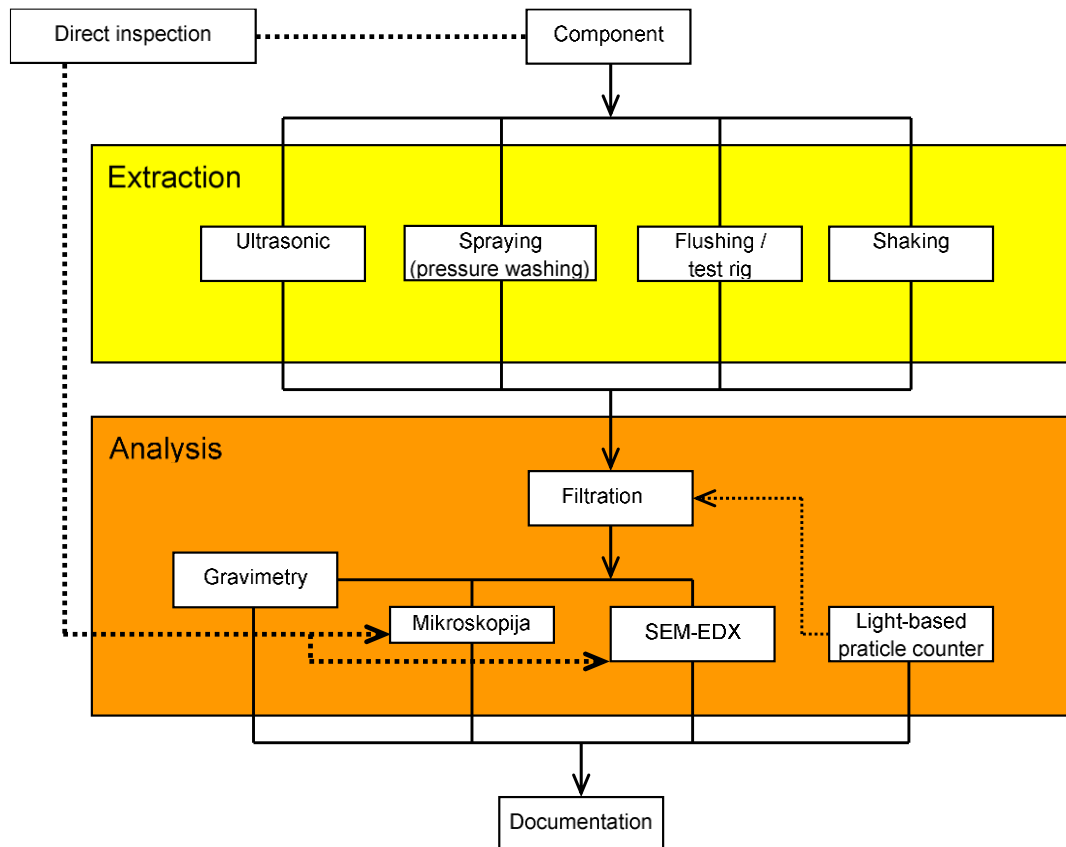


Figure 3: Various extraction methods for determining the quantity of residual contamination on components according to VDA 19-1 (source: TESCA)

2.2.1 Preparation of samples

Samples are taken randomly, at the production stage for which control is required. It is necessary to ensure that no additional contamination of the surface occurs when taking the sample, storing and transporting the sample to the measuring point.

2.2.2 Separation of the solid contamination from the sample

Separation of solid particles from the sample is a preparatory step for measurement analysis. It is carried out using a liquid in which particles are retained.

In the diversity of the size and shape of the sample, the following methods are distinguished:

- Ultrasonic method (for components of smaller dimensions, castings, components having mechanically treated all surfaces);
- Shaking (for components of smaller dimensions, components with openings);
- Rinse under pressure (for tubular components);
- Spraying (for complete or defined surfaces of components or assemblies of all shapes and dimensions). It is performed with dedicated test devices.

Different methods can be combined in order to achieve the best possible separation of particles.

2.2.3 Metrological analysis of particulate matter

The metrological particle analysis is carried out using gravimetry, light microscopy, electron microscopy, automatic particle counters, and direct inspection. The choice of the method depends on the size or the size. Characteristics required (g, g/m², g/component, maximum particle size, particle size in a certain size class, particle size, particle composition, etc.). Different methods can be combined to achieve perfect insight in quantity, size and type of particles.

Gravimetry as the only method can only be considered in case of need for information on the quantity (masses) of particles. Usually, this method is not sufficient because it does not provide data on the number, size, and composition of particles.

Light and electron microscopy is used if an analysis of the type and shape of particles and for counting a small number of large particles is required. In the case of particle counting, there is a great chance of a subjective error of the analyst.

Automatic particle counting is used for analysis. The result is the number of particles in individual size categories according to the applicable standards. The error option is negligible.

Direct inspection is the only method in which no particulate matter is excised. We do not separate them from the surface of the component. A direct inspection is a visual overview of smaller components or surfaces on components in the purpose of determining the type of particles and, in particular, the state of the surface.

2.2.4 Evaluation of results

Regardless of the chosen metrology method, the exact measurement protocol must be determined, and so called "zero value" for each type of component.

The effectiveness of the extraction method is essential for the accuracy of the results. Unfortunately, there were no precise rules that ensure the success of the exclusionary method and the correct results. It is necessary to find an optimal combination of the type of liquid for washing, temperature, metrological methods and rinsing time.

When checking the cleanliness of the surface by washing, there is a risk that the liquid also contains particles that were not on this surface. If the content of particles of foreign origin (zero value) is large, it can distort the results of the measurements. The zero value must be less than 10 % of the maximum measured value (Figure 4).

To determine the protocol, we must first select the metrology method and the type of fluid, and determine the zero value. After that, we choose different combinations of parameters: the quantity and temperature of the liquid, the mode and the duration of the rinsing, and for each combination, six rinses of the same surface are carried out on one component. The results are evaluated by decay behaviour (Figure 2). If the purity level decreases, it means that an optimal combination of parameters has been selected. All the information needs to be documented, and on the basis of them write the precise protocol for controlling the purity of the surface on a particular component.

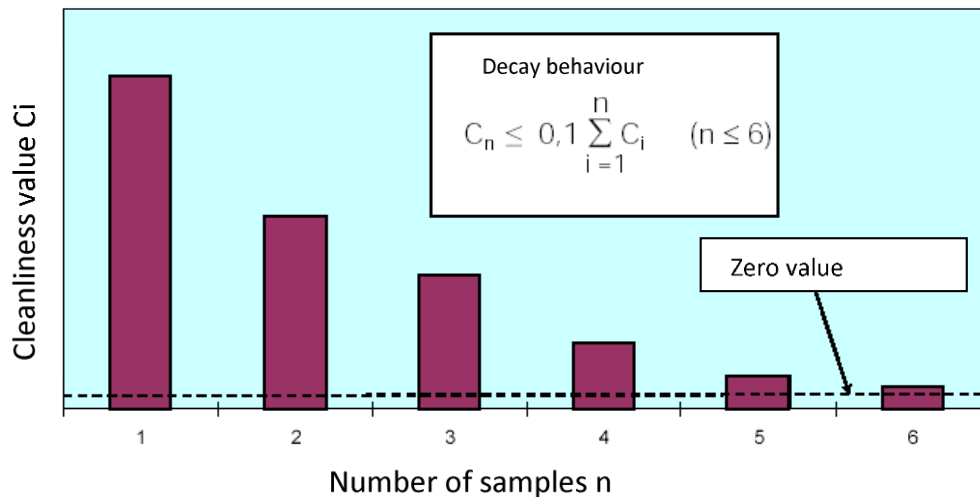


Figure 4: Example of a successful decay behaviour (source: TESCA)

2.2.5 Documentation

The documentation covers the complete specification of the cleanliness of the testing sample and is closely related to the appropriate control specification. As an independent document, the control specification describes the conditions and details of the process used in the cleanliness control. The cleanliness control is documented in the form of a control report. This is a transparent document summarizing information on the method and parameters of the separation of particulate matter from the surface of the component, the methods and parameters of the analysis, the level of surface purity and all other data related to the control.

2.2.6 Cleanliness specifications

Companies in the automotive, agricultural and construction machine industry apply and use these procedures to determine the technical cleanliness. So-called cleanliness specifications are drawn up and forwarded to suppliers so that component requirements can be met and monitored. These analyses are carried out predominantly in-house or in independent laboratories established specifically to analyse component cleanliness.

Production of components and systems according to cleanliness specifications ensures that the supplied quality is consistent. Before drawing up the specification it is important to establish which are the most sensitive components in the system. Individual components or system areas should be divided into categories according to sensitivity.

A = not very particle-sensitive, e.g. low pressure systems with large gap tolerances

B = particle-sensitive, e.g. low pressure systems with small gap tolerances

C = highly particle-sensitive, e.g. high pressure systems with small gap tolerances and exacting requirements, safety-related systems.

For each of these cleanliness categories a maximum value for the particle contamination is specified. In addition, the fluid cleanliness for the individual system and process fluids is defined.

The following points are generally included in the cleanliness specification for the components:

1. Objective of the cleanliness specification
2. Scope of application

3. Scope of tests and test cycles
4. Sample taking
5. Analysis procedure
6. Evaluation procedure
7. Accuracy
8. Test fluid to be used
9. Documentation
10. Limits
11. Procedure for non-compliance with the specification

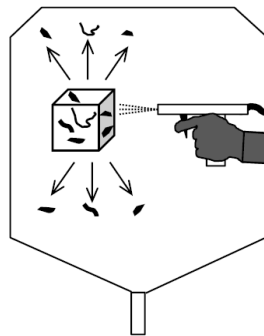
3 Air extraction

The use of air extraction has been part of the VDA 19-1 since 2015. The process described methods and the device technique refers to the blow-off process. The development of the process is due, among other things, to the need to provide a method of wet sampling, which does not damage components and thus allow non-destructive material testing. Example: electronic components, these are examined for particle loading in order to prevent short circuits on the circuit boards by metallic particles. The wet process used so far saturates the boards with moisture and these can not be traced back into the production process.

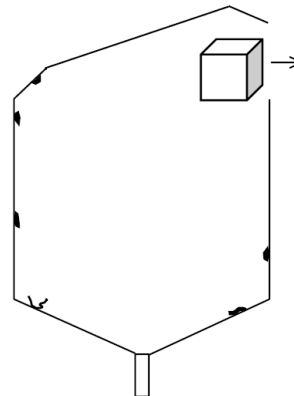
Anhang 6.5.1 Abblasen

A 6.5.1.1 Prinzip und Ablauf bei der Extraktion durch Abblasen

Schritt 1: Abblasen des Prüfteils mit **Druckluft**, Extraktion der Partikel



Schritt 2: Entnehmen des Prüfteils



Schritt 3: Nachspülen der Kammer ohne Prüfteil mit **Flüssigkeit**

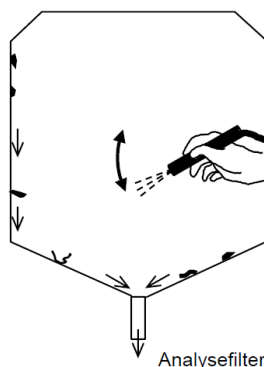


Figure 5: Dry extraction using the following methods: blow-off and flow-through
(source VDA 19-1)

The method is mainly applied to the following component types:

- Destruction-free testing of electronic components
- Quick test, in which a wet application is not desired
- For plastic components that swell during sampling and thus give incorrect results
- Component surfaces which are destroyed by the use of liquid, e.g. composite materials paper / metal.

4 Rinsing extraction volume flow up to 18 L/min

Due to the increasing demands on the extraction parameters due to the expansion to mobile hydraulics and trucks, high volume flows are required for the components with large suction volumes and passages. The VDA 19 -1 does not describe the required parameters, but describes this via the evaluation method of the decay curve.

The method is basically simple in technical terms. The required test volume flow is generated via a defined supply of test liquid to the component. This can be supported with pulsation if the critical Reynolds number can not be reached. The analytical liquid discharged from the component (the name change of test liquid in analytical liquid is due to the loading with particle loads) is collected in a sample container and filtered through an evaluation filter. This filter is sent to the later analysis.

One example of high volume flows extraction procedures:

Cooler tested with HYDAC CTM-3xxx SC+EF Modul (Figure 6). Testfluid in CTM-3xxx SC device is crossing through the cooler, been collected and filtered in EF Module and send back to SC Modul (Figure 7). Flow rate during testing is 18 L/min with adjustable pulsation, volume SC Modul is 60 L and volume EF Modul is 40 liters. Testing is carried out 5 times successively with the duration 1min each.



Figure 6: HYDAC CTM-3xxx SC+EF Modul
(source HYDAC International documentation)

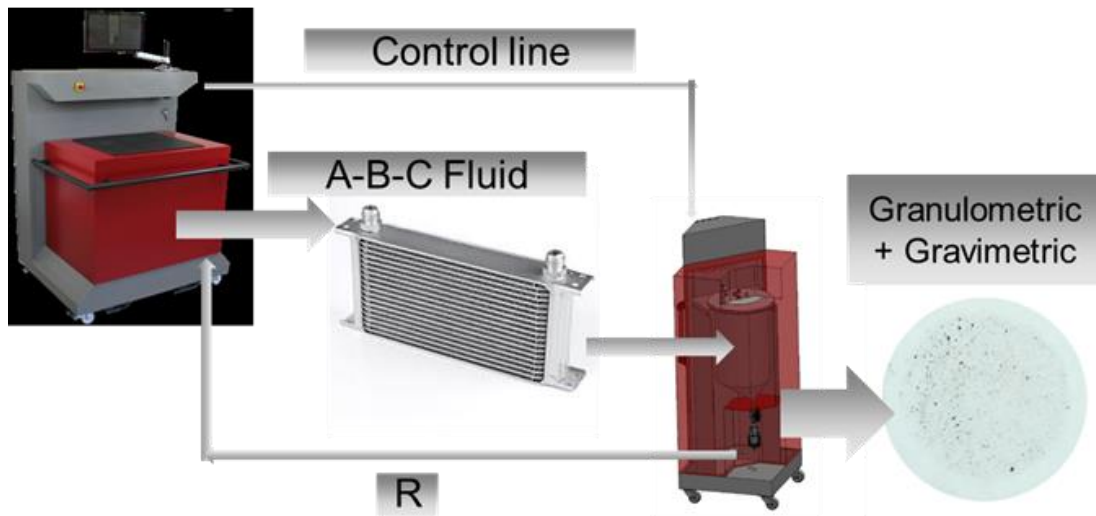


Figure 7: High volume flows extraction procedure with HYDAC CTM-3xxx SC+EF Modul
 (source HYDAC International documentation)

References

- [1] HYDAC Filbertechnik GmbH: Practical Contamination Management From Processing to Delivery, HYDAC Filbertechnik GmbH, Sulzbach/Saar, 2003
- [2] Amela Krajnc, POVRŠINSKA ČISTOST KOMPONENT IN SKLOPOV V AVTOMOBILSKI INDUSTRIJI, Zbornik prispevkov, Inovativna avtomobilska tehnologija – IAT '05, Bled, 21.-22. April, 2005
- [3] Frank Jung: HYDAC Service Technology, Filtersystems Sales Meeting 2005, HYDAC Filbertechnik GmbH, Sulzbach/Saar, 2005
- [4] HYDAC Filbertechnik GmbH: CTU 2000 Series – Operating and Maintenance Instructions, HYDAC Filbertechnik GmbH, Sulzbach/Saar, 2004
- [5] Fraunhofer Institut Produktionstechnik und Automatisierung: Guideline (Draft): Inspection of Technical Cleanliness – Particulate Contamination of Functionally- Relevant Automotive Components, Fraunhofer Institut Produktionstechnik und Automatisierung, Stuttgart, 2004
- [6] Different internal documentation of Hydac Group
- [7] HYDAC Filbertechnik GmbH: Technical Cleanliness – Doc. No. E10.110.1.0/07.13, Sulzbach/Saar, 2013

MPC-Test: An introduction and examples of test results

MANJA MODER & URŠKA CAFUTA

Abstract In-service lubricating oils are subjected to degradation processes as aging, additive depletion or contamination. Oxidation processes are probably the major cause for the degradation of lubricating oil. An oxidation process is the initiating process which may result in the formation of insoluble deposits, called varnish. These are mainly organic nature but of higher polarity and molecular weight, which start to agglomerate into sticky deposits at oil-wetted surfaces.

Condition monitoring of in-service lubricating oil is important throughout the entire life cycle of the lubricating oil. It involves different test methods in order to determine the properties of the in-service lubricating oil. One of the latest test methods used mainly for turbine and hydraulic oils is referred to as Membrane Patch Colorimetry (MPC).

This paper presents the standard MPC-Test and a modified MPC-Test applied in Laboratory Petrol. The modifications are listed. Some examples of MPC-Test results are demonstrated and discussed, respectively.

Keywords: • lubricating oil • oxidation • varnish • condition monitoring • MPC •

CORRESPONDENCE ADDRESS: Manja Moder, Petrol d.d., Dunajska cesta 50, 1000 Ljubljana, Slovenia,
e-mail: manja.moder@petrol.si. Urška Cafuta, Petrol d.d., Dunajska cesta 50, 1000 Ljubljana, Slovenia,
e-mail: urska.cafuta@petrol.si.

1 Introduction

Condition monitoring of in-service lubricating oil is important throughout the entire life cycle of the lubricating oil [1, 2]. Condition monitoring also involves performing different test methods (density, viscosity, VI, TAN, TBN, additive and wear elements, water content,...) in order to determine the properties of the in-service lubricating oil. One of the latest test methods used mainly for turbine and hydraulic oils is referred to as Membrane Patch Colorimetry (MPC) [3, 4]. The standard test procedure is prescribed in ASTM D7843 (Standard Test Method for Measurement of Lubricant Generated Insoluble Color Bodies in In-Service Turbine Oils using Membrane Patch Colorimetry) [3].

In Laboratory Petrol we perform a modified MPC-Test. The modifications are the following: a) we do not apply sample preheating (aging) and b) we do not apply a spectrophotometric determination of the color of the membrane patch reported as the CIE LAB ΔE values. From the color and intensity of the filter - membrane patch (insoluble deposits on the filter) a direct correlation to oil degradation is made using the ASTM Color Standards and calculating the MPC value.

2 MPC-Test: ASTM D7843 standard test procedure

The sample is heated to 60°C to 65°C for 23 h to 25 h and then stored at between 15°C to 25°C, away from UV light for an incubation period of 68 h to 76 h. (Samples that are analyzed prior to this aging period may produce fewer color bodies on the patch which may lower the value of trend analysis.)

The sample is vigorously mixed for a minimum of 15 s to resuspend insolubles uniformly. 50 ml ± 1 ml of sample is transferred into a clean flask/beaker and mixed with 50 ml ± 1 ml of petroleum ether for 30 s. This mixture is filtered (vacuum pressure of 71 ± 5 kPa) through a 0,45 μm nitro-cellulose membrane filter within 1 min to 2 min after initial mixing and rinsed twice with a suitable amount (minimum 35 ml) of filtered petroleum ether. Any adhering insolubles are washed from the funnel onto the filter - membrane patch. The filter - membrane patch is washed gently, particularly the edges. A dry filter - membrane patch is analyzed using a spectrophotometer in the range of 400 nm to 700 nm.

The total difference ΔE^*_{ab} between two colors each given in terms of L^* , a^* , b^* is calculated as:

$$\Delta E^*_{ab} = [(\Delta L^*)^2 + (\Delta a^*)^2 + (\Delta b^*)^2]^{1/2} \quad (1)$$

where L^* , a^* , b^* are:

$$\begin{aligned} L^* &= 116 \cdot (Y/Y_n)^{1/3} - 16 \\ a^* &= 500 \cdot [(X/X_n)^{1/3} - (Y/Y_n)^{1/3}] \\ b^* &= 200 \cdot [(Y/Y_n)^{1/3} - (Z/Z_n)^{1/3}] \\ X/X_n ; Y/Y_n ; Z/Z_n &> 0,01 \end{aligned}$$

The CIE LAB ΔE values are reported to one decimal place [3].

3 Modified MPC-Test (mod. ASTM D7843)

Modifications: a) we do not apply sample preheating (aging) but perform the test on a received sample and b) we do not apply a spectrophotometric determination of the colour of the membrane

patch as the CIE LAB ΔE values. Note: The UV-VIS spectrometer is not equipped with CIELAB measuring indices.

A 0,45 μm nitro-cellulose filter is weighed before filtration to 0,1 mg precise. First the sample is visually inspected for any impurities or water content and then vigorously mixed for at least 15 s. 50 ml \pm 1 ml of sample is mixed with 50 ml \pm 1 ml of filtered petroleum ether in a sample beaker for 30 s. Within 1 min to 2 min after initial mixing the sample is poured into a filter funnel and filtered with a vacuum pressure of 71 \pm 5 kPa. The sample beaker and stopper are rinsed twice with a minimum of 35 ml filtered petroleum ether. The rinse is poured into the filter funnel and permitted the filtrate completely. Any adherent insoluble are washed from the filter funnel onto the filter - membrane patch. The filter - membrane patch is washed gently, particularly the edges and dried in a heating cabinet ($T = 50 - 80^\circ\text{C}$). The filter - membrane patch is visually inspected for any wear particles or an inhomogeneous appearance and weighed to 0,1 mg precise. The colour of the membrane patch is compared with ASTM Color Standards. The test result of the modified MPC-test is the ASTM Color Standards rating from which the MPC value is calculated and reported to the whole number [3, 6].

Example:

1) filter - membrane patch with ASTM Color Standards rating = B-2/B-3:

B-2 has: $L^* = 91,08 / a^* = -0,70 / b^* = 8,05$

B-3 has: $L^* = 86,21 / a^* = 0,13 / b^* = 14,89$

For the calculation of the MPC value the average values for L^* , a^* , b^* are used:

B-2/B-3: $L^* = 88,645 / a^* = -0,285 / b^* = 11,47$

For the blank filter the values for rating A-1 are used: $L^* = 98,99 / a^* = 0 / b^* = -0,01$ [6]

$$\Delta E^*_{ab} = [(\Delta L^*)^2 + (\Delta a^*)^2 + (\Delta b^*)^2]^{1/2} =$$

$$= [(88,645-98,99)^2 + (-0,285-0)^2 + (11,47-(-0,01))^2]^{1/2} = 15 \dots \text{MPC value}$$

4 Test results and evaluation

In literature, different recommendations for evaluating the warning and alarm limits of the MPC value can be found:

“Values up to 15 are regarded as normal with no risk of varnish deposition. Values between 15 - 45 represent moderate risk, and results above represent severe risk of varnish deposits, immediate action is required to prevent machinery failure” [4].

“CIE ΔE Varnish Rating: Fresh Oil: <15; Normal Used: 15 – 30; Potential Varnish Formation 30 – 40; Varnish Formation >40” [5].

In Laboratory Petrol the following interpretation is applied:

MPC values <10 are considered as appropriate, MPC values between 10 – 40 are considered as acceptable, MPC values >40 are considered as inadequate. The warning limit is between 30 – 40.

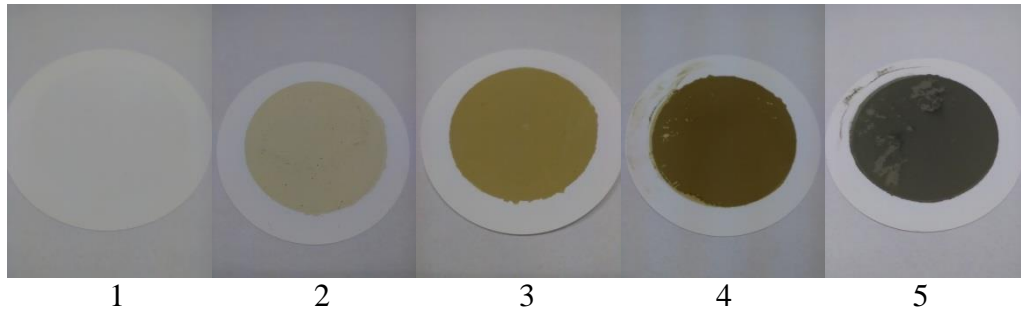


Figure 1: Examples of different filters - membrane patches with corresponding MPC values (from left to right): 1 = <10, 2 = 15, 3 = 32, 4 = 47 and 5 = 64

The MPC value for sample 1 is acceptable and the potential risk for varnish deposits is low. The in-service lubricating oil (oil charge) is considered as appropriate.

The MPC value for sample 5 is inadequate, not acceptable and the potential risk for varnish deposits is severe. The in-service lubricating oil (oil charge) is not appropriate and immediate actions are needed. A recommendation for this in-service lubricating oil / oil system would be to change the lubricating oil (oil charge).

In order to provide a sound statement on the status (compliance) of the in-service lubricating oil (oil charge) a “complete picture” is needed. The test results for other measured test properties have to be considered as well.

5 Conclusions

The MPC-test or the modified MPC-test is an important tool for predicting the creation of deposits. For end users (laboratory customers) the MPC value is important. Especially for evaluating the status (compliance) of an in-service turbine and hydraulic oil sample.

Despite the fact that we do not have an appropriate spectrophotometer, the condition of the filter - membrane patch reflects the state of the oil system. The filter - membrane patch often contains solid particles, which are usually wear metals. The filter - membrane patch can be further analyzed with an XRF technique to determine the type of wear metals or it can be put under a microscope to obtain additional information.

References

- [1] Busch, A.: Fluid Condition Monitoring, 2013, OilDoc Conference.
- [2] Tič, V., Tašner, T., Lovrec, D.: Enhanced lubricant management to reduce costs and minimise environmental impact, *Energy*, ISSN 0360-5442. [Print ed.], 1 Dec. 2014, vol. 77, str. 108-116.
- [3] Standard Test Method for Measurement of Lubricant Generated Insoluble Color Bodies in In-Service Turbine Oils using Membrane Patch Colorimetry; American Society for Testing and Materials (ASTM) D7843-16.
- [4] Fischer, T., Krethe, R.: MPC-Test; Sample preparation and repeatability of test results, 2017, OilDoc Conference.
- [5] Billings, L., Sapiano, H., Shahfoort, T.: New Wave: Next Generation Low Varnish Turbine Fluids, 2017, OilDoc Conference.
- [6] Standard Test Method for Particulate Contaminant in Aviation Fuel by Line Sampling; American Society for Testing and Materials (ASTM) D2276-06; (2014).

Hydraulic pump pulsation using Ionic Liquid

BERNHARD MANHARTSGRUBER & VITO TIČ

Abstract The research objective was to evaluate pressure pulsation and flow ripple of a hydraulic pump using two different ionic liquids with high bulk modulus in comparison to HLP standard mineral hydraulic oil.

The two most adequate ionic liquids for hydraulic application with highest bulk modulus were chosen, and a special test rig was built using a bent axis 7-piston pump powered by a servo motor.

Measurements of pressure pulsation were done at two different pressures of 100 and 200 bar, two different viscosities and several different rotational speeds, ranging from 1000 to 4000 rpms in 100 rpm steps.

Results show change of resonance frequencies of the entire hydraulic system due to the higher bulk modulus and higher density of the ionic liquids. On the other hand, there is no significant change in pump pressure pulsation in the non-resonance frequency range below 2500 rpm.

Keywords: • hydraulic • pump • flow-ripple • pulsation • ionic liquid •

CORRESPONDENCE ADDRESS: Bernhard Manhartsgruber, Ph.D., Associate Professor, Johannes Kepler University Linz, Institute of Machine Design and Hydraulic Drives, Altenberger Straße 69, 4040 Linz, Austria, e-mail: bernhard.manhartsgruber@jku.at. Vito Tič, Ph.D., Assistant Professor, University of Maribor, Faculty of Mechanical Engineering, Smetanova ulica 17, 2000 Maribor, Slovenia, e-mail: vito.tic@um.si.

1 Introduction

The most common and frequently used hydraulic fluid in the past decades is HLP hydraulic mineral oil, which has well-known properties that make it ideal to be used as a hydraulic fluid. Some of its properties are not particularly superior, and could be improved by using other new types of hydraulic fluid. One of the drawbacks of HLP oil is its high compressibility, which influences the performance of the entire hydraulic system. Thus, ionic liquids have been proposed as possible alternatives to be used as a hydraulic fluid with higher bulk modulus [1].

In this pilot stage of research – using ionic liquids as hydraulic fluids – we first have to evaluate the adequacy of pump design for use with ionic liquids that have higher density and bulk modulus which affect the operation of the hydraulic pump.

Hydraulic pumps, as all positive displacement pumps, have typical pulsation. The hydraulic pump cannot provide absolutely constant flow at constant speed. These small pulsations in the flow speed are called flow-ripple. The flow-ripple and also, consequently, pressure pulsation, generated by an axial piston pump, are relatively large compared to the rest of the positive-displacement pumps [2].

In the case of an axial piston pump (Figure 1), the piston movement is sinusoidal, where the flow rate by each piston is the product of piston area and speed. The pump delivery is the summation of the flow rate delivered by all of the pistons in connection with the delivery port [3].

However, the pressure pulsation is not only related to the pump, but also to the system which the pump is feeding [2]. Since this can make simulations and calculations complicated, we have tried to build as simple a test rig as possible.

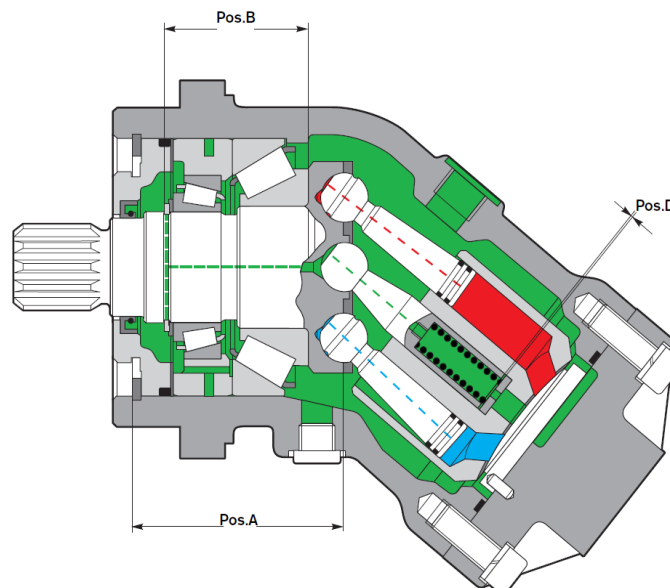


Figure 1: Cross-section of A2F5 type pump used in the test

2 Test setup

2.1 Hydraulic fluids

Three different hydraulic fluids were studied and compared in order to evaluate the effects of high bulk modulus and higher density of ionic liquids on the pressure pulsation and flow-ripple of

hydraulic pumps. The two most adequate ionic liquids with high bulk modulus were chosen (IL1 and IL2), and tested against HLP ISO VG 32 standard mineral hydraulic oil. The most important properties of the tested fluids are presented in Table 1, while detailed information on bulk modulus of the fluids is given in Figure 2.

Table 1: Properties of tested hydraulic fluids

Property	HLP VG 32	IL1	IL2
Density @ 15°C [g/cm ³]	0,869	1,266	1,241
Viscosity @ 40°C [mm ² /s]	31,56	15,42	39,44
Viscosity @ 100°C [mm ² /s]	5,41	4,313	7,66
Viscosity index	106	208	168
Bulk modulus [Pa · 10 ⁹] @ 0 bar	1,64	2,85	3,09
Bulk modulus [Pa · 10 ⁹] @ 100 bar	1,74	2,91	3,20
Bulk modulus [Pa · 10 ⁹] @ 200 bar	1,86	2,97	3,32
Bulk modulus [Pa · 10 ⁹] @ 400 bar	2,15	3,08	3,60

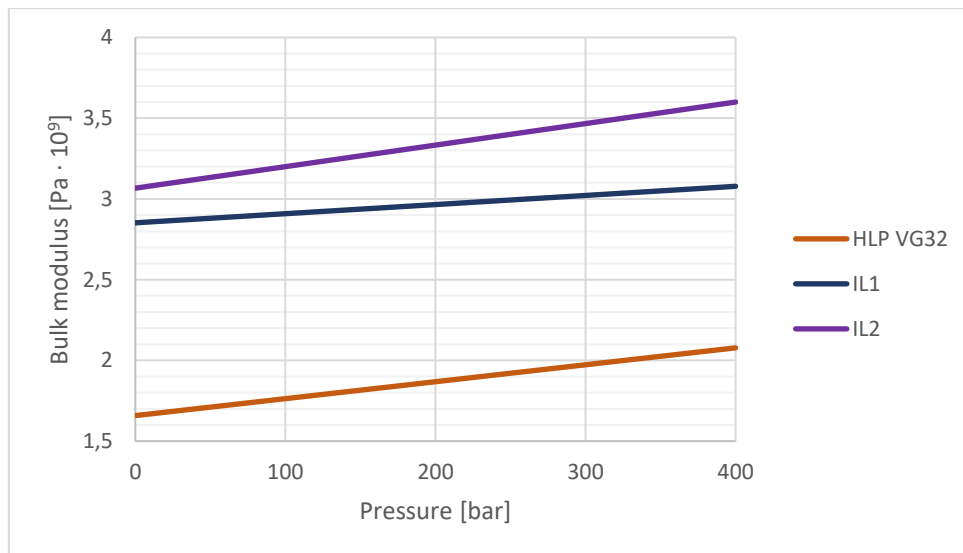


Figure 2: Bulk modulus of tested liquids

All liquids were tested at two different viscosities, approx. 15,6 and 31,6 cSt, which were achieved by performing the test at different temperatures to match the viscosities of the liquids. These two viscosities were chosen because they represent the lower and upper temperature limits the usual hydraulic oil applications (40 and 60 °C). Table 2 presents viscosities and temperatures of the fluids at which the tests were performed.

Table 2: Viscosities and temperatures of liquids at which the tests were performed

	Temperature [°C]	Viscosity [cSt]
HLP 32	59,0	15,6
IL1	39,5	15,6
IL2	69,0	15,6
HLP 32	40,0	31,6
IL1	18,3	31,6
IL2	46,0	31,7

2.2 Hydraulic test rig

The test rig was designed and constructed as simply as possible to allow comparison between the test and the simulation model, which will be developed in the future. Each additional component in the system would only introduce more and more unknown variables into the simulation model. The pressure pulsation and flow-ripple were studied on a Rexroth A2F5/60W-C3 pump, which is a 4,93 cc bent axis 7-piston pump that can also be used as a motor. The pump was driven by a servomotor with closed-loop speed control at different rotational speeds.

The test rig setup is presented in Figure 3. The pump was placed into a simple hydraulic circuit with 4 pressure sensors and a variable orifice at the end. A pressure relief valve, set to 300 bar, was placed at the end of the line for safety reasons. The lengths of pipelines (Φ 12 mm x 2 mm) between each component are also presented in Figure 3. A smaller hydraulic tank was used, filled with approx. 15 L of tested liquid and equipped with a temperature probe to measure the temperature of the liquid near the suction line.

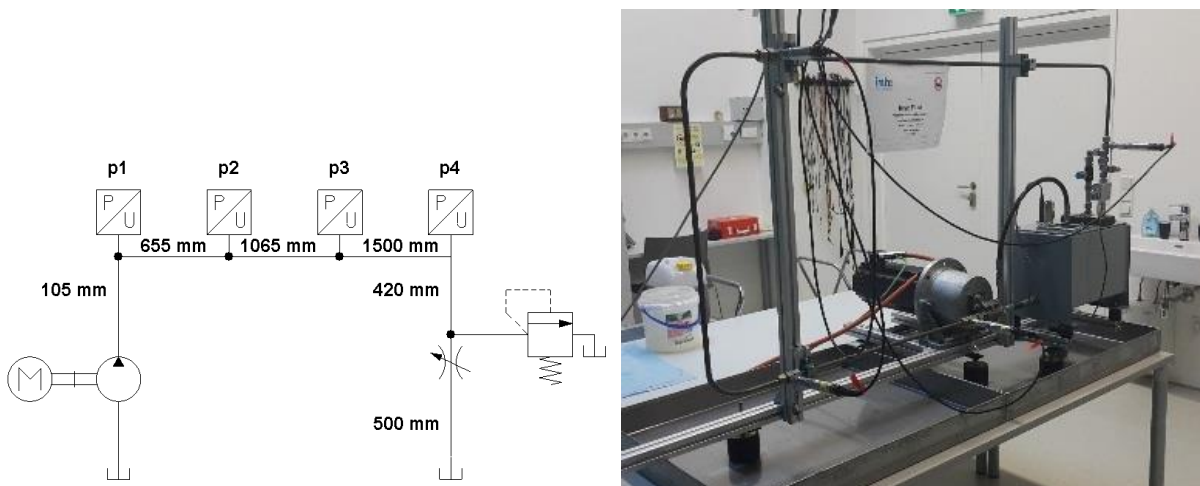


Figure 3: Test rig setup

2.3 Measurement system setup

Four precision GE PDCR 4060 pressure sensors were installed into the pipeline, as presented in Figure 3, and were coupled to an NI 9237 data acquisition unit (± 25 mV/V, Bridge Analog Input, 50 kS/s/ch, 4 Ch Module) driven by National Instruments cRIO-9024 Real-Time FPGA Controller. The measurement system allowed us to take pressure readings at 4 different locations in the pipeline at a 50kHz sample rate. To compensate the temperature drift of the pressure sensors, the sensors were calibrated after each measurement series at a given temperature.

3 Results

Measurements of pump pulsation were made at two different pressures of 100 and 200 bar, two different viscosities of 15,6 and 31,6 cSt, and several different rotational speeds ranging from 1000 to 4000 rpms in 100 rpm steps.

There were some additional limitations while performing measurements:

- If the resonance of the system was too excessive, the measurements were not taken in high-resonance rotational speeds,

- Measurements with IL1 at high viscosity of 31,6 cSt at $T = 18,3 \text{ }^\circ\text{C}$ were only taken at 500 rpm steps due to ineffective cooling.

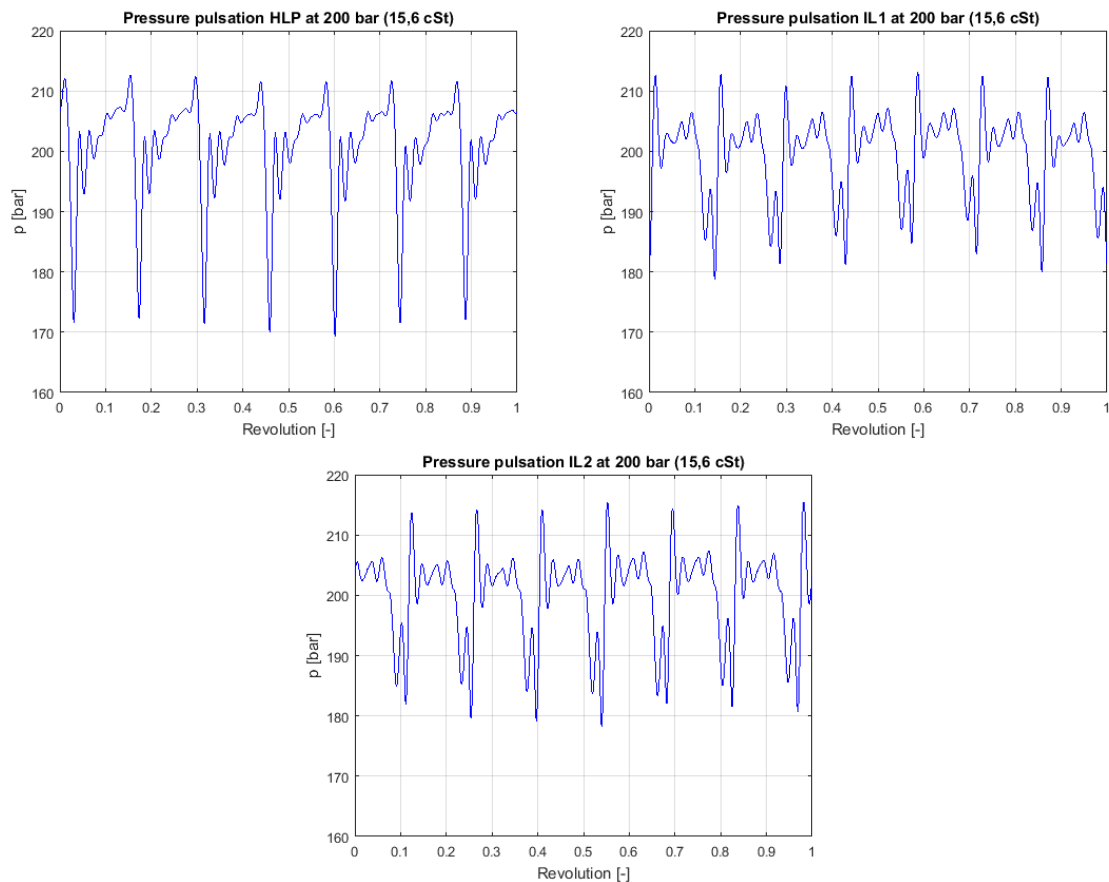


Figure 4: Hydraulic pump pressure pulsation using tested fluids at $n = 1500 \text{ rpm}$

As described above, there were approx. 360 measurements made (3 fluids at 2 viscosities and 2 pressures in 30 steps by 100 rpm steps), thus, it is impossible to present all measurements in this paper.

Figure 4 presents hydraulic pump pressure pulsation (measuring point p_1 , just after the pump) at nominal speed of $n = 1500 \text{ rpm}$, at 200 bar and viscosity of 15,6 cSt using different tested fluids. Pressure pulsation is shown only for 1 revolution, although 6 revolutions were recorded for each measurement and used for all further calculations.

Further on, the pressure pulsation was evaluated in two ways, as shown in Figure 5:

- $p_{max} - p_{min}$: the absolute difference between maximal and minimal pressure reading
- RMS: RMS value of pulsation was calculated by subtracting the average pressure from the measured pressure signal.

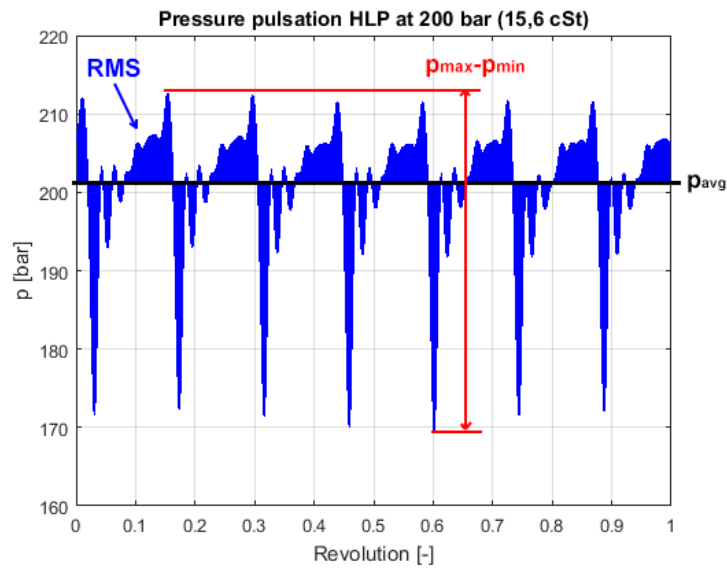


Figure 5: Representation of pressure pulsation calculation

Figure 6 presents $p_{max} - p_{min}$ and RMS value of pressure pulsation from 1000 to 4000 rpm for each tested fluid at (low) viscosity that corresponds to HLP VG 32 viscosity at 60 °C and at pressure 200 bar. Note that the $p_{max} - p_{min}$ values and lines are divided by 5 in order to fit the same y-axis scale as RMS values.

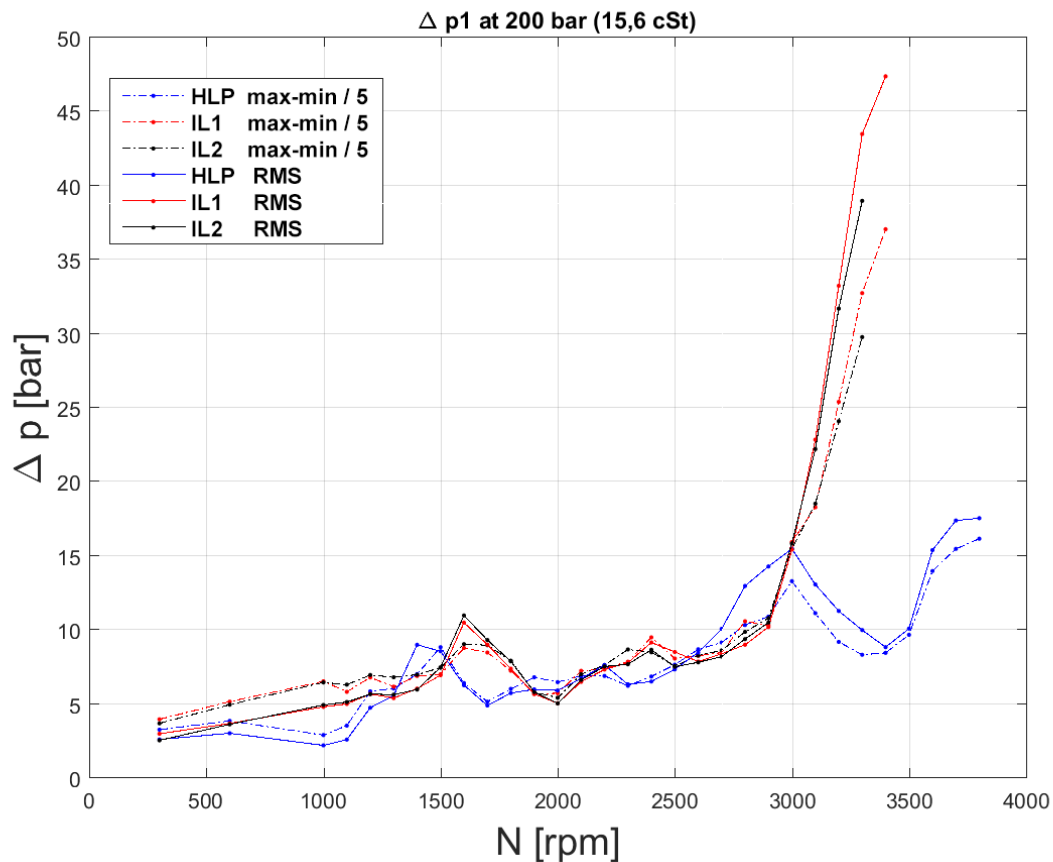


Figure 6: Pressure pulsation represented as $p_{max} - p_{min}$ and RMS value from 1000 to 4000 rpm for each tested fluid at viscosity 15,6 cSt and at pressure 200 bar

Figure 6 shows clearly that the resonance frequencies of the system have changed due to using fluids with different bulk modulus and different densities. We also notice that the resonance was much more severe with high bulk modulus and high density ionic liquids.

On the other hand, there is no significant change in pump pressure pulsation in the non-resonance frequency range below 2500 rpm. Thus, data for non-resonance frequency was investigated further and is shown in Table 3.

Table 3 shows the hydraulic pump pressure pulsation in the non-resonance frequency range below 2500 rpm in comparison to standard HLP VG 32 oil:

- For IL1 it was approx. 6 % higher at low viscosity (15,6 cSt),
- For IL2 it was approx. 11 % higher at low viscosity (15,6 cSt),
- For IL1 it was approx. 19 % higher at high viscosity (31,6 cSt),
- For IL2 it was approx. 16 % higher at low viscosity (15,6 cSt).

Table 3: Viscosities and temperatures of liquids at which the tests were performed

Viscosity [cst]	p [bar]	Fluid	Average pulsation for non-resonance speeds from $n = 1000 \text{ min}^{-1}$ to $n = 2500 \text{ min}^{-1}$			
			$p_{\max} - p_{\min}$ [bar]	RMS [bar]	$p_{\max} - p_{\min}$ vs HLP32	RMS vs HLP32
Low 15,6	100	HLP32	13,12	2,41		
		IL1	14,12	2,55	+8 %	+5 %
		IL2	15,00	2,68	+14 %	+11 %
	200	HLP32	23,68	4,58		
		IL1	25,21	4,85	+6 %	+6 %
		IL2	26,13	4,99	+10 %	+9 %
High 31,6 cSt	100	HLP32	11,83	2,19		
		IL1	13,39	2,56	+13 %	+17 %
		IL2	13,56	2,49	+15 %	+14 %
	200	HLP32	20,34	3,99		
		IL1	25,25	4,84	+24 %	+21 %
		IL2	23,84	4,61	+17 %	+16 %

3 Conclusion

The aim of the research was to evaluate the adequacy of hydraulic pump design for use with ionic liquids that have higher density and bulk modulus than common hydraulic fluids. A special test rig was built to investigate the pump flow-ripple and pressure pulsation.

Based on the numerous measurements made, we can conclude that both ionic liquids performed very well as a hydraulic fluid in a hydraulic system with no extra modifications.

The paper presents the first simple data processing results that were made on the measurements. The results revealed that there is little to no increase in pump pulsation while using ionic liquids at non-resonance frequencies below 2500 rpm. However, since the pressure pulsation is not only related to the pump, but also to the system which the pump is feeding, we can notice significant change of resonance frequency of the hydraulic system and pipeline.

References

- [1] Kambič, M., Kalb, R., Tašner, T., Lovrec, D.: High Bulk Modulus of Ionic Liquid and Effects on Performance of Hydraulic System. *The scientific world journal*, ISSN 1537-744X, 2014, vol. 2014, art. no. 504762, str. 1-10. <http://dx.doi.org/10.1155/2014/504762>, doi: 10.1155/2014/504762
- [2] Minav T. A., Laurila, L. I. E., Pyrhönen J. J.: Axial piston pump flow-ripple compensation by adjusting the pump speed with an electric drive; *The Twelfth Scandinavian International Conference on Fluid Power*, May 18-20, 2011, Tampere, Finland
- [3] Patil, B. J., Sondur V. B.: Investigation into the Causes of Pulsation of Flow of Hydraulic Pumps and Its Effects; *International Journal of Innovative Research in Science, Engineering and Technology*, Vol. 4, Issue 1, January 2015

Mathematical Modelling and Experimental Research of Characteristic Parameters of aviation hydraulic piston pump

RADOVAN PETROVIĆ, HUAYONG YANG, MAJA ANDJELKOVIĆ & RADOJE CVEJIĆ

Abstract Axial piston pumps with constant pressure and variable flow have extraordinary possibilities for controlling the flow by change of pressure. Owing to pressure feedback, volumetric control of the pump provides a wide application of these pumps in complex hydraulic systems, particularly in aeronautics and space engineering. Some dynamic processes developing in control cycle have been analyzed by mathematical model and a large number of process simulations have been done by means of programming language Matlab. On that occasion some diagrams have been made which have been a basis for analysis of time-constants of transient and it has been concluded that the characteristics comply with the requirements defined by the aeronautics standards.

Keywords: • axial piston pump • constant pressure • experimental research
• mathematical modelling • dynamics •

CORRESPONDENCE ADDRESS: Radovan Petrović, Ph.D., Professor, University “Union - Nikola Tesla” of Belgrade, Faculty for Strategic and Operational Management, Sajmište 29, 11070 Belgrade, Serbia; e-mail: radovan4700@yahoo.com. Huayong Yang, Ph.D., Professor, Zhejiang University, The State Key Laboratory of Fluid Power and Mechatronic Systems, 38 Zheda Road, Hangzhou, China, e-mail: yhy@zju.edu.cn. Maja Andjelković, Ph.D., Professor, University “Union - Nikola Tesla” of Belgrade, Faculty for Strategic and Operational Management, Sajmište 29, 11070 Belgrade, Serbia; e-mail: maja.andjelkovic@fsp.edu.rs. Radoje Cvejić, Ph.D., Professor, University “Union - Nikola Tesla” of Belgrade, Faculty for Strategic and Operational Management, Sajmište 29, 11070 Belgrade, Serbia; e-mail: radoje.cvejic@fsom.edu.rs.

1 Introduction

A review of the axial piston pump with constant pressure variable displacement. These pumps have found wide application in complex hydraulic system in the field of aviation [1]. Demands placed stations in aviation are numerous but the most significant reliability in operation, exceptional efficiency in the supply of highly complex branch system and economical operation and request that the maximum energy saving.

Contents of the paper, in an attempt to provide further improve the performance of the devices from the structure of the hydro system of the aircraft. In particular, these activities are related to the components that generate certain kinds of power, namely, first of all, pumps and motors [2], [3].

Besides causing of the compression losses, changes of the pressure inside the cylinder at short intervals are causing hydraulic impacts in the fluid that spread through the housing and cause the noise. There is a tendency of development of new pumps with constant increase of the operating pressure, which results in increase of the efficiency coefficient while increasing the noise. It is interesting to study what possibilities exist to reduce the noise while the pressure rises at the same time. One way is selection of optimal angles of suction and suppression openings on valve plate to obtain certain angles – compression angle and expansion angle.

2 Mathematical model

Axial piston pumps with constant pressure and variable flow have extraordinary possibilities for controlling the flow by change of pressure [4], [5], [6]. Owing to pressure feedback, volumetric control of the pump provides a wide application of these pumps in complex hydraulic systems, particularly in aeronautics and space engineering. Some dynamic processes developing in control cycle have been analysed by mathematical model and a large number of process simulations have been done by means of programming language Matlab. On that occasion, some diagrams have been made which have been a basis for analysis of time-constants of transient and it has been concluded that the characteristics comply with the requirements defined by the aeronautics standards.

Figure 1a. shows a schematic view of an axial piston pump with swash plate and with shown angles on valve plate α_k and α_e .

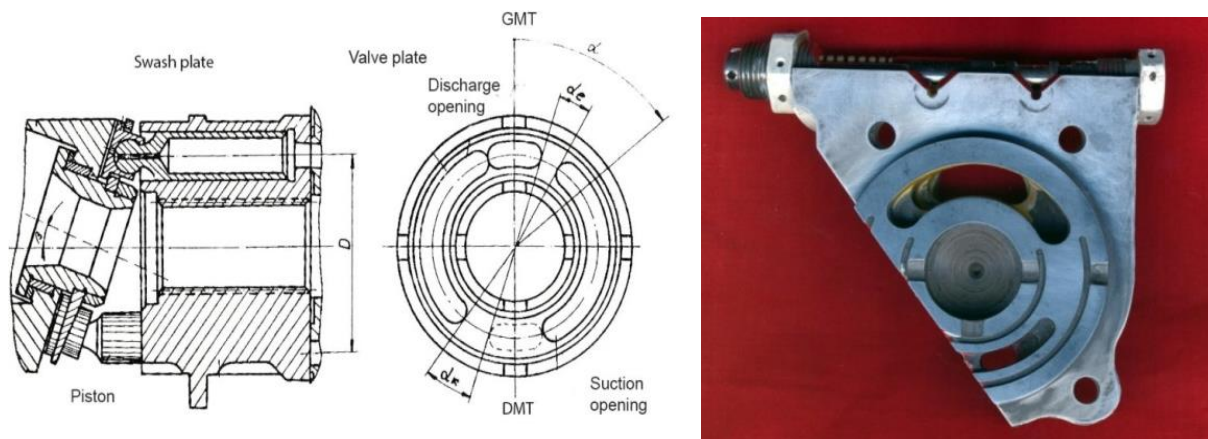


Figure 1a: axial piston pump with swash plate, b) detail of valve port plate

The following equation satisfies the compression and expansion of the fluid:

$$\frac{dV}{dp} = -\frac{V}{E} \quad (1)$$

where:

- E – compressibility module
- V – volume of the working fluid in the cylinder.

The volume of the working fluid in the cylinder of the cylinder block can be expressed by the equations:

$$V = V_0 + RA \operatorname{tg} \beta_{max} - RA \operatorname{tg} \beta \cos \alpha \quad (2)$$

where:

- R=D/2- radius of divider circle of the cylinder block
- A - surface of the piston

The cycle of compression and expansion of the fluid in cylinders is shown in the diagram, points ABCD. At point B the pressure of the fluid in the cylinder rises rapidly and reaches a discharge value, while at point D the pressure begins to decrease rapidly and reaches a filling value. The shock waves that cause noise occur because of these rapid pressure changes. In the case of right choice of compression angle, fluid in the cylinder is compressed and then discharged into suppression opening, point F. The shock wave is avoided in this way since the fluid is compressed to the pressure that exists in the suppression opening. In the same way, by choosing the correct angle of expansion, the pressure in the point D can be reduced to the pressure in the point E. In the first case when $\alpha_k = \alpha_e = 0$, the required mechanical work is equal to the surface of the rectangle ABCD, and in the second case the required work is equal to the surface EBFD. By analyzing this we find that in both cases the generated hydraulic energy is represented with surface EBFD. In case when $\alpha_k = \alpha_e = 0$, the higher work is required which is spent on compression losses to a certain extent. Compression losses in the lower dead point (DMT) are shown with surface of the triangle BCF, while losses in the upper dead point (GMT) are shown with surface of the triangle ADE [7].

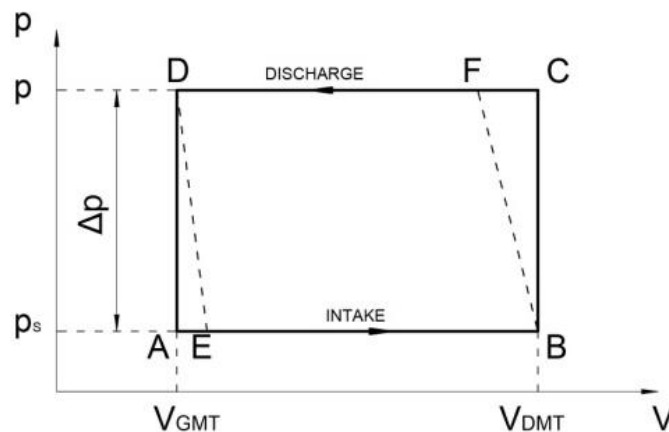


Figure 2: The cycle of compression and expansion of the fluid in cylinders

Using the equations (1) and (2), we get

$$\frac{\Delta p_0}{E} = \frac{V_{GMT} - V_\alpha}{V_{GMT}}; \quad \alpha = \pi + \alpha_k \quad (3)$$

where:

V_{GMT} - The volume of the fluid in the upper dead point.

Δp_0 - The optimum pressure difference at the lower dead point.

V_α - The volume of the working fluid in the cylinder when it is turned for the angle α .

This equation can also be written in another form

$$\Delta p_0 = \frac{ERA(1 - \cos \alpha_k)}{V + RA \operatorname{tg} \beta_{max} + RA \operatorname{tg} \beta} \quad (4)$$

If the requirement that $\Delta p = \Delta p_b$ is fulfilled, then the losses do not occur in the upper dead point for the expansion angle α_e .

Analogously to equation (4), the equation (5) is obtained:

$$\Delta p_b = \frac{ERA(1 - \cos \alpha_e)}{V_0 + RA \operatorname{tg} \beta_{max} + RA \operatorname{tg} \beta} \quad (5)$$

The compression losses in the upper dead point for the pressure difference Δp will be:

$$W_{GMT} = \frac{1}{2} (\Delta p - \Delta p_b)^2 \cdot \frac{V_{GMT}}{E} = \frac{1}{2E} (\Delta p - \Delta p_0)^2 \cdot (V_0 + RA \operatorname{tg} \beta_{max} + RA \operatorname{tg} \beta) \quad (6)$$

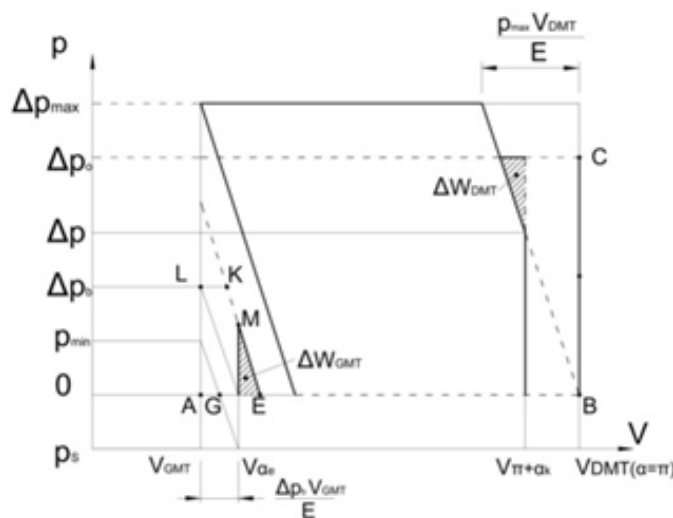


Figure 3: Diagram for $\Delta p \geq \Delta p_{min}$

We can write the equation of the compression losses in the lower dead point:

$$W_{DMT} = \frac{1}{2E} (\Delta p - \Delta p_0)^2 \cdot (V_0 + RA \operatorname{tg} \beta_{max} - RA \operatorname{tg} \beta) \quad (7)$$

In case $\alpha_e = \alpha_k = 0$, losses can be expressed as:

$$W = W_{GMT} + W_{DMT} = \frac{\Delta p^2}{E} (V_0 RA \operatorname{tg} \beta_{max}) \quad (8)$$

The relative compression loss in percentage can be expressed by equation:

$$\Delta W[\%] = \frac{\Delta W}{P_{ABCD}} 100\% = \frac{1}{2E} \Delta p \left(1 + \frac{V_0}{RA \operatorname{tg} \beta_{max}} \right) \quad (9)$$

where:

P_{ABCD} - surface defined in Figure 2.

If the pressure difference Δp is below Δp_{min} , where $\Delta p_{min} = \Delta p_b - p_s$, and p_s is supply pressure, the under-pressure must not occur in cylinder [8, 9].

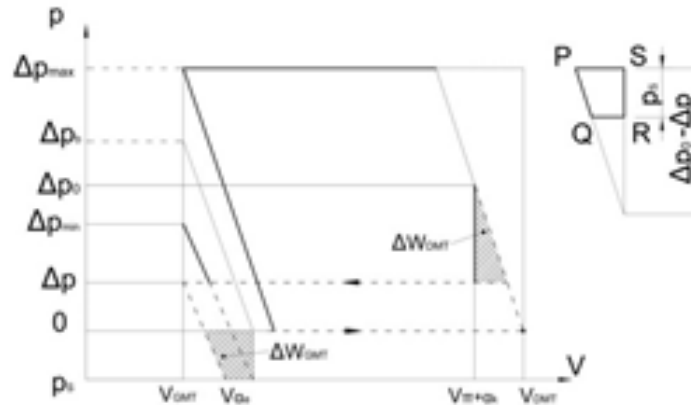


Figure 4: Diagram for $\Delta p \leq \Delta p_{min}$

The expansion losses in the lower dead point can be expressed by the following equation:

$$\Delta W_{DMT} = P_{PORS} = \frac{1}{2E} (\Delta p_o - \Delta p)^2 \cdot V_{DMT} - \frac{1}{2E} (\Delta p_b - \Delta p - p_s) \cdot V_{DMT} = \frac{1}{2E} \cdot V_{DMT} \cdot p_s (2\Delta p_b - 2\Delta p - p_s) \quad (10)$$

Diagram of the losses depending of the compression and expansion angles can be obtained by these equations. The pressure differences Δp_o and Δp_b are calculated first, and then W_{GMT} and W_{DMT} .

3 Experimental results

Technical data of axial piston pump with variable flow which has the swash plate with these properties:

$D = 43 \cdot 10^{-3} \text{ m}$ - diameter of divider circle of the cylinder block

$V_0 = 0,581 \cdot 10^{-6} \text{ m}^3$ - minimum volume of fluid in the cylinder

$\beta = 19^\circ$, -angle of swash plate

$A = 0,785 \cdot 10^{-4} \text{ m}^2$ - surface of the piston

$E = 1,542 \cdot 10^3 \text{ MPa}$ - compressibility module of fluid AMG10 at temperature $t=60^\circ$ and pressure $p=20\text{MPa}$.

Figure 5 shows a diagram of changes of some losses depending on the change in fluid pressure in the pressure pipe. Compression losses and losses due to the leakage are linearly increasing with the increase of the pressure. On the other hand, the mechanical losses are firstly reduced to a certain limit and then are increasing with increase of the pressure [9, 10].

Compression losses depend largely on the following values:

- Compressibility module of the working fluid,
- The pressure difference,
- The minimum volume of the cylinder

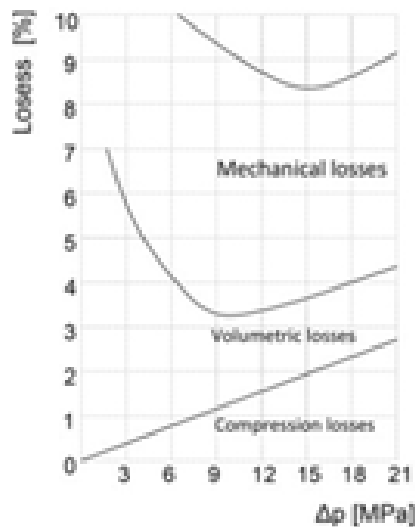


Figure 5: Diagram of some losses of axial piston pump

Minimum volume and compressibility module are taken as a constant, although the compressibility module depends on the temperature and pressure. It is noted that at constant values of the angle of swash plate inclination β and the pressure difference Δp , compression losses can be reduced to minimum by proper choice of angles α_k and α_e . The problem is that inclination angle β and pressure difference Δp are constantly changing during the operation of the pump, so the optimum pre-compression and pre-expansion are not done at certain angles α_k and α_e . Diagrams ΔW_{DMT} and ΔW_{GMT} for one cylinder and one revolution depending on the angles α_k and α_e are shown in Figures 6 and 7, as a result of these calculations. It should be noted that any change in the inclination angle of the swash plate affects the change of losses ΔW_{DMT} and ΔW_{GMT} . By doing the analysis it can be determined that the compression loss in GMT is much smaller than in the DMT at higher values of the angle α_e . The optimal compression angle α_k for a specified working range can be chosen from the diagram shown in Figure 6.

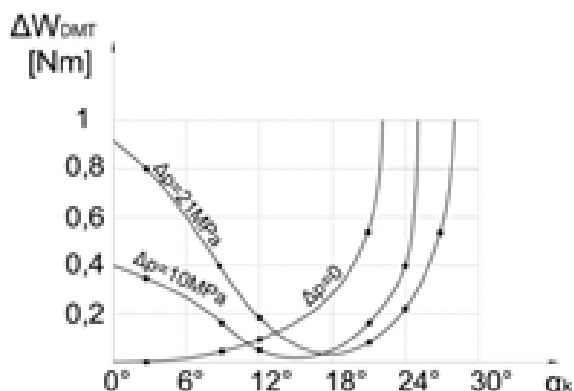


Figure 6: Diagrams of compression losses in DMT for one cylinder and one revolution

For example, if it is assumed that the angle $\beta=19^\circ$ and the pressure difference is $0 < p < 21 \text{ MPa}$, then $\alpha_k(\text{opt}) = 14$. For the angle $\alpha_k = 14^\circ$ compression loss per cylinder and revolution is maximum 0.13 Nm , if the pressure difference Δp varies from 0 to 21 MPa. However, if the another angle β is chosen or another range of the pressure difference Δp , then, from the diagram, we can find the optimal value of the compression angle α_k . Table I shows the compression losses for various values of the inclination angle β and compression angle α_k . By analyzing the mean values of losses it can be concluded that for certain angles of inclination the compression angle α_k has an optimum value which is 14° .

Table 1: The compression losses for various values of the angle β and compression angle α_k

$\beta \backslash \alpha_k$	10°	11°	12°	13°	14°	15°	16°	17°
19°	0,29	0,24	0,20	0,15	0,13	0,19	0,22	0,29
15°	0,31	0,27	0,22	0,20	0,14	0,12	0,14	0,22
10°	0,31	0,29	0,27	0,24	0,20	0,18	0,19	0,21
5°	0,33	0,33	0,31	0,29	0,28	0,27	0,25	0,22
Average value	0,31	0,28	0,25	0,22	0,18	0,19	0,20	0,23

Figure 7 shows a diagram of losses depending on expansion angle α_e , at particular inclination angle β , supply pressure p_s and minimum volume of the cylinder V_0 . It can be seen from the diagram that for large enough expansion angle α_e the losses ΔW_{gmt} can be neglected. The optimum angle of expansion α_e for above mentioned data is in the range from 12 to 16° .

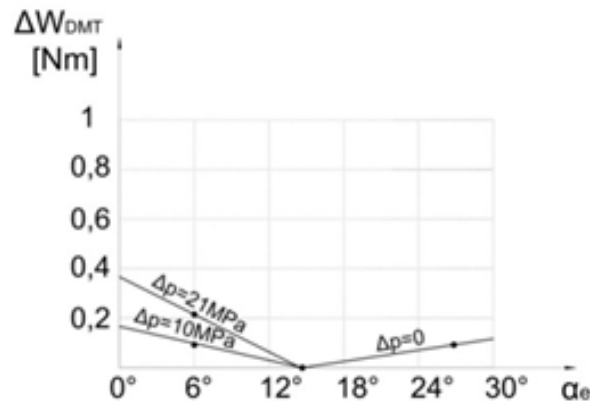


Figure 7: Diagrams of compression losses in GMT for one cylinder and one revolution

This paper also considers the noise problems and the tests were performed on the same pump where the compression losses were measured. Noise level was measured using a device for measuring the noise with C filter. The microphone was attached to the stand at a distance of 5cm from the frontal area of the valve plate.

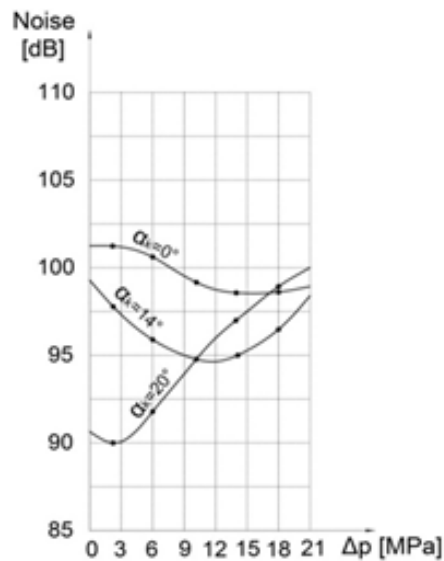


Figure 8: Results of measurements of noise depending on the pressure
 $n=1980 \text{ min}^{-1}$, $\beta=19^\circ$, $\alpha_e=0$

This place was chosen because the loudest noise occurs in the area of the valve plate, and to rule out the effect of noise from other devices. Figure 8 shows results of measurements of noise depending on the pressure of the fluid in the pressure pipe. In this case, the expansion angle is $\alpha_e=0$, rotation frequency $n=1500 \text{ min}^{-1}$, inclination angle of the swash plate is $\beta=19^\circ$, while the compression angle was changed and had values $\alpha_{k1}=0$, $\alpha_{k2}=14$, $\alpha_{k3}=20$. It can be concluded that at the lowest pressure and the highest compression angle $\alpha_k=20^\circ$ noise is greater than with the first pump, in which compression angle was $\alpha_k=0^\circ$. If the compression angle is $\alpha_k=14^\circ$, reduction of noise will occur at the pressure of 6MPa.

Figure 9 shows results of noise measurements under the same conditions as in the previous case, with the exception in compression and expansion angles α_k and α_e . The compression angle was $\alpha_k=0^\circ$, and the expansion angle was changed and had values $\alpha_{e1}=0$, $\alpha_{e2}=12$, $\alpha_{e3}=14^\circ$. By

analyzing a diagram it can be concluded that for these test conditions the optimal expansion angle is $\alpha_e = 12^\circ$.

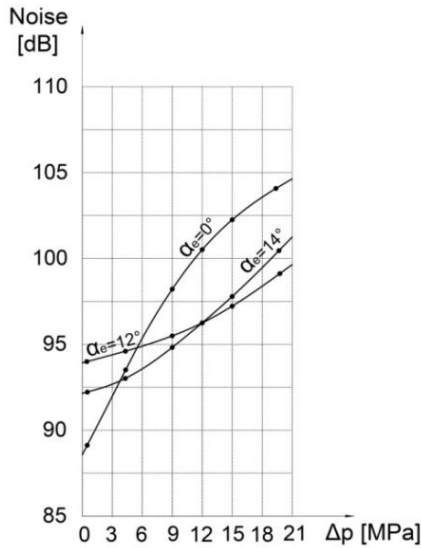


Figure 9: Results of measurements of noise depending on the pressure $n=1980 \text{ min}^{-1}$, $\beta=19^\circ, \alpha_k=0$

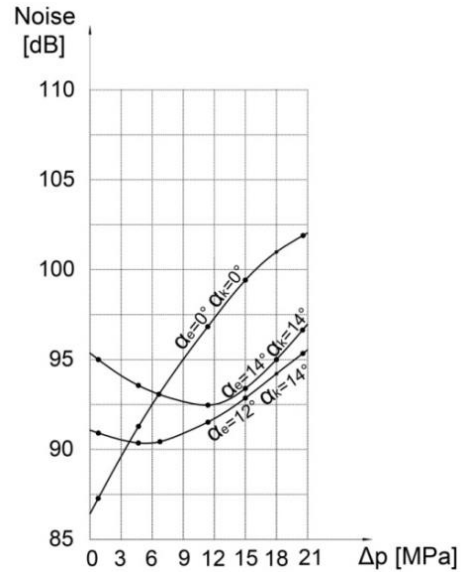


Figure 10: Results of measurements of noise depending on the pressure $n=1500 \text{ min}^{-1}$, $\beta=19^\circ, \alpha_k=0$

Figures 10, 11 and 12 show the results of noise measurements depending on the pressure for different rotation frequencies $n_1=1500 \text{ min}^{-1}, n_2=1980 \text{ min}^{-1}, n_3=3000 \text{ min}^{-1}$ and for the different expansion angles $\alpha_{e1} = 0^\circ, \alpha_{k1} = 0^\circ, \alpha_{e2} = 12^\circ, \alpha_{k2} = 14^\circ, \alpha_{e3} = 14^\circ, \alpha_{k3} = 14^\circ$.

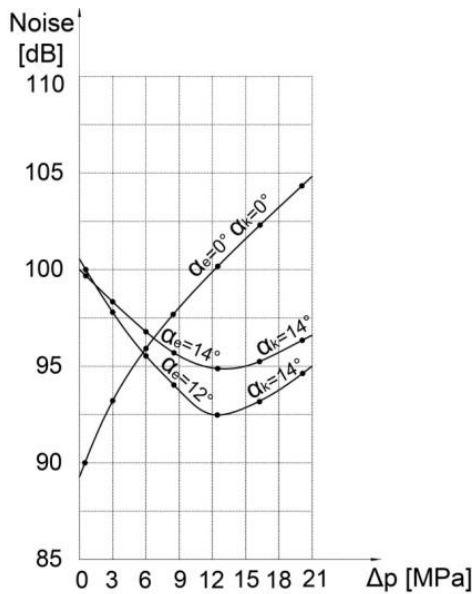


Figure 11: Results of measurements of noise depending on the pressure $n=1980 \text{ min}^{-1}, \beta=19^\circ$

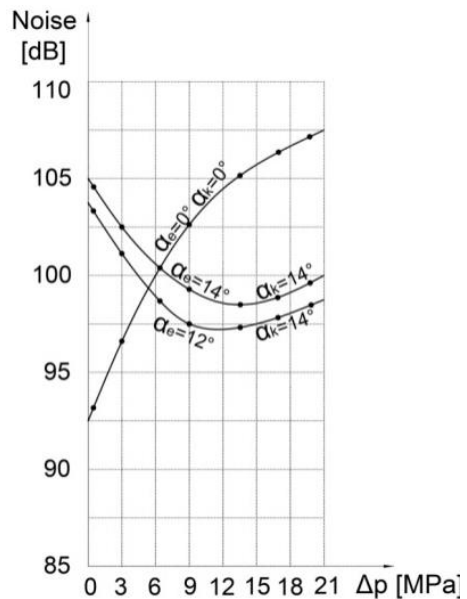


Figure 12: Results of measurements of noise depending on the pressure $n=3000 \text{ min}^{-1}, \beta=19^\circ$

Since the optimal value of the expansion angle $\alpha_e = 12^\circ$ is near the optimal value of the compression angle $\alpha_k = 14^\circ$, the case when $\alpha_e = \alpha_k = 14^\circ$ is considered. Symmetry of openings of the pump distribution is present in this case, so the pump can be the two-way with the same valve plate, which reduces the production cost with a slight increase in noise.

4 Conclusion

The basic fact that producers and users of axial piston pumps must accept is that every increase in the operating pressure leads to the increase in pump noise. The greater influence on the noise level has the increase of rotation frequency of pump's drive shaft than the increase of pressure in the pressure pipe. Since the rotation frequency has a large impact on noise, it is often reduced in order to neutralize the noise caused by increasing pressure. If the rotation frequency is reduced, we have to use larger pump that is heavier and more expensive to remain the same flow. In case of increasing flow two times (which means that the rotation frequency can be reduced two times), the pump price increases by 30 %. In addition, the weight increases by approximately 50 % and the larger space is required for installation due to increase of built-in measures. Reducing the rotation frequency in order to reduce the noise has a negative effect also, but if the pump is assembled in places where noise must be as small as possible, then this solution is used. Cavitations that occur as a result of insufficient supplying of the pump can affect the noise level. Bearings and gears also contribute to the increase of noise. It should also be noted that the choice of appropriate materials can attenuate certain vibrations that also lead to increase of the noise. The pump noise can be minimized if all these factors are taken into account.

References

- [1] Petrovic, R., Mathematical modelling and identification of multi cylindrical axial piston pump parameters. PhD Thesis, Faculty of Mechanical Engineering, 1999, Belgrade, Serbia, 1999.
- [2] Petrović, R.: Mathematical Modelling and Experimental Research of Characteristic Parameters of Hydrodynamic Processes of an Axial Piston Pump, *Strojniški vestnik - Journal of Mechanical Engineering* 55 (2009) 4, UDK 621.785.4, 2009
- [3] Petrović, R., Pezdirnik, J., Banaszek, A.: Mathematical Modelling and Experimental Research of novel seawater hydraulic axial piston pump, *The Twelfth Scandinavian International Conference on Fluid Power*, ISBN=978-952-15-2521-6(Vol.4), May 18-20, 2011, Tampere, Finland, p.459-469, 2011
- [4] Ivanović, P., Petrović, R., Todić, N.: Experimental research of characteristic parameters of hydrodynamic processes of axial piston pumps with constant pressure and variable flow, *Tractors and power machines*, ISSN 0354-9496, 2008, Novi Sad, Serbia, Vol. 13, No. 1, p. 52 – 59, 2008
- [5] Petrović, R., Gašić, H., Živković, M.: Influence of Compressibility of Working Fluid on Hydrodynamic Processes in the Axial Piston Pump, *21st International Conference on Hydraulics and Pneumatics, ICHP 2011*, ISBN=978-80-248-2430-7, June 1st – 3rd 2011, Ostrava, Czech Republic, p.145-151, 2011
- [6] Petrović, R., Pezdirnik, J., Banaszek, A.: Influence of Compressibility of Working Fluid on Hydrodynamic Processes in The Axial Piston Pump With Combined Distribution/Flow of Working Fluid, *Proceedings of the 2011 International Conference on Fluid Power and Mechatronics*, IEEE Catalogue number: CFP1199K-CDR ISBN: 978-1-4244-8449-2, 17 – 20 August 2011 Beijing, China, p.335-339, 2011
- [7] Petrović, R., Živković, M., Gašić, M.: Mathematical Modelling, Experimental Research and Optimization of Characteristic Parameters of the Valve Plate of the Axial Piston Pump/Motor, ISBN=4-931070-08-6, 8th JFPS International Symposium on Fluid Power October 25-28, 2011, Okinawa, Japan, p.175-181, 2011

- [8] Todić, N., Filipović, N., Petrović, R.: Modelling of torque with friction effect for water hydraulic axial piston pump/motor, Fourth Serbian (29th Yu) Congress on Theoretical and Applied Mechanics, ISBN: 978-86-909973-5-0, 4-7 June 2013 Vrnjačka Banja, Serbia, p. 843–848, 2013
- [9] Petrovic, R., Andjelkovic, M., Radosavljevic, M., Todic, N.: Experimental Research and Optimization of Characteristic Parameters of the Valve Plate of the Axial Piston Pump/Motor, ISBN: 978-80-01-05542-7, International Conference of Machine Design Departments (ICMD2014), September 9 – 12, 2014, Beroun, Czech Republic, p.161-170, 2014

Mathematical Modelling and Experimental Research of Characteristic Parameters barrel-valve plate of aviation hydraulic piston pumps

RADOVAN PETROVIĆ, SHAOPING WANG, MAJA ANDJELKOVIĆ & RADOJE CVEJIĆ

Abstract Hydraulic pump is the heart of aircraft hydraulic system. Performance degradation based on mixed wear theory of aviation hydraulic piston pumps: its reliability and safety is very important; complicated structure; high pressure; high speed; strong vibration, multi field coupling, high reliability and long life.

This paper establish detailed model based on mixed lubrication-wear mechanism. Experiment and validation indicate that the proposed mathematical model can reflect the integrated development process of hydraulic pump.

Mechanical analysis of barrel-valve plate covers: film thickness, pressure distribution in different angles, contact pressure considering machined roughness, elastic and plastic deformation, comparison of contact force and fluid force, elastic and plastic deformation, viscosity and deformation compensation.

Keywords: • hydraulic piston pump • mathematical modelling • experimental research • strong vibration • lubrication-wear mechanism •

CORRESPONDENCE ADDRESS: Radovan Petrović, Ph.D., Professor, University “Union - Nikola Tesla” of Belgrade, Faculty for Strategic and Operational Management, Sajmište 29, 11070 Belgrade, Serbia; e-mail: radovan4700@yahoo.com. Shaoping Wang, Ph.D., Cheung Kong Scholar Chair Professor, Beihang University, College of Automation Science and Electrical Engineering, 37 Xueyuanlu, Haidian District, Beijing 100191, P.R. China, e-mail: shaopingwang@vip.sina.com. Maja Andjelković, Ph.D., Professor, University “Union - Nikola Tesla” of Belgrade, Faculty for Strategic and Operational Management, Sajmište 29, 11070 Belgrade, Serbia; e-mail: maja.andjelkovic@fpp.edu.rs. Radoje Cvejić, Ph.D., Professor, University “Union - Nikola Tesla” of Belgrade, Faculty for Strategic and Operational Management, Sajmište 29, 11070 Belgrade, Serbia; e-mail: radoje.cvejic@fsom.edu.rs.

1 Introduction

The main friction pairs of axial piston pump consist of cylinder block/valve plate, piston/plunger chamber and piston shoes/swash plate. In normal condition, the main friction pairs operate in good lubrication condition. However, the complicated operational principle makes it easy enter boundary lubrication even abrasion, so the wear and tear plays major role in failures of axial piston pump. The failure analysis of axial piston pump divides into two types: one focuses on the lubrication and another emphasizes on the wear and tear. In 1986, Yagaguchi studied the lubrication between the valve plate and cylinder block, and gives the mathematical model of fluid oil [1].

Based on studied model, he established the dynamic model of cylinder block, calculated its force and torque, and provided the stable condition of constant oil film between the valve plate and the cylinder barrel [2]. Through fixing up the displacement sensors along the valve plate, he got the oil film thickness between the valve plate and the cylinder block [2]. In order to get the variation of oil film, Maring measured the oil film pressure between piston shoes and swash plate through experiment [3]. At the same time, Ivantysynova established the oil film model of cylinder block and valve plate considering the elastic deformation of the contact surface under high pressure [4]. She also analysed the temperature influence between this friction pair considering the effects of viscosity and pressure change [5], [6]. With the continuous operation of the axial piston pump, Greenwood and Williamson discovered the local contact when the oil film thickness is less than the roughness of the two surfaces, and built the Greenwood-Williamson model based on the elastic contact of rough surfaces [7]. In order to connect the bridge between the lubrication and abrasion of friction pairs, Patir and Cheng proposed a kind of Reynolds equation to solve the lubrication problem under local contact condition for the axial piston pump [8], [9].

Yamaguchi analysed the mixed lubrication based on Greenwood Williamson model and Patir equation and built the test rig [10]. The corresponding experiment indicated that the proposed model can give the predict friction force and flow rate. Subsequently, many researches presented a series models to describe the multi scale characteristics of rough peak curvature in two surface contact [11], [12]. Majumdar and Bhushan established the classification model of elastic plastic contact process on the rough peak, which means the plastic deformation connect each other and develop them to the elastic state [13]. Considering the rough peak deformation, Liou proposed a contact model based on height distribution of non Gauss distribution [14].

From the real micro profile monitoring, the wear and tear of friction pairs of axial piston pump depends on the pressure distribution, temperature distribution, oil film thickness variant and contact wear principle, so this paper establishes the mixed wear model considering the lubrication, boundary lubrication and abrasion, provides the performance degradation law and gives the estimation based on the on line wear debris monitoring.

2 Modelling of axial piston pump

Figure 1 shows the structure of axial piston pump, in which the valve plate and swash plate are fixed, the shaft drives the cylinder block rotation and the pistons reciprocate in it when the axial piston pump operates. There are three friction pairs in axial piston pump, that is, cylinder block/valve plate, slipper/swash plate and piston/ plunger cavity. The cylinder block-valve plate plays important role in axial piston pump because its failures predominate in maintenance.

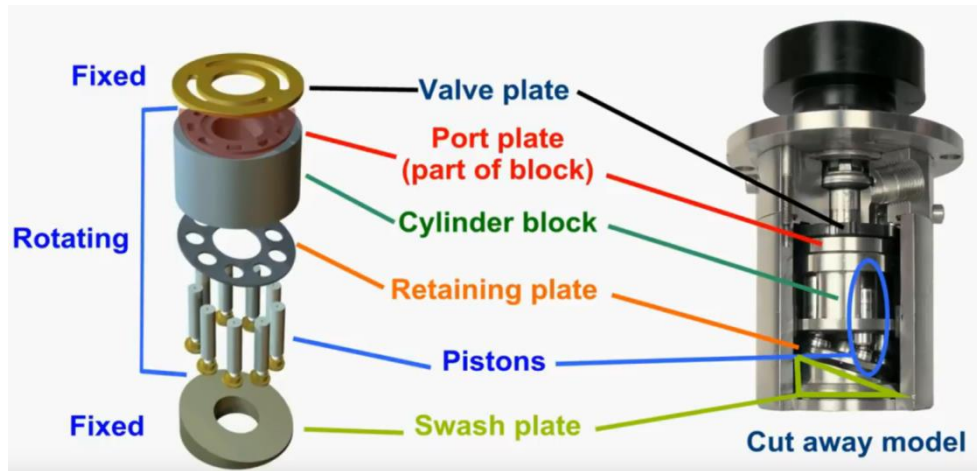


Figure 1: The structure of axial piston pump

Through analysing the surface morphology of the worn valve plate, its eccentric wear in high-pressure area occupies the primary position. Since the axial piston pump is full of oil, its normal operation depends on the lubrication between friction pairs. Based on the tribology theory, most of the abrasive wear of the axial piston pump is caused by oil film damage between friction pair surfaces.

In order to describe the failure development of abrasive wear, it is necessary to investigate the dynamic variation of the fluid film and abrasion rule between valve plate and cylinder block.

2.1 Model of cylinder block and valve plate

Since the imbalance pressure distribution between cylinder block and valve plate, the oil film between the friction pair is wedge-shaped shown in Figure 2.

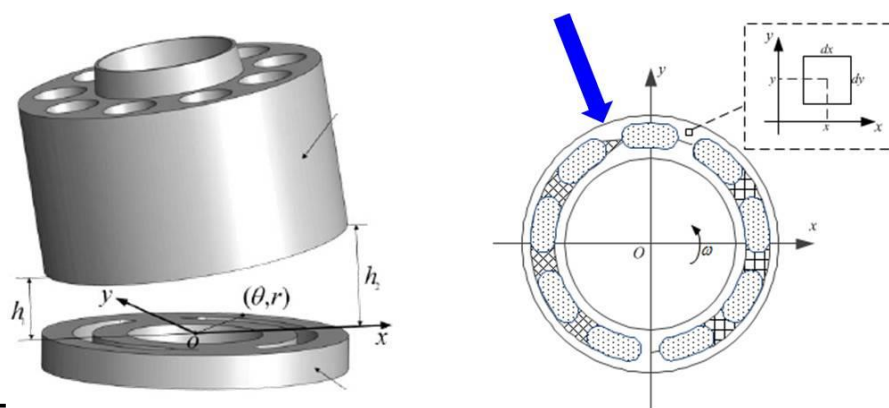


Figure 2: Wedge-shaped oil film between cylinder block and valve plate

For wedge-shaped oil film, the position of the whole cylinder block can be determined through measuring the height of 3 fixed points. Suppose three points in cylinder block are shown in Figure 4, the oil film thickness at arbitrary point can be determined as follows:

$$h(x, y) = \frac{h_3 - h_2}{\sqrt{3}r_r} x + \frac{2h_1 - h_2 - h_3}{3r_r} y + \frac{h_1 + h_2 + h_3}{3}$$

(1)

Where x, y is the coordinate at arbitrary point of valve plate, r_r is reference radius, h_1, h_2, h_3 are the height of oil film in distributed three points of valve plate. According to the Reynolds equation, the relation of support force and velocity can be described as:

$$\frac{\partial}{\partial x} \left(\frac{\rho h^3}{\mu} \frac{\partial p}{\partial x} \right) + \frac{\partial}{\partial y} \left(\frac{\rho h^3}{\mu} \frac{\partial p}{\partial y} \right) = 6 \left[\frac{\partial}{\partial x} (v_x \rho h) + \frac{\partial}{\partial y} (v_y \rho h) + 2\rho \frac{\partial h}{\partial t} \right] \quad (2)$$

Where p_l is the support force of oil film, h is oil thickness, μ is dynamic viscosity which is related to the temperature and pressure.

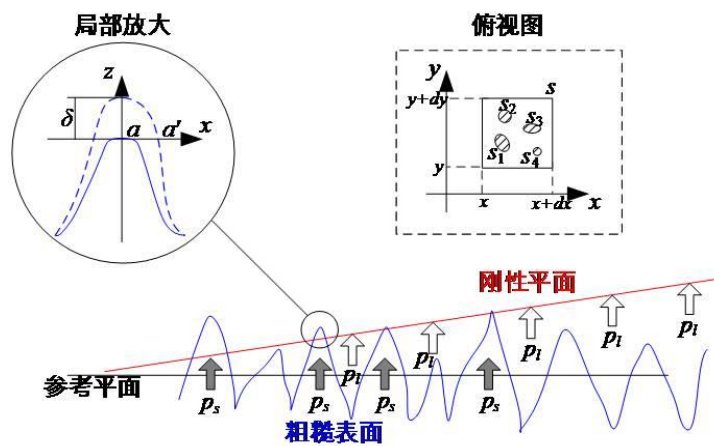


Figure 3: Mixed lubrication state

2.2 Analysis of cylinder block and valve plate

Under ideal condition, there exists a layer of oil film between valve plate and cylinder block, which lubricate the operation of the friction pair shown in Figure 4.

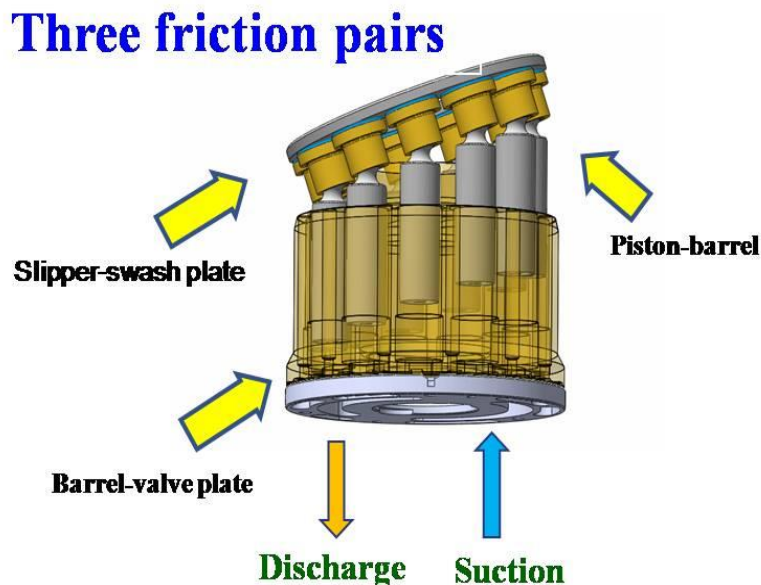


Figure 4: Valve plate and cylinder block

Since the sealing strips separates the high pressure area of outlet and low pressure area of inlet, the periodic eccentric moment exists in valve plate to cause out-of-balance between downward *compressive stress* and *upward support*.

Suppose the contact surface between cylinder block and valve plate has the following characteristics:

- 1) The surface of cylinder block is ideal rigid smooth plane;
- 2) The surface of valve plate is non-rigid rough surface;
- 3) The top of the rough peak on a rough surface is nearly half spherical;
- 4) The curvature of rough peak is related to the sectional area of rough peak.

3 Simulation and validation

Based on the technical documentation was developed model valve plate of axial pump. In computer program FEMAP (*Finite Element Modeling And Postprocessing*) created finite element model.

Valve plate is modeled 3D tetra elements with intermediate nodes. Model consists of 307,644 nodes and 205,323 elements. The analysis assumed that the plate is fixed on one side (Figure 6) and on the other hand, the pressure released in Figure 5. On the part of the pressure distribution plate is loaded with a pressure of 80 bar, and the air duct pressure is 1.2 bar.

In Figures 7 and 8, there is the field of vertical movements, distribution boards made of a material that is PEEK1 PEEK2, respectively, Table 1.

Table 1. Material properties

Material	PEEK 1	PEEK 2
Additive	10 % carbon, 10 % graphite, 10 % PTFE	
Young's modulus [MPa]	9500	3500
Poisson ratio [-]	0.394	0.400
Density [kg/m ³]	1480	1300
Tensile strength, Yield [MPa]	119	97
Compressive yield strength [MPa]	152	118
Friction coefficient [-]	0.19	0.34

The maximum displacement of the **Valve plate** made of materials PEEK1 is 5.86 microns, the material is PEEK2 15.8 microns. For the analysed cases, stresses in the **Valve plate** did not differ significantly. Based on the analysis, it can be concluded that the use of better materials PEEK1 to the **Valve plate**. In future work will be considered as a pump assembly.

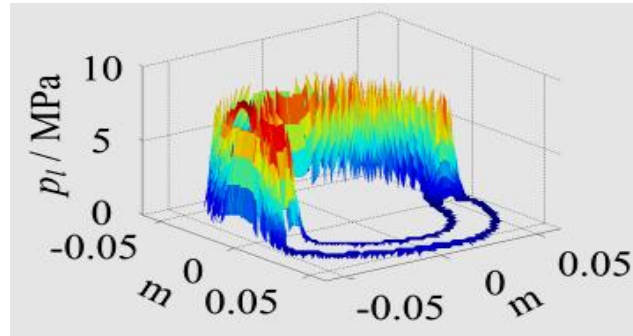


Figure 5: Pressure distribution

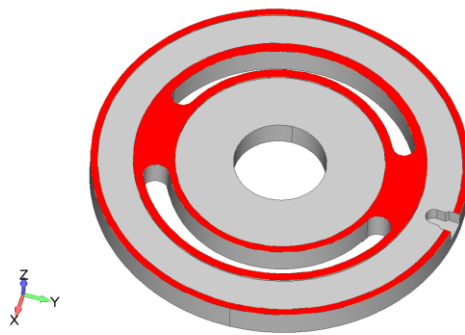


Figure 6: Surfaces to which the specified boundary condition

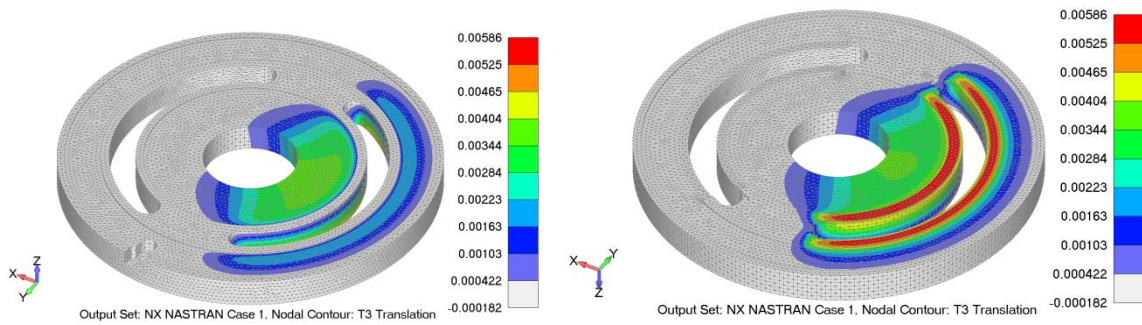


Figure 7: Vertical displacement field [mm], PEEK1

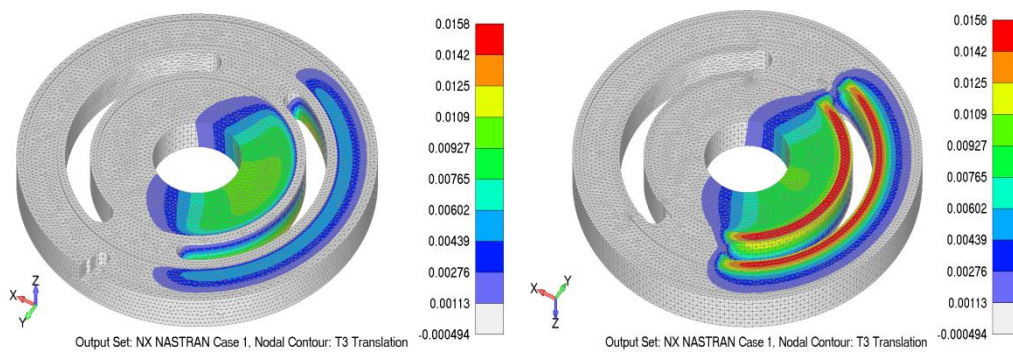


Figure 8: Vertical displacement field [mm] PEEK2

4 Conclusion

The oil film thickness is time dependent and angle position dependent. The oil film thickness decreases from discharge port (150°) to inlet port (330°). The average film thickness of inner sealing strip is smaller than that of outer sealing strip in the angular range of 60° to 240°. The simulation results demonstrate good agreement with reference [15], [16].

This paper studies the performance degradation based on the complicated failure process including lubrication, mixed lubrication and abrasion. Based on Reynolds equation and Hertz abrasion theory, this paper establishes the dynamic abrasive wear model of cylinder block and valve plate from normal lubrication, partial abrasion to wear and tear. Simulation and validation indicate that the proposed mathematical model can reflect the integrated failure development process of axial piston pump, so its performance degradation is more consistent with the actual application [17].

References

- [1] Yamaguchi, A.: Formation of a fluid film between a valve plate and a cylinder block of piston pumps and motors: 1st Report, A Valve Plate with Hydrodynamic Pads, Bulletin of JSME, Vol.29, No.251, pp.1494-1498, 1986
- [2] Yamaguchi, A.: Formation of a fluid film between a valve plate and a cylinder block of 16 15th International Conference on Tribology – Serbiatrib '17 piston pumps and motors.(2nd report A valve plate with hydrostatic pads, JSME international journal, Vol. 30, No.259, pp. 87-92, 1987
- [3] Manring, N. D.: Friction forces within the cylinder bores of swash-plate type axial-piston pumps and motors, Journal of dynamic systems, measurement, and control, Vol. 212, No.3, pp.531-537, 1999
- [4] Ivantysynova, M., Lasaar, R.: An investigation into micro-and macrogeometric design of piston/cylinder assembly of swash plate machines, International Journal of Fluid Power, Vol. 5, No. 1, pp. 23-36, 2004
- [5] Huang, C., Ivantysynova, M.: A new approach to predict the load carrying ability of the gap between valve plate and cylinder block, Bath Workshop on Power Transmission and Motion Control, pp.225-240, 2003
- [6] Jouini, N., Ivantysynova, M.: Valve plate surface temperature prediction in axial piston machines, in: Proceedings of the 5th FPNI PhD symposium, Cracow, Poland, pp. 95-110, 2008
- [7] Greenwood, J., Williamson, J.: Developments in the theory of surface roughness, in : Proc. 4th Leeds–Lyon Symp. on Tribology, D. Dowson et al.[Eds.], Mechanical Engineering Publications, London, pp.167-177, 1977
- [8] Patir, N., Cheng, H. S.: An Average flow model for determining effects of three-dimensional roughness on partial hydrodynamic lubrication, Journal of Lubrication Technology, Vol. 100, No.1, pp. 12-17, 1978
- [9] Patir, N., Cheng, H.: Application of average flow model to lubrication between rough sliding surfaces, Journal of Lubrication Technology, Vol. 101, No.2, pp.220-229, 1979
- [10] Yamaguchi, A., Matsuoka, H.: A mixed lubrication model applicable to bearing/seal parts of hydraulic equipment, Journal of tribology, Vol. 114, No.1, pp.116-121, 1992
- [11] Kazama, T., Yamaguchi, A.: Application of a mixed lubrication model for hydrostatic thrust bearings of hydraulic equipment, Journal of tribology, Vol. 115, No.4, pp. 686-691, 1993
- [12] Kazama, T., Yamaguchi, A.: Experiment on mixed lubrication of hydrostatic thrust bearings for hydraulic equipment, Journal of tribology, Vol. 117, No. 3, pp. 399-402, 1995
- [13] Majumdar, A., Bhushan, B.: Role of fractal geometry in roughness characterization and contact mechanics of surfaces, ASME J. Tribol, Vol. 112, No. 2, pp.205-216, 1990
- [14] Liou, J. L., Tsai, C. M., Lin, J. F.: A micro contact model developed for sphere-and cylinder-based fractal bodies in contact with a rigid flat surface, Wear, Vol. 268, No. 3, pp. 431-442, 2010

R. Petrović, S. Wang, M. Andjelković & R. Cvejić: Mathematical Modeling and Experimental Research of Characteristic Parameters barrel-valve plate of aviation hydraulic piston pumps

- [15] Bergada, J. M., Davies, D. L., Kumar, S., Watton, W.: The effect of oil pressure and temperature on barrel film thickness and barrel dynamics of an axial piston pump, *Meccanica*, No. 47, pp. 639-654, 2012
- [16] Hong, W., Wang, S., Tomovic, M.: A hybrid method based on band pass filter and correlation algorithm to improve debris sensor capacity, *Mechanical Systems and Signal Processing*, No.82, pp.1-12, 2017
- [17] Wang, S., Tomovic, M., Liu, H.: *Commercial aircraft hydraulic systems*, Academic Press of Elsevier, 2016

The nonlinear mathematical model of electrohydraulic position servo system

MITJA KASTREVC & EDVARD DETIČEK

Abstract Highly nonlinear nature of electrohydraulic servo system is well known. Main reasons for nonlinear and non-differentiable mathematical description of systems dynamics are the fluid compressibility, leakage flows, friction forces and nonlinear fluid flow through servo valve orifices.

Accurate nonlinear mathematical models based on physical analysis are necessary for construction of computer simulation models. These models are used for detailed analysis of nonlinear dynamic behaviour and for development of different control strategies.

Keywords: • electrohydraulic servo system • position servo system • nonlinear model • computer simulation • dynamic behaviour • analysis

CORRESPONDENCE ADDRESS: Mitja Kastrevc, Ph.D., Assistant Professor, University of Maribor, Faculty of Mechanical Engineering, Smetanova ulica 17, 2000 Maribor, Slovenia, e-mail: mitja.kastrevc@um.si.
Edvart Detiček, Ph.D., Assistant Professor, University of Maribor, Faculty of Mechanical Engineering, Smetanova ulica 17, 2000 Maribor, Slovenia, e-mail: edvard.deticek@um.si.

1 Introduction

Conventional hydraulic systems have been widely used as power units because they can generate very large power compared with their size. Combining these actuators with electro hydraulic servo-valves and sensors as well as appropriate control electronics, we get electrohydraulic servo systems.

Detecting, transmitting and processing the signal by use of electric and electronic components, driving the load with hydraulic transmission in the electro-hydraulic servo control system. So it can make full use of electrical system for its convenience and aptitude, make full use of hydraulic system for its rapid response speed, big load stiffness and accurate positioning characteristics to make the whole system more adaptable.

Electro-Hydraulic Actuators (EHA) are highly non-linear systems with uncertain dynamics in which the mathematical representation of the system cannot sufficiently represent the practical circumstances [1]], [2], [3]. The actuator plays a vital role in industrial processes and manufacturing line. The electro-hydraulic actuator can use either proportional valve or servo valve. It converts electrical signal to hydraulic power [4], as well as conversion to the pneumatic power [5].

Hydraulic servo systems are characterized by their ability to impart large forces at high speeds and are used in many industrial motion systems. The goal of this paper is to present a mathematical model of a complete hydraulic servo system. Mathematical modeling is a description of a system in terms of equations. In order to acquire the highest performance of the electro-hydraulic actuator, a suitable controller has to be designed. As the controller design require mathematical model of the system under control, a method of identifying the actuator need to be chosen so that the best accuracy of the model can be obtained.

For a computer simulation a Matlab Simulink is used. Simulink is a graphical environment for dynamic system modelling, simulation and analysis interactively [5], [6]. Using Simulink environment, can build complex system simulation model, using the mask function to simplify the model, using M files to initial the module variables, which provides great convenience for PID parameters setting and change the variable value of the various modules [7].

2 Analysis and mathematical modelling of electrohydraulic system

A typical electrohydraulic positioning servo system consists of a hydraulic power supply e.-g. constant pressure hydraulic pump with relief valve and accumulator, a flow control servo valve(SV), a hydraulic cylinder, a position sensor and an electronic controller unit (Figure 1).

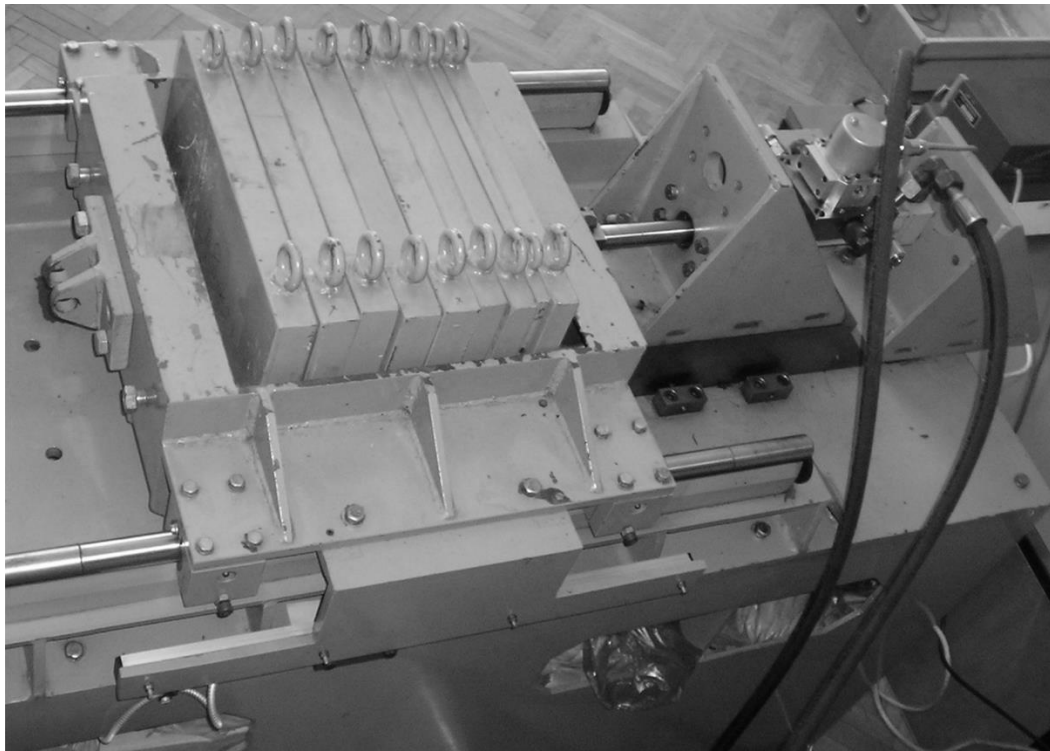


Figure 1: Electro-hydraulic servo system with load

Before of closed loop controller design for electrohydraulic servo system, the analysis of the system dynamics is required, as well as, mathematical modelling and computer simulation of dynamic behaviour [7]. The complete mathematical model of the system is based on physical laws that expresses dynamic behaviour and are described through differential equations. However, this task is troublesome due to the multidisciplinary nature of the electrohydraulic system that requires electric, magnetic, mechanical and hydraulic knowledge. Meanwhile, the nonlinearities of this type of system, such as fluid nonlinear properties, nonlinear servovalve dynamics and flow rate characteristics, as well as, nonlinearities associated with hydraulic actuator by converting hydraulic power into mechanical power, increase a model complexity. The methodology in this work is that a theoretical model is presented first, where each individual component is expressed in a phenomenological description context e.g. basic physical law.

2.1 Description of the SV dynamics

Two stages SV consist of three main parts: the electrical torque motor, the hydraulic amplifier and the valve spool assembly (Figure 2). In these SVs, the motor torque is commanded by an electrical current resulting in the flapper plate movement from its central position. The first stage is the so called flapper-nozzle system which allows the spool motion by adjusting the flapper via a low power electrical signal. The second stage relates the small spool motions ($[\mu\text{m}]$) into a large fluid flow through the spool ports.

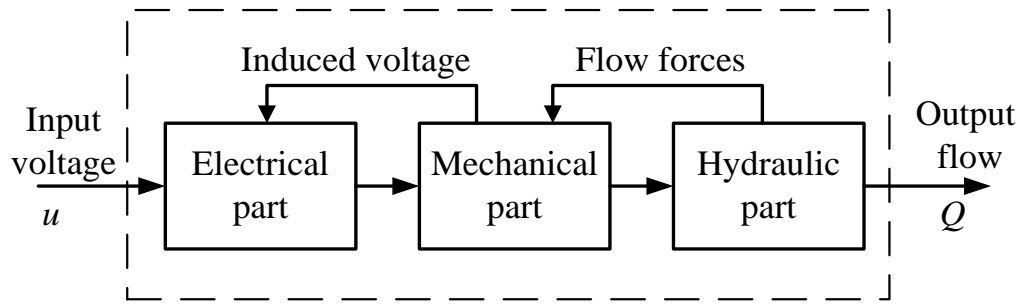


Figure 2: Main parts of two-stage servo valve

The flows in the SV concerns two parts: one is involved in the pilot stage and the other in the second stage.

In the first stage, the flapper deflects due to the torque generated by the torque motor. This force is the result of the current through the two coils fixed around the armature, which is connected to the flapper. As a result of this displacement, the cross sections of the orifices associated with the nozzles change. Schematic of SV cross section is shown in Figure 3.

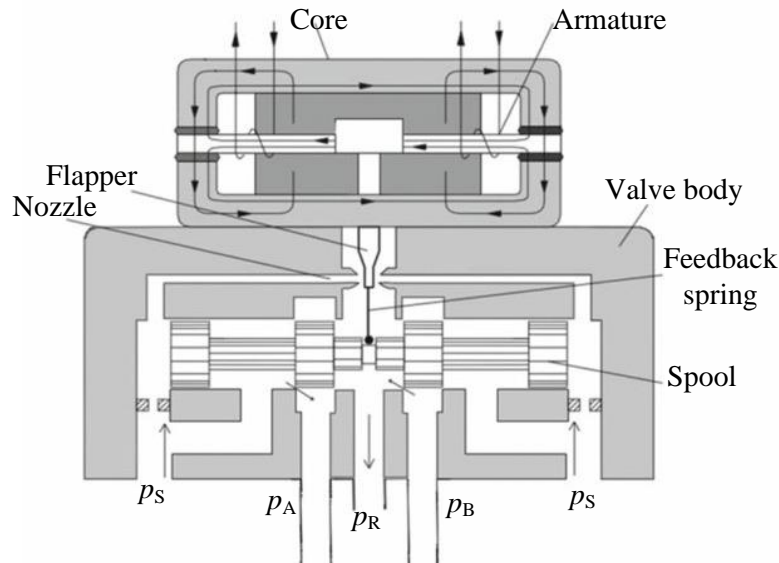


Figure 3: Schematic of SV

Dynamic behaviour of valves involves a large number of parameters. An accurate analytical description would be time consuming and extremely difficult to validate for details. Therefore, it is useful to use manufacturer's catalogue information that provides the well-known step responses and frequency responses for various sizes and types of valves. The inspection of step responses and frequency diagrams suggests an approximation of the SV by a second order model of the form [8].

$$\frac{1}{\omega_v^2} \ddot{x}_v + \frac{2\xi_v}{\omega_v} \dot{x}_v + x_v + f_{HS} \operatorname{sgn}(\dot{x}_v) = k_v \cdot u \quad (1)$$

where: ω_v – is a valve natural frequency, ξ_v - damping coefficient, x_v –valve spool displacement, f_{HS} – takes into account the valve hysteresis and response sensitivity, k_v – valve flow gain, u – valve input signal.

2.2 Hydraulic actuator dynamics

Hydraulic actuator (cylinder) converts hydraulic power into mechanical power. Hydraulic cylinder consists mainly of hollow cylindrical body and a piston. The chamber pressure dynamics is a well-known expression proposed by [4] and can be obtained by applying the conversation principle to each individual chamber, as follows:

$$\dot{p}_A = \frac{\beta_{Aeff}}{V_A} [Q_A - A_p \dot{x}_p + Q_{Li} - Q_{LeA}] \quad (2)$$

$$\dot{p}_B = \frac{\beta_{Beff}}{V_B} [Q_B + \alpha A_p \dot{x}_p - Q_{Li} - Q_{LeB}] \quad (3)$$

The effective bulk modulus essentially depends on pressure, entrained air and mechanical compliance. The commonly used empirical equation for calculation of the effective bulk modulus for hydraulic cylinders is expressed as [9]:

$$\beta_{Aeff} = a_1 \beta_{max} \cdot \log \left(a_2 \frac{p_A}{p_{max}} + a_3 \right) \quad (4)$$

$$\beta_{Beff} = a_1 \beta_{max} \cdot \log \left(a_2 \frac{p_B}{p_{max}} + a_3 \right) \quad (5)$$

with the parameters $a_1=0.5$, $a_2=90$, $a_3=3$, $\beta_{max}=18000$ [bar], $p_{max}=280$ [bar].

The cylinder chambers volumes are given by

$$V_A = V_{A0} + [A_p (x_0 + x_p)] \quad (6)$$

$$V_B = V_{B0} + [\alpha A_p (x_0 - x_p)] \quad (7)$$

Where x_0 is initial piston position, x_p actual piston position and V_{A0}, V_{B0} are the initial chamber volumes which consist of an efficient part (the volume required to fill only the chambers) and inefficient part (volume of the pipelines between the valve and actuator) for the side A and B respectively. $A_A = A_p$ is a piston surface area and the $A_B = \alpha A_p$ rod side area where $\alpha = A_B/A_A$ is a ratio of cylinder bore area and the annulus effective area at the rod side.

Q_{Li} and Q_{Le} denote the internal leakage flow and the external leakage flow respectively. Leakage from one cylinder chamber to another, known as internal leakage flow, by assumption of laminal flow can be calculated:

$$Q_{Li} = k_L (p_B - p_A) \quad (8)$$

where k_L is internal leakage flow coefficient, while the external leakage can be neglected.

The mechanical subsystem dynamics of the piston and the moving mass is described by dynamic equations:

$$m_t \cdot \ddot{x}_p + F_f(\dot{x}_p) = (p_A - \alpha \cdot p_B) A_p - F_{ext} \quad (9)$$

where m_t is total mass, F_f friction force and F_{ext} external load force.

The total mass m_t consists of the piston mass and the mass of hydraulic fluid in the cylinder chambers and the pipelines. However, mass of fluid can usually be neglected with the piston mass.

An important part of above equation is a friction force. Friction is a complex natural phenomenon. It occurs at the physical interface of two surfaces in contact and tangential reaction between them. It can lead to tracking errors, limit cycle oscillations and undesirable stick-slip motion. Friction is commonly modelled as a discontinuous static mapping between the velocity and the friction force:

$$F_f(\dot{x}_p) = F_v(\dot{x}_p) + F_c(\dot{x}_p) + F_s(\dot{x}_p) = \sigma_{vf} \cdot \dot{x}_p + F_{co} \cdot \text{sgn}(\dot{x}_p) + \text{sgn}(\dot{x}_p) \cdot F_{so} \cdot e^{-\frac{|\dot{x}_p|}{c_s}} \quad (10)$$

with σ_{vf} is the parameter for viscous friction, F_{co} - static friction force, F_{so} - Stribeck friction force, c_s - Stribeck velocity. This friction force depends on the velocity sign and is restricted to viscous friction and Coloumb friction with Stribeck effect. Moreover, the friction force must be considered in order to obtain acceptable tracking accuracy.

Natural frequency can be also calculated based on the system design parameters. The natural frequency for the overall system equals the natural frequency of the hydro-mechanical part. Therefore, an electro-hydraulic control system natural frequency will be:

$$\omega_H = \sqrt{\frac{C_H}{m}} \quad (11)$$

In order to calculate the natural frequency of hydraulic cylinder, the hydraulic cylinder stiffness must be found in advance. The total stiffness of differential cylinder is defined with equation [8]:

$$C_H = \frac{\beta_{Aeff} \cdot A_A^2}{V_A} + \frac{\beta_{Beff} \cdot A_B^2}{V_B} \quad (12)$$

In case of synchronous cylinder (double rod of equal area) AA is equal AB. For performance calculation, only the minimum stiffness will be considered since it has the worst effect on the system dynamics.

3 Simulation model

In standard Simulink module library contains many modules, such as Sinks (output module group), Source (input module group), Linear (Linear link module group), Nonlinear (non-linear links module group), Math (mathematical operation module group), Continuous and Connections modules group and so on. Each module contains many sub-module. Models are supported with constants (due the simulation) which can be used as exact numbers or symbol constants. Therefore, the Matlab script is used. M file is the file with a letter M for its extension and is the executable

file in Matlab [6]. For the simulation M file is used to transfer parameters, which are not input or output parameter but refers to the use of variable in M files to passes parameters. Because the variables that M files created are variables of Matlab working space, when a program run to the end, the variables store in the working space. The other programs or simulation model can directly call these variables, in order to achieve the purpose of transmitting parameters.

A complex Simulink model, in order to be versatile and portable, each module parameter often set in parameter name rather than specific value. Assign or initialize these variables before simulation. Figure 4 shows the Simulink model used for compare two models, nonlinear model (in upper part of figure) and linearized model (lower part of figure).

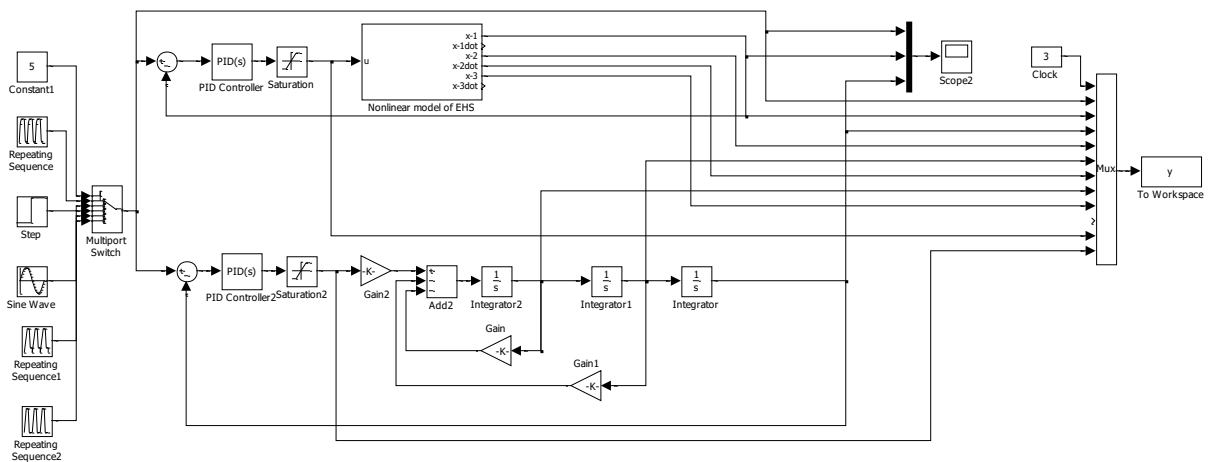


Figure 4: Matlab-Simulink simulation scheme

Figure 5 shows the inside of the subsystem - nonlinear model. The Matlab script is used for initialize the start constants and parameters needed for simulation. For represents the results of simulation the Matlab graphic representation is used, customized by usage of Matlab graphics commands and script file.

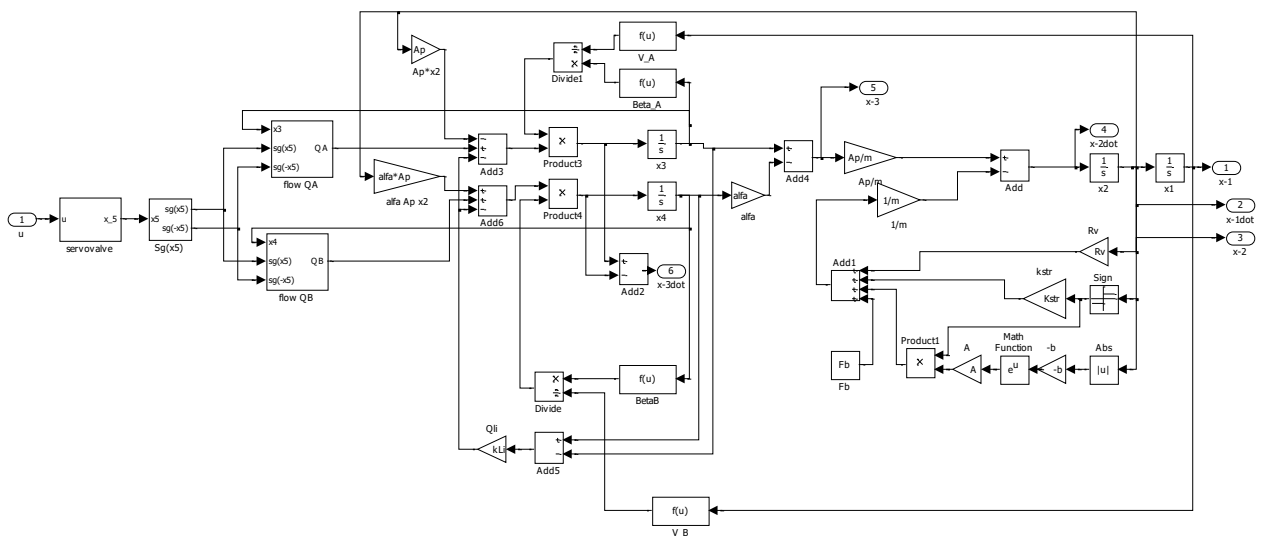


Figure 5: Matlab-Simulink subsystem Nonlinear model of EHS

4 Results

For position control system, dynamically aperiodic response is demanded. The final position accuracy is tested at small steps of reference value.

Table 1: Main parameters of the EHS system

Par.	Value	Par.	Value	Par.	Value	Par.	Value
A_p	$6.4 \cdot 10^{-4} \text{ m}^2$	m	200 kg	F_{ext}	[N]	p_s	210 bar
σ_{vf}	70 Ns/m	V_t	$131.85 \cdot 10^{-6} \text{ m}^3$	k_L	$3 \cdot 10^{-13} \text{ m}^5/\text{Ns}$	ρ	850 kg/m ³
F_{co}	19.62 N	β	$1.5 \cdot 10^9 \text{ Pa}$	C_d	0.63	k_V	$5.53 \cdot 10^{-7} \text{ m}^2/\text{V}$

Because the tracking precision and the positioning accuracy are two most important index of electro-hydraulic position servo control system, so need to examine the variation of these two indexes. The unit step signal is selected as Simulation test signal to check localization accuracy of the system. Figure 6 shows the result of simulation on step response reference.

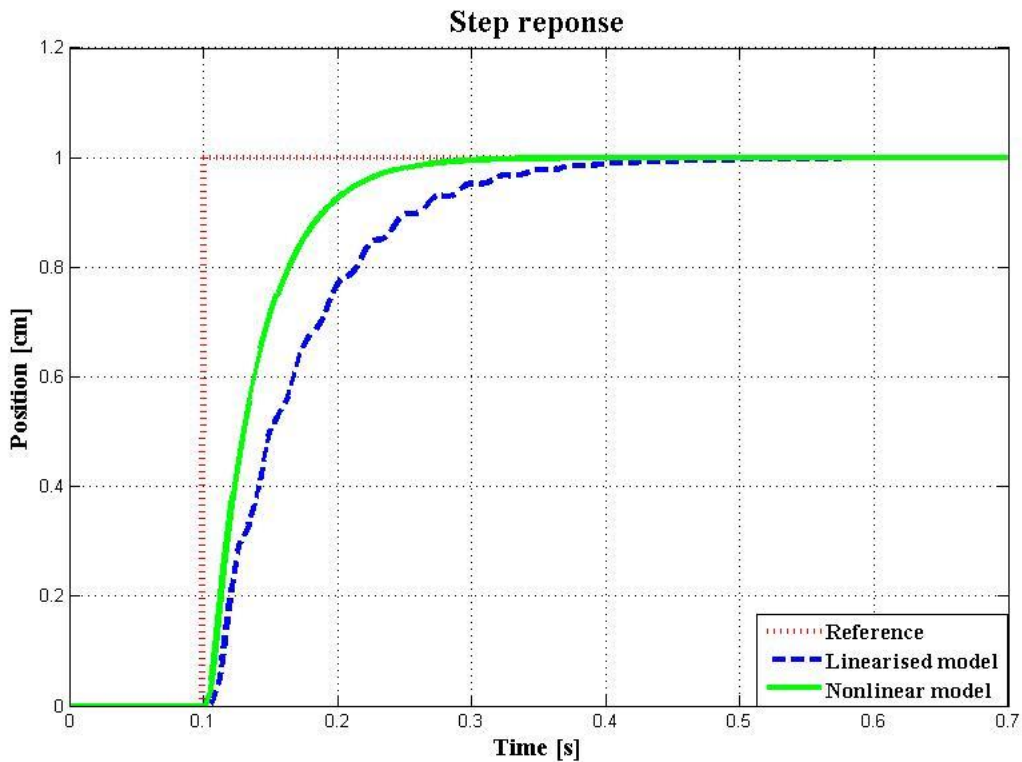


Figure 6: Step response

On Figure 7, the ramp signal is selected as simulation test signal to compare tracking precision of the system on both used mathematical models.

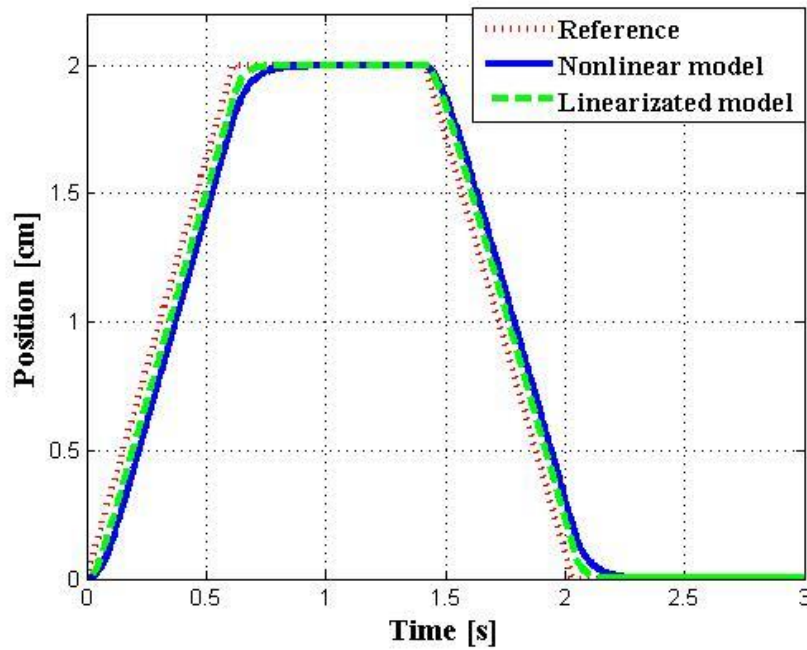


Figure 7: Ramp reference response

Figure 8 represents the ramp signal comparison between simulated data (nonlinear model) and experimental data. On Figures 9 and 10 the details shown on Figure 8 are presented.

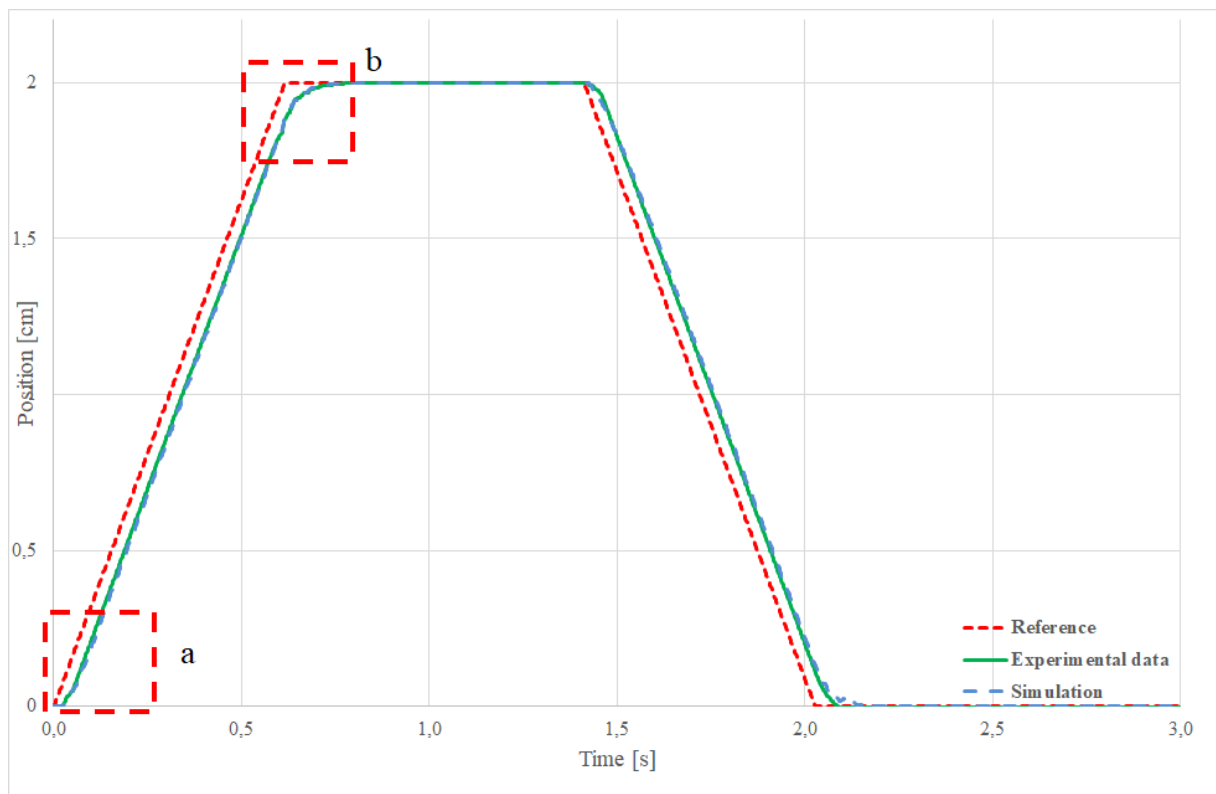


Figure 8. Ramp reference response comparison with experimental data

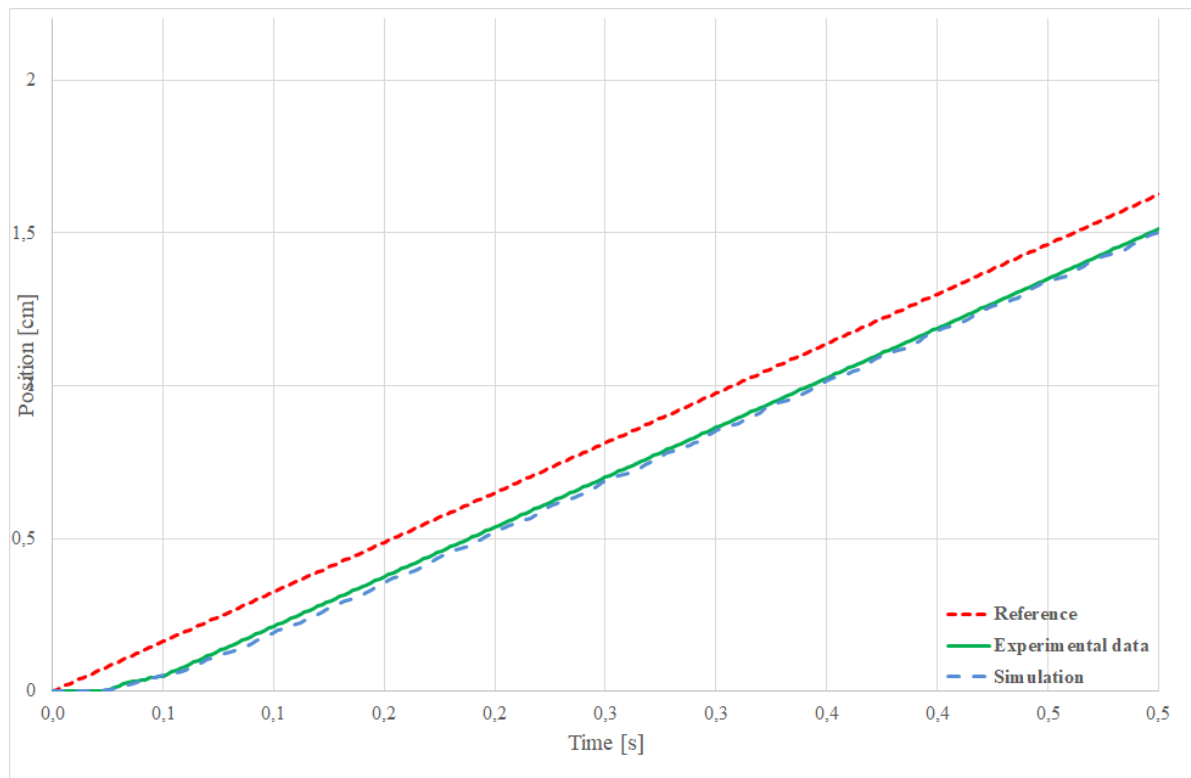


Figure 9: Detail “a” of Figure 8

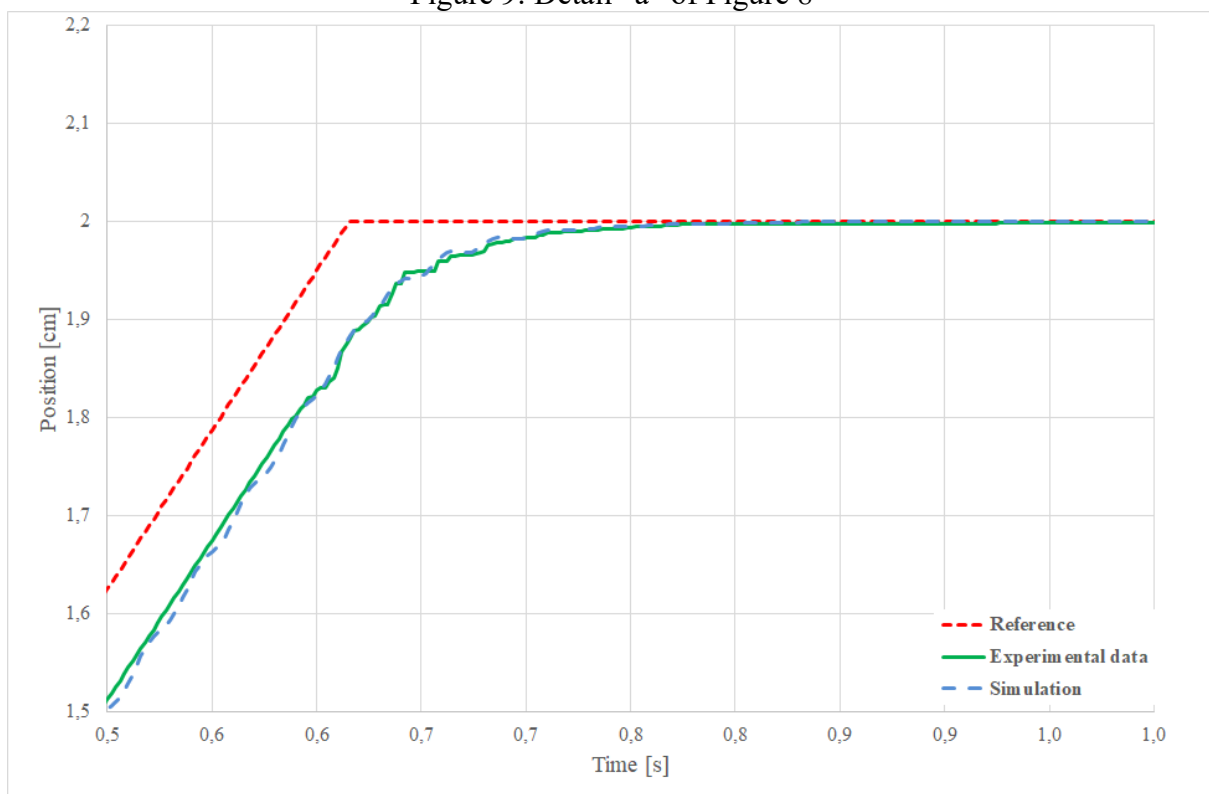


Figure 10: Detail “b” of Figure 8

5 Conclusions

In this paper, a development of nonlinear model for electrohydraulic linear positioning servo system is presented. Comprehensive investigation was carried out on the mathematical modelling

and computer simulation of dynamic behaviour of whole system, based on real laboratory experimental data.

Results of simulation shows the difference between presented models. Linearized models are commonly used, but for detailed analysis are not suitable. This is confirmed with differences shown in Figures 6 and 7. The comparison between experimental data and data archived with use of nonlinear model shows that differences are very small.

Described model was used for development of nonlinear type of controllers.

References

- [1] Merritt, H. E.: Hydraulic Control Systems. Wiley, New York, 1967
- [2] Kovari, A.: Effect of Leakage in Electrohydraulic Servo Systems Based on Complex Nonlinear Mathematical Model and Experimental Results, Acta Polytechnica Hungarica, Vol. 12, No. 3, p. 129-146, 2015
- [3] Wang, Z., Shao, J., Lin, J., Han, G.: Research on controller design and simulation of electrohydraulic servo system, Proceeding of the International Conference on Mechatronic and Automation, Aug. 9-12, IEEE Xplore Press, Changchun, pp: 380-338. DOI: 10.1109/ICMA.2009.52450952009, 2009
- [4] Zulfatman, R. A., Rahmat, M. F.: Modeling and controller design of electro-hydraulic actuator. Proceeding of the 2nd International Conference on Control, Instrumentation and Mechatronic Engineering, June 9-9, UTM Publisher, Malacca, Melaka, Malaysia, pp: 225-231, 2009
- [5] Šitum, Ž.: Control of a Pneumatic Drive Using Electronic Pressure Valves, Transaction of the institute of Measurement and Control 35, No. 8, 2013
- [6] Lopez, C. P.: MATLAB Control System Engineering, Press Academic, Springer Verlag, London, Berlin, Heidelberg, 2014
- [7] Bang, B., Draxler, J., James, G.: Dynamic Hydraulic System Simulation-An Integrated Approach, SAE Technical Paper 902003, 1990
- [8] Wright, H., Alleyne, A., Liu, R.: On the stability and performance of two-state hydraulic servovalves, Proceedings of the ASME Dynamic Systems and Control Division, Vol. 63, p. 215-222, 1997
- [9] Jelali, M., Kroll, A.: Hydraulic Servo-systems: modelling, identification and control, Springer Verlag, London, Berlin, Heidelberg, 2003

Verification of a simulation model to predict the transmission behaviour of hydrostatic bearing on machine tools

JÖRG EDLER & MATTHIAS STEFFAN

Abstract Hydrostatic bearings in machine tools are used for qualitative highest demands. They are used in precision machines, for example in grinding machines, to get a high precision and highest quality in the production, or in machines with high forces during the production process. Generally, hydrostatic bearings are characterized by a good damping behaviour and a good stiffness of the bearing.

To predict the transmission-behaviour of hydrostatic bearings a simulation model was developed. The model considers different geometries of the bearing and also different kinds of fluid supply. To predict the transmission-behaviour it is possible to apply forces and accelerations in the simulation model. In this work the verification of the simulation model by measurement of a hydrostatic test bench is presented. By the verification of the model, it should be possible to dimension hydrostatic bearings and adjust the transmission-behaviour to the working process of the machine tool.

Keywords: • machine tools • hydrostatic bearing • geometry • simulation model • experimental research •

CORRESPONDENCE ADDRESS: Jörg Edler, Dr.techn., Assistant Professor, Graz University of Technology, Kopernikusgasse 24, 8010 Graz, Austria, e-mail: joerg.edler@tugraz.at. Matthias Steffan, Graz University of Technology, Kopernikusgasse 24, 8010 Graz, Austria, e-mail: matthias.steffan@tugraz.at.

<https://doi.org/978-961-286-086-8.18>

ISBN 978-961-286-086-8

© 2017 University of Maribor Press

Available at: <http://press.um.si>.

1 Introduction

Hydrostatic bearings are widely used in technical applications. For instance, as bearing in axial and radial piston machines or as bearings of ship propellers [1]. In the machine tool industry, hydrostatic bearings are used especially in precision machines. They are used for bearing of spindles as well as bearings of linear slides. Machine tools, on the other hand, are subject to the dynamics of the movement process, on the other hand, to the cutting forces during machining. From the movement of the machine low-frequency loads are produced on the machine, see Figure 1.

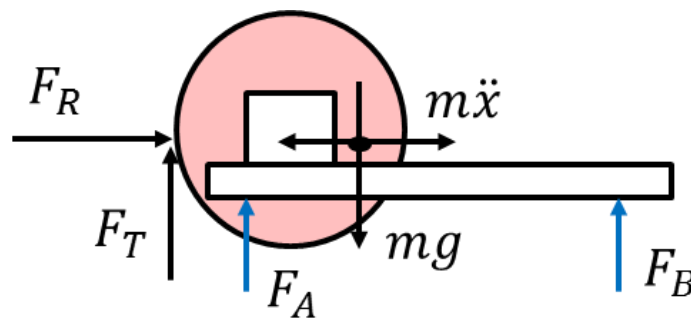


Figure 1: Forces on the linear slides of a grinding machine

The cutting forces cause a high-frequency load on the hydrostatic bearing [3], see Figure 2. The exact knowledge of the transmission behavior of the hydrostatic bearing is of great importance during dimensioning precision machines. The presented model in the following section allows to predict the transmission behavior of hydrostatic bearings. This makes conclusions about the accuracy and surface quality of the machine tool possible. The model can be used to simulate different control strategies, such as the use of progressive flow controllers [4], in the hydrostatic bearing.

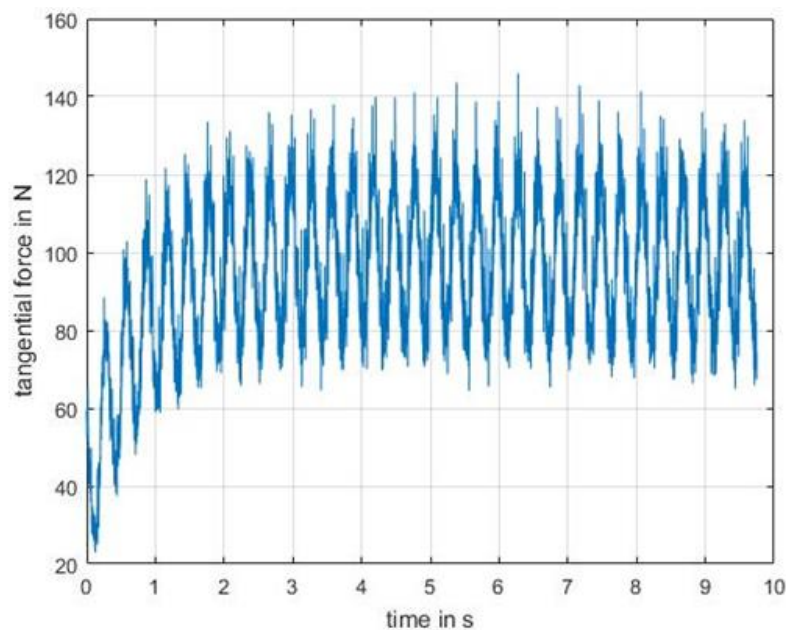


Figure 2: Cutting forces of a dynamic grinding process

2 Model

Hydrostatic Bearing are described by the Hagen-Poiseuille-Equation. In this case, a relationship between the geometry of the hydrostatic bearing and pressure drop across the gap of the bearing is established. In the derivation of the Hagen-Poiseuille-Equation, is a linear pressure drop over the gap assumed, see Figure 3. This assumption is permissible for rectangular pockets (except for the corners of the pockets).

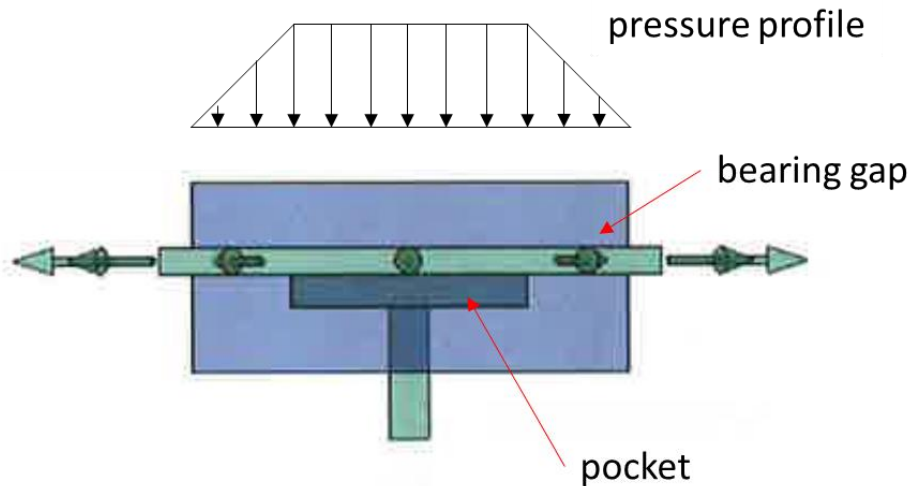


Figure 3: Hydrostatic bearing, pressure profile

For circular pockets is also a linear pressure drop assumed [5]. This assumption is a rough approximation, because the area of the circular pocket increases quadratically with the radius. The in the evaluation used test rig is equipped with rectangular pockets, therefore the equation for the rectangular pocket is used in mathematical modeling, see Equation 1.

$$Q = \frac{b h^3 \Delta p}{12 \eta l} \quad (1)$$

In this case b , h , and l represent the geometric dimensions of the bearing, Δp the pressure drop over the bearing, and η the dynamic viscosity of the pressure fluid. In order to obtain the function of a hydrostatic bearing, which is a throttle, a further throttle must be installed in front of the bearing, see Figure 4.

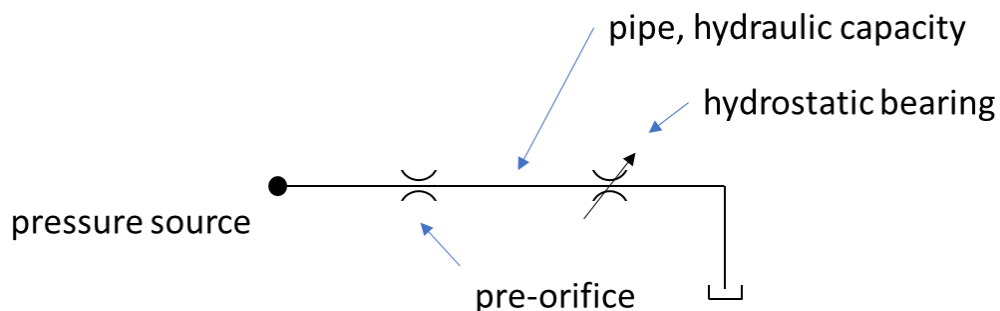


Figure 4: Hydraulic circuit diagram, hydrostatic bearing

This pre-throttle ensures, that not the entire pump pressure is passed to the hydrostatic bearing. The result is a system with a constant pre-throttle and a variable throttle (hydrostatic bearing).

Which type of throttling is used has an affect on the behavior of the hydrostatic bearing. Four different possibilities for pre-throttling can be distinguished:

- by a capillary,
- by a throttle,
- by a orifice,
- by a progressive quantity regulator.

Each of the four different types of throttling has a different characteristic. This results in a different behavior on load changes of the hydrostatic bearing. The capillary can be regarded as a thin tube with a laminar flow inside. The flow depends on the pressure drop and on the viscosity of the fluid, see Equation 2.

$$Q = \frac{\pi r^4 \Delta p}{8 \eta l} \quad (2)$$

The only difference to the hydrostatic bearing is that the geometry is constant. Is an orifice used as pre-resistance, then depends the flow on the geometry of the orifice and the density of the fluid. In addition, the pressure drop across the orifice is quadratic in the equation, see Equation 3.

$$Q = \alpha A \sqrt{\frac{2 \Delta p}{\rho}} \quad (3)$$

If a progressive flow regulator is used, the flow through the pre-resistance should be proportional to the pressure in the hydrostatic bearing. As a result, a constant gap height can be achieved in the hydrostatic bearing [4]. For describing the time behavior of the progressive quantity controller, either a characteristic curve can be stored or the controller can be described in a hydraulic-mechanical system.

To describe the transfer behaviour of a hydrostatic bearing a hydraulic-mechanical model must be developed. The hydraulic part of the system will be described with hydraulic resistances, capacitances and inductances. The mechanics of the hydrostatic bearing will be described with Newton's law of motion. In Figure 5 can be seen the model of a hydrostatic bearing consisting of the hydraulic network and the mechanic.

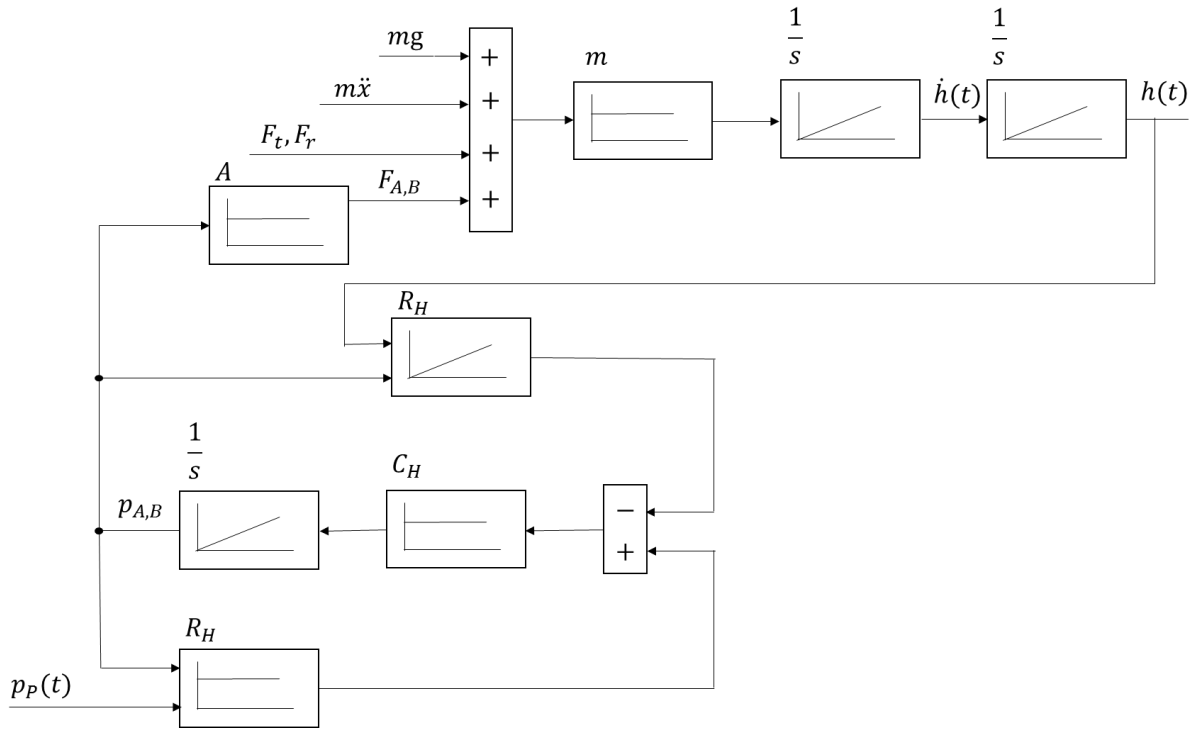


Figure 5: Equivalent circuit, hydrostatic bearing

While the resistors have already been treated in the description of the hydraulic network, see Equations 1, 2 and 3, the hydraulic inductance is neglected by the small volume of oil and the low flow rate in the bearing. However, the hydraulic capacity C_h can not be neglected. It represents the compression of an oil volume due to the elasticity of the fluid, see Equation 4. At high pressures, the stiffness of the components must also be considered.

$$C_h = \frac{Q}{\dot{p}} \quad (4)$$

For the enclosed oil volume can the hydraulic capacity be written, see Equation 5, where E the compression modulus of the fluid is.

$$C_h = \frac{V_0}{E_{\dot{O}l}} \quad (5)$$

The compression modulus of mineral oil depends on the pressure and the free unresolved air, see Equation 6 [6].

$$E_{\dot{O}l} = \frac{(1-\alpha) \left(1 + \frac{m p}{E}\right)^{\frac{1}{m}} + \alpha \left(\frac{p_0}{p}\right)^{\frac{1}{n}}}{\frac{1}{E_0} (1-\alpha) \left(1 + \frac{m p}{E_0}\right)^{\frac{m+1}{m}} + \frac{\alpha}{n p_0} \left(\frac{p_0}{p}\right)^{\frac{n+1}{n}}} \quad (6)$$

With the air content α , the pressure dependence coefficient m and the polytropic exponent n . The pressure dependence of the free unresolved air is described by Henry-Dalton's law. This dependence is not considered in this case because it is a 1-d model. The solubility in the oil is not infinitely fast and with a 1-d Model it is not possible to consider it.

For the description of the hydraulic network, the continuity equation is applied over the hydrostatic bearing, see Equation 7.

$$Q_{zu} - Q_{ch} - Q_{ab} = 0 \quad (7)$$

Where Q_{zu} is described by the prethrottle, Q_{ch} by the hydraulic capacity, and Q_{ab} by the hydrostatic bearing. Substituting the equation 1, 3 and 4 in Equation 7 results the differential equation for the hydraulic network.

$$\dot{p}_{Po} = \frac{E_0 l}{V_0} \left(\alpha A \sqrt{\frac{2(p_{Pu} - p_{Po})}{\rho}} - \frac{b h^3 p_{Po}}{12 \eta l} \right) \quad (8)$$

By the parameters E-modulus, percent air and viscosity the used the hydraulic fluid is taken into account. The equation of the hydrostatic bearing includes the gap height of the bearing and the pressure drop. These two parameters are related to the equation of motion, see Equation 9, of the hydrostatic bearing.

$$m \ddot{x} = \Sigma F \quad (9)$$

The force F represents external forces on the bearing, inertial forces and also forces through the hydrostatic bearing. The current gap height is obtained by integrating twice, see equation 10. This gap height is used in the calculation of the hydraulic network. This results in a differential equation system for the calculation of the hydrostatic bearing.

$$x(t) = \frac{\Sigma F t^2}{2m} + h_0 \quad (10)$$

3 Test Rig

Since it is usually difficult to measure both the pocket pressures and the gap heights on existing machine tools, a test bench is used to validate the simulation. The geometry of the hydrostatic bearings on the test rig corresponds to the hydrostatic bearings of the research grinding machine at the institute. Figure 6 shows the test rig for measuring hydrostatic bearings. It consists of three axial bearings which represent the bearings to be investigated and a cover disc. The cover disk is centered by three hydrostatic bearings. The test rig can be loaded by weights and spring pretension. The dynamic loads are applied by a hydrostatic cylinder. It is possible to simulate jumps, sinus and square loads.

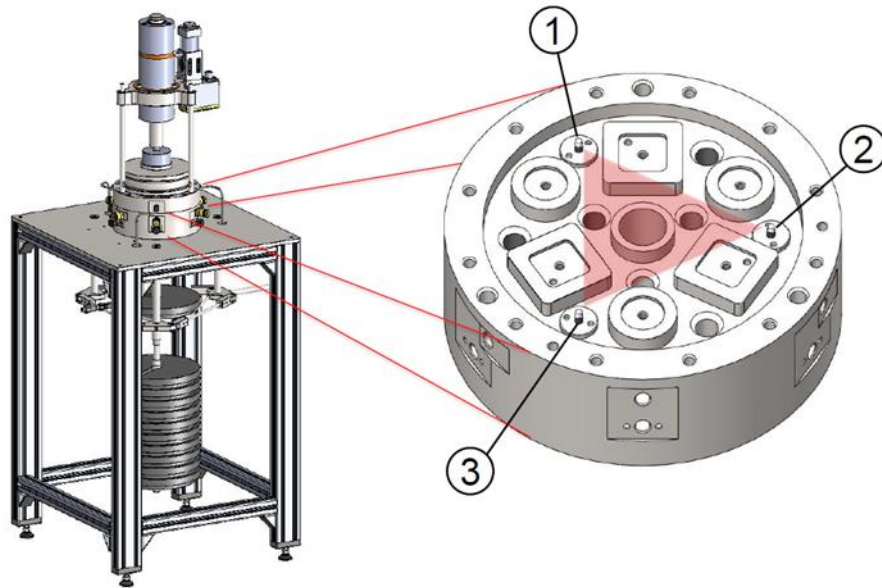


Figure 6: Test rig

4 Results

For the validation of the model, the jump response of the hydrostatic bearing is considered. During the jump response test, the bearing is previously loaded with a static load of 40 kN. The pressure supply is then activated and the gap height and pocket pressure are measured. The pre-orifice of the hydrostatic bearing is adjusted so that a gap height of 40 μm is obtained. In order to take the dynamics of the switch-on process into account, the measured pressure build-up upstream of the pre-throttle is used as a boundary condition in the simulation, see Figure 7.

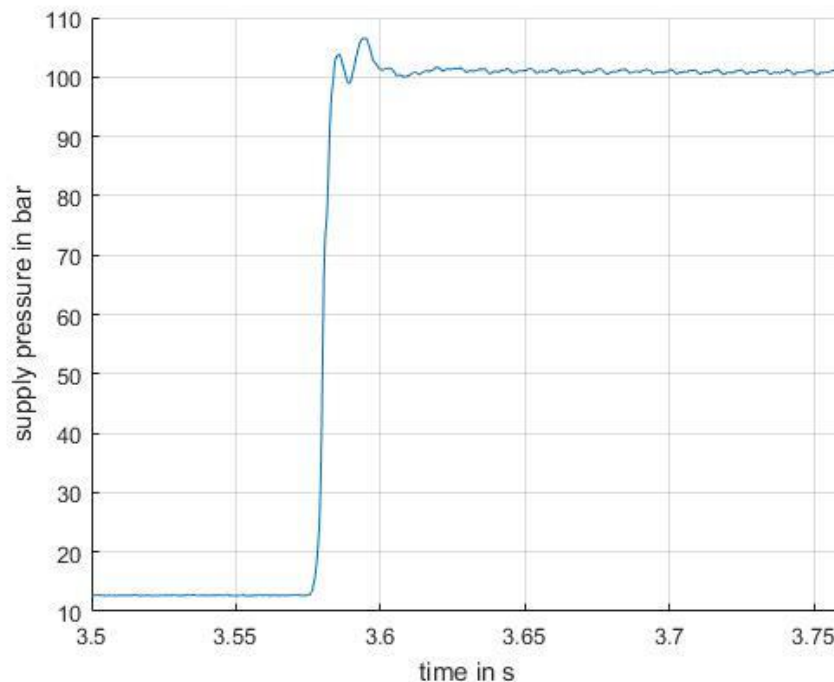


Figure 7: Supply pressure

Figure 8 shows the measured and the simulated pressure profile. The pressure build-up shows a good match, while the pressure reduction after the overshoot matches not so good.

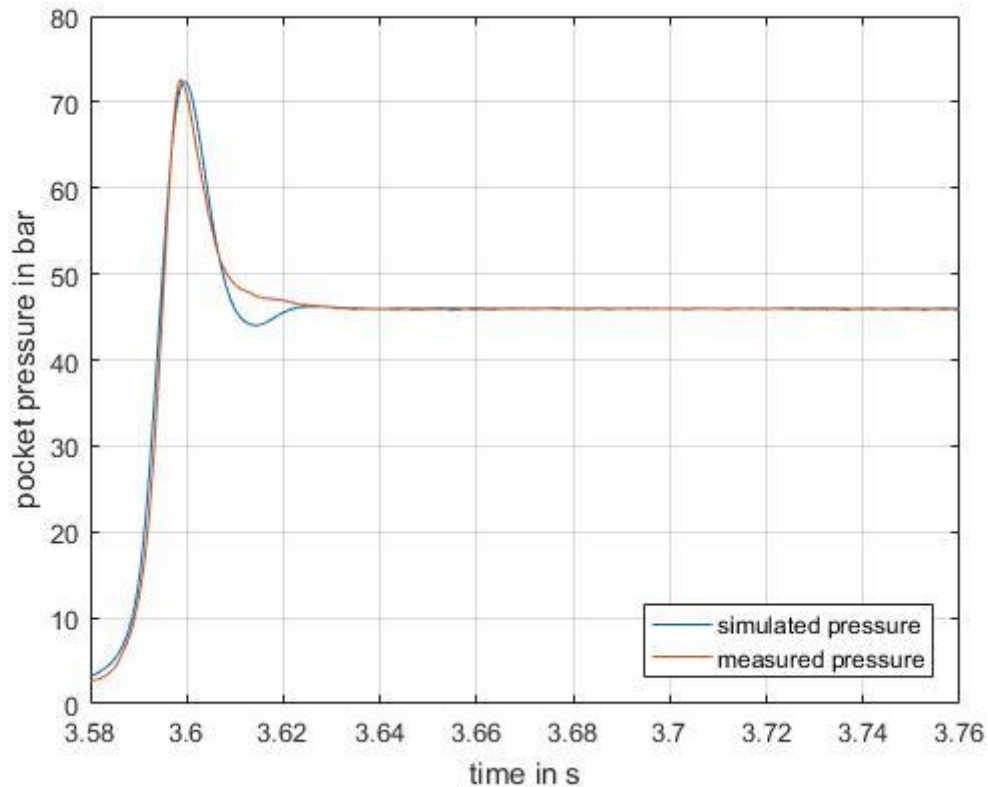


Figure 8: Simulated and measured pocket pressure

This deviation can be explained by the pressure distribution in the bearing gap during the gap height reduction. In the model, a linear pressure reduction over the bearing gap is assumed. In the case of the reduction of the gap height, the excess fluid must be squeezed out of the gap. This results in a non-linear pressure distribution in the gap and a deviation in the simulated pressure profile. Figure 9 shows the corresponding gap height profile, here it can be seen, that the deviation is only present during the gap height reduction.

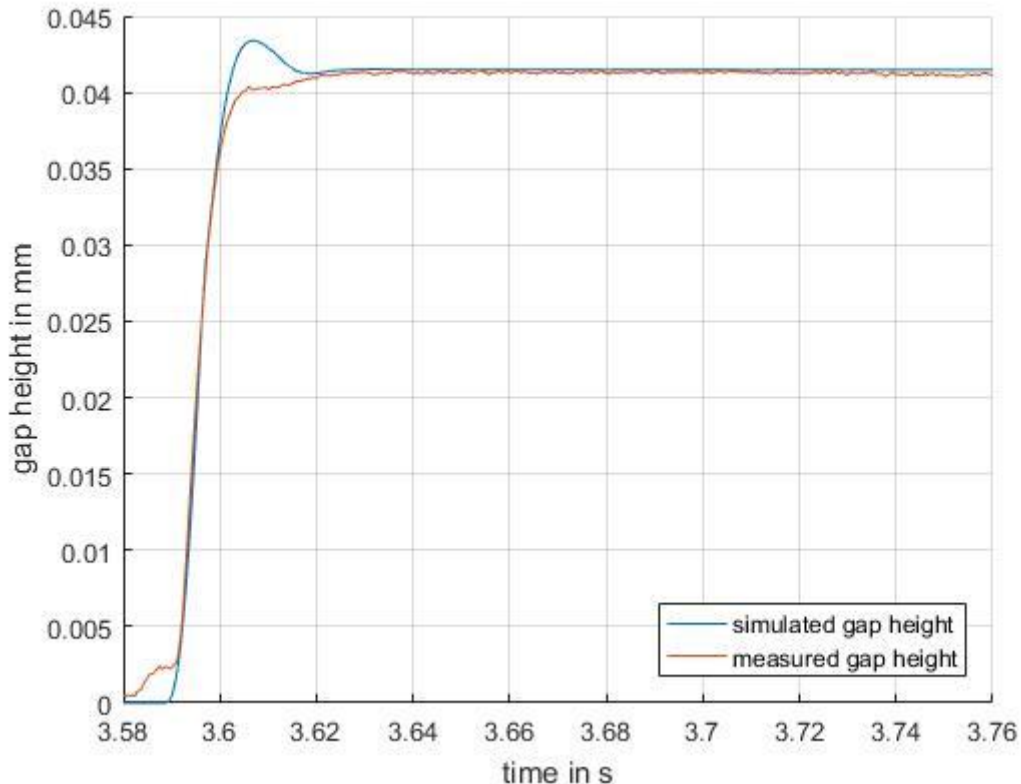


Figure 9: Simulated and measured gap height

5 Conclusion

The developed 1-d model makes it possible to depict the time behavior of hydrostatic bearings. Both the geometry of the bearing as well as different boundary conditions can be adapted to the respective application of the hydrostatic bearing. As a future development, the nonlinear pressure distribution in the bearing and the time air solvency should be included into the model. In this way, the prediction of the operating behavior of hydrostatic bearings, especially for applications in machine tools, should be even more predictable.

References

- [1] Gold, S.; Weber, J.: New Plain Bearing Concept for Support of the Propeller Shaft in Pod-drives of Large Ships; 8. Internationales Fluidtechnisches Kolloquium, proceedings; Dresden; 2012
- [2] Haas, F.: Werkzeugmaschinen, Umdruck zur Vorlesung, 1.Auflage, IFT Graz, 2015
- [3] Steffan, M., Haas, F., Zopf, P., Edler, J.: Optimierung der Schleifbearbeitung mittels OPC UA: Neue Prozessregelung zur Vermeidung von thermischer Randzonenschädigung. Zeitschrift für wirtschaftlichen Fabrikbetrieb. 2017 Mar 1;112(3/2017):137, 2017
- [4] Mörwald, G., Edler, J., Tic, V.: Calculation of Control Edges with Simulation, Fluid Power conference 2015, University of Maribor, p. 249-254, 2015
- [5] Hochleitner, H.: Grundlagen der Fluidtechnik, Teil 1, 1.Auflage, IFT Graz, 2010
- [6] Murrenhoff, H.: Grundlagen der Fluidtechnik, Teil 1: Hydraulik, Umdruck zur Vorlesung, 2.Auflage, IFAS-RWTH Aachen, 1998

Design challenges of modern hydraulic power packs

TADEJ TAŠNER, PETER HACE & KRISTIAN LES

Abstract Engineers nowadays face numerous challenges while designing hydraulic power packs. One of the more challenging is meeting the short design times required by most of the customers. This forces engineers to use simple and accurate tools to help them in the design process. This article will focus on Excel based calculation tools. Moreover, it will expose advanced features of modern CAD/PLM software packages, which help to shorten the design times even further.

Keywords: • hydraulic • power packs • design • Excel • CAD/PLM •

CORRESPONDENCE ADDRESS: Tadej Tašner, HAWE Hidravlika d.o.o., Petrovče 225, 3301 Petrovče, Slovenia, e-mail: t.tasner@hawe.si. Peter Hace, HAWE Hidravlika d.o.o., Petrovče 225, 3301 Petrovče, Slovenia, e-mail: p.hace @hawe.si. Kristian Les, HAWE Hidravlika d.o.o., Petrovče 225, 3301 Petrovče, Slovenia, e-mail: k.les@hawe.si.

<https://doi.org/978-961-286-086-8.19>
© 2017 University of Maribor Press
Available at: <http://press.um.si>.

ISBN 978-961-286-086-8

1 Introduction

Why modern hydraulic power packs? There were no major breakthroughs in the field of hydraulic power packs; therefore, the hydraulic power packs are built from same component types as 20 years ago. They consist of electric motor, hydraulic pump, some valves and filters. So there is nothing modern in there, except that most of the components have improved. They still have the same function, are still mostly compatible, but require less material for production and are generally cheaper. Who knows if they last longer than old components or not?

The word modern is used mainly because the design process of the hydraulic power packs has changed. The time from first customer inquiry to working hydraulic power pack has reduced dramatically in last years. Such trend is forcing engineers to use suitable modern computer aided design tools to speed up and automate the design process. The design and manufacturing process must be really short, because sometimes the customer wants the power pack produced before he sends in his inquiry. Maybe the future will bring tools to serve such customers too.

Next chapters will present the hydraulic power pack design process. After that, focus will be on methods of automating, simplifying and speeding-up the design process. All of the presented methods are examples of good practices that have been already implemented and are being used in the actual design process.

1.1 Design process

The design process starts with customer inquiry for a new hydraulic power pack. If enough details are provided engineers can prepare a quote with draft hydraulic schematic and a bill of material. The customer then takes his time to choose the best (the cheapest) quote (because he sent his inquiries to more companies) and places the order. After the order has been placed, a detailed technical calculation and final hydraulic schematic are created. Next, a 3D model of the power pack is drawn from which dimensional and assembly drawings are derived. The drawings are sent to production, but the design process does not end here. The designers need to prepare product documentation, which includes user manual, technical data sheets, declarations and test protocol. It can be seen that the design process is quite extensive. Therefore it requires a lot of experience to get through the whole process without mistakes and as fast as possible. As the experience is very hard to pack into a tool for speeding up the design process, there are more suitable parts for automation, which include calculation, 3D modelling / drawing and documentation.

The next chapter will present techniques used for automation in the calculation phase, the 3D modelling phase and documentation preparation phase.

2 Automation of the design process

The design process is shown in Figure 1, where lighter circles represent customer actions and darker circles parts of the design process. The uppercase text represents design process actions and the bulleted lists represent the outcome of those actions. The next chapters will focus on design process actions and possibilities of their simplification and automation.

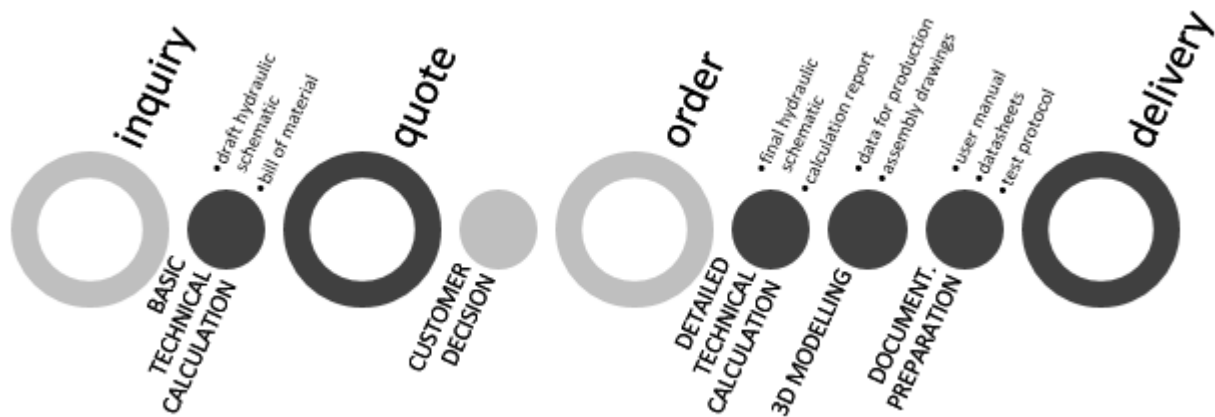


Figure 1: Design process flowchart

2.1 Technical Calculation

There are numerous of calculation programs for hydraulic systems. Some of them are even capable of simulating an entire hydraulic schematic. [1], [2] But are such programs really suitable for quick technical calculations of hydraulic power packs? Unfortunately no, because the programs are too complex for such calculations, as they require too much input data for simple calculations and are therefore too time consuming. An alternative to such calculation programs are Excel based calculation programs tailored by engineers who know which data is important for them.

For most of the power packs the customer knows hydraulic loads (cylinder dimensions, required forces and speeds), operation timeline of the machine (order of machine operations) and ambient conditions. All parts of the hydraulic power pack can be calculated out of this data. [3], [4], [5] The flowcharts below represent calculation order; when A and B is taken to calculate C and D such action is represented as “A+B→C+D”.

- cylinder dimensions → volume change
- volume change + speed → flow rates → piping ID¹; valve, filter types and sizes
- flow rates + piping ID, valve, filter types and sizes → pressure losses
- required force + pressure losses → required pressure
- required pressure + piping ID → piping size
- flow rates → pump + accumulator sizes
- flow rates + required pressure → motor size and power
- volume change + accumulator size → tank size → oil pan size
- pressure losses + flow rates → cooler size
- ambient temperature + flow rates → heater size

Such calculations require a database of basic parameters of mostly used components (valves, filters, pumps, ...), a table that holds customer input data and some basic hydraulic equations which are used to create final calculation report as shown in Figure 2.

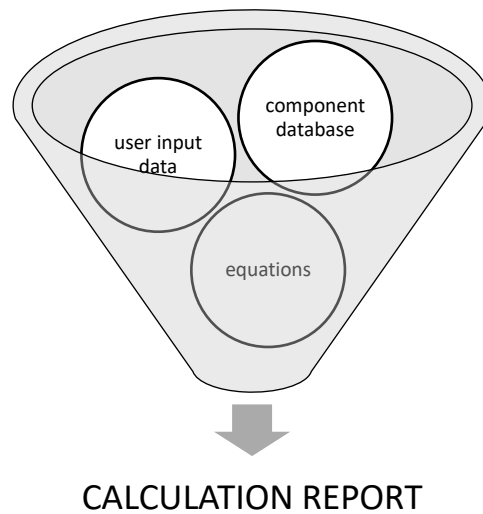


Figure 2: Calculation program as a funnel

The advantages of such calculation program are:

- simple component database (component parameters can be read from any datasheet)
- instant calculation (no long computation times)
- equations and component database are reused in new projects

Everything mentioned above can be packed into an Excel file, which is a well known and relatively cheap solution, as it is a must have application in every office. First page of the report generated in Excel is shown in Figure 3.

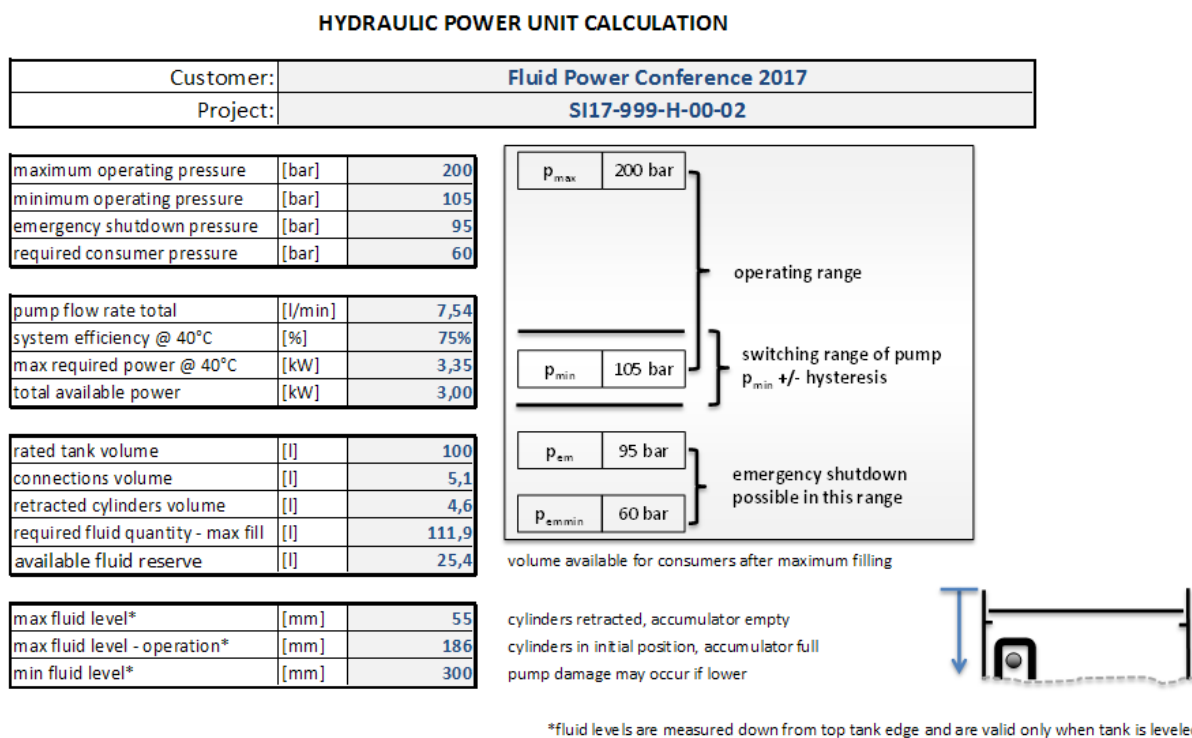


Figure 3: First page of a report generated with Excel based calculation program

2.2 3D modelling of the hydraulic power pack

There are a lot of different CAD software packages available on the market (Inventor, SolidWorks, ProEngineer, Catia, Geomagic, ...). Most of them have similar functionality and offer comparable features. This chapter will point out the most useful features for speeding up the 3D modelling of the hydraulic power packs, which are parametric modeling, library features (iFeatures) and finite element method (FEM) analysis. An example 3D model of a hydraulic power pack is shown in Figure 4.



Figure 4: Render of a 3D model of a modern hydraulic power pack

2.2.1 Parametric modelling

Each company that produces a lot of hydraulic power packs, has or should have internal standard parts (eg. tanks, oil pans, manifold brackets, flanges, ...) which they frequently use. It is nonsense to model new parts for each project but reuse the standard parts. There is the point where parametric modeling comes in. Each component is drawn using parameters, which are stored in a table (eg. height, width, depth and wall thickness of a tank). Example table is shown in Figure 5. When a designer needs a tank, it places a tank in the 3D model and chooses the desired size. The benefit of such modelling comes to light when changes have to be made. When changing a parametrically drawn component a change is done with a few clicks (by highlighting new table row). Moreover the constraints (mates) don't have to be reattached, which saves a lot of time and simplifies redesigns and changes.

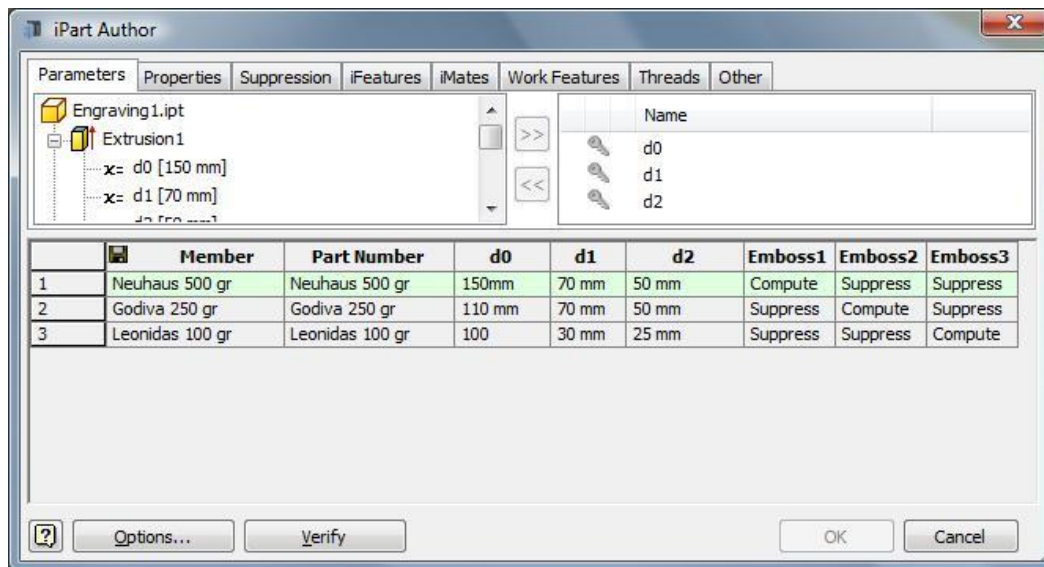


Figure 5: Parametric table in Inventor

Parametric modelling is suitable for components that don't have a lot of variations. Parametric modelling requires more time for creating the first component variant, but saves a lot of time on further similar components. The only drawback of parametric modelling is the complexity of making unexpected design changes. [6], [7], [8]

Parametric modelling can also be used for purchased parts, which have little differences. For example electrical level indicator that has different standard lengths. Although it takes more time to draw the parametric model or modify manufacturer's model to parametric, such approach pays off when replacing the components, due to customer requests.

2.2.2 Library features (iFeatures)

Another interesting feature of modern CAD software packages are library features (Solidworks [9]) or iFeatures (Inventor [10]). Library features are useful for tank cover hole patterns of components (return filters, filler filters, bell housings...). When placing a new component on the tank cover, its "footprint" (usually a hole with more threaded holes around it) is dropped on the cover from the library and correctly positioned. After that, the actual component is constrained to its "footprint".

Using library features can help designers to create tank covers faster and with fewer errors as footprints in library were already verified. "Footprints" can be easily replaced (similarly to replacing a parametrically modelled part) when a component change is desired and no constraints brake during its replacement.

2.2.3 FEM analysis

FEM analysis is useful for calculating mechanical strength of manifold mounting brackets for example. FEM is already built in many modern software packages, therefore it is easy to use. FEM analysis is executed using only a few clicks, its results help engineers to determine whether the component would withstand the forces and where the component could be improved. The results also enable more efficient use of the material and therefore further reduce manufacturing costs of analysed components. [11]

2.3 Documentation preparation

Every hydraulic power pack needs some documentation, which includes technical datasheets, user manual, declaration of incorporation (mostly) and test protocol. All those documents are based on templates, which have some fields that have to be filled out. Each new power pack has different documentation, which may be in different languages when selling power packs to foreign customers.

Because some documents have a lot of fields to edit and sometimes a customer wants multilingual documentation (meaning filling out same data for each language), this procedure is extensive and time consuming. Even though it is straightforward, a lot of errors can happen due to repetitive tasks.

Because of its nature, the preparation of documentation is relatively simple to automate. The documentation templates are prepared using Word application. All the fields that need to be filled out are marked using Word's built in content controls. Templates in such form can be easily edited using a master Excel document, which serves as a container of additional power pack properties and as a link between bill of material and Word templates. Macros based on Visual Basic for Applications (VBA) in master Excel open the Word templates, fill out the fields, paste in the relevant images, save word files and create PDFs in all the required languages. Such procedure is illustrated in figure 6 where grey boxes represent inputs to the master Excel file and black boxes represent Word templates, which are converted to normal Word documents during creation and finally converted to PDF.

Such approach requires little VBA knowledge plus intermediate Excel and Word experience for initial system creation [12]. Using such system is afterwards simple and straightforward, so anyone can generate all the relevant documentation in a few minutes.

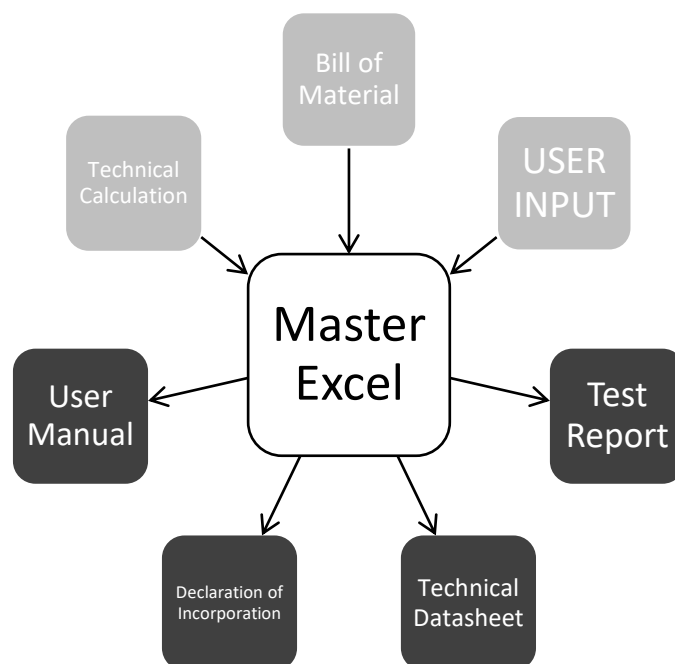


Figure 6: Block diagram of documentation generation procedure

The user must manually add only documents that originate from another programs, for example hydraulic schematic from HyDRAW, dimensional drawing from Inventor, electrical schematic from Caddy, etc.

3 Conclusion

This article illustrated the design process of modern hydraulic power packs. It has been shown, that time is one of the biggest challenges that engineers have to face, throughout the whole design process. Therefore it is suitable to optimize the parts of the workflow that is repeating from one power pack to another. These steps are technical calculation of the power pack, 3D modelling of the power pack and preparing power pack's documentation.

The most elegant solution is to get the most out of the tools that engineers already use every day: 3D CAD software package and Microsoft Office programs.

Excel is an indispensable tool for any calculation, therefore it was used as a fundament for hydraulic power pack calculation program. When combined together with Word templates it such combination was turned into a powerful documentation generator, which can generate documentation of the power pack in the matter of minutes.

There are a lot of features hidden in every 3D CAD software package. Some of them are very useful for modelling the hydraulic power packs. Especially parametric modelling, library features and FEM analysis have been proven as very useful in the field. Parametric modeling serves for fast tank, oil pan and frame generation, where as library features speed up tank cover design. When there is a doubt in load capacity of construction, mounting brackets or frames FEM analysis helps to determine whether the construction will withstand the loads or not.

Perfectly modelled power packs don't only look nice but can also save a lot of time in the manufacturing phase. If one change in calculation phase takes 1 minute, the same change in modelling phase takes 10 minutes and in manufacturing phase 100 minutes. Use all the presented techniques to save precious time and to make power packs look perfect on the computer screen and in reality – Figure 7.

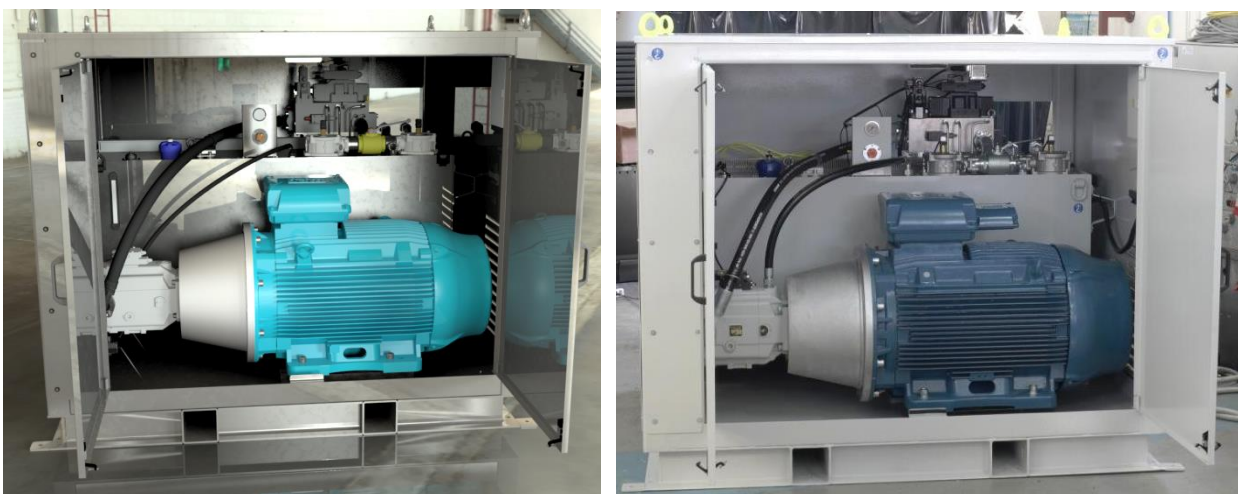


Figure 7: Render of 3D model of a hydraulic power pack (left), actual product (right)

References

- [1] Famic Technologies Inc., "Automation Studio P6 Professional Edition," [Online]. Available: <http://www.famictech.com/pro/index.html>. [Accessed 8 2017].

- [2] MathWorks, "Modeling a Hydraulic Actuation System," [Online]. Available: <https://www.mathworks.com/videos/modeling-a-hydraulic-actuation-system-68833.html>. [Accessed 2017].
- [3] Hunt, T., Vaughan, N.: The Hydraulic Handbook, Oxford: Elsevier, 1996.
- [4] Evett, B. J., Liu, C.: 2500 Solved Problems in Fluid Mechanics and Hydraulics, New York: McGraw Hill, 1989
- [5] Watton, J.: Fundamentals of Fluid Power Control, Cambridge: Cambridge University Press, 2009
- [6] Brunelli, M.: Parametric vs. Direct Modeling: Which Side Are You On?
- [7] Shih, R.: Parametric Modeling with Autodesk Inventor 2017, Mission: SDC Publications, 2016
- [8] Owan, C. P.: Advanced Design Based Parametric Modeling Using Solidworks® for Electro-Mechanical Industrial Products, Primedia E-launch LLC, 2015
- [9] Reyes, A.: Beginner's Guide to SOLIDWORKS 2016 - Level II, Mission: SDC Publications, 2016
- [10] Munford, P., Normand, P.: Mastering Autodesk Inventor 2016 and Autodesk Inventor LT 2016: Autodesk Official Press, Indianapolis: John Wiley & Sons, 2016
- [11] Kurowski, P. M.: Finite Element Analysis For Design Engineers, SAE international, 2004
- [12] Driza, S.: Word 2007 Document Automation with VBA and VSTO, Plano: Wordware Publishing inc 2009

Hydrostatic Transmission Design – Closed-loop Trailer Assist Drive

LUKA JELOVČAN & ALEŠ NOVAK

Abstract The article presents design study, production and commissioning of heavy-duty forestry trailer equipped with hydrostatic transmission. The aim of the project is to build heavy duty, highly productive and compact, cost-effective and user-friendly machine, which will be able to operate on severe terrains and can be at the same time driven with standard agriculture tractor.

The aim of the trailer transmission is to generate additional tractive effort on terrains where tractive effort of the tractor does not guarantee correct and safe driving conditions. Trailer transmission design is done in way to provide additional tractive effort when traveling uphill and provide sufficient hydrostatic braking when traveling downhill.

Trailer Assist is diagnosed via several sensors and consequently controlled by micro controller, which is a part of the transmission and provides on-time speed synchronization between the tractor and the trailer. An additional integrated display provides effective interface between the machine and the user.

Keywords: • forestry trailer • hydrostatic transmission • assist drive design • compact • cost-effective • user-friendly •

CORRESPONDENCE ADDRESS: Luka Jelovčan, Poclain Hydraulics d.o.o., Industrijska ulica 2, 4226 Žiri, Slovenia, e-mail: luka.jelovcan@poclain.com. Aleš Novak, Poclain Hydraulics d.o.o., Industrijska ulica 2, 4226 Žiri, Slovenia, e-mail: ales.novak @poclain.com.

1 Aim of the project

On the market there are many systems to transport wooden logs. There are solutions from very simple winches to more sophisticated forestry machines as are tower yarders, to skidders and forwarders and finally even helicopter transportation.



Figure 1: Several concepts of wood transportation

General aim is to transport heavy wooden logs from difficult terrains to the territory near roads that can be easily reached with standard trucks.

Focus on basic log transportation “on-wheels” generally show two solutions; transportation with tractor trailers and transportation with forestry forwarders. Forwarders are very effective and comfortable solution, but at the same time also expensive due to input costs of complex machine and regular machine operational costs. Transportation with tractor trailers is at the same time inexpensive (tractor is one of the basic equipment on the farm), but causing several deficiency. One of the most important is that many difficult terrains are impossible to reach.

On the market there are many different tractor forestry trailers options. From very simple to very sophisticated solutions. Weaknesses generally stay the same – classic forestry trailer has to be in combination with heavy and powerful agriculture tractor to be able to transport heavy loads. Basic idea of the company Pro Jernač was to develop forestry trailer which can be used also in combination with smaller agriculture tractor and can at the same time reach heavy terrains which are normally reachable only with forestry forwarders.

2 Input requests

Input requests were following:

- Trailer solution has to be as much universal as possible and useful with any agriculture tractor as possible. Minimal size of tractor is 4 tons and 90kW engine power.
- Trailer size has to allow loading, transportation and unloading up to 10 m³ of logs at once.
- Solution must allow greater manoeuvrability compared to standard trailers solutions.
- Trailer transmission has to be able to transform as much input power in additional tractive effort when composition traveling uphill and at the same time need to provide reliable retain torque when traveling downhill.

Almost all points above can and at the end were reached with proper trailer transmission. This was the point where innovative ideas of Pro Jernač have met Poclain Hydraulics' heavy duty transmission solutions.



Figure 2: Pro Jernač prototype trailer

3 Transmission solution

Generally trailer transmission is closed loop electronically controlled hydraulic transmission. It consists from four general types of components; PW heavy duty closed loop hydraulic pump, MSE18 radial piston hydraulic motors, closed loop hydraulic control valves and electronic control unit. On the trailer there is also additional open loop hydraulic system provided by Poclain Hydraulics to control additional functions on the trailer; steering, wheels position control etc...). Transmission was designed in a way that speed of the trailer is synchronized with speed of the tractor and at the same time can provide additional tractive effort according to operator demand. To achieve those requests, so called constant pressure control principle were used. Beside that there are several driving modes:

- I. On-road mode: Assistance is completely stopped and system needs only energy to provide correct lubricating of the hydraulic motors and ability to operate in freewheeling mode.

- II. Freewheeling mode: Assistance operates, but it is not used to provide any additional torque.
- III. Assist mode in forward or reverse: Assistance needs to provide requested torque to trailer's wheels to increase moving ability of the composition.
- IV. Retain mode in forward and reverse: Assistance needs to provide requested hydrostatic braking torque to avoid uncontrolled moving of the composition when traveling downhill.

Operational principle is following:

- Composition starts to move; tractor demand speed of composition.
- One of the trailer wheels is equipped with speed sensor which independently detects and measures the speed of composition.
- Dedicated software calculates pump displacement according to wheels speed. Electronic control unit provide on time adjusting of pump displacement regarding to speed variations.
- At the same time operator set requested additional torque – on the control panel operator directly set percentage of additional torque.
- Software re-calculate requested torque – regarding of wheels size and motors displacement – in needed pressure level.
- Electronic control unit sets the pump to maintain calculated pressure in the high pressure lines of the system and at the same time maintain requested speed of the composition.
- Retain mode is done on the same way the only difference is, that opposite lines are pressurized.

This concept gives very effective hydraulic transmission for off-road towed vehicles. Key point of system performances is initially correct setting.

4 Hydraulic system

a. Hydraulic motors

There are two low speed high torque (LSHT) radial piston wheel hydraulic motors. Motors are used on trailer front wheels due to increase gradeability of the wheels with ground. First wheels normally (in case of equal weight distribution) generate greater tractive effort in comparison with rear wheels. Motors on the trailer are MS range, that is already well proven on the different forestry machines.

Motors used are 2340 ccm radial piston motors with “stepped piston” technology. Stepped technology allows higher displacement inside same overall dimensions. At the same time maximal pressure for those motors is limited to 410 bar, which is enough for trailer assistance.

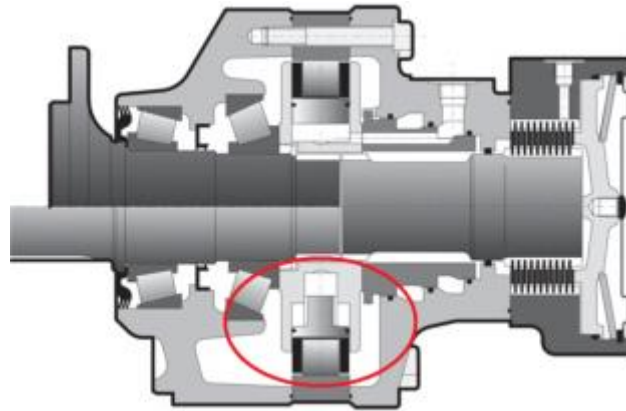


Figure 3: Stepped piston technology

Motors are wheel type with dedicated bearing support that can take the complete load of the loaded trailer. End of the motors are equipped with additional drum brake system provided by company Colaert from France. With this braking system trailer comply all regulations for on-road use in area of European Union. Brakes can be hydraulic or pneumatic controlled. Braking energy is provided and controlled by the tractor.



Figure 4: Wheel type hydraulic motors

One of the motors is equipped with additional rear gear pump, which provides necessary hydraulic energy when the main pump is stopped. Gear pump is driven by the motor which is driven by the wheel when trailer is towed. Additional energy is needed for motor's lubricating and maintaining freewheeling of the motors. Freewheeling means light pressurization of motor case ($\sim 2\text{bar}$) to avoid uncontrolled movement of motor's pistons.

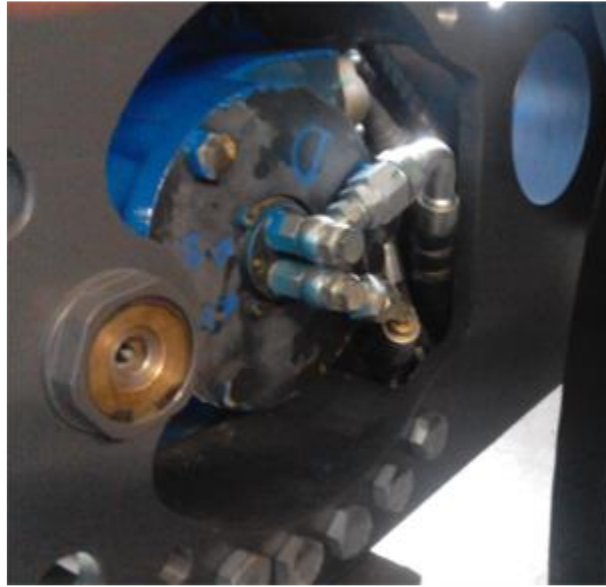


Figure 5: Additional pump on the rear of the motor

b. Hydraulic pump

At first Poclain Hydraulics medium duty PM50 pump was used. But based on results of first tests decision was taken to switch to new Poclain Hydraulic heavy duty PW096 pump. PW096 is closed loop axial piston pump. High development on this product provide effective and reliable product that can be used in several mobile and industrial applications. Key point of the pump is unique piston – sliding plate joint which provide less wear of key pump components, higher response time due to lighter components and less temperature dependant.

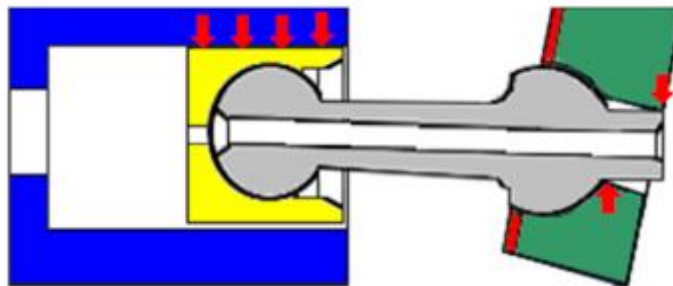


Figure 6: Piston – slide plate joint on PW096 pump

Pump is 96 ccm electro-proportional controlled unit with integrated 22ccm g-rotor charge pump. Integrated and closed loop flushing valve importantly decrease piping which still – based on machine complexity – remains heavy. Integrated pump speed sensor on time monitor pump speed and transmit information to main electronic control unit. Pump speed is also important information to adjust it's displacement.

Pump is driven by 3:1 multiplicator which is driven by tractors PTO. This allows pump operating in most optimal speed frequency. Open-loop pump for the crane is mounted directly on the rear side of PW closed loop pump.

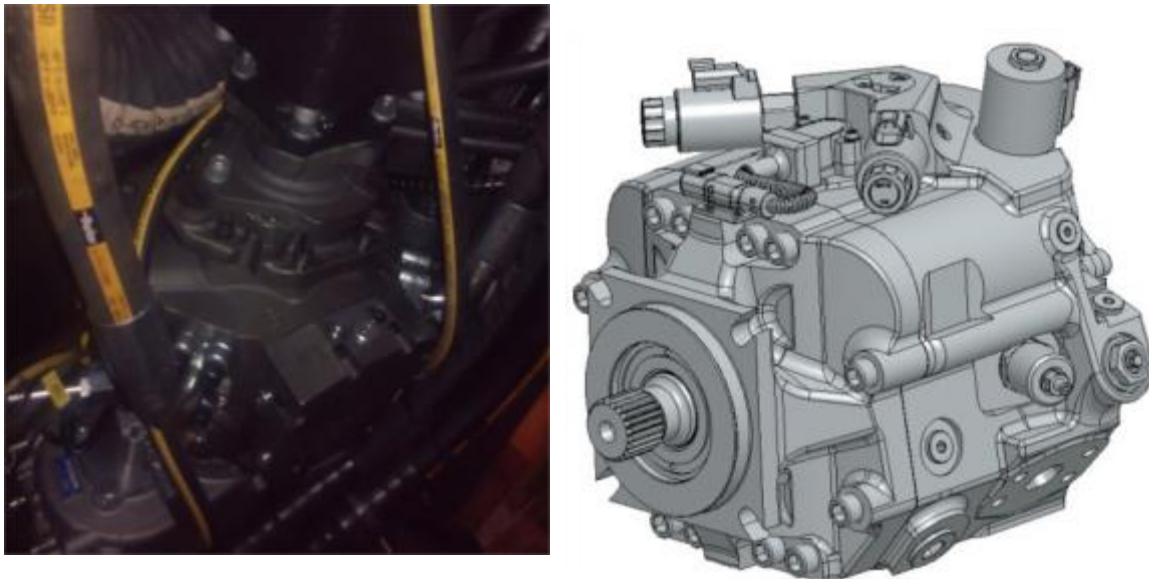


Figure 7: PW096 pump on trailer and overall view

c. Closed loop hydraulic control valves

Additional hydraulic controls (beside control provided with pump) are: freewheeling valve, traction control valve and motor case pressurization valve.

Freewheeling valve is high pressure, high flow electro controlled hydraulic valve. Its function is to enable freewheeling of the motors. At the same time its function is to engage and disengage the transmission when pump is running. Freewheeling valve also provides quick transmission disengaging in case of emergency. Large internal sections provide low pressure drops through the valve.

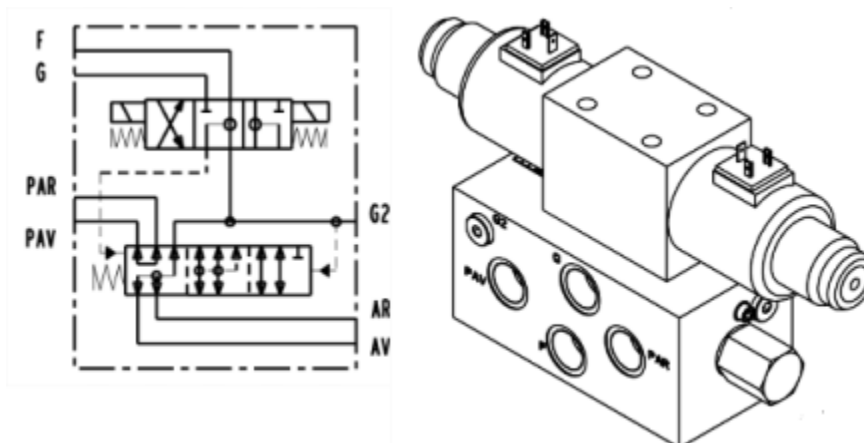


Figure 8: Freewheeling valve VDF-H15

Traction control valve is basically high pressure flow divider, equipped with bypass and control system. It is heavy duty FD-H2 type, a new product of Poclain Hydraulics in Žiri. Valve splits the pump flow into two independent ways to independently supply each motor. In reverse way it combines flow to supply the return line of the pump. Demand when to engage this function is given from operator via control panel.

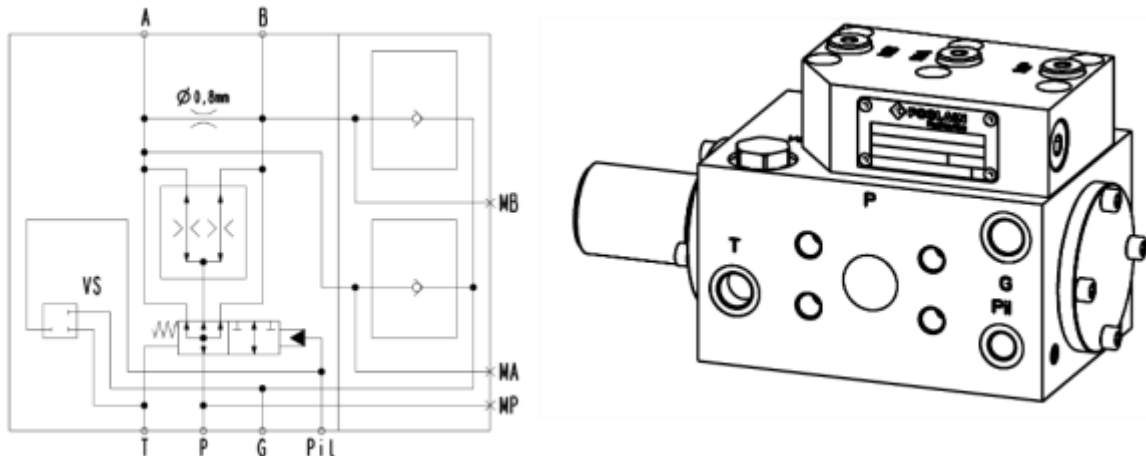


Figure 9: Traction control valve FD-H2

Case pressurization valve is hydraulic wheatstone bridge and it is used in combination with additional gear pump driven by hydraulic motor. Motor can run in both directions and consequently pump suction and pressure line must change regarding to pump rotating direction. That provide case pressurization valve.

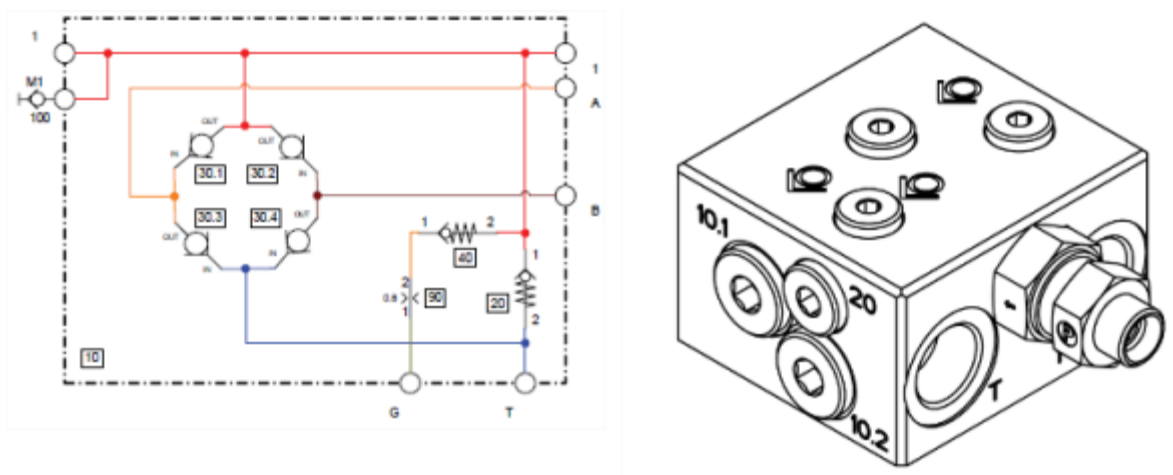


Figure 10: Case pressurization valve

d. Electronic control components

Electronic controls components exist from four main units; electronic microcontroller with high power outputs, dedicated software, control panel and several sensors integrated in hydraulic system.

Electronic control unit is Poclairn Hydraulics SMARTDRIVE EASY programmable module with several high power outputs to control hydraulic pump and several electro controlled hydraulic valves.



Figure 11: Electronic control unit and control display

Software is dedicated to the trailer assistance. Parameters also allow to control the main trailer functions like maximum speed, wheels/tyre size etc.

There are two control panels for the trailer – one for trailer transmission, second for trailer auxiliary functions. Trailer transmission control panel is programmable display with several control buttons where required functions can be set. Pressure command is given by rotatable potentiometer. On the display chosen function is graphically shown. Also important parameters like trailer speed or hydraulic oil temperature are shown.

On the trailer there are several sensors of three types: speed sensors, pressure sensors and temperature sensors. Outputs are used to provide correct system control and necessary safety functions like power or pressure limitation.



Figure 12: Trailer electro cabinet

e. System hydraulic schematic

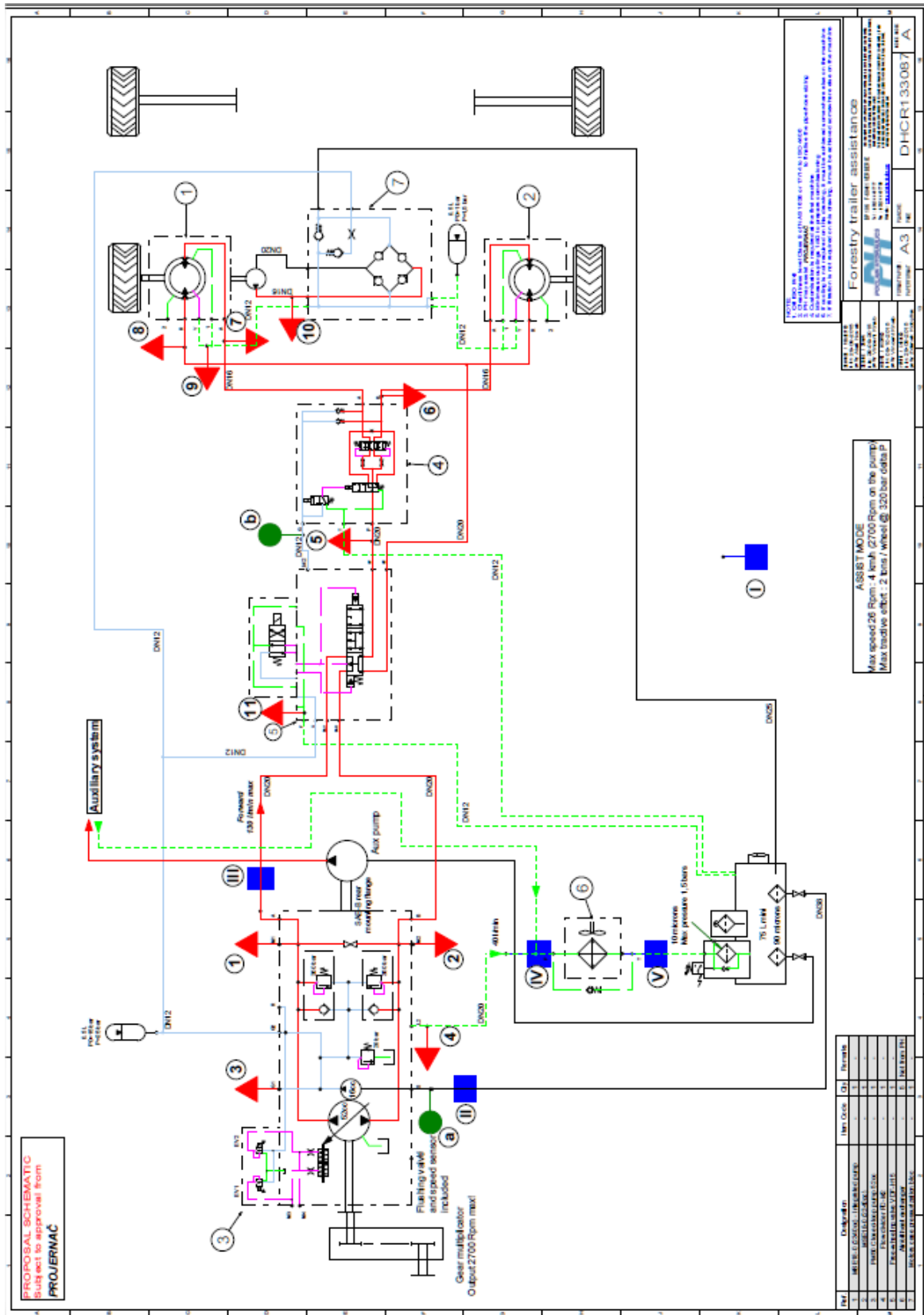


Figure 13: Trailer hydraulic schematic

5 On field testing

Intensive on-field setting and testing show many trailer assistance advantages as far as many advantages of the trailer as complete unit. Assistance can be used up to 7 km/h and can provide up to 2,75 tons of tractive effort per wheel. That findings show, that trailer assistance in many cases is not an additional transmission, but becomes the main transmission. Tractor in that case only provides power to run the pump. Fact is also that loaded trailer can weight up to 18 tons, when weight of the tractor is 4 tons.



Figure 14: On field trailer testing

System can operate up to 410 bar. Temperature stabilization is 82,5 °C. System provides performances according to initial calculations. Special care were put on retain mode. After a fine tuning also this function was fine adapted, especially with use of heavy duty hydraulic pump. That was also one of general conclusions of the testing – the complete machine works properly with heavy duty components and at the same time best-in-class components that can be found today on the market.

Commissioning also exposed one weak point of the transmission - hydraulic hoses. After a longer high pressure testing many of them start to leak and need to be replaced. Even high pressure hoses were not long term solution.

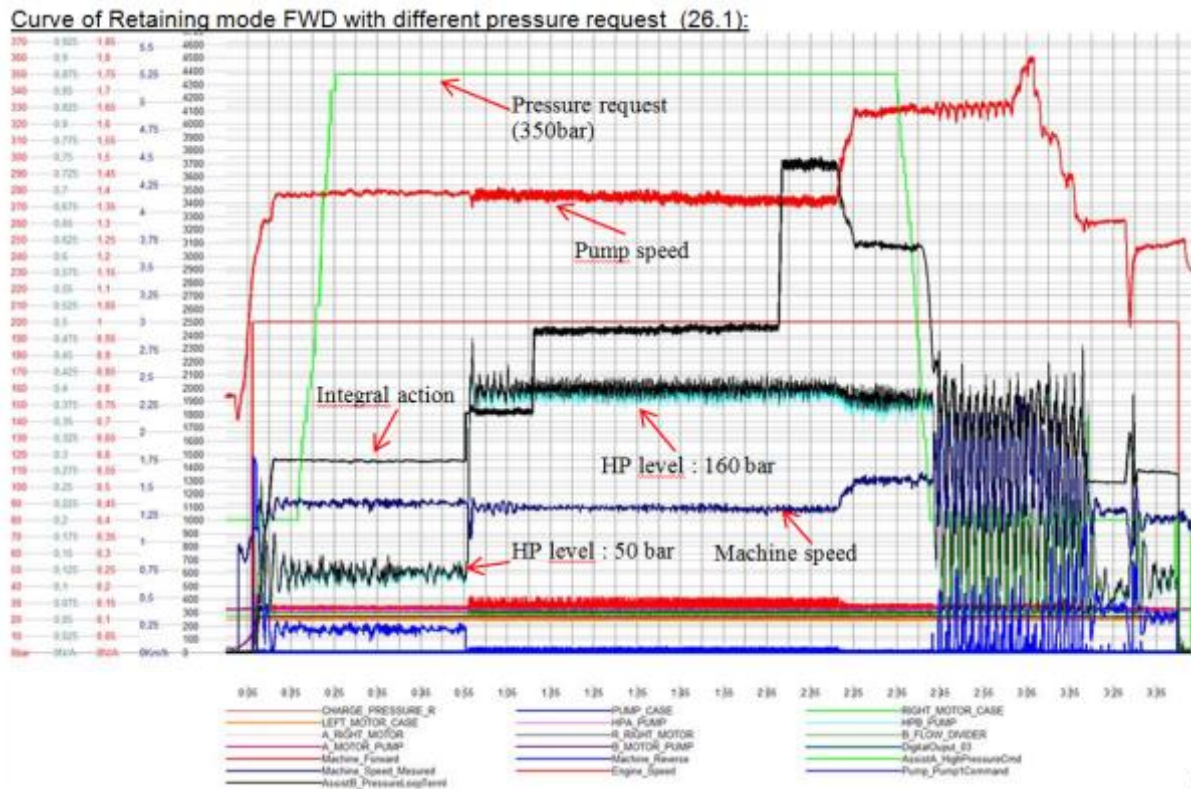


Figure 15: Measurements during commissioning

6 Conclusions

Generally looking hydrostatic transmission is the solution for that kind of heavy duty applications. Energy transition via hydraulic hoses allows complex architecture of the machine which at the end allows many others functionalities.

Also some further developments steps can be defined: increasing end speed of the transmission using two speed hydraulic motors, integration of several components (hydraulic valves) into one valve block to simplify piping and some other improvements on trailer geometry and auxiliary hydraulic system.

Acknowledgment

Kind regards to the company Pro Jernač s.p. to allow Poclairn Hydraulics d.o.o. to mention their product in this paper.

References

- [1] N.N.: Poclairn Hydraulics internal Sources and documentation

Piezo actuators for the use in hydraulic and pneumatic valves

MARKO SIMIC & NIKO HERAKOVIČ

Abstract The paper presents different types of piezo actuators that can be used in hydraulic and pneumatic valves. Despite their high-performance characteristics, high dynamic response and reduced energy consumption, piezo valves are still not used in commercial applications.

The main purpose of the paper is to presents basics of piezo technology and the main influence parameters. Several different types of piezo elements and actuator designs are presented which were used in hydraulic and pneumatic prototype valves. The main parameters that have major impact on static and dynamic characteristics of the piezo actuators and piezo valves are highlighted. Especially the direct drive piezo valves used for digital hydraulics and pilot stage driven servo valves are described in detail. The paper describes theoretical background as well as results of experimental analysis. At the end some development guidelines for the use of piezo technology in the field of valves are pointed.

Keywords: • piezo actuators • valves • hydraulic • pneumatics • influence parameters •

CORRESPONDENCE ADDRESS: Marko Simic, Ph.D., Assistant Professor, University of Ljubljana, Faculty of Mechanical Engineering, Aškerčeva cesta 6, 1000 Ljubljana, Slovenia, e-mail: marko.simic@fs.uni-lj.si.
Niko Herakovic, Ph.D., Full Professor, University of Ljubljana, Faculty of Mechanical Engineering, Aškerčeva cesta 6, 1000 Ljubljana, Slovenia, e-mail: niko.herakovic@fs.uni-lj.si.

1 Introduction

Design and development of hydraulic and pneumatic valves constantly dictates improvements in valve miniaturization, lower price, better dynamic characteristics and lower energy consumption ([1] to [4]). Better dynamics of valves can be achieved with use of light-weight piston materials and alternative actuators for their actuation. The most commonly used actuators in industry are electromagnetic actuators (solenoids) which are robust and reasonably priced, however, they are questionable when shorter switchover and response times are needed, which is desirable in high dynamic systems. Shorter switchover and response times occur due to magnetic induction and eddy current when switching the current on. With the use of alternative actuators, among which piezoelectric actuators (piezo actuators) offer the best possibilities for practical use ([4] to [9]), much shorter response times and lower electric energy consumption can be achieved. On the one hand, switchover times of the electromagnetic actuators lie in the range between 10 to 20 ms, whereas on the other hand, piezo actuators achieve shorter switchover times in the range of 0.1 to 0.5 ms [3], [10].

The last twenty years the development of piezo valves presents an important area in the field of hydraulic and pneumatic systems. The research works are focused on development of high-response and energy efficient piezo actuators that can replace the conventional actuators of proportional and high-response servovalves. On the other hand high-response piezo actuators installed in conventional or new valves can be successfully used in proportional, servo and digital hydraulics. Especially the digital hydraulics is the reason that the piezo technology has become more interesting in the field of hydraulic valves. The state of the art technology of piezo actuators used in hydraulic valves is still in the prototype phase, some of the valves have already been used in hydraulic linear drives to analyse the drives characteristics.

A piezo actuator works on the principle of the inverse piezo effect. It converts electric energy directly to mechanical energy, while the solenoid (electromagnetic) actuator converts electric energy indirectly to mechanical energy (Figure 1). Because of the indirect energy conversion, longer response times are achieved with solenoids and consequently, worse dynamic characteristics of a hydraulic valve [11].

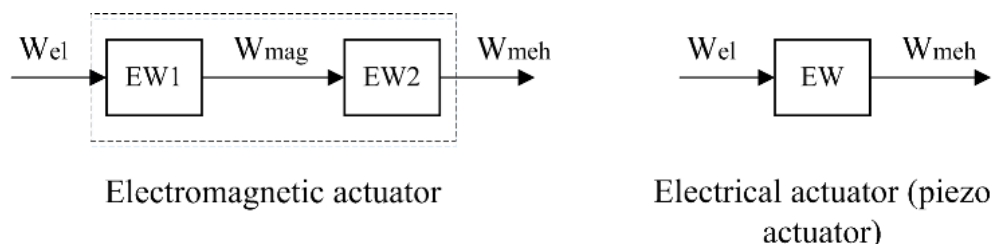


Figure 1: Conversion of electric energy in mechanical for electromagnetic and piezo actuator

2 Piezo actuators

In 1880 it was discovered that electric potential could be generated if pressure is applied to quartz crystals (piezoelectric material). This is called piezo effect. Vice versa, if electric potential is applied to piezoelectric material it changes its shape – inverse piezo effect. Piezo effect exhibited by natural materials as quartz, tourmaline, Rochelle salt etc. is very small so new materials with improved characteristics of piezo effect were developed. These materials are polycrystalline ferroelectric ceramic materials such as barium titanate and lead (plumbum) zirconate titanate (*PZT*), which is also a most widely used material for actuator applications today [11].

The biggest advantages of piezo actuators over electromagnetic actuators are short response time and low energy consumption in the stationary state. Other advantages and also disadvantages are presented in Table 1 [5], [11], [12].

Table 1: Properties of piezo actuators

Advantages	Disadvantages
High resolution	Hysteresis
High generated force (stack actuators)	Drift, creep (1% displacement/time decade)
Good efficiency	Small displacement, stroke (0.1-0.2%)
Short response time (below 1 ms)	Problem of depolarization
No wear (no moving parts)	High supply voltage (60-1000V)
High stiffness of <i>PZT</i> material	Sensitive to radial loads and torsion
Low energy consumption (stationary state)	
Operation at cryogenic temperature	

The most common used piezo elements for the technical applications are still linear multilayer stack piezo elements and bending bimorph piezo elements presented in Figure 2. Main properties for selecting the right piezo actuator for a particular application are: force generation, deflection/extension, dimensions and response time. Stack actuators (Figure 2a) can consist of monocrystal or of several piezoceramic plates. An advantage of the construction made of several plates is that a lower voltage is required for supplying the stack actuator, which is especially important for applications in fluid power technology and in assembly automation. They also generate high forces up to several kN but have small extension – several 10 μm . A bending actuator usually consists of a passive metal substrate which is glued to a piezoceramic strip – bimorph actuator [11]. There are also bending actuators with several layers – trimorph or multimorph. Two types of bending piezo actuators, cantilever piezo actuator (Figure 2b) and crossbow piezo actuator (Figure 2c), are more suitable for the use in pneumatic applications. A bending piezo actuator has high deflection – greater than 1 mm but generated forces are very low, up to several N. The bending cantilever piezo element is fixed only at one end; it has higher deflection and smaller forces than the crossbow piezo element. The crossbow piezo element is fixed on both ends [3], [11].

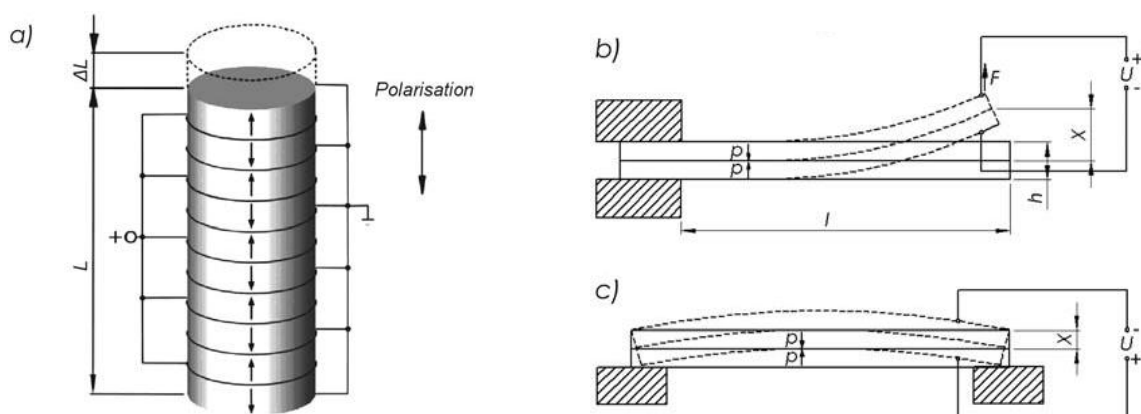


Figure 2: Different types of piezo actuators: a) stack; b) cantilever and c) crossbow

Based on the previous research works multilayer stack actuator (Figure 2a) is more suitable for use in hydraulic valves. Their mechanical performances can be described with two basic mathematical expressions which defines the electro-mechanical correlation [13]. Equation (1) presents the electrical charge of piezo actuator Q_{pzt} while Equation (2) describes the piezo actuator displacement x_{pzt} .

$$Q_{pzt} = C_{pzt} \cdot U_{pzt} - x_0 \cdot F_{pzt} \quad (1)$$

$$x_{pzt} = x_0 \cdot U_{pzt} - \frac{1}{k_{pzt}} \cdot F_{pzt} \quad (2)$$

Where:

Q_{pzt} – electric charge of piezo stack [C]

F_{pzt} – blocking force of piezo stack [N]

C_{pzt} – capacity of piezo stack [F]

x_{pzt} – displacement of piezo stack [m]

U_{pzt} – supply voltage [V]

k_{pzt} – stiffness of piezo stack [N/m]

x_0 – stress-free displacement of piezo stack per unit volt [m/V]

Under free operation, or no load, the stack does not exert any force and Equation (2) reduces to Equation (3). Thus, x_{pzt} becomes the free displacement of the stack, it varies linearly with voltage, and it will be denoted as x_{free} . In the same manner, if the stack operates under a very large load, its output displacement x_{pzt} is zero and Equation (2) reduces to Equation (4). This is the blocked force of the *PZT* stack and it will be denoted as F_{block} . Furthermore, for the operation of the stack under the maximum voltage allowed, U_{max} , Equation (2) can be rearranged in the form (5).

$$x_{pzt} = x_0 \cdot U_{pzt} \quad (3)$$

$$F_{block} = k_{pzt} \cdot x_0 \cdot U_{pzt} \quad (4)$$

$$F_{pzt} = -k_{pzt} \cdot x_{pzt} + k_{pzt} \cdot x_0 \cdot U_{max} \quad (5)$$

Equation (5) represents the force-displacement characteristic curve for a piezo stack and can be plotted as shown in Figure 3. It describes the mechanical performance of the *PZT* stack. The characteristic curve defines the operating point of a *PZT* stack (*OP*), given the loading conditions it is operating under.

In the same manner, Equation (1) yields to the charge-voltage characteristic shown in Figure 4, and it is related to the electrical performance of the *PZT* stack.

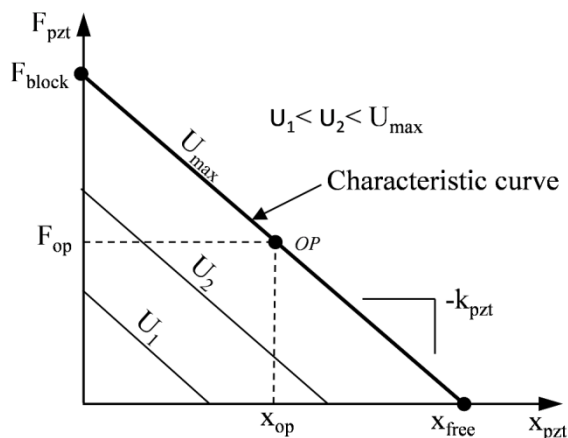


Figure 3: Force-displacement curve for a multilayer stack piezo actuator

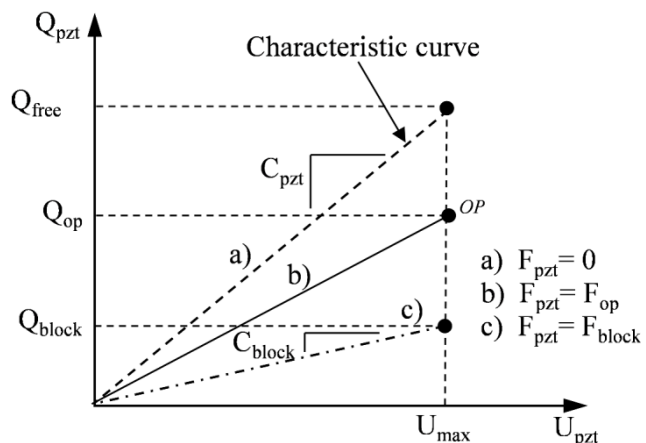


Figure 4: Electrical charge versus electrical voltage

One important fact when using the piezo actuator in real applications is the type of preload. As described in [13], a piezo actuator is an elastic body with a given stiffness, and from a mechanical standpoint it will be represented with a k_{pzt} . Furthermore, it can be operated under two different types of loading.

The first case represents the load which remains constant during the expansion process. This is represented in Figure 5, where a mass exerts a constant force on the piezo stack. The force of the mass m compresses the piezo stack until equilibrium is reached. Thus, the initial position of the stack changes by the amount of $\Delta x = F/k_{pzt}$. However, and as represented in the Figure 5, the constant force and the nonzero initial condition does not affect the stack's free displacement capability ($x_{freeA} = x_{freeB}$). Absolute displacement of piezo stack is defined with Equation (6).

$$x_{pzt} = x_{freeA} = x_{freeB} + \Delta x \quad (6)$$

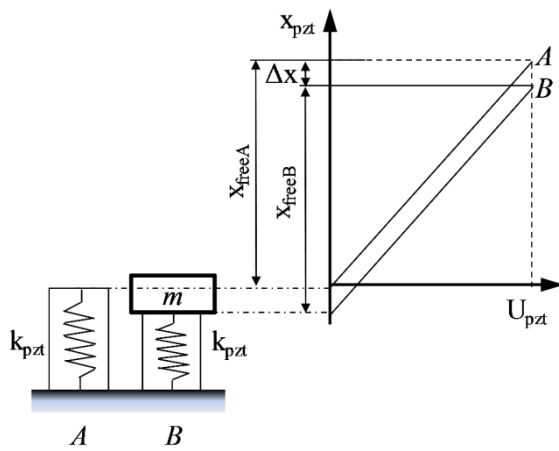


Figure 5: Effect of a constant force pre-load on a piezo stack

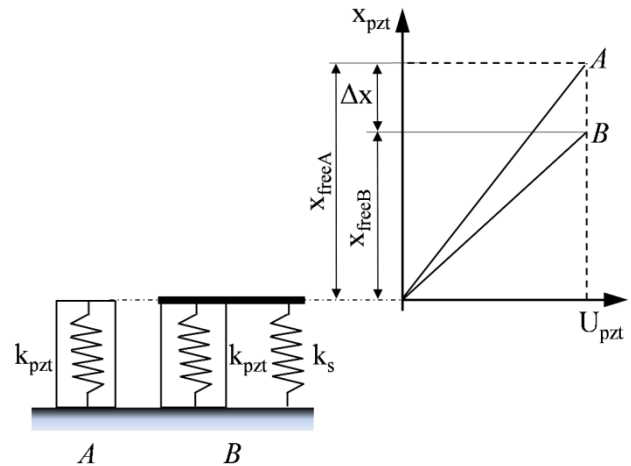


Figure 6: Effect of a spring pre-load on a piezo stack

The second case occurs when the load on the stack changes during the expansion process. In Figure 6 the stack is loaded with a spring of stiffness k_s that is coupled in parallel to it. Therefore, the free displacement of the unloaded stack is expressed with Equation (7) (case A), while the free displacement of the spring loaded stack (shown as case B) is expressed with Equation (8).

$$x_{freeA} = \frac{F_p}{k_p} \quad (7)$$

$$x_{freeB} = \frac{F_p}{k_p + k_v} \quad (8)$$

Thus, a spring load does affect the free displacement capability of the piezo stack, reducing the free displacement by Δx , Equation (9). Furthermore, the free displacement of the loaded case can be also expressed as a function of the original free displacement, Equation (10).

$$\Delta x = x_{freeA} \cdot \left(1 - \frac{k_{pzt}}{k_{pzt} + k_s} \right) \quad (9)$$

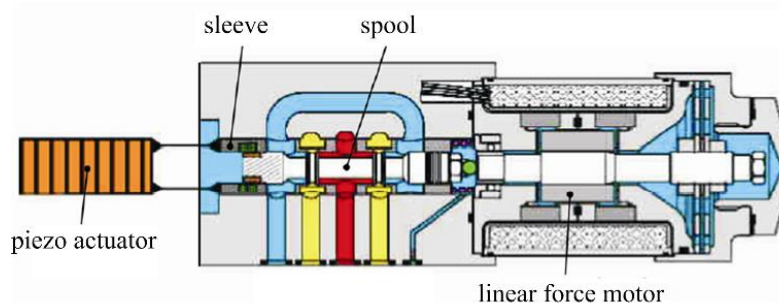
$$x_{freeB} = \frac{k_{pzt}}{(k_{pzt} + k_s)} \cdot x_{freeA} \quad (10)$$

3 Piezo actuators used in hydraulic and pneumatic valves

Hydraulic and pneumatic valves can be directly-operated or pilot-operated. In the first case usually the multilayer stack actuators in combination with hydraulic or mechanical amplifiers are used for high response servovalves. The stroke of piezo stack actuators (several 10 microns) can be amplified up to several 100 microns. In some cases, digital hydraulics, the amplification is not necessary. Digital hydraulics and digital fluid control units (DFCU) demands small-size switching valves. That can be achieved with the appropriate design of the valve and small displacement of the spool driven with direct-driven piezo actuator. The pilot-operated valves can use stack as well as bending piezo actuators. In this case the construction modification is usually performed due to low generated forces of the bending piezo actuators.

3.1 Directly-operated piezo valves

Interesting concept of a high response piezo servovalve, presented in Figure 7, implies a modification of a conventional direct driven servovalve [14]. In contrast to the conventional actuation of a spool in an immovable sleeve this concept includes the actuation of both the spool and the sleeve. This design allows reacting faster by driving the sleeve in the opposite direction to the spool and thereby enlarging the valve control orifice. The spool is driven by a conventional actuator (linear force motor) and the sleeve is actuated by a piezo stack. The actuators drive the spool and the sleeve in the opposite directions which results in a faster opening of the control orifice within a small signal operation till the piezo actuator achieves the full stroke. Both the spool and the sleeve are driven in a position closed loop in order to avoid a drift of a conventional actuator, to compensate a hysteresis of a piezo-actuator and to hold a required position at changing external forces (i.e. flow forces, friction forces). Due to the lower mass of the spool it can be advantageous to drive the spool with a piezo actuator and to actuate a sleeve with a conventional valve drive. Generally, the force of the piezo actuator reduces with an increasing stroke. External forces acting on a piezo-actuator should be considered as they cause an offset of the stroke or reduce it. The new concept of hybrid servovalve results in much better dynamic characteristics of the valve in the range of small openings. The step response of the sleeve is below 1 ms (maximal stroke of the sleeve) while the frequency response is around 620 Hz (-3dB) and 850 Hz (phase shift -90°). The delay time of piezo actuated sleeve is much lower (0.1 ms) compared to the conventional actuation of the spool (1 ms).



Source: IFAS

Figure 7: Hybrid proportional piezo valve [14]

A product of company Hydraulik Ring can be taken as an example of a directly driven piezo-valve with a mechanical stroke amplifier [15], [16]. Figure 8 shows the valve and its schematic mechanical stroke amplification system. The amplification ratio is set by the distances between the pivot point and the joints. The valve has improved dynamic characteristics (750 Hz at -90° phase shift). However, the amplified stroke of the spool (ΔLa) of $\pm 150 \mu\text{m}$ leads to extremely narrow manufacturing tolerances and a small nominal flow rate.

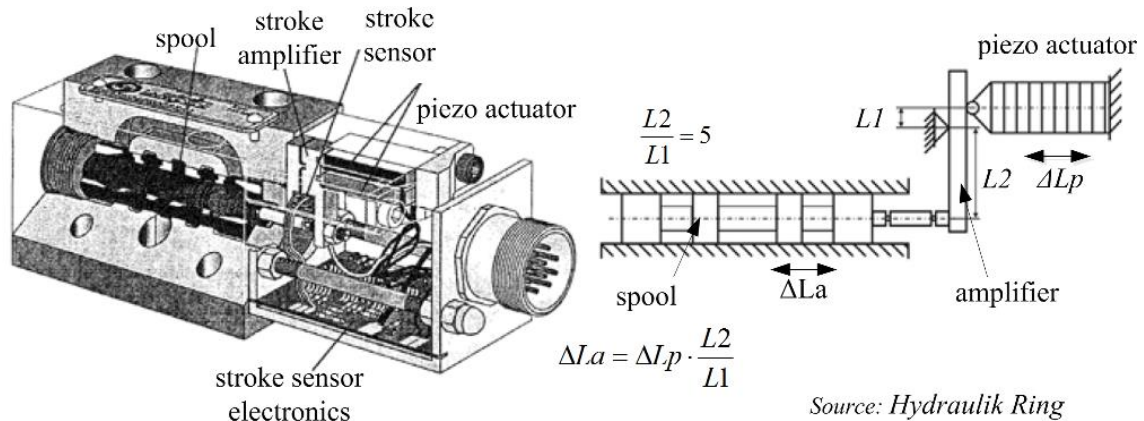


Figure 8: Hydraulic piezo valve using the mechanical amplifier [15], [16]

Very similar to the mechanically amplified actuator the hydraulically amplified piezo actuator is presented in Figure 9 [17]. The amplification ratio is defined by the areas of the pistons at the input D and output d side of the amplifier. In order to avoid oil leakage, the amplification system of this valve consists of a membrane on the actuator side and a flexible metal bellow on the spool side. Thermal expansion of the actuators and the oil is compensated by the opposed arrangement of the actuator packages. Some of the authors use silicon filling (instead of oil chamber) in the hydraulic amplifiers to avoid leakage. The response time of the valve, size 10, is around 1 ms.

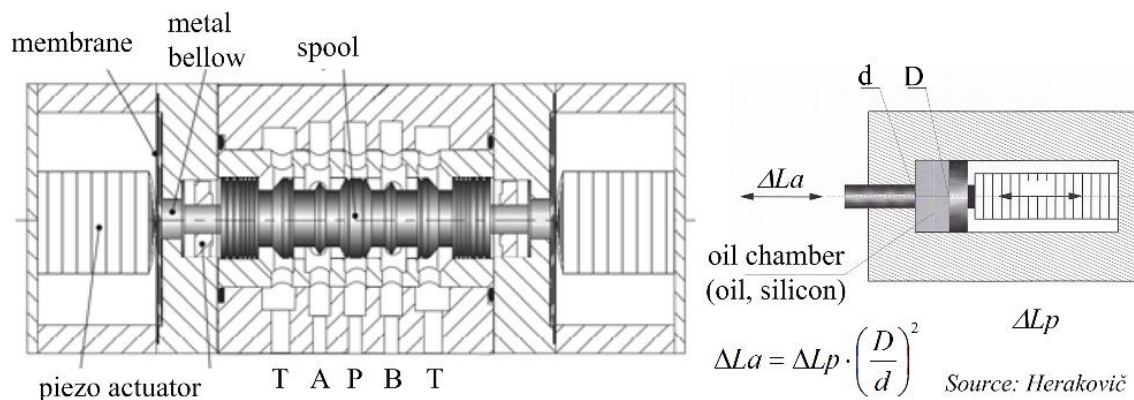
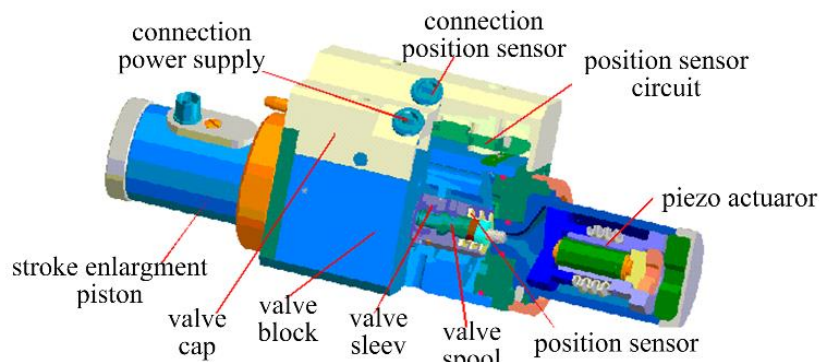


Figure 9: Hydraulic piezo valve using the hydraulic amplifier [17]

The next example uses a piezo driven spool valve shows Figure 10 [18]. It provides a partly cross sectional view of the valve (Size 10, $Q_N = 70$ l/min, $\Delta p = 70$ bar) being developed at IFAS. A stack of piezo discs provides only a small stroke of about 1/1000 of the stack length. For that reason a stroke amplification system is necessary. It features a hydrostatic transformer filled with silicone and allows a 40 times stroke amplification. The valve spool is flow force compensated to minimize forces required from the piezo drive. It is not easily accessible for stroke measurement and for this reason a special eddy current sensor was developed which is integrated into the valve sleeve.

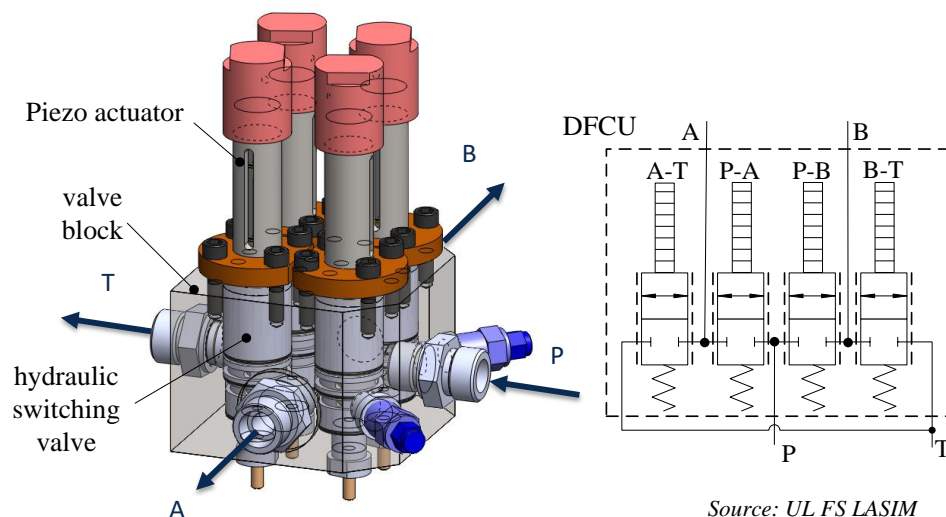


Source: IFAS

Figure 10: Piezo driven servovalve with stroke amplifier [18]

High response hydraulic drives, controlled with servovalves, can be replaced with digital fluid control units (*DFCU*) presented in Figure 11 [10]. New *DFCU* was developed by *UL FS LASIM* and is suitable for the use as 4/3 spool valve in high performance hydraulic linear drives. The functionality of conventional servovalve is achieved with the use of four on/off valves (functional states: $P \rightarrow A$, $B \rightarrow T$ and $P \rightarrow B$, $A \rightarrow T$). Valve in combination with proper control electronic and control algorithm allows controlling the flow rate (from 0.08 to 20 l/min at pressure drop per metering edge $\Delta p = 3.5 \text{ MPa}$) of individual on/off valve independently which results in high flexibility of the valve.

The major advantage of the new digital piezo valve, compared to proportional and servovalves, is high step response (short delay time-below 0.1 ms, short switching time-below 0.3 ms) in all range of valve opening (from 0% to 100 %). The frequency response of the piezo actuator is approximately 1.4 kHz (-3dB) and 1.7 kHz (-90° phase shift) while the frequency response of the valve is 1.17 kHz (-3dB) and 1.18 kHz (-90° phase shift). The new construction of the seat valve is developed in order to reduce the static and dynamic flow forces which results also on reduction of the electrical energy consumption.



Source: UL FS LASIM

Figure 11: Digital hydraulic piezo valve [10]

The cross-section view of piezoelectric actuator is shown in Figure 12. It consists of: 1-screw cap that allows proper preload of the piezo stacks, 2-spacer in combination with ball bearing to eliminate torsion, 3-actuator housing with the proper stiffness, 4-flange (for installation in hydraulic valve), 5-disk springs, 6-control piston and PE-piezo stack.

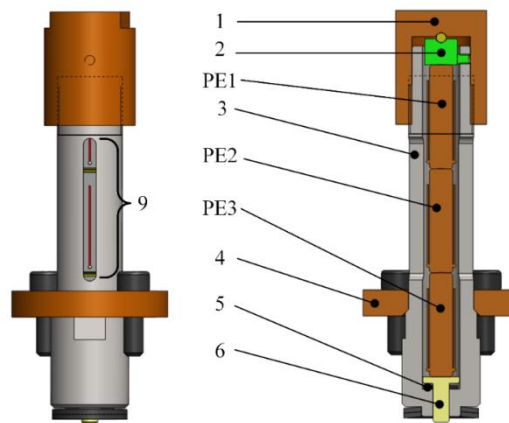


Figure 12: Construction design of piezoelectric actuator [10]

3.2 Pilot-operated piezo valves

A newly developed piloted hydraulic servovalve at IFAS [19] aims at two limits given today:

1. increase of dynamic performance by the use of piezo crossbow actuators
2. reduction of quiescent leakage using two independently controlled nozzles.

A cross sectional view of this valve can be taken from Figure 13. To increase performance of the piezo crossbow actuators the static force of the nozzle acting on it is compensated by a small piston fed by supply pressure. During static operation conditions both nozzles can almost be closed increasing the pressure in both spool driving chambers thus decreasing quiescent leakage. The valve spool is optimized with regard to its mass and is compensated for static flow forces. Spool displacement is measured by a small eddy current sensor which delivers a linear output signal.

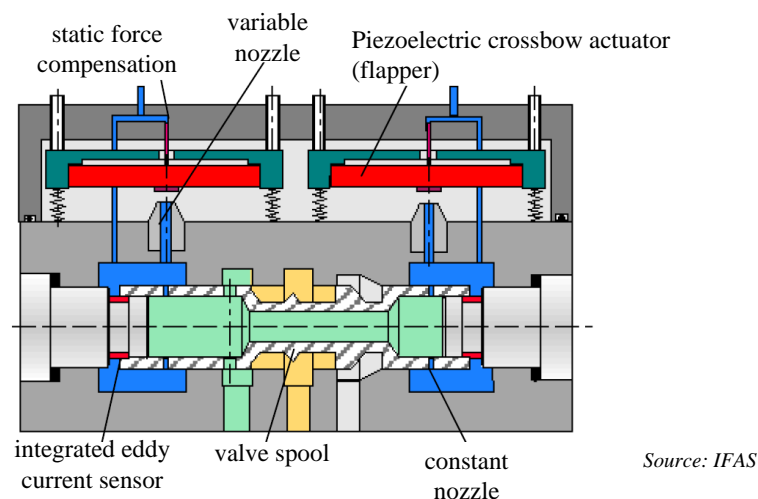
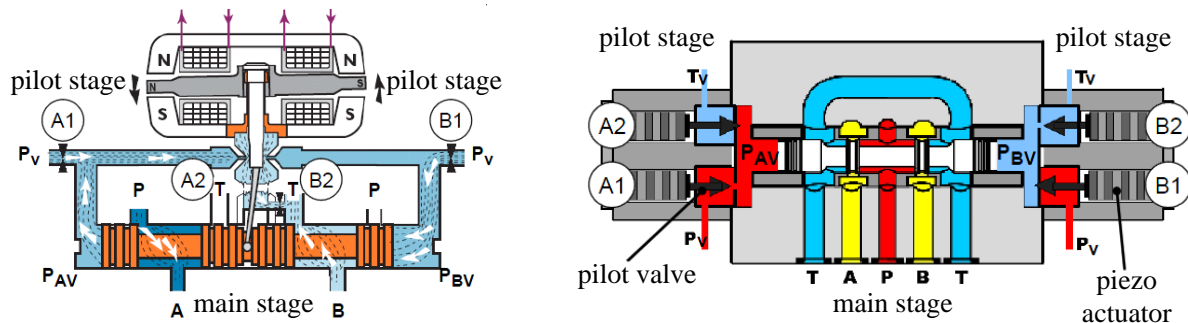


Figure 13: Pilot stage servovalve using the piezo crossbow actuators [19]

Figure 14 shows another concept how to modify the conventional nozzle flapper pilot stage servovalve (Figure 14 left) with two variable flow resistors A2 and B2 and two constant flow resistors A1 and B1. The concept (Figure 14 right) deals with a use of piezo-driven pilot stage as a hydraulic amplifier for the main stage with a higher nominal flow rate. The pilot stage comprises of four variable hydraulic flow resistors. Each flow resistor is implemented as a piezo-actuated 2/2-way poppet valve. The pilot stage is mounted on a main stage of a conventional servovalve. The pilot stage pressures P_{AV} and P_{BV} are varied by a continuous displacement of the pilot valves.

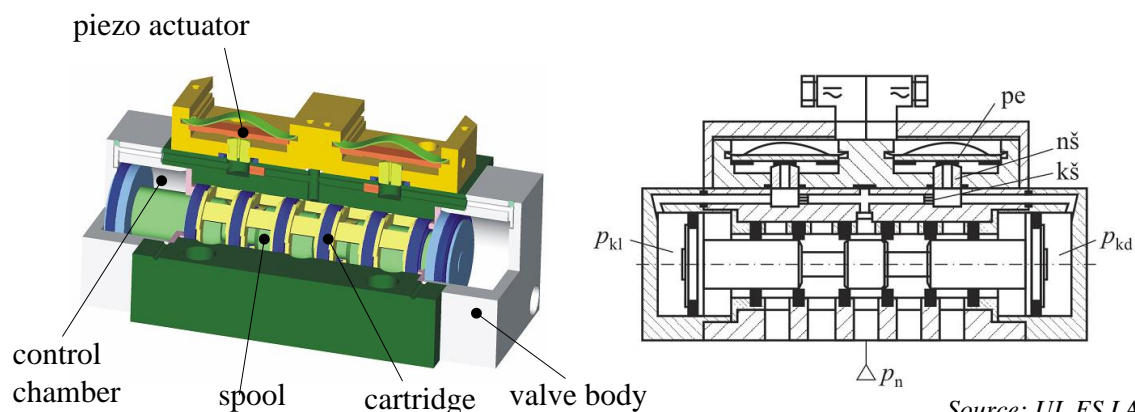
The spool of the main stage is driven by these pressures in a position control loop. One of the operation modes of the pilot stage is driving the pilot valves pairwise in opposite directions. While valves A2 and B1 are closing, valves B2 and A1 are opening and vice versa. By changing the stroke of each pilot valve and the phase lag between them, different operation modes of the pilot stage can be achieved. The use of the highest hydraulic power amplification of four variable resistors on the one hand and fast piezo actuators on the other hand provides the valve high dynamics. The step response of the piezo valve is approximately 1.3 ms (maximal stroke of the sleeve) while the frequency response is around 340 Hz (-3dB) and 300 Hz (phase shift -90°).



Source: IFAS

Figure 14: Pilot-operated piezo servovalve [14]

Very similar to the concept of hydraulic valve shown in Figure 13, Figure 15 shows pneumatic directional valve of the size ISO 3, 5/2 with a pilot-stage piezo actuator [3]. The research into the possibilities of using piezo actuators with bending elements has shown that for controlling a 5/2 directional valve it is possible to use the crossbow piezo element with a flapper/nozzle system. In the pilot-stage two crossbow piezo elements were used. The supply pressure p_n is led from the main power supply on the main directional valve. The supply air flows through the constant nozzle to the adjustable nozzle. At standstill both piezo elements are unloaded and the air flows from both nozzles into the atmosphere. By switching ON one of the pilot-stage valves, the piezo actuator bends and moves towards the nozzle. Due to greater blockage of the air outflow, the pressure p_k in the chamber rises. When the pressure force in the chamber is big enough, the valve is switched over into a new position. The research also includes the energy consumption analysis by taking into account the energy needed for one switch of the main spool. The results shows that piezo actuator consume up to 30 % less energy compared to the conventional solenoid.



Source: UL FS LASIM

Figure 15: Pneumatic piezo valve ISO 3, 5/2 with a pilot-stage piezo actuator [3]

4 Conclusion

The paper presents different types of piezo actuators that can be used in hydraulic and pneumatic valves. In the first part basic theoretical background of the piezo technology which should be taken into account when developing the new piezo actuators is presented in detail. Further on three most useful piezo actuators, multilayer stack, cantilever and crossbow, are presented.

Piezo stack actuators are more suitable for the use in direct-operated hydraulic valves due to their high blocking forces. Very small displacement of the piezo stack actuators demands mechanical and hydraulic stroke amplifiers to increase the stroke to a demanded value. In the case of servovalve with the torque motor the piezo stack actuators can be used in pilot operated when small flow rates of the pilot stage is needed to control the main spool.

Piezo stack actuators are very suitable for the use in digital hydraulics as actuators of fast switching valves. Based on existing researches the combination of pilot-operated high flow rate switching piezo valve and the small flow rate direct-operated piezo valve should give the best results in terms of robustness, functionality, price and dynamic performance of the entire DFCU.

Bending piezo actuators are usually used in pilot-operated hydraulic and pneumatic valves. Hydraulic valves demands modifications of the pilot-stage chambers in order to achieve the static force compensation needed to open the pilot-stage nozzle. Otherwise these types of actuators don't provide functionality due to small generated forces.

The mechanical components such as actuator body, preloading components of the actuator system, valve spools, valve sleeve, valve body, and other mechanical elements effecting the static and dynamic characteristics of the actuator or the valve need special treatment and the use of advanced numerical approach such as CFD (Computer Fluid Dynamics) and FEM (Finite Element Method) methods. Otherwise the problems in terms of valve stability and performance of the valve cannot be achieved. Especially the dead volume of the pilot-stage chamber could have major impact on valve dynamics.

By taking into account all the requirements the improved characteristics of the valves can be achieved. The experimental results of the existing piezo valves prototypes shows that piezo valves can be used as alternative to conventional servo valve for driving the high-performance and energy efficient hydraulic and pneumatic drives.

References

- [1] Herakovič, N.: Alternativni aktuatorji in mehatronski sistemi – pregled in uporaba v fluidni tehniki, Ventil, (1997) 3–4, 135–141, 1997
- [2] Murrenhoff, H.: Trends in valve Development; 3rd International Fluid Power Conference (Volume 1); Shaker Verlag GmbH, Aachen, 2002
- [3] Herakovič, N., Noe, D.: Analiza delovanja pnevmaticnega ventila s predkrmilnim piezoventilom, Strojnikski vestnik, (2006) 12. 834–851, 2006
- [4] Bevk, T.: Eksperimentalna analiza dinamičnih lastnosti pnevmatičnega ventila in optimizacija energetske porabe; diplomska naloga univerzitetnega študija; UL FS, Ljubljana, 2008
- [5] Herakovic, N.: Die Untersuchung der Nutzung des Piezoeffektes zur Ansteuerung fluidtechnischer Ventile; Verlag Mainz, 1996

- [6] Topçu E., Yüksel I., Kamý° Z.: Development of electro-pneumatic fast switching valve and investigation of its characteristics; *Mechatronics*, (2006) 6, 365–378
- [7] Choi, S. B., Yoo, J. K., Cho, M. S., Lee, Y.S.: Position control of a cylinder system using a piezoactuator-driven pump; *Mechatronics*, 2005, št. 2, str. 239–249
- [8] Choi, S. B., Han, S. S., Lee, Y. S.: Fine motion control of a moving stage using a piezoactuator associated with a displacement amplifier; *Smart Materials and Structures*, (2005) 1, 222–230
- [9] Miyajima, T., Fujita T., Sakaki K., Kawashima K., Kagawa T.: Development of a digital control system for high-performance pneumatic servo valve; *Precision Engineering*, (2007) 2, 156–161
- [10] Šimic, M.: Karakterizacija in modeliranje hidravličnega digitalnega piezoventila, doktorsko delo; UL FS, Ljubljana 2013
- [11] Herakovič, N., Bevk, T. Analiza vpliva materiala in aktuatorjev na lastnosti pnevmatičnega ventila; *Materiali in Tehnologije*, 37-40, 44 (2010)
- [12] Physik Instrumente: PZT Fundamentals, Catalog: Products for Micropositioning, 1999
- [13] Nasser, K.M.: Development and Analysis of the Lumped Parameter Model of a PiezoHydraulic Actuator; Faculty of the Virginia Polytechnic Institute, Blacksburg, 2000
- [14] Reichert, M.: Development of High-Response Piezo-Servo Valves for Improved Performance of Electrohydraulic Cylinder Drives; Von der Fakultät für Maschinenwesen der Rheinisch-Westfälischen Technischen Hochschule Aachen zur Erlangung des akademischen Grades eines Doktors der Ingenieurwissenschaften genehmigte Dissertation, 04.02.2010
- [15] Matten, N., Ohmenhäuser, M.: Stetigwirkendes Wegeventil mit piezoelektrischem Stellelement; O+P „Ölhydraulik und Pneumatik“ 38 Nr.6, pp. 350-355, 1994
- [16] Ohmenhäuser, M., Glöckler, M.: Hochdynamisches Stetigventil mit Piezoaktor, Lageregelseminar; Institut für Steuerungstechnik der Werkzeugmaschinen und Fertigungseinrichtungen ISW; Universität Stuttgart, Germany, February 16-17, 1996
- [17] Herakovič, N.: Die Untersuchung der Nutzung des Piezoeffektes zur Ansteuerung fluidtechnischer Ventile: Der Fakultät für Maschinenwesen der Rheinisch-Westfälischen Technischen Hochschule Aachen; vorgelegte Dissertation zur Erlangung des akademischen Grades eines Doktors der Ingenieurwissenschaften. Aachen; 1995. IV, 152 f., illustr
- [18] Linden, D.: Entwicklung eines piezobetätigten Servoventils für die hydraulische Werkstückprüfung; Dissertation, RWTH Aachen, 2001
- [19] Hagemeister, W.: Auslegung von hochdynamischen servohydraulischen Antrieben für eine aktive Frässpindellagerung; Dissertation RWTH Aachen, 1999

Development of the heavy-duty flow divider (FD-H2) for mobile applications

ANŽE ČELIK & LUKA PETERNEL

Abstract A two-way heavy-duty flow divider assures parallel operation of wheels of the same axle and/or between different axles by dividing or combining flow. In generally, it can be operated in open or closed loop circuits.

The paper shows development procedure of a heavy-duty flow divider of spool type for mobile applications: starting with basic principle of flow dividing, over development activities including benchmarking, concept design to experimental validation, to patenting problems. The latter normally refers to high pressure (up to 500 bar) and high flow rates (up to 300 L/min in by-pass mode). For such applications, it is highly desired to establish stable valve operation as well as dividing/combining accuracy in the widest possible flow range.

Keywords: • mobile hydraulic • wheels drive • parallel operation • flow divider • development procedure •

CORRESPONDENCE ADDRESS: Anže Čelik, Poclain Hydraulics d.o.o., Industrijska ulica 2, 4226 Žiri, Slovenia, e-mail: anze.celik@poclain.com. Luka Peternel, Poclain Hydraulics d.o.o., Industrijska ulica 2, 4226 Žiri, Slovenia, e-mail: luka.peternel@poclain.com.

<https://doi.org/978-961-286-086-8.22>

ISBN 978-961-286-086-8

© 2017 University of Maribor Press

Available at: <http://press.um.si>.

1 Introduction

If there is a need to split a single hydraulic line into two or more identical flow paths, a tee (i.e. hydraulic T-junction component) or several tees can be a solution. However, if the resistance in all lines is not identical, flow can vary in each line. Adding flow control valve at the tee outlets allows changing resistance and equalizing flow in each line. In the machine operating condition, work resistance changes often require constant flow modifications. A special flow control valve, called a flow divider, splits flow and compensates for pressure differences. A flow divider can split flow equally, unequally, and into single or more paths [6]. There are two types of flow dividers: a spool type and a motor type (usually gear). This is shown on Figure 27.

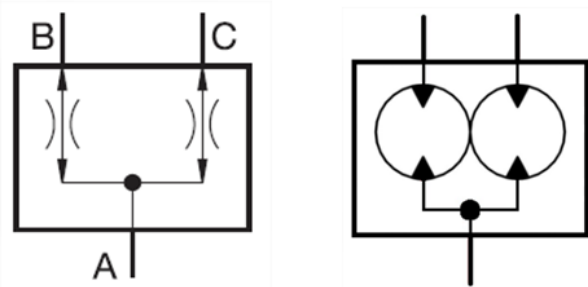


Figure 27: Hydraulic symbol of a flow divider: spool type (left) and motor type (right) [5]

If this valve also combines the flows, it is named a flow divider/combiner. However, for this paper purposes, only a flow divider/combiner of a spool type is taken into account. For the sake of simplicity, flow divider/combiner will be called, hereafter, only a flow divider.

A typical flow divider has two functions, dividing and combining of a fluid flow. The valve divides a fluid flow in the direction from A to B and C, and combines flows in the direction from B and C to A (refer to Figure 27). The dividing/combining ratio is usually 50 % : 50 % (although any other ratio is possible), independent of a pressure in respective pipelines, B or C. Typically, the valve consists of housing (4), outer spool (3), two dividing spools (2) and three weak springs (1). See Figure 33 for more details.

Flow dividing: The fluid flows in the direction from A to B and C. The flow in chamber A is divided and flows through the orifices with constant cross-section (i.e. fixed orifices) and throttles (i.e. variable orifices) into chambers B and C.

Flow combining: The oil flows in the direction from B and C to A. The operation is identical as at dividing of the flow.

The principle of operation depends on the pressure loss, which again depends on the fluid flow. For this reason, the divider works properly only within the defined flow range. Limitation of a maximal flow directly affects the rate of pressure loss; limitation of minimal pressure has a direct impact on dividing and combining accuracy [1].

A typical position of a flow divider in a closed loop hydraulic circuit is depicted on Figure 28. Inlet flow from a pump is distributed equally to the left and right hydraulic motors and assures parallel operation of wheels of the same axle and/or between different axles. If there is no flow divider integrated into hydraulic circuit and there is a loss of adherence on one wheel, a vehicle will not move ahead anymore since all the flow passes through this motor (→ oil under pressure will take the easy way out).

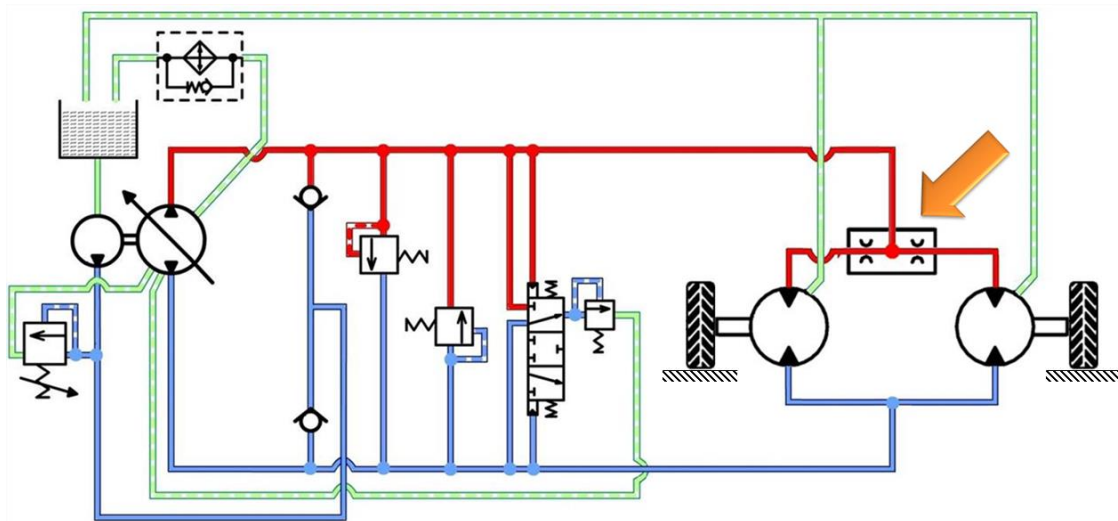


Figure 28: Position of a flow divider in a closed loop hydraulic circuit [5]

Figure 29 depicts position of a flow divider in an open loop hydraulic circuit (depicted in a simplified representation). In this case, inlet flow from a pump is distributed equally to the both hydraulic cylinders and therefore assures parallel operation of both cylinders. If there is no flow divider integrated into hydraulic circuit and cylinders are not loaded equally, cylinders may not reach the end of stroke together (the low-loaded cylinder will make full stroke first).

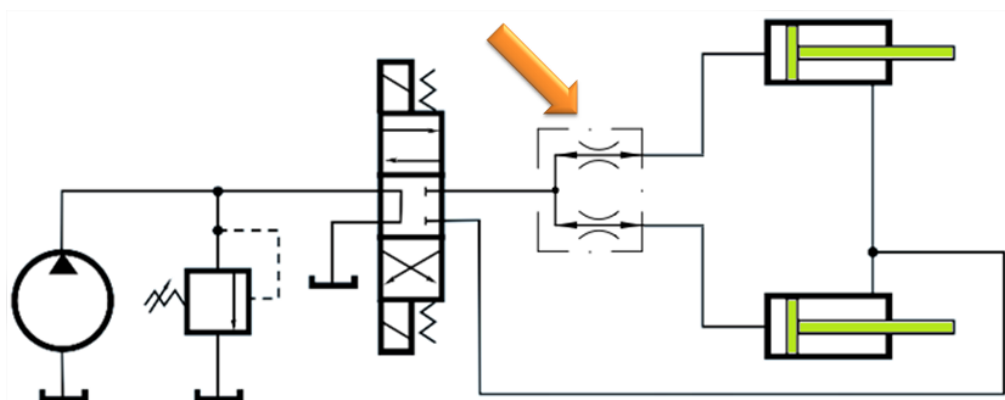


Figure 29: Position of a flow divider in an open loop hydraulic circuit [5]

1.1 Basics of dividing/combining principle

As the principle of dividing and combining mode is the same, the dividing mode will be presented hereafter only. For the explanation simplicity, it is assumed that dividing (or combining) ratio is 50 % : 50 %.

1.1.1 Hydraulic orifice

The fundamental principle of a flow divider is the fluid flow repartition through (two) orifices in parallel connection. The prescribed repartition ratio depends solely on fixed orifices (Figure 30).



Figure 30: Fixed orifice (constant cross section)

Fluid flow through the (fixed, variable) orifice is governed by the Bernoulli equation which relates the flow rate and pressure loss:

$$Q = A \cdot v = C_q \cdot A \cdot \sqrt{\frac{2 \cdot \Delta p}{\rho}} \quad (1)$$

where v , A , C_q , Δp and ρ refer to fluid velocity, orifice cross section area, flow coefficient, pressure loss and fluid density, respectively.

- **Orifice cross section area**, A , could be fixed (i.e. non-adjustable $\rightarrow A = \text{const.}$) or variable (i.e. adjustable $\rightarrow A \neq \text{const.}$). In the first case, orifice is known as fixed orifice; in the second case, orifice is said to be variable orifice. Figure 31 depicts these two types of orifices on Poclair Hydraulic existing flow divider (DTP).

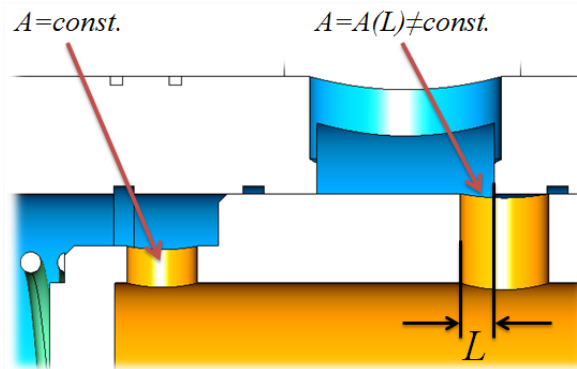


Figure 31: Orifice examples: fixed orifice (left) and variable orifice (right)

- **Flow coefficient**, C_q , represent the hydraulic efficiency of a component. Flow coefficient has mainly a constant value in turbulent area (i.e. at high flow number λ), but linearly increases at laminar flow (i.e. at low flow number λ).

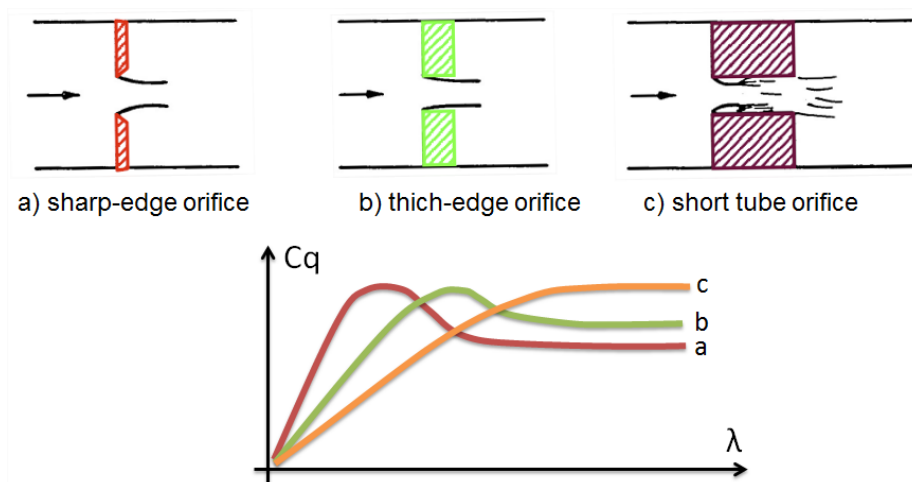


Figure 32: Characteristic of flow coefficient versus lambda [3]

- **Pressure loss**, Δp , refers to the pressure difference between upstream and downstream pressures. Therefore, if a flow direction on Figure 30 is $A \rightarrow B$, then the pressure loss is $\Delta p = p_A - p_B$. For pressure loss calculation according equation (1), minimum cross section area should always be taken into account.

Based on the equation (1), two orifices with the same flow rate (Q) have the same pressure loss (Δp) if their cross section area (A) is the same.

1.1.2 Dividing principle – centric spool position

Combination of fixed and variable orifices is used on the existing Poclair Hydraulic flow divider. Variable hydraulic orifice is designed as “spool-in-spool” where cross section area varies and depends on relative positions of both spools.

In this particular case, it is assumed that inlet flow rate (Q) divides into C and B hydraulic lines equally (i.e. $p_B = p_C \rightarrow Q_B = Q_C$) and fixed orifices are of the same size. Therefore, oil passes through the control (fixed) orifices and spools remain in the central position, as shown on Figure 33. Although it depends on a particular design, variable orifices on inner spools in centric position are normally fully uncovered by the outer spool.

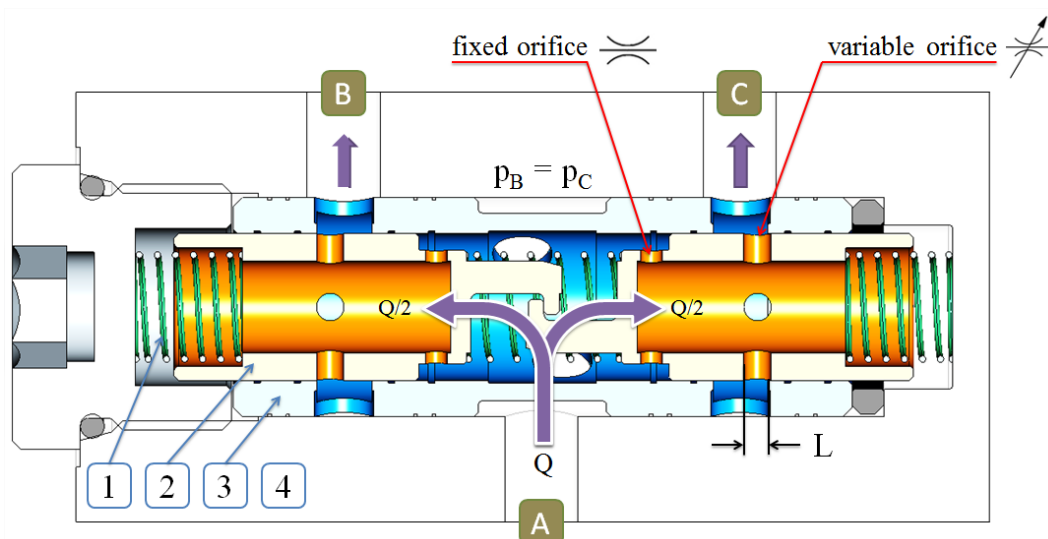


Figure 33: Cross section view of flow divider (DTP) in centric position

Therefore, in this centric inner spool position, fixed orifices play the essential role for maintaining equal pressure loss and consequently, equal flow rate on both sides of the valve.

1.1.3 Dividing principle – eccentric spool position

If, due to a change in outlet pressures p_B or p_C , there is a tendency for more oil to pass through one side than the other (i.e. B or C), the pressure loss increases in that side causing inner spool to shift the other inner spool across eventually restricting the outlet of the higher flow side (thanks to variable orifice) while keeping the lower flow side open (Figure 34). As soon as the pressure loss through the fixed orifice in both inner spools is equal, the spools will maintain a metering position keeping the flow from both legs equal. Any change in the outlet pressures will cause the inner spool to move accommodating the change by metering the oil through the path of least resistance [8].

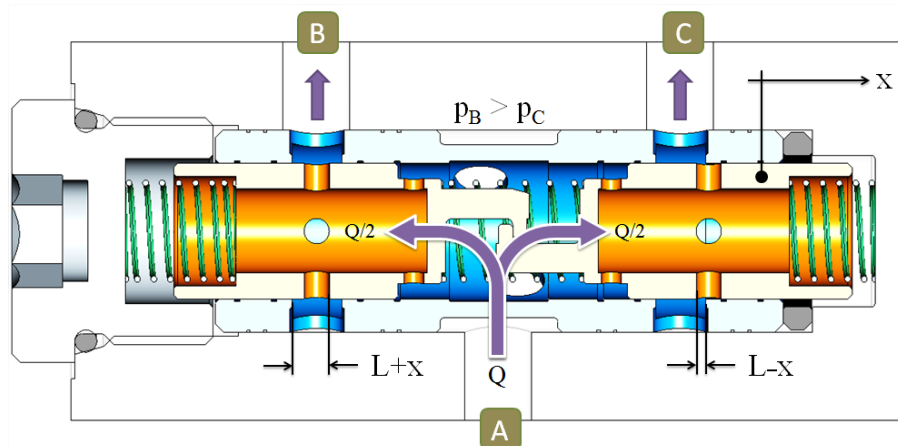


Figure 34: Cross section view of flow divider (DTP) in eccentric position

In this particular scenario, all orifices (i.e. fixed and variable) are essentially important in order to assure equal flow rates on both sides of the flow divider. Thus, variable orifices adjust their position in order to equalize pressures on both sides of a valve (i.e. B and C) and therefore equalize pressure loss between the inlet port and the outlet ports.

2 The scope of investigation

Since last few years, power transmission valves (i.e. VPT – a dedicated branch of valves in Poclain Hydraulic) experience an increase of market needs and demands. VPT hydraulic valves are mainly used on mobile applications. Due to space and weight limitations, such valves need to handle high power density at minimum overall dimensions. This could be mainly achieved by increasing a working pressure. Along with rigorous demands for valve operating conditions (e.g. high flow rates, high pressures), there is also an undesired consequence of higher energy losses.

Poclain Hydraulics strives to offer a complete hydrostatic transmission solution for high pressure applications. In order to fulfil this aim, the new “HP” (i.e. high pressure) series of pumps, motors, valves and electronics are released for most demanding applications (Figure 35). The latter usually refers to pressures up to 500 bar.

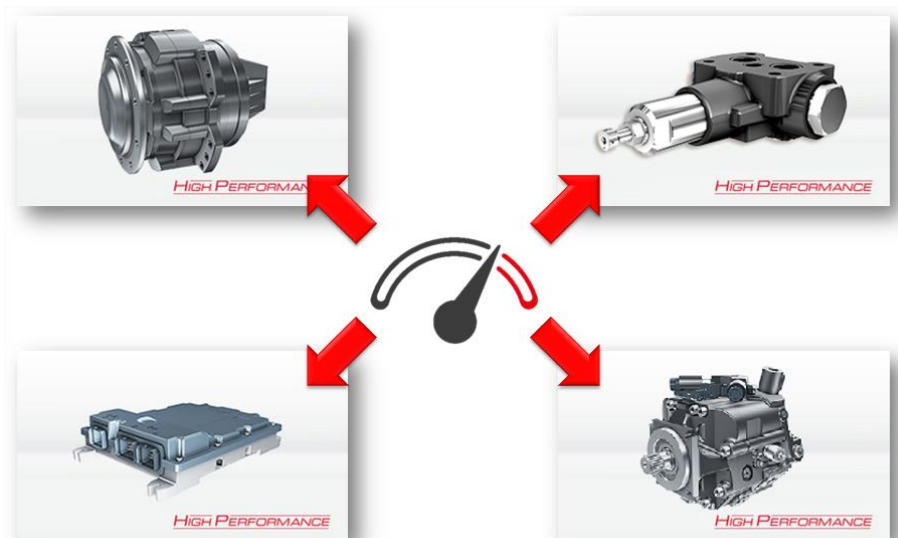


Figure 35: Poclain Hydraulics high performance portfolio

The new generation flow divider (FD-H2) has been developed in order to satisfy the needs for high performance product portfolio.

2.1 Existing solutions

Prior to a development of the new high pressure flow divider FD-H2, Poclairn Hydraulics already offers solutions for synchronizing motor speed on mobile applications (Figure 36). There are the following products:

- FD-MX flow dividers (FD-M2, FD-M3, FD-M4) for medium duty applications (i.e. for pressures up to 420 bar). It allows dividing/combining flow into 4 hydraulic lines.
- FDB-2X flow dividers (FDB-20, FDB-25) for high pressure applications (i.e. for pressures up to 450 bar). It is designed and produced in subcontracting.

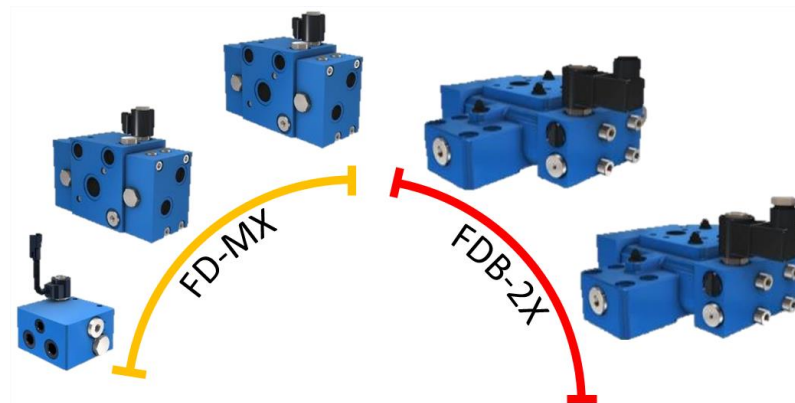


Figure 36: Existing solutions for flow dividing/combining

2.2 The needs for a new development

Existing solutions for heavy duty application are out of the market needs and also out of Poclairn Hydraulics needs. Based on Poclairn Hydraulics past experiences and new market research, the following needs/goals have been defined regarding flow divider basic function:

- *performances of HP range (i.e. pressures up to 500 bar, flow rates up to 200 l/min in dividing/combining mode),*
- *good dividing/combining accuracy over entirely flow range,*
- *operational stability (no oscillations),*
- *compact design,*
- *modularity,*
- *higher profitability,*
- *faster delivery.*

Along with these goals, several other needs have been defined, such as: develop and produce components in-house in order fulfil customer needs faster, better control over the quality, achieve higher profitability and assure faster end-product delivery to customers.

3 Benchmark analysis

Four different flow dividers from competitors are analysed hereafter. All of them could be used for mobile applications. The following output variables are tracked:

- pressure loss (Δp),
- accuracy in dividing and combining mode.

Accuracy is measured over the entire flow range at five different Δp (i.e. at min pressure, ± 200 bar, ± 350 bar) between input/output ports. Figures below show averaged values of accuracy calculated based on the equation (2):

$$T[\%] = \frac{\sum_{i=1}^5 \frac{Q_{Ai} - Q_{Bi}}{Q_{Ai} + Q_{Bi}}}{5} \cdot 100\% \quad (2)$$

3.1 Hydraulic measurements of the competitor valves

3.1.1 Pressure losses

This type of analysis indicates significant differences in pressure losses at nominal flow rates. Figure 37 depicts pressure losses in dividing mode according to the ratio between actual (Q_A) and nominal (Q_N) flow rates. Pressure losses at nominal flow rate in dividing mode differ from 12 bar to almost 48 bar. Therefore, at given pressure loss, a significant difference in flow rate among competitor “A” and competitor “C” could be obtained.

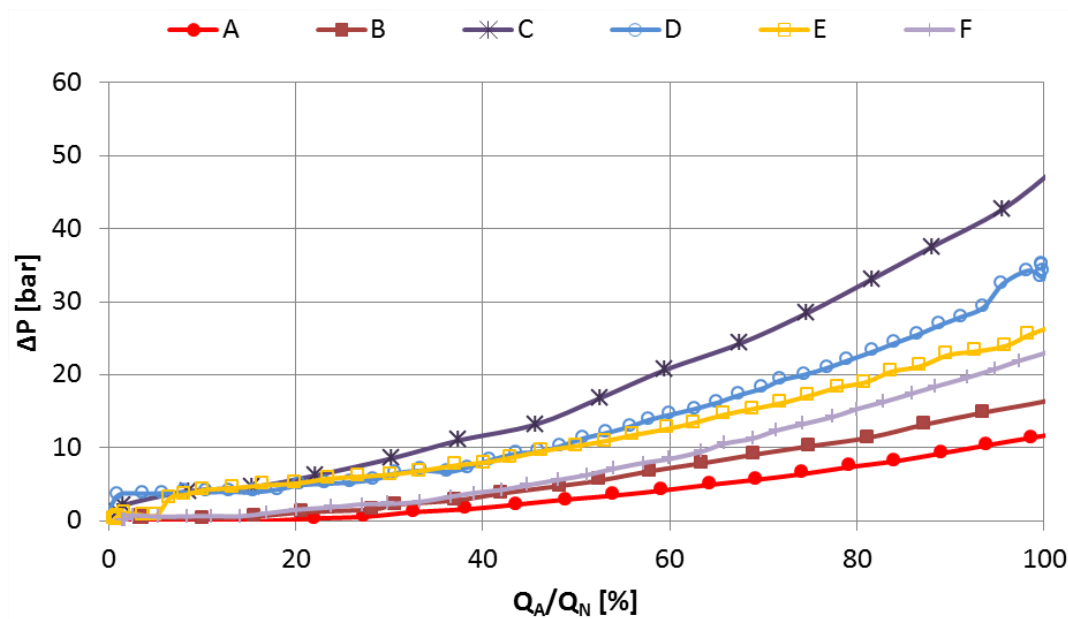


Figure 37: Pressure loss in dividing mode

Differences are also observed between pressure losses in dividing and combining modes. For example: valve from competitor »D« has 19 bar difference in pressure loss at nominal flow rate comparing dividing and combining mode (see Figure 38).

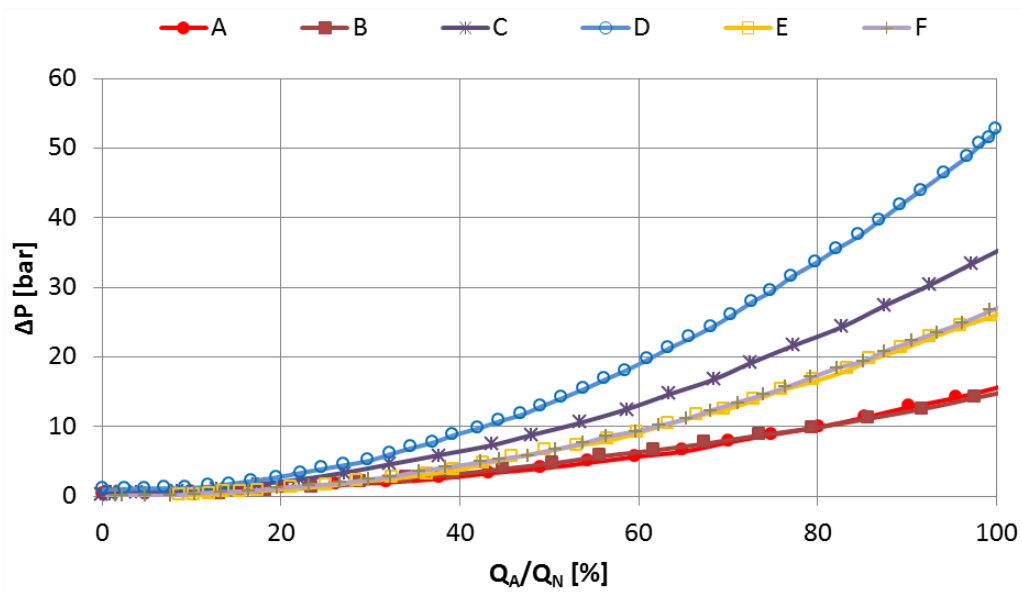


Figure 38: Pressure loss in combining mode

3.1.2 Accuracy

In dividing mode, all analysed valves operate stable (i.e. no oscillations observed). There are some differences with respect to accuracy, especially at lower flow rates (Figure 39). For mobile applications, it is desirable to have constant accuracy over entire flow range.

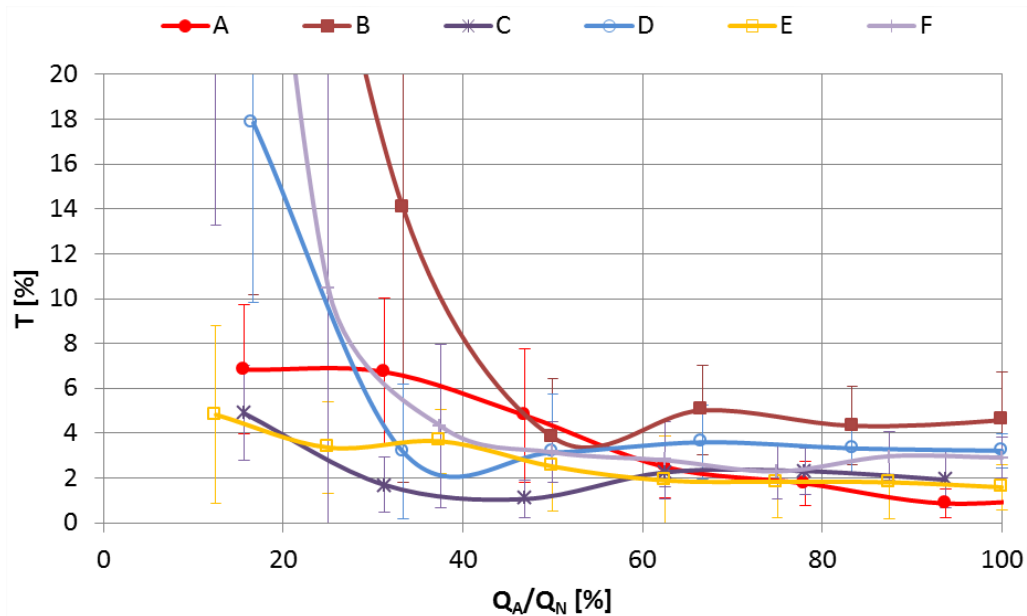


Figure 39: Accuracy in dividing mode

Figures for accuracy versus flow ratio (i.e. Figure 39 and Figure 40) depict averaged values for accuracy with additional (vertical) lines that represent the standard deviation.

Differences between analysed valves become even more obvious in combining mode. In this particular mode, the worst accuracy is observed in general and three out of five valves start to oscillate (Figure 40). Valves with detected instabilities (i.e. oscillations) are shown as dotted lines.

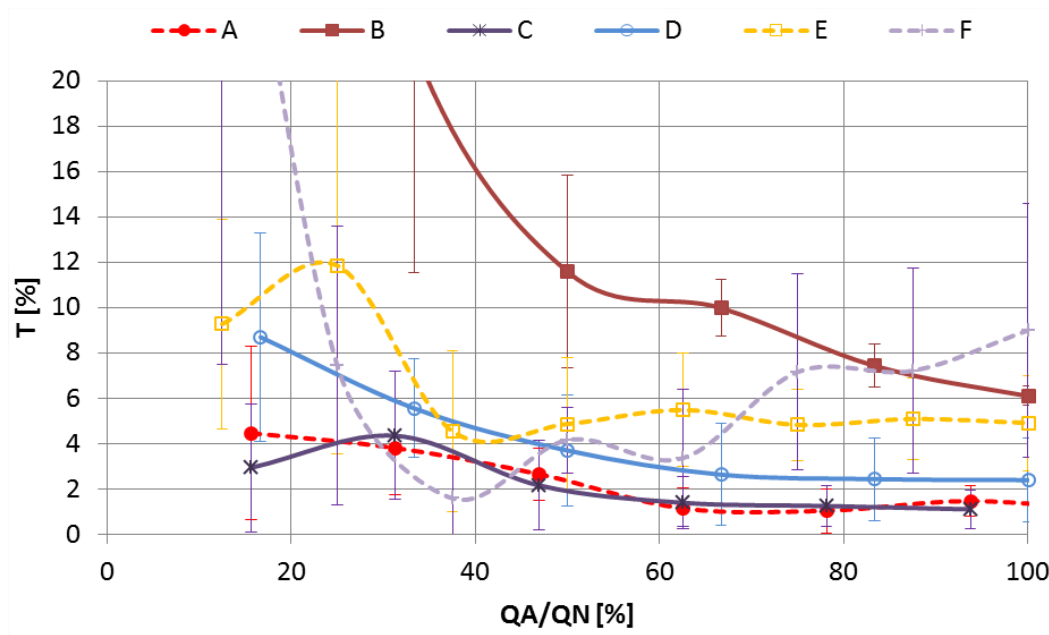


Figure 40: Accuracy in combining mode

3.2 Conclusions

Benchmark analysis shows that the combining mode is the most critical mode with respect to accuracy and also with respect to operation stability. In the beginning of benchmark analyses, there were some uncertainties on the Poclair Hydraulic measurement protocol. This is because oscillations occur at several “brand name” competitor products. Among others, the appropriateness of the experimental approach has been approved thanks to feedback from the market – some valves experience instabilities also on the field.

4 Development workflow

Many different design concepts of a flow divider basic function exist on the market. However, a basic operating principle for many of those concepts is the same as described in beginning of this paper (see chapter 0). For the Poclair Hydraulics new development procedure, the spool-in-spool type flow divider is taken into account, patented by Japanese inventor Masao Yoshino (see Figure 41). Patent protection already expired and, consequently, design is public available.

United States Patent

[11] **3,554,213**

[72] Inventor **Masao Yoshino**
 No. 26-8, 1-Chome, Numabukuro, Nakano-
 Ku, Tokyo, Japan
 [21] Appl. No. **815,632**
 [22] Filed **Apr. 14, 1969**
 [45] Patented **Jan. 12, 1971**

3,113,581 12/1963 Presnell..... 137/101
 3,347,254 10/1967 Compton et al. 137/101

Primary Examiner—William F. O’Dea
Assistant Examiner—David J. Zobkiw
Attorney—McGlew and Toren

[54] **FLOW CONTROL VALVE**
6 Claims, 6 Drawing Figs.

[52] U.S. Cl. **137/101,**
 137/111, 137/118

[51] Int. Cl. **G05d 11/00**

[50] Field of Search. 137/100,
 101

[56] **References Cited**
UNITED STATES PATENTS
 2,386,291 10/1945 Browne 137/101
 2,985,184 5/1961 Bowers et al. 137/101

ABSTRACT: A flow control valve is formed of valve body having a longitudinally extending bore containing a main spool axially, slidably positionable within the bore and arranged to be centered along its axis. A pair of slidable subsidiary spools is positioned within an axially extending passageway in the main spool with each of the spools being located on an opposite side of a transverse plane dividing the main spool in half. Each of the subsidiary spools has an axially extending passage which is divided by a partition into two chambers with a sharp-edged orifice in the partition affording communication between the two chambers. Openings through the valve body, the main and subsidiary spools afford fluid flow through the chambers in the subsidiary spools so that the fluid can be passed in either direction through the sharp-edged orifices in the partitions.

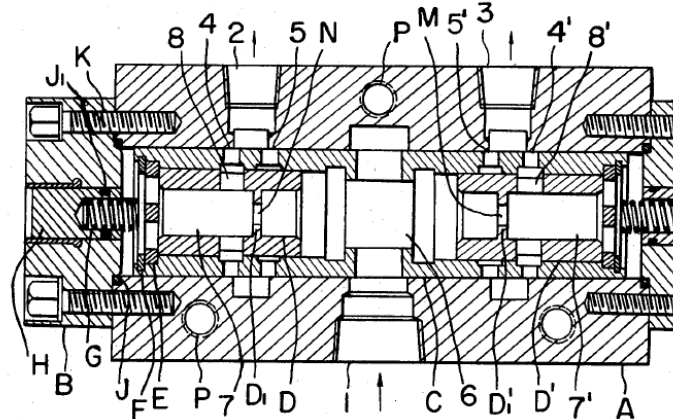


Figure 41: Extraction from the US patent [11]

4.1 Conceptions

Designs of flow dividers mostly use two spools in parallel, connected with a leg (named also tooth or rod, see Figure 33). Main benefit of spool-in-spool design is a single-piece outer spool and consequently no lateral forces due to spool connection. This has a beneficial consequence in a less friction force.

In order to additionally improve the valve performances, a tangential connecting hole between main hole and ports is used. According to experiences, this should reduce deformations of connecting hole due to tightening torque on fittings (see Figure 43).

Figure 42 depicts a cross section view of the first concept, made by the Poclairn Hydraulics development team.

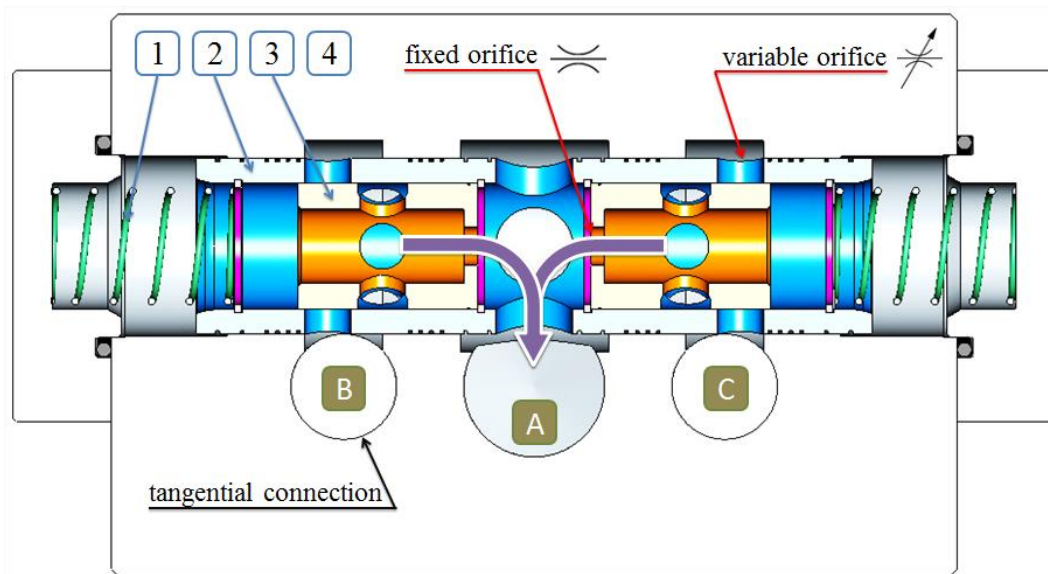


Figure 42: Cross section view of the first concept

The prototype has been made and tested. Although that all known past experiences on similar valves together with best practices and results of the benchmark analyses were taken into account, valve did not work as expected. In particular, accuracy in combining mode was out of expectation and acceptance criteria. In addition, oscillations in combining mode did not allow for valve to be functional.

4.2 Improved functionality

Additional design loops were necessary in order to improve most of weak points of the flow divider. Some of them are described and explained hereafter in order to emphasize the difficulty and expertise of the task.

The result of intensive development is a bunch of acquired knowledge on hydraulic components design, their interactions as well as on validation procedure of the end product.

4.2.1 Turbine effect

The visual inspection of outer spool after the first characteristic test shows scratches in circumferential direction on the outer spool external surface. One of the main contributors for such phenomena is angular rotation of the outer spool (i.e. rotation around spool axis). Applied tangential connection between main hole and external ports decrease deformations of valve housing. In the same time, a so-called turbine effect is obtained. Consequently, radial (i.e. centric) connection between main hole and external ports has been used. This situation is depicted on Figure 43.

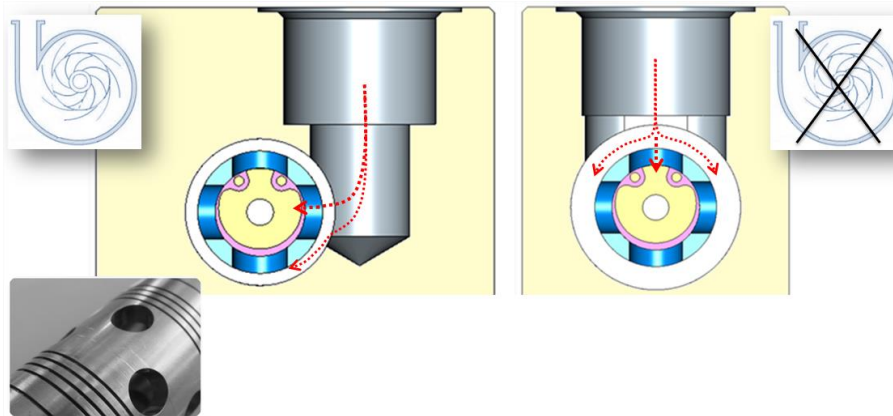


Figure 43: Different types of connections (radial and tangential)

4.2.2 Flow split disc

In combining mode, fluid flow from B and C side of the valve meet each other inside the outer spool (Figure 44). Collision of fluid flow from both sides influence the pressure upstream the fixed orifices and therefore directly impact the combining accuracy (oscillations appears). In order to avoid this phenomenon, a special flat barrier (called flow split disc) has been integrated in the middle of both inner spools. This solution partially solved the oscillations but makes valve noisier.

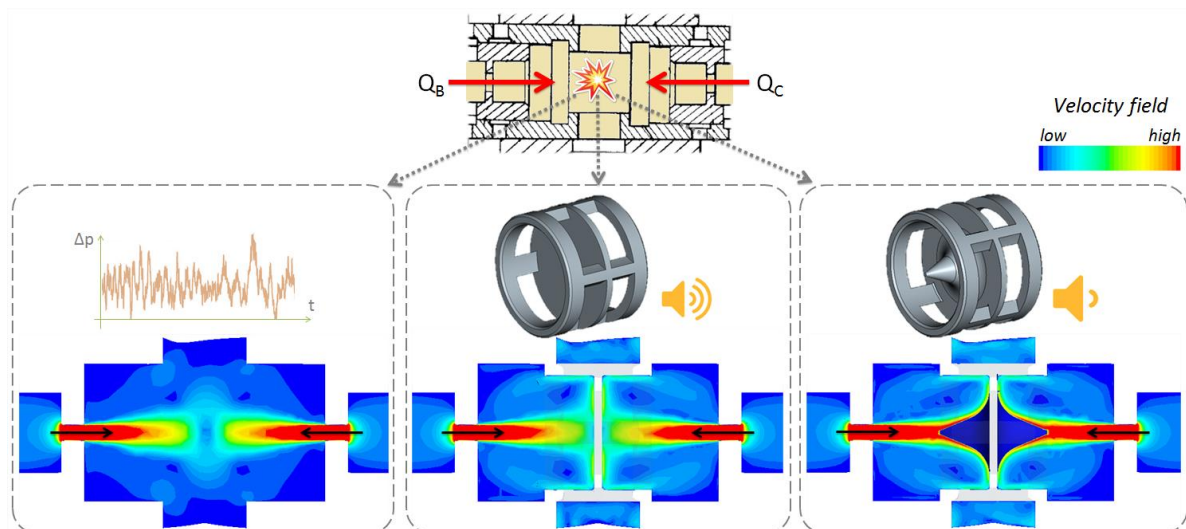


Figure 44: Installation of FSD between inner spools

In order to decrease the noise, a flat shape has been replaced by the special cone shape (proposed by LFT), which makes valve less noise.

4.2.3 Number of fixed orifices

In the first design concept, inner spool includes only a single (fixed) orifice with the appropriate diameter. Numerical simulations show that this design scenario locally produces higher (stagnation) pressure that directly affects required pressure to shift the outer spool. This phenomenon was also proved by the experimental investigation.

Then, the improved design scenario of inner spool includes multiple (fixed) orifices that give similar pressure loss as that from a single orifice configuration. This situation is depicted on Figure 45.

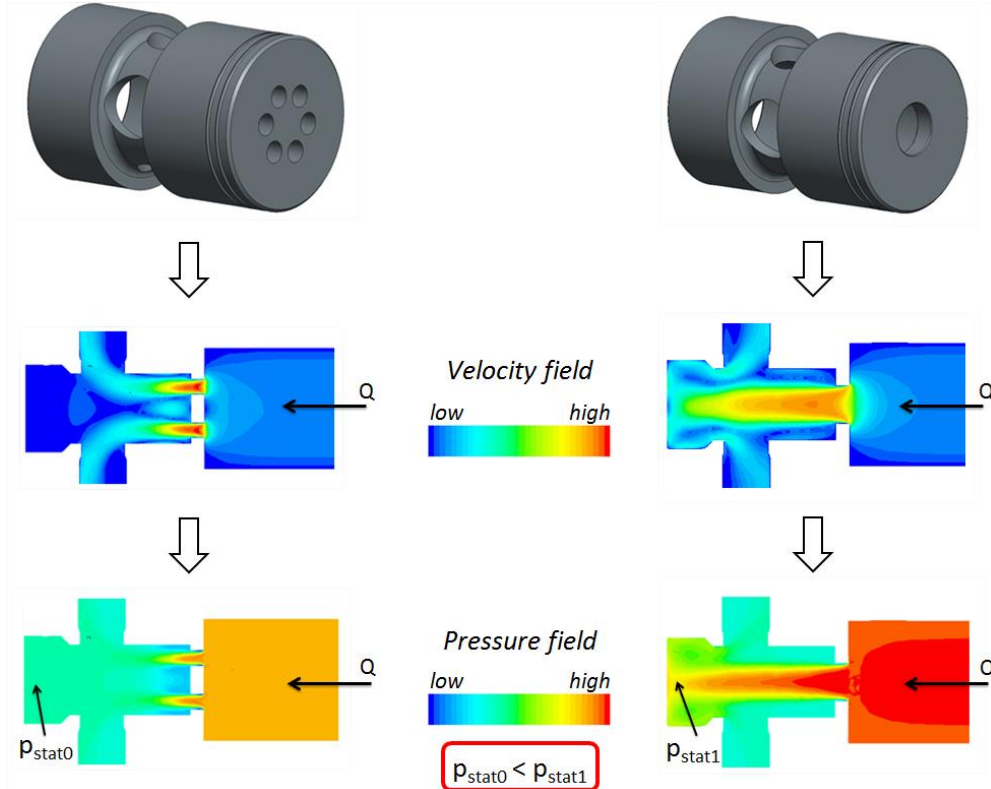


Figure 45: Effect of different number of orifices on pressure/velocity field

4.2.4 Milled grooves on outer spool

As explained previously, combining mode is the critical one with respect to accuracy and instabilities (i.e. oscillations). Deeper numerical investigation explains the source of instabilities. Flow force (also called jet force), which is a consequence of unequal static pressure distribution, causes outer spool to become unstable. These instabilities could be decreased if flow force is increased. The latter could be achieved if the flow angle is decreased (Figure 46).

The flow force on a valve is found by evaluating the momentum changes. This force tends to close the valve. For a steady state flow of a liquid, the flow force F_{jet} is evaluated according to the equation (3):

$$F_{jet} = 2 \cdot C_q \cdot A \cdot \Delta p \cdot \cos \alpha \quad (3)$$

where C_q , A , Δp and α refer to flow coefficient, orifice cross section area, pressure difference and flow angle, respectively.

According to the equation (3), the smaller the flow angle α the bigger the value of cosine and bigger the flow force.

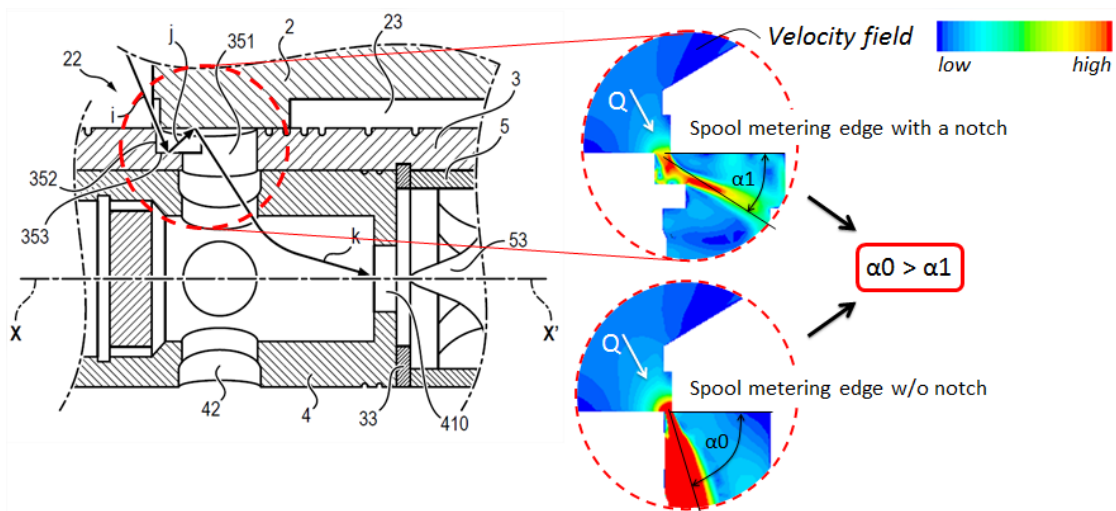


Figure 46: Variable orifice design scenarios

4.3 Conclusion

After several design iterations, numerical simulations (1D and 3D) and experimental investigations contribute to acceptable valve functionality. Valve instabilities are eliminated and a good accuracy in dividing and combining mode is achieved over a wide flow range. This has been approved also by the full characteristic test. In the very last step, valve durability has been checked by the endurance test.

4.3.1 Characteristic tests

- *Pressure losses*

A fundamental characteristic of any flow divider is the amount of pressure loss at given flow rate. Such a curve of FD-H2 main function is depicted on Figure 47. It can be clearly seen that pressure loss in dividing mode is much lower compare to pressure loss in combining mode. Therefore, flow direction has direct impact on energy losses of the component.

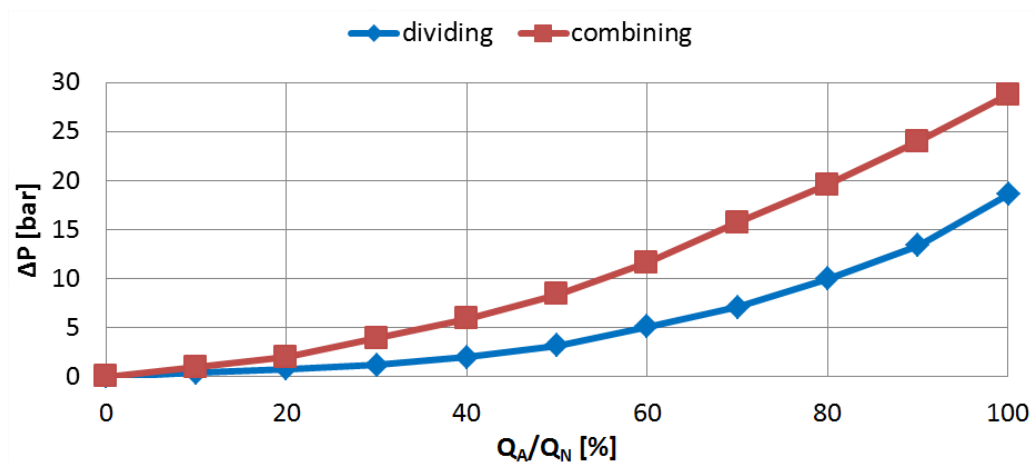


Figure 47: Pressure loss of the FD-H2 (dividing/combining)

- Accuracy

Average values of dividing accuracy are depicted on Figure 48. For the smaller flow rates, dividing accuracy $|T|$ is high and it is not recommended to operate in this area. However, for higher flow rates, dividing accuracy $|T|$ significantly decrease and gets stabilized at approx. 2 %. Dotted lines on figure below represent the standard deviation (s) of dividing accuracy. Note that average value refers to measurement of accuracy at several pressure differences.

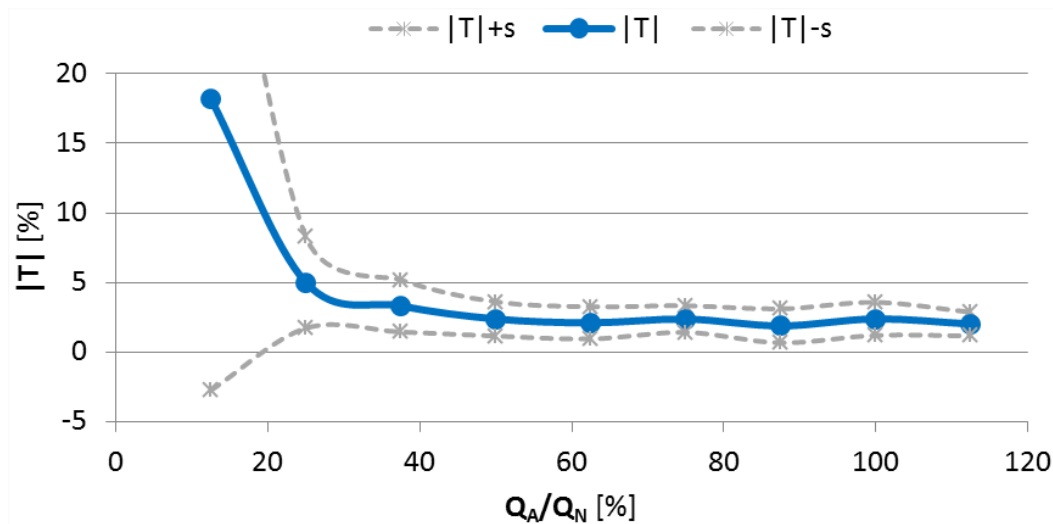


Figure 48: Average of absolute dividing accuracy

Figure 49 depicts average values of combining accuracy. At higher flow rates, combining accuracy $|T|$ gets stabilized at approx. 3 %.

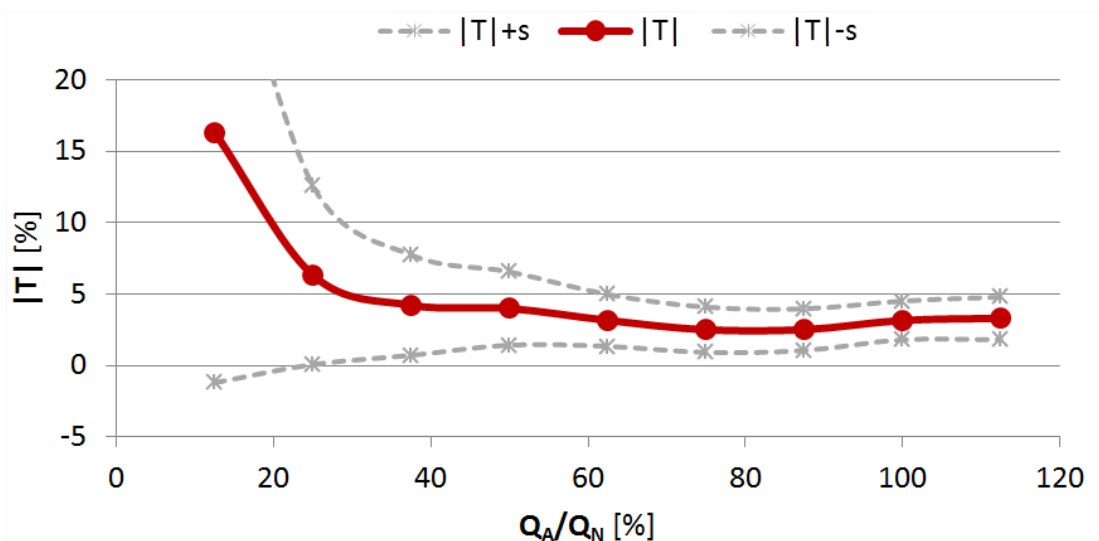


Figure 49: Average of absolute combining accuracy

All characteristic curves in this chapter are obtained on the product B25301A, FD-H2-2A20-E300-42B-313-000.

4.3.2 Intellectual property

It needs to be noted that complete design (including several design improvements) is already patented (Figure 50). The patent application is published under the publication number FR3032244 in France; EP3051147 in Europe and CN105840880 and US20160223091 in the USA.



(19) United States		
(12) Patent Application Publication		(10) Pub. No.: US 2016/0223091 A1
Peternel et al.		(43) Pub. Date: Aug. 4, 2016
<hr/>		
(54) FLOW CONTROL VALVE	(52) U.S. CL.	
(71) Applicant: Poclair Hydraulics Industrie, Verberie (FR)	CPC	<i>F16K 11/0716</i> (2013.01)
(72) Inventors: Luka Peternel, Ziri (SI); Matej Erznovnik, Ziri (SI); Franc Majdic, Moravce (SI); Alen Ljoki, Semce (SI)	(57) ABSTRACT	
(73) Assignee: Poclair Hydraulics Industrie, Verberie (FR)	The invention relates to a flow control valve adapted for use as a flow-dividing and flow-combining valve in hydraulic devices, comprising: a valve body having a first longitudinally extending bore, an outer spool slidably positioned within the bore, the outer spool having an axially extending passageway, a pair of axially extending inner spools slidably positioned within the passageway, the valve body having a first port and a pair of second ports, the outer spool having at least a first opening communicating with the first port and with the passageway, and at least two pairs of second openings therethrough. At least one second opening of each pair is of non-constant longitudinal section narrowing from the outer face of the outer spool on at least a part of the thickness of the second opening, so that a lateral side of the second opening offers an obstacle where a part of the fluid flow entering the second opening crashes before entering the inner spool.	
(21) Appl. No.: 15/006,594		
(22) Filed: Jan. 26, 2016		
(30) Foreign Application Priority Data		
Jan. 29, 2015 (FR)	1550708	
Oct. 22, 2015 (FR)	1560112	
Publication Classification		
(51) Int. Cl.		
<i>F16K 11/07</i>	(2006.01)	

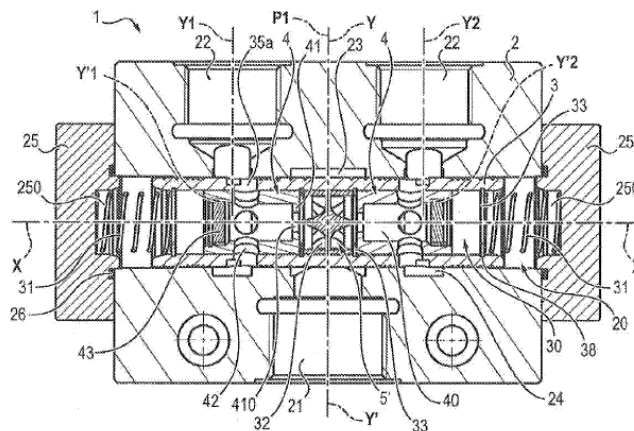


Figure 50: Extraction from the US patent [12]

4.3.3 Simulation models

The new heavy-duty flow divider has been extensively evaluated also via numerical approach. This refers to the usage of several different numerical models, such as:

- fundamental linear finite element (FEM) model which allows for static characterization of mechanical response of numerous valve components,
- steady-state computational fluid dynamic (CFD) model that enables to evaluate pressure field at various boundary conditions and design scenarios,
- advanced 1D dynamic model (built in AMESim) for prediction of valve fundamental characteristics (e.g. Δp -Q), evaluation of valve temporal characteristics (e.g. transient and stabilization zones) and for evaluation of component interactions.

The important output of numerical investigations is 1D dynamic model for valve design exploration (Figure 51). It allows for quick and accurate evaluation of different design scenarios (i.e. variation of input parameters). In addition, functional model of a flow divider is also used on a system level in order to assure more predictable and accurate functionality of a complete virtual machine.

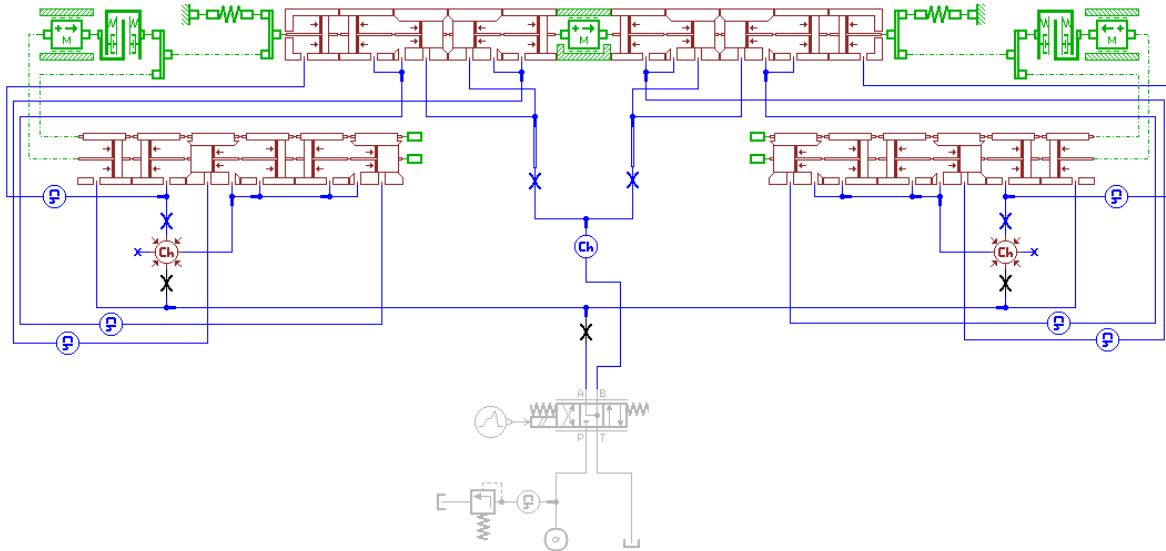


Figure 51: 1D numerical model for design exploration and validation

5 Multi-purpose functionality of the new flow divider

The basic functionality of a flow divider is presented on Figure 28 and Figure 29 above. In such cases, entire inlet flow needs to pass the valve even that flow divider basic function (i.e. flow repartition) is currently not required (e.g. all wheels have the same traction, loads on hydraulic cylinders are of the same magnitude etc.). Consequently, additional pressure loss appears as it would be in the case, if flow could pass a flow divider. Thus, additional energy is needed which make the system less efficient.

For that sake, flow divider main function has been upgraded in order to minimize the energy losses and extend valve functionality. It is a compact integrated „all in one” design. The important improvement refers to the integrated by-pass valve (pos. 4 on Figure 53) which allows for flow to pass the flow divider when its main function is not required. This function is activated by the driver, manually. In addition, several auxiliary functions are also available, if needed (pos. 5 on Figure 53).



Figure 52: Flow divider FD-H2: no auxiliaries (left) and with auxiliaries (right) [9]

Hydraulic schema of the new FD-H2 without auxiliaries is depicted on Figure 53. It can be seen that there are several other components beside the core one – flow divider on pos. 3.

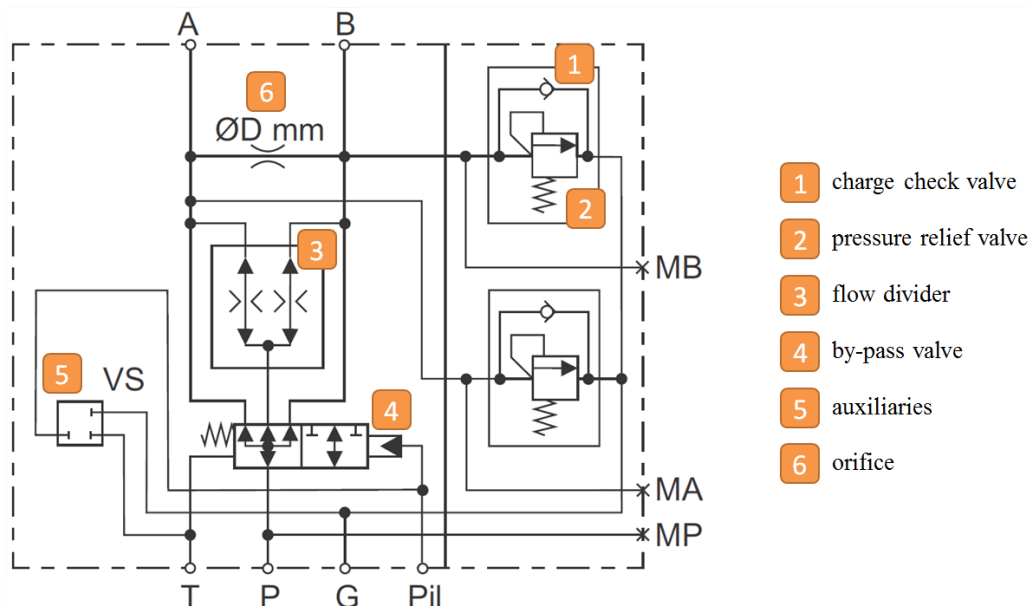


Figure 53: Hydraulic schema of the new FD-H2 (no auxiliaries) [9]

Check valves (pos. 1) are needed in order to feed the lines A and B with charge pressure (usually to avoid cavitation on motor side). Pressure relief valves (pos. 2) are used to protect high pressure lines (A and B) against overpressure. Then, flow divider (pos. 3) assures prescribed flow repartition on A and B lines, respectively. By-pass valve (pos. 4) allows for flow to pass the flow divider. A single or several auxiliaries (pos. 5) could be added in order to extend the valve functionality (e.g. feeding other lines, such as motors 1C/2C spool, motor brake deactivation, etc.). Fixed orifice (pos. 6) is needed in order to compensate flow rates during steering manoeuvre.

5.1 Catalogue product

Basically, there are two types of the new flow divider: medium duty (FD-MX) and heavy duty (FD-HX) valve where X refers to the number of outlet ports. Medium duty is designed for maximal pressure of 420 bar and flow rates up to 150 l/min. Heavy duty refers to maximal pressure up to 500 bar and flow rates up to 300 l/min. Modularity of each type of flow divider allows for wide range of product portfolio. In that manner, there are several different possibilities.

5.1.1 Electric by-pass

Different possibilities with electric by-pass are depicted on Figure 54: with and without auxiliaries, with and without pressure relief valves.

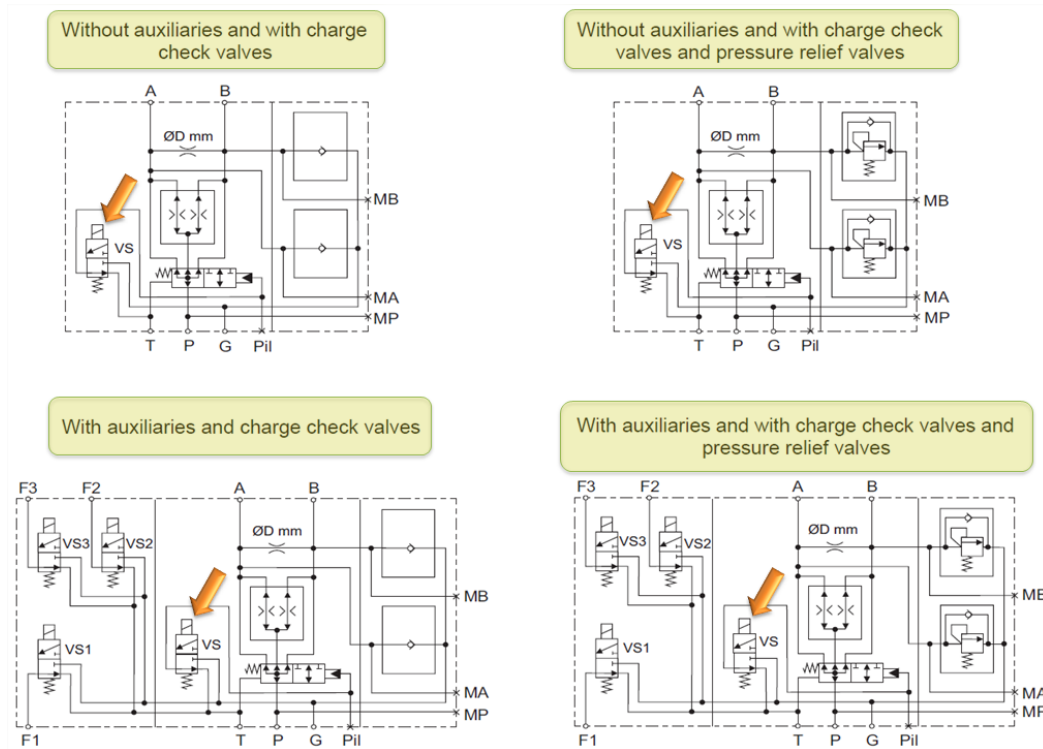


Figure 54: Different possibilities with electric by-pass [1]

5.1.2 Hydraulic by-pass

Figure 55 shows different possibilities with hydraulic by-pass. The main difference here compare to electric by-pass is that by-pass valve is activated hydraulically → pilot port (Pil) is not plugged but rather connect to external supply.

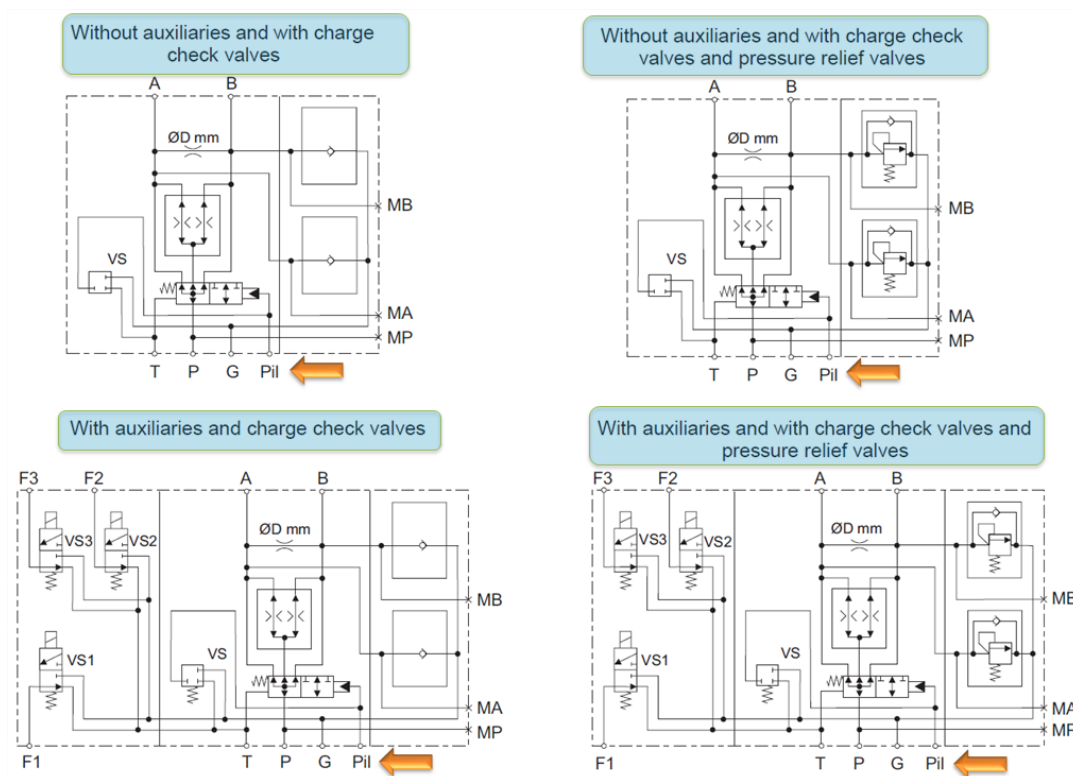


Figure 55: Different possibilities with hydraulic by-pass [1]

5.2 Mobile applications

The target markets for multifunction flow divider depend on their requirements. However, flow divider is mainly used for mobile applications. Medium duty flow divider is used for tool carriers, combi rollers/harvesters (e.g. fruits, apples, blueberry), rice field sprayer, small loaders, boat carrier, compactors, airport equipment, lift platforms, rock slingers, cold milling machines, forestry trailers (Figure 56).

Heavy duty flow divider could be used on the same fields, but is essentially recommended on every mobile application where pressure exceeds 420 bar and flow rates exceed 150 l/min. This situation is typically for agriculture (Figure 57) and road machinery platforms (Figure 58).



Figure 56: Platform market for FD-H2: forestry trailer [5]



Figure 57: Platform market for FD-H2: agriculture [5]



Figure 58: Platform market for FD-H2: road machinery [5]

References

- [1] Poclain Hydraulics: Flow control valves; Hydraulic components: 2017
- [2] Merrit, H. E.: Hydraulic control system, John Wiley and Sons, New York, 1967.
- [3] AMEHelp, rev. 15 SL1
- [4] Peternel L.: Hydraulic flow divider/combiner optimisation, diploma thesis, Ljubljana, 2012
- [5] Poclain Hydraulics training centre (various internal literature)
- [6] <http://www.hydraulicspneumatics.com/other-technologies/book-2-chapter-11-flow-divider-circuits>; last visited on 27.7.2017
- [7] http://www.sunhydraulics.com/sites/default/files/media_library/tech_resources/TT_US_FlowDivider-New.pdf; last visited on 26.7.2017
- [8] http://www.eaton.com/ecm/groups/public/@pub/@eaton/@hyd/documents/content/pct_273379.pdf; last visited on 27.7.2017
- [9] <http://www.poclain-hydraulics.com/en/products/valves/flow-divider>; last visited on 1.8.2017
- [10] <http://www.poclain-hydraulics.com/en/high-performance>; last visited on 27.7.2017
- [11] <https://www.google.com/patents/US3554213>; last visited on 17.7.2017
- [12] <https://www.google.com/patents/US20160223091>; last visited on 17.7.2017

Influence of the Hydrodynamic Bearing on the Flow Characteristics of a Dynamically Operated Displacement Meter

OTHMAR BERNHARD & JÖRG EDLER

Abstract In a time in which efficiency enhancement has become such a major issue in the development of internal combustion engines, it is critical to be able to rely on precise consumption measurement. To do so, it is essential to be capable of both identifying and assigning systematic errors occurring in a consumption measurement chain.

This paper specifically analyses the change in the volume delivered by a dynamically operated displacement meter due to position-change processes in the gear wheels. These dislocation processes are examined using an eddy current sensor based on the dislocation of the ring gear, which, at the same time, assumes the function of a hydrodynamic bearing.

The objective is to map how the current gear-wheel position is linked to the delivered volume and, ultimately, to develop a model that, based on the characteristic parameters, confirms the measured results.

Keywords: • hydrodynamic bearing • flow measuring method • flow sensor • flow characteristic • analysis of results •

CORRESPONDENCE ADDRESS: Othmar Bernhard, Graz University of Technology, Kopernikusgasse 24, 8010 Graz, Austria, e-mail: othmar.bernhard@student.tugraz.at. Jörg Edler, Dr.techn., Assistant Professor, Graz University of Technology, Kopernikusgasse 24, 8010 Graz, Austria, e-mail: joerg.edler@tugraz.at.

<https://doi.org/978-961-286-086-8.23>

ISBN 978-961-286-086-8

© 2017 University of Maribor Press

Available at: <http://press.um.si>.

1 Introduction

1.1 Problem Statement

Hydrodynamic bearings have been used successfully for a very long time in a broad variety of fields. One specific area of application results from their use in a volumetric flow meter based on a displacement meter. Due to the extensive measurement range, its operation covers a high speed range. Since the lower speed range is not traversed quickly as with normal applications but represents an operating mode instead, the design poses additional challenges.

1.2 Aim of the Paper

The aim of this paper is to develop a method for describing positional changes which occur in the real-life operation of hydrodynamic bearings. It additionally seeks to describe and assign characteristic influencing factors. It should be possible to present a detailed description of the state of the hydrodynamic bearing across all areas of tribology. Finally, the paper seeks to make some statements about stability in the individual operating points. Furthermore, conclusions are to be drawn on the link between changes in speed and the gear pump's delivery characteristics.

1.3 State of the Art

Hydrodynamic bearings (fluid dynamic bearings) in all their forms as parts of machinery, as well as related disciplines such as tribology, have already been the subject of extensive investigation. Prominent research in this field was conducted by Arnold Sommerfeld and Ludwig Gümbel. Hydrodynamic fluid bearings and their shifting processes were already the focus of publications by Adolf Fränkel based on work by Gümbel et al [1]. To date, the author has no knowledge of papers dealing with the correlation between the delivery characteristics of a flow meter and positional displacement.

2 Basic Principles

2.1 Volumetric Flow Meters

Displacement meters are based on the principle of volumetric displacement by means of rotating wheels or spindles. The wheel geometry determines the individual volumes and the way in which the individual volumes are sealed from each other. Total displacement per revolution, V , results from the summation of the individual volumes ΔV .

$$V = \sum_{i=1}^N V_i \quad (1)$$

Displacement meters are operated either actively or passively.

PLU flow sensors are volumetric flow meters for liquid media that operate on a servo-controlled gear counter basis. Due to the fast response time and the low system interference, this type of displacement meter is preferably used for dynamic consumption measurement. The flow meter device AVL PLUtron – based on an actively driven displacement meter designed as an internal gear pump – is used for the following examinations, see Figure 1.



Figure 1: AVL PLUtron Classic Flow Meter

The PLU principle, named after Pierburg und Luftfahrtgeräteunion (PLU), combines a servo-controlled gear counter with a dynamic piston sensor. A gear counter driven by a servo motor with encoder defines a geometric volume to pulse frequency ratio at an adjusted speed. A bypass ensures zero pressure difference ($\Delta p = 0$) between inlet and outlet, preventing leakage flow. Any flow changes immediately displace a zero-friction piston in either direction.

A piston position sensor and a servo controller provide a fast control loop, keeping the piston centred.

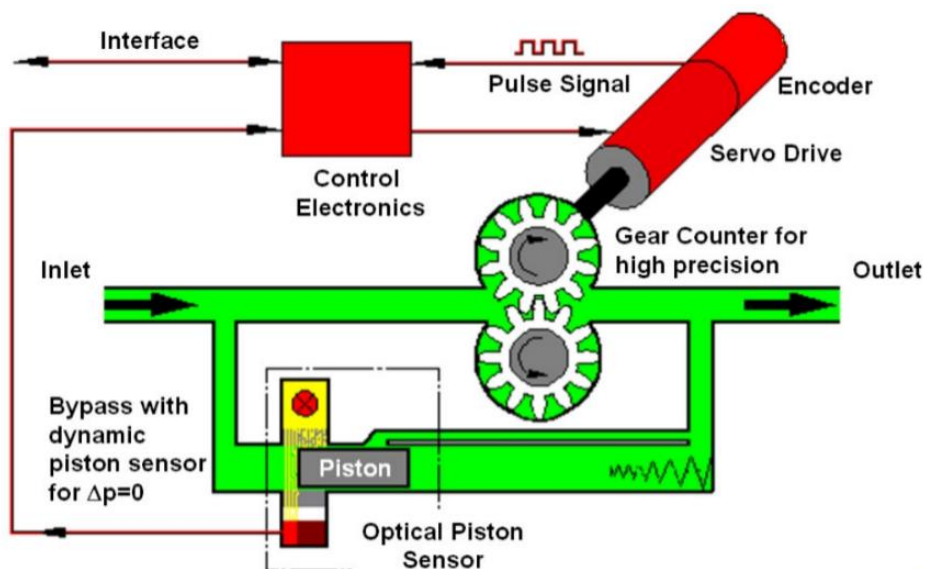


Figure 59: PLU principle servo-controlled displacement meter

3 Preparations

This paper is based on the characterization of gap geometries in a flow sensor, which was already the subject of an analysis as part of a bachelor project. By means of a differential flow measurement, a leakage flow was applied to the gap of a gear pump operated at steady state and from the produced leakage it is possible to draw conclusions about the gap geometries. Changes made to the parameters allow you to separate and allocate leakages proportionately. Alterations made to the tooth flank leakage in particular allow making statements about how the two gear-wheels' position to each other changes. As these investigations are restricted to a low speed range, the intention is to map a position characterization across the entire speed range.

4 Measuring Methods

4.1 Position Sensors

Position measurements are based on the principle of eddy current formation. Eddy current sensors belong to a sub-category of inductive displacement transducers. Any changes in the distance between an eddy current sensor and the device under test, which requires electrical conductivity, manifest themselves in changes in the level of impedance. Alternating current flowing through a coil produces a primary alternating magnetic field, which, following the law of induction generates eddy currents in the device under test.

The principle works both with ferromagnetic and non-ferromagnetic devices under test. Compared to conventional inductive displacement transducers, eddy current sensors have a higher resolution coupled with high dynamics. Another reason for choosing this type of sensor was its dirt resistance and the low impact of external magnetic fields. [2]

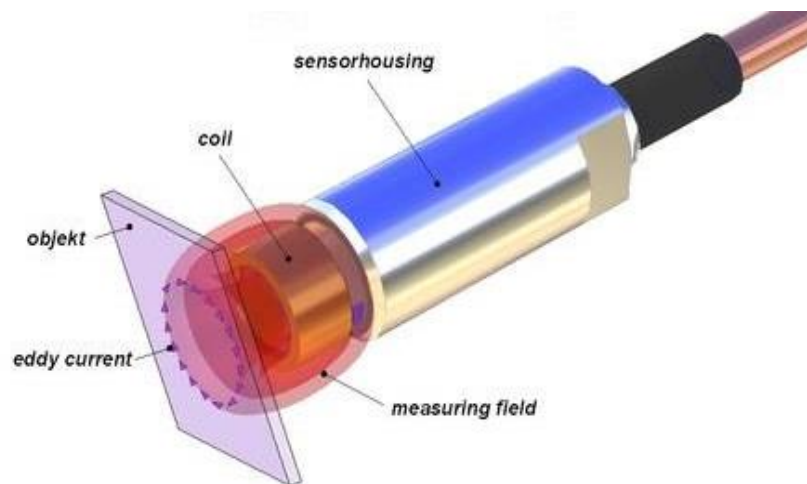


Figure 60: Eddy current principle

Figure 61 shows a schematic diagram of the position measurement test setup. The three eddy current sensors are arranged at an angle of 120° to each other in order to describe the position of the ring gear on a plane.

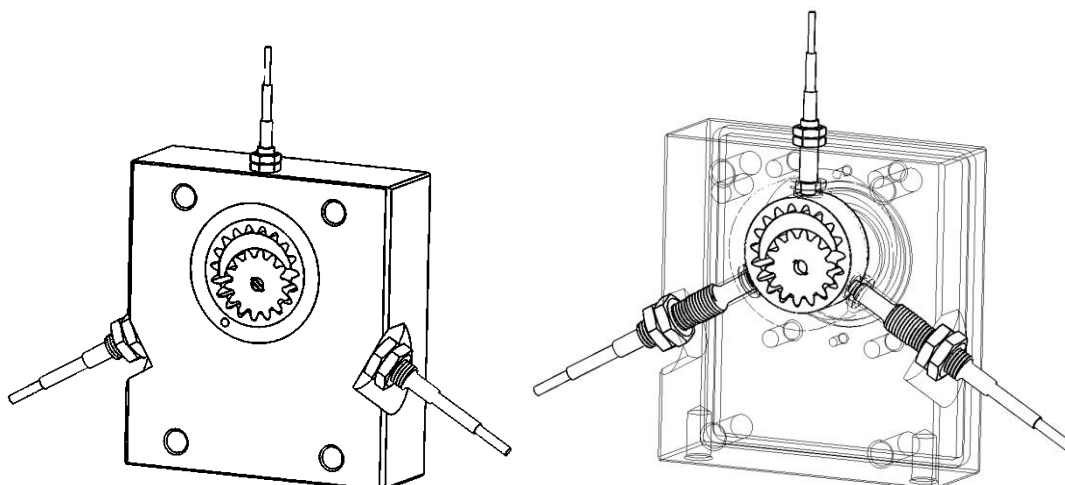


Figure 61: Schematic figure of measurement setup

4.2 Evaluation

In order to generate meaningful data from the three eddy current sensors' raw signals, angle-based data are created with the help of the data acquisition system AVL IndiModul and the post-processing tool AVL Concerto by means of a mathematical model. These data are then filtered using a low pass filter and a cut-off frequency of 200 Hz.

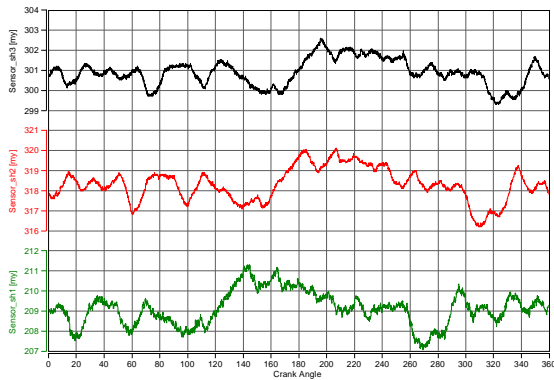


Figure 62: Eddy current sensor signals, unfiltered

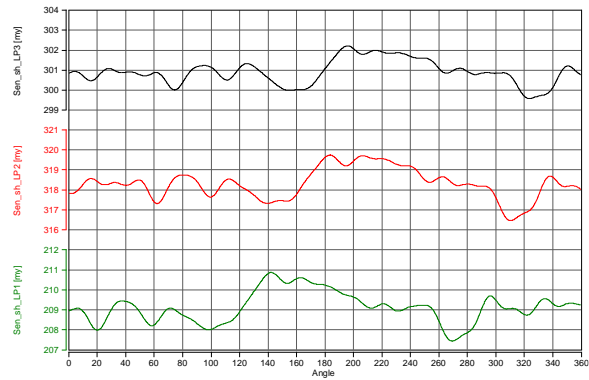


Figure 63: Eddy current sensor signals, filtered at 200 Hz cut-off frequency

After that, the conversion to the center point of the ring gear was calculated, assuming an ideal geometrical model. In Figure 64 you can see the trajectory of the ring gear's center point during one gear revolution. Figure 65 shows the same ring gear center point trajectory in relation to the hydrodynamic bearing bushing center point. The circle represents the maximum deflection of the ring gear center point in relation to the bushing center point.

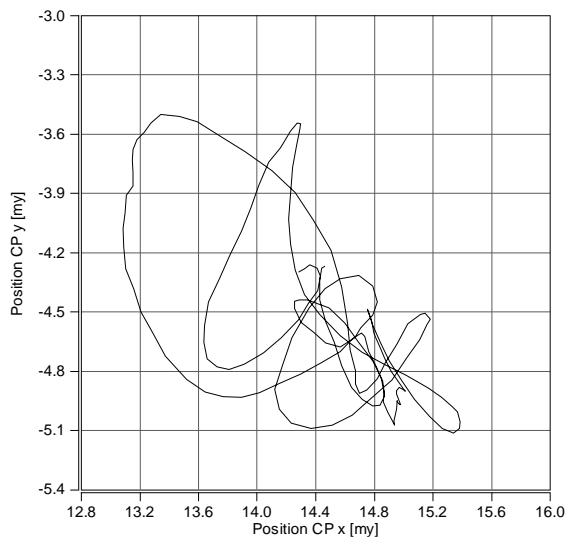


Figure 64: Trajectory center point

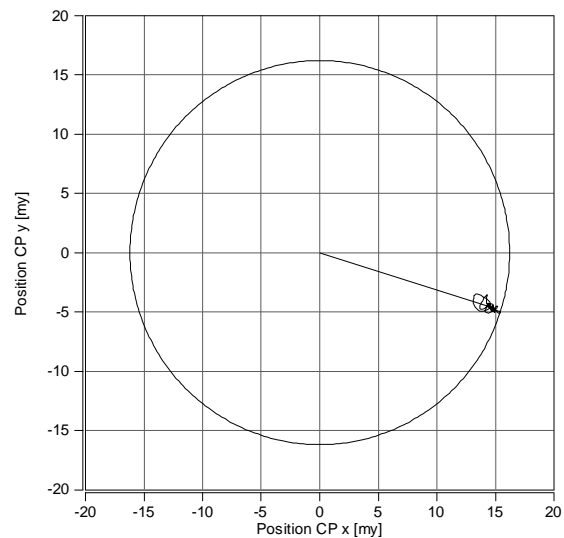


Figure 65: Trajectory in relation to bushing

5 Current Results

The following measurements conducted so far are limited to an examination of the speed impact. Figure 66 shows the ring gear center point's trajectory in relation to the bushing during one revolution (360°) of the ring gear. In this measurement, a speed of 1000rpm was chosen and kept constant. Figure 67 shows the distribution of the mean trajectory center point over 200 revolutions.

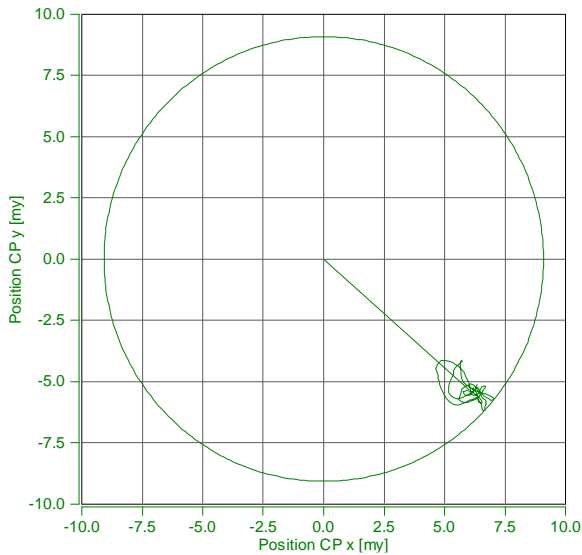


Figure 66: Dislocation of center point
80 rpm

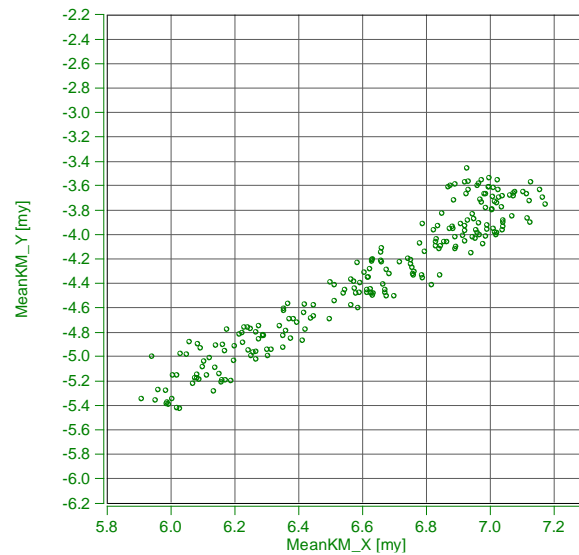


Figure 67: Distribution of center point
80 rpm

If you compare Figure 66, conducted at 80 rpm, and Figure 68, conducted at 1000 rpm, it becomes evident that although the distance from the center of the bushing becomes wider with an increasing speed, the trajectory within one revolution decreases.

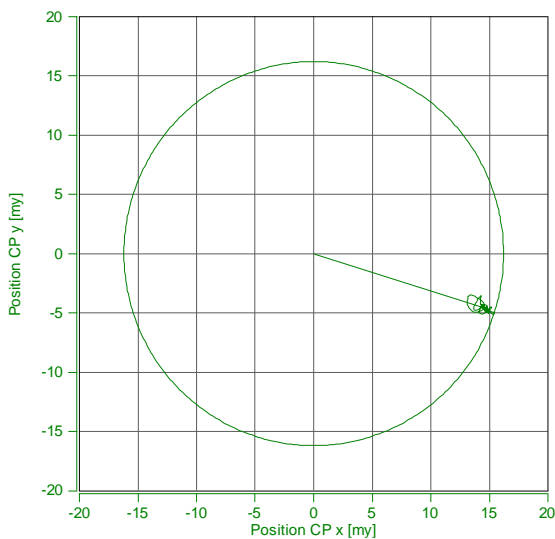


Figure 68: Dislocation of center point
1000 rpm

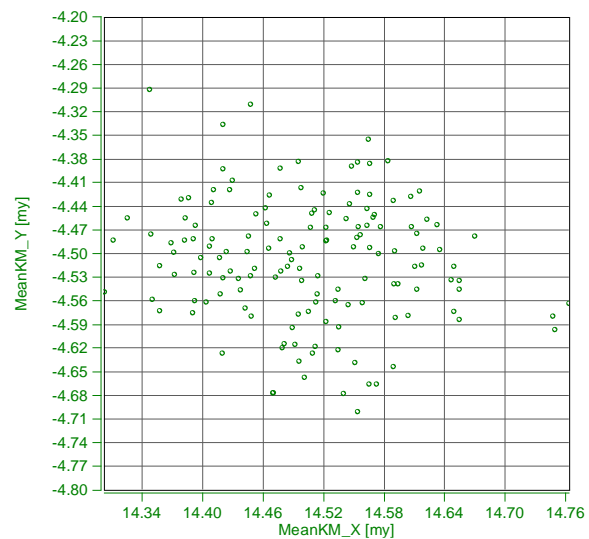


Figure 69: Distribution of center point
1000 rpm

Figure 70 and Figure 71 show the trajectory difference when measured at 80rpm and at 1000 rpm. A direct comparison results in a similar trajectory. In subsequent measurements, it is necessary to ascertain whether differences in the tooth geometry and resulting tooth force fluctuations are decisive factors for this pronounced trajectory.

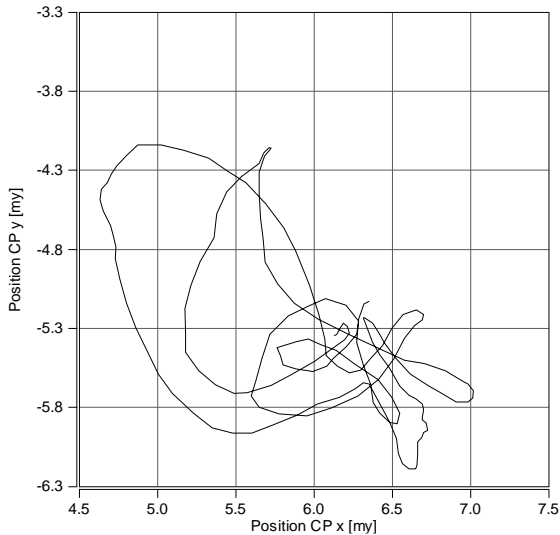


Figure 70: Trajectory center point 80 rpm

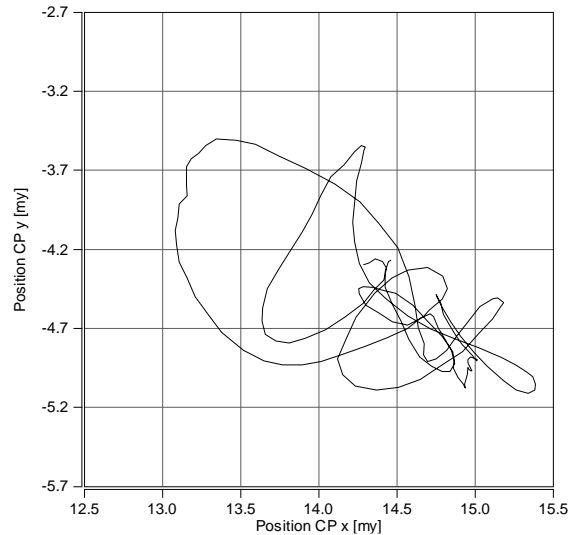


Figure 71: Trajectory center point 1000 rpm

Passing through a speed range from standstill to a maximum speed of 2800rpm produces a displacement curve that clearly reveals two characteristic positional changes. Large positional changes are achieved in the lower speed range before the position starts to stabilize. Another transition point can be found in a higher speed range - see Figure 72.

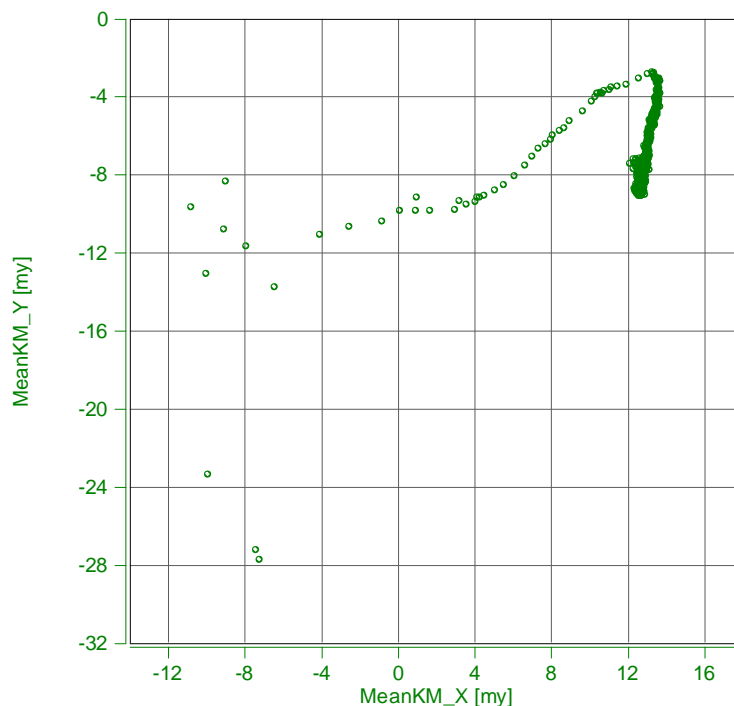


Figure 72: Distribution of center point 1600 revolutions

Before any sound statements can be made on the behaviour of the hydrodynamic bearing in these ranges, further measurements will be necessary in the speed ranges where these pronounced positional changes are found.

6 Outlook

Further questions that arise concern the main factors for displacement characteristics as well as the correlation between the speed and the delivery characteristics.

Another need is to establish clarity about whether the significant changes in position are attributable to transitional friction states (as described by Stribeck).

References

- [1] Fränkel, A.: Berechnung von zylindrischen Gleitlagern, Dissertation an der ETH Zürich, 1944
- [2] Tränkler, H. R., Reindl, L. M.: Sensortechnik Handbuch für Praxis und Wissenschaft, Berlin Heidelberg: Springer Vieweg, 2014

Testing based analysis of the gerotor orbital hydraulic motor

ERVIN STRMČNIK & FRANC MAJDIČ

Abstract In this study, the efficiency characteristics of hydraulic gerotor motor was investigated. A gerotor with the floating outer ring is a low speed high torque hydraulic motor.

The main purpose of this paper was to analyse the influence of the size of the holes in the valve plate on the total efficiency of the gerotor. The total efficiency is the most important and prominent information about an energy conversion of hydraulic components such as hydraulic motors and pumps.

The operation of gerotor is briefly described as well as some equations for the efficiency determination. Within the used methodology, a measurement procedure is presented in detail. A test rig with hydraulic components and sensors was introduced. A very high total efficiency was obtained with the hole size of $\Phi 6,3$ mm - the total efficiency was on average 5 % higher in comparison to the initial hole size of $\Phi 5,5$ mm.

Keywords: • hydraulic motor • gerotor principle • design details • testing • efficiency • analysis •

CORRESPONDENCE ADDRESS: Ervin Strmčnik, MS, University of Ljubljana, Faculty of Mechanical Engineering, Aškerčeva cesta 6, 1000 Ljubljana, Slovenia, e-mail: ervin.strmcnik@fs.uni-lj.si. Franc Majdič, Ph.D., Assistant Professor, Aškerčeva cesta 6, 1000 Ljubljana, Slovenia, e-mail: franc.majdic@fs.uni-lj.si.

1 Introduction

In this paper, the results of the measurement of low speed high torque orbital hydraulic motor are presented. The rapid development of the hydraulic components in the last few years has contributed many novelties, innovations and improvements in hydraulics. One of the groups of hydraulic component is hydraulic motor group. Hydraulic motors convert hydraulic energy into the mechanical energy. The most crucial measure of performance of the hydraulic motor is the total efficiency. There are many factors which influence the hydraulic motor performance. They are related to hydraulic, tribological, material and other challenges. The performance of the hydraulic motor depends on the construction parameters as well. A gear pair has the largest influence on performance, whereas other parameters are also very important. We investigated the influence of the size of the holes in the valve plate. The holes are important for inlet and outlet flow of the fluid. Fluid takes care of the relative movement of the gear pair and lubrication of the main parts of the hydraulic motor. Within research we found out that the diameter of the holes in the valve plate influences hydraulic motor performance significantly. With the right choice of hole diameter, we can raise the total efficiency on average around 5 %. The paper is structured as follows. In the introduction is described an objective and the purpose of the research. Section 2 presents the theoretical framework of the conducted research. Hydraulic gerotor motor was described as well as procedure for the determination of the volumetric, mechanical-hydraulic and total efficiency. Furthermore, the calculation of the gerotor's derived displacement volume is proposed according to the international standard ISO 8426. Methodology is described in section 3. A test rig of the experiment is shown in section 4. The Results are presented in section 5 and conclusions are summarized in section 6. In the last two sections, there is a list of references and a nomenclature explanation.

1.1 Literature review

There are many factors which influence the performance of the gerotor. The viscosity, viscosity index, high-shear viscosity, piezoviscosity and shear stability of prototype fluids have been characterized in the research of fluid properties influence on the total efficiency of low-speed high torque hydraulic motors [1]. In literature, there exists very little scientific papers which deal with hydraulic gerotor motor with the floating outer ring. Usually the classical orbital hydraulic motor with inner rotor and gerotor's housing are analysed. In the past few decades, many designs have been disclosed in relative patents, but many of them were not feasible for actual motor production. A kind of deep analysis of multiple performance attributes and structural design of the gerotor motor has been extensively investigated through multi-objective optimization design of the gerotor motor [2]. Pressure distribution within gerotor and some other physical quantities were analysed through a CFD model for orbital gerotor motor [3].

A CFD analysis helps us to understand the physics of gerotor's operation and enable us a rapid development of new hydraulic motors [4]. The total efficiency is very much related to losses. Experimental and torque losses in gerotor were investigated in case of hydrostatic machines which represent complex fluid dynamic systems due to intricate and partially unknown dynamics [5]. Some losses are related to tribological behaviour. The most important are friction [6] and wear [7], [8]. Regarding rotational speed, there are two types of hydraulic motors. A low speed hydraulic motor doesn't exceed the rotational speed of 250 min^{-1} . On the other hand, a high speed hydraulic motor reaches rotational speed higher than 250 min^{-1} . A difference between the above mentioned group is shown in the Figure 73 [9]. The low speed hydraulic motors achieve a higher total efficiency when they rotate relatively slowly (Figure 73, line 1). The total efficiency of the high speed hydraulic motor increases in case of the rising rotational speed (Figure 73, line 2).

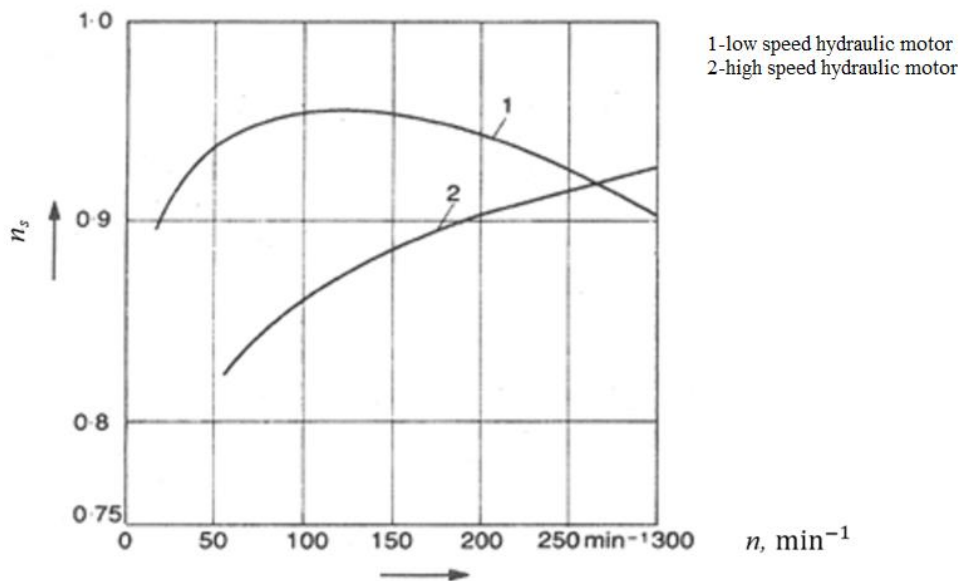


Figure 73: The total efficiency of low and high speed hydraulic motor

Nowadays, there are many different types of hydraulic motors. Gear, vane, axial piston and radial piston hydraulic motor. Geroller and gerotor are two special types of gear hydraulic motors. Our scientific paper deals with the gerotor, which has two special characteristics. It is a low speed hydraulic motor with high torque capability. In literature, it is often abbreviated as LSHT (“low speed high torque”). Other precedences and limitations are listed in Table 1.

Table 1: Precedence and limitations of the hydraulic gerotor motor

Precedences	Limitations
relatively simple construction compared to other types of hydraulic motors	friction
high torque	wear
low speed	low sealing ability of lobes between the inner rotor and outer ring
self-braking ability	low total efficiency
relatively small and light	
relatively cheap	

2 Hydraulic gerotor motor with the floating outer ring

The hydraulic gerotor motor with the floating outer ring, its design, and principle of operation are presented in this section. At the end of the section we will introduce the procedure of displacement volume and efficiency determination for such a type of hydraulic motor.

2.1 Design and principle of operation of the gerotor

Gerotor has a mass of around 20 kg. Its working pressure is up to 35 MPa. The hydraulic gerotor motor consists of thirty different parts. The maximum diameter is $\Phi 174$ mm, whereas the maximum dimension represents the length of the gerotor – it is 250 mm (Figure 74).

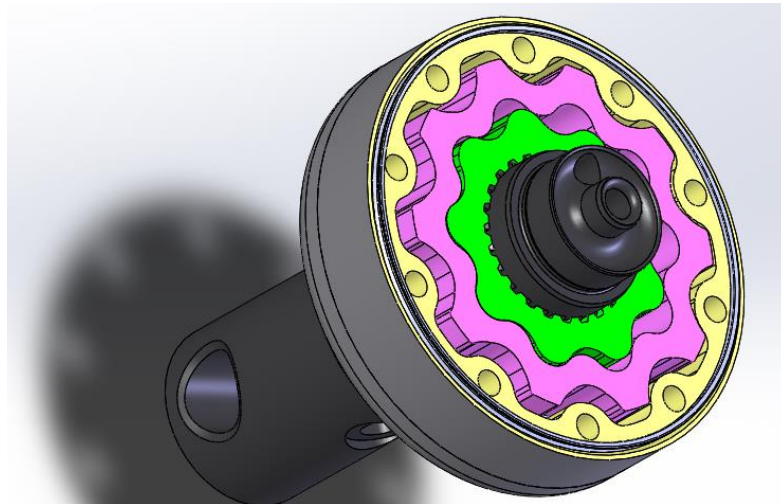


Figure 74: The hydraulic gerotor motor design ($\Phi 174 \text{ mm} \times 250 \text{ mm}$)

There are four very important parts according to the functionality of the gerotor. The most influential elements of the hydraulic motor regarding principle of operation are: 1-the inner rotor, 2-the outer ring, 3-the gerotor housing and 4-the valve plate (Figure 75).

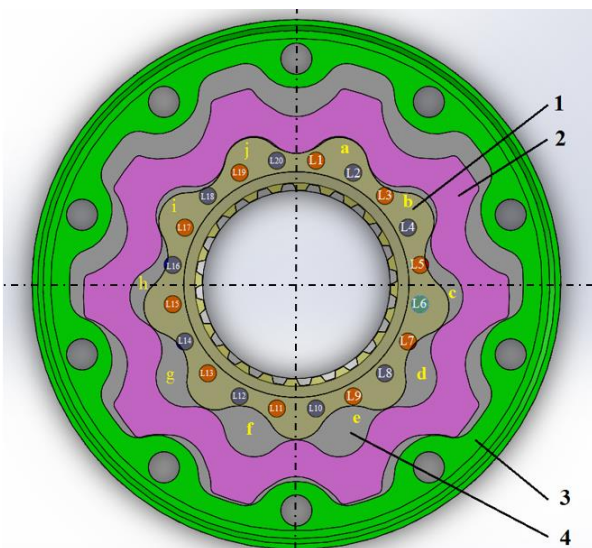


Figure 75: Four basic parts of the hydraulic motor ($\Phi 174 \text{ mm}$)

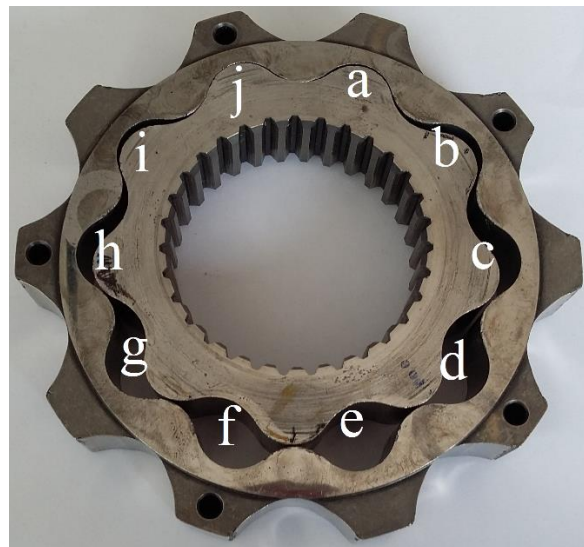


Figure 76: Lobes

The outer ring has 10 teeth, whereas the inner rotor has 9 teeth and. They together constitute 10 lobes, which are designated with the small letters on Figure 75 and Figure 76. On the figure 75 we can recognize twenty holes, which are part of valve plate. The first hole has the mark L1, and the last one L20. Odd numbers represent holes which are connected with the high pressure zone, and even numbers represent holes which are linked to the low pressure zone. As operators, we can change low and high pressure zone with the control valve. A main function of the gerotor housing is the limitation of motion of the outer ring.

2.2 Gerotor displacement volume (ISO 8426)

In theory, there are two kinds of displacement volumes. The first one is the theoretical VG and the second one is the derived displacement volume VI. The difference between them is that the derived displacement volume considers the real production tolerances. The estimated deviation between VG and VI was 2 to 3 % [10]. Gerotor displacement volume is very important information that

helps us to determine the volumetric and hydraulic-mechanical efficiency of the hydraulic motor. There exist three methods of determination of derived displacement volume [9]: a) Measurement of displacement volume with the two reservoirs; b) Toet-method; c) Method regarding ISO 8426. Due to international accepted standard, we decided to use the third method. The above mentioned standard ISO 8426 [11] proposes the measurement of volume flow rate with different pressure differences, whereas the speed of shaft of the hydraulic motor is the constant value. We have to determine the volume flow rate for $\Delta p = 0$. We can do this graphically either with the help of the method of least squares as it is shown in equation 1.

$$V_i = \left\{ \left(\frac{1}{k} \sum_{i=1}^k Q_i \right) - \left[\frac{\frac{1}{k} \sum_{i=1}^k (\Delta p_i Q_i) - \frac{1}{k^2} (\sum_{i=1}^k \Delta p_i) (\sum_{i=1}^k Q_i)}{\left(\frac{1}{k} \sum_{i=1}^k \Delta p_i^2 \right) - \left(\frac{1}{k} \sum_{i=1}^k \Delta p_i \right)^2} \right] \left(\frac{1}{k} \sum_{i=1}^k \Delta p_i \right) \right\} \frac{1}{n} \quad (1)$$

2.3 Gerotor efficiency

In reality, there are many kind of losses. Volumetric losses include external volumetric losses, internal volumetric losses, losses due to compressibility, losses due to incomplete filing. Hydraulic-mechanical losses represent viscosity friction, friction losses due to turbulent flows, due to pressure differences. The most important fact related to energy consumption of the hydraulic component is efficiency. It represents the ratio between the useful output to the total input, in energy terms. According to hydraulic gerotor motor there are three different types of efficiency:

- total efficiency,
- volumetric efficiency,
- hydraulic-mechanical efficiency.

It's not possible that any of these efficiencies would be greater than 100 % in real applications.

A conversion of hydraulic energy into mechanical energy is the main purpose of the hydraulic motor. Hydraulic energy (equation 2) is a function of volume flow rate and pressure difference, whereas mechanical energy (equation 3) depends on rotational speed and torque.

$$E_h = Q_1 \cdot (p_1 - p_2) \quad (2)$$

$$E_m = 2 \cdot \pi \cdot n \cdot M \quad (3)$$

The total efficiency of the hydraulic motor is ratio between input hydraulic energy and output mechanical energy as it is shown in equation 4.

$$\eta_t = \frac{2 \cdot \pi \cdot n \cdot M}{Q_1 \cdot (p_1 - p_2)} \quad (4)$$

If we would like to determine volumetric and hydraulic-mechanical efficiency, we have to have information about the derivate displacement volume of hydraulic motor. Volumetric efficiency of the hydraulic motor is a function of rotational speed, derivate displacement volume, and volumetric input flow rate into the hydraulic motor.

$$\eta_v = \frac{n \cdot V_i}{Q_1} \quad (5)$$

Hydraulic-mechanical efficiency of the hydraulic motor depends on effective torque, pressure difference and derivate displacement volume of the hydraulic motor.

$$\eta_{hm} = \frac{M \cdot 2\pi}{(p_1 - p_2) \cdot V_i} \quad (6)$$

3 Methodology

According to the previous research activities, we decided to observe hydraulic motor operation in eighteenth different measured points which are stated in the Table 2. We chose two different rotational speeds: 15 min⁻¹, 17 min⁻¹ and nine different pressure differences: 16 MPa, 17 MPa, 18 MPa, 19 MPa, 20 MPa, 21 MPa, 22 MPa, 23 MPa, 24 MPa. Within the wide set of the measurement activities we took into account recommendations and guidelines from different international standards, whereas we would like to emphasise the importance of the international standard ISO 8426 [11] as well as other standards which are related to different types of hydraulic motor efficiency. Our main purpose was to determine hydraulic motor displacement volume and total, volumetric, and hydraulic-mechanical efficiency of the investigated hydraulic motor

Table 2: List of eighteen selected measured points

#	Rotational speed n, min^{-1}	Pressure difference $\Delta p, \text{MPa}$	#	Rotational speed n, min^{-1}	Pressure difference $\Delta p, \text{MPa}$
1	15	16	10	17	16
2	15	17	11	17	17
3	15	18	12	17	18
4	15	19	13	17	19
5	15	20	14	17	20
6	15	21	15	17	21
7	15	22	16	17	22
8	15	23	17	17	23
9	15	24	18	17	24

The ambient temperature was 25 °C, whereas the fluid's temperature was 60 °C. One set of the measurements represents 18 measurements points with the one specific hole diameter in valve plate – for example, $\Phi 5,9$ mm. For the testing of one set of the measurements we spent around four hours. Two hours for the preparation and measuring installation, and additional two hours for determination of physical quantities, which are represented in equations for hydraulic motor efficiency. All measurements were accomplished in the laboratory for fluid power and controls at the Faculty of Mechanical Engineering, University of Ljubljana. The uncertainty analysis was done according to the international standard JCGM 100:2008-BIMP [12]. International standard ISO 8426 addresses three classes of measurement accuracy: A, B and C. In the Table 3 are permissible systematic measuring instruments errors for each class.

Table 3: Permissible systematic measuring instrument errors [11]

Parameter	Permissible systematic measuring instrument errors for each class of measurement accuracy		
	A	B	C
Rotational frequency (%)	± 0,5	± 1	± 2
Flow rate (%)	± 0,5	± 1,5	± 2,5
Pressure, MPa gauge where $p < 0,15$	± 0,001	± 0,003	± 0,005
Pressure, MPa gauge where $p \geq 0,15$	± 0,05	± 0,15	± 0,25
Test fluid temperature (°C)	± 0,5	± 1	± 2

Within measurement, we were able to ensure the following errors for desired physical quantities: Pressure difference: ± 0,05 MPa, Rotational speed: ± 0,1 min⁻¹, Fluid Temperature: ± 1 °C. The original diameter of holes in the valve plate was Φ5,5 mm (Figure 77). It was the first set of the measurements. Every additional set had 0,4 mm incremental increase in hole diameter. The maximal hole diameter was Φ7,1 mm (Figure 78).



Figure 77: The minimal hole size (Φ5,5 mm) in the valve plate (Φ174 mm × 15 mm)



Figure 78: The desired maximal hole size (Φ7,1 mm) in the valve plate (Φ174 mm × 15 mm)

To conclude, hole diameter in the valve plate was the only parameter which was being changed. As an objective function we selected the total efficiency of hydraulic gerotor motor.

4 Test rig

The test rig of the experiment consisted of sixteen different hydraulic components (Figure 79), whereas we would like to describe just the most important parts. The experiment was carried out by (1)-the electromotor and (2)-variable displacement pump. The tested hydraulic motor is denoted with the number (3). We used (7)-pressure reduction valve and (8)-pressure relief valve. Five different physical quantities have been measured. We applied (12)-volume flow rate meter, (13)-torque sensor, (14)-rotational speed sensor, (15)-pressure sensor and (16)-temperature sensor. If we would like to determine different kind of efficiencies of the hydraulic motor, we have to measure the physical units properly in sense of location of sensors. We would like to emphasize

that on the inlet flow side we have to measure flow rate (Q_1) and pressure (p_1). On the other hand, outlet pressure (p_2) is absolutely essential, because the pressure difference of the inlet and outlet flow of the hydraulic motor is very important.

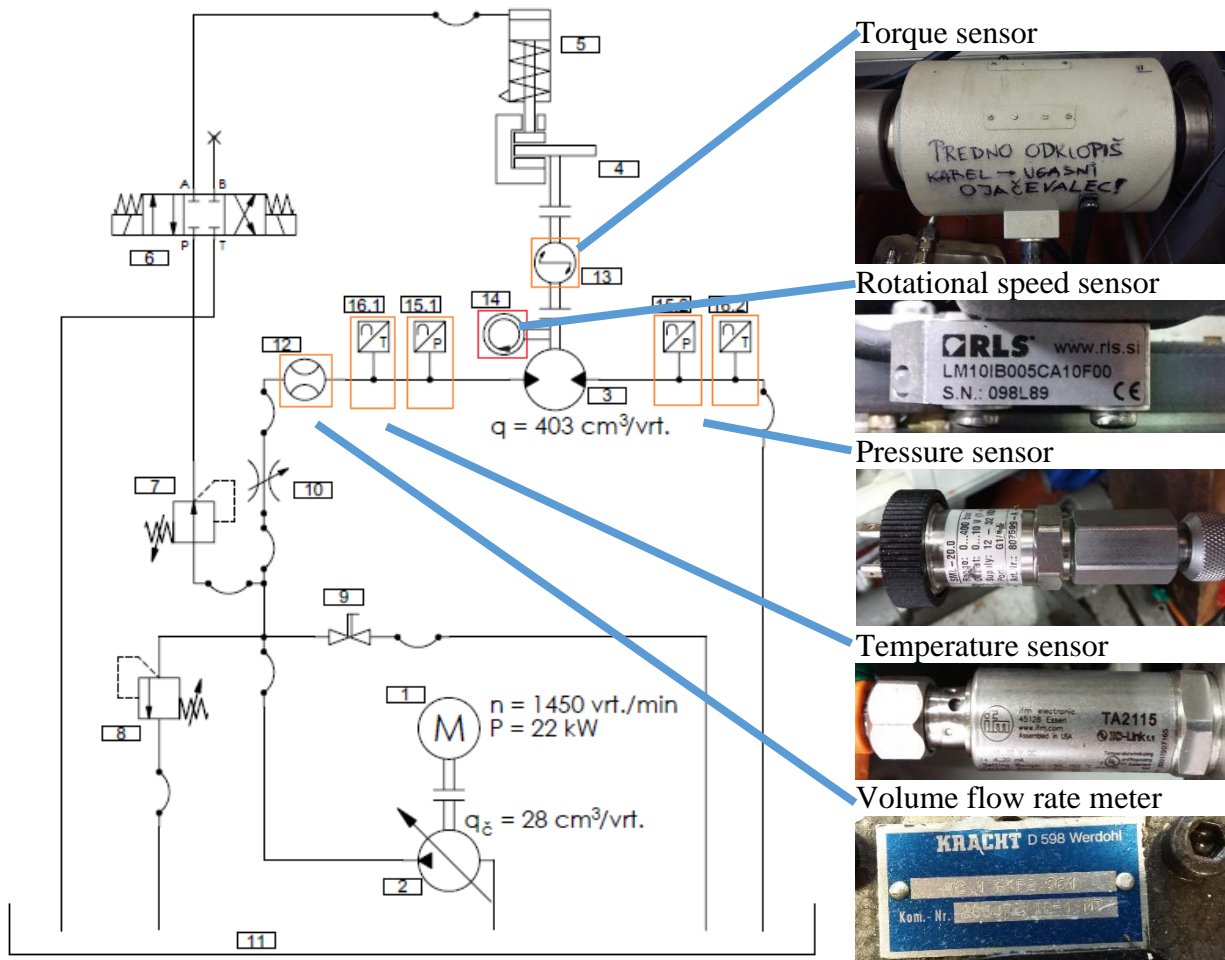


Figure 79: Test rig of the experiment

5 Results and discussion

The result of research is presented in two sections. In the first section is presented the influence of the size of the holes in the valve plate on efficiency. In the second half is introduced the uncertainty analysis.

5.1 Influence of the size of the holes in the valve plate on efficiency

The results of the research are presented in figure 80, which show a relationship between pressure difference, size of the holes in the valve plate and total efficiency. Different colours represent different holes' size. There is pressure difference (range: from 160 bar to 240 bar) on the y-axis and total efficiency (range: 0 % – 45 %) on the x-axis. The length of a row represents a value of the total efficiency in a specific measured point. The longer the length of the row, the greater the total efficiency of the hydraulic gerotor motor. In the case of rotational speed 15 min^{-1} , the initial total efficiency of gerotor with the valve plate with the diameter $\Phi 5,5 \text{ mm}$ was 30,7 %. The highest total efficiency was 36,2 %, returning an 18 % higher total efficiency compared to the initial state. The highest total efficiency was obtained with the hole diameter of $\Phi 6,3 \text{ mm}$. The additional increase of the hole diameter had a negative influence on the gerotor characteristics - total efficiency dropped down dramatically. For example, the total efficiency of the gerotor with the

valve plate with hole diameter $\Phi 7,1$ mm was just 11,4 %. There exists almost the same trend for every set of pressure differences. In general, we found out that the total efficiency increases with the increase of pressure differences if we observe the total efficiency of one specific hole diameter. For example, the total efficiency values for hole diameter of $\Phi 6,7$ mm were increasing in the following way: 20,5 %, 24,3 %, 26,5 %, 29,5 %, 32,0 %, 33,3 %, 35,1 %, 35,5 %, 36,2 %. When we accomplished the measurement of the gerotor with rotational speed 17 min^{-1} (Figure 80), we found out that there exist similarities with the results of gerotor with rotational speed 15 min^{-1} . If we look at the results in the second case, we can find out that gerotor has a slightly lower total efficiency. There exists the increasing and the decreasing trend of total efficiency within every set of measurements. If we focus on the total efficiency in both cases ($n = 15 \text{ min}^{-1}$, $n = 17 \text{ min}^{-1}$), we can see that the total efficiency was higher in case of slightly larger holes. In the initial state, total efficiency was relatively low. When we enlarged hole diameter from $\Phi 5,5$ mm to $\Phi 6,3$ mm, the hydraulic motor reached the maximum total efficiency in a few sets of measurements. Additional escalation of the hole diameter led to lower total efficiency. In some cases, the holes are so big that the hydraulic motor couldn't operate.

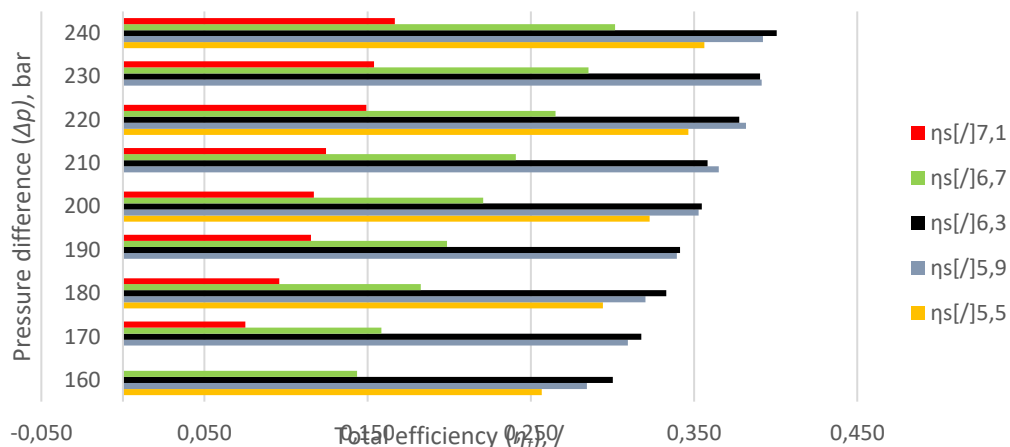


Figure 80: Total efficiency of the gerotor (operating point: $n = 17 \text{ min}^{-1}$)

To summarize, we found out that a hole diameter of $\Phi 6,3$ mm is the most appropriate size of holes in the valve plate regarding total efficiency of the hydraulic gerotor motor. In this case, the total efficiency is around 5 % higher on average.

5.2 Uncertainty analysis

The uncertainty analysis gave us information about the confidence in the results. Within the study, we measured five physical quantities: pressure, flow rate, torque, rotational speed, and temperature. Briefly, we would like to present the uncertainty analysis for the first four physical units. The expanded uncertainty analysis was done by assuming triangular and rectangular distribution and a coverage factor = 2 (Table 4).

Table 4: Expanded uncertainty analysis

	Rectangular distribution [%]	Triangular distribution [%]
Pressure	1,50	1,06
Flow rate	1,73	1,22
Torque	2,02	1,43
Rotational speed	1,73	1,22

6 Conclusion

A research of the hydraulic gerotor motor efficiency with the floating outer ring is presented in this paper. The findings of this study can be summarized as follows: The diameter of holes in the valve plate influences the total efficiency of the hydraulic gerotor motor. For each set of the measurements exists an optimal diameter of holes. Very high total efficiencies were reached with holes' diameter being $\Phi 6,3$ mm in most cases. The highest total efficiency was on average 5 % higher than the total efficiency of the original hole size. It means that a hydraulic motor with the hole diameter $\Phi 6,3$ mm in the valve plate has on average 5 % better operation characteristic in every measured point than a hydraulic motor with the hole size $\Phi 5,5$ mm in the valve plate. We can conclude that we would be able to optimize the gerotor's operation with some simple mechanical operation. With drilling we can make hole diameter larger to raise the total efficiency of the gerotor around 5 % on average. This happens if the diameter of holes in the valve plate is $\Phi 6,3$ mm. The results and research findings present a very important contribution to science. Hydraulic gerotor motors with the floating outer ring were very rarely discussed in scientific papers. There is a lack of such analysis in literature. An influence of hole diameter in the valve plate on the total efficiency of hydraulic gerotor motors represents novelty and original insight in the gerotor's group of hydraulic motors.

Acknowledgement

The authors greatly acknowledge the company KGL d.o.o. Slovenia.

References

- [1] Michael, P., Burgess, K., Kimball, A., Wanke, T.: Hydraulic Fluid Efficiency Studies in Low-Speed High-Torque Motors; SAE Technical Paper 2009-01-2848 (2009), Nr.7; doi:10.4271/2009-01-2848
- [2] Dong, X.: Multi-Objective Optimization Design of Gerotor Orbit Motors; SAE Technical Paper 2002-01-1350 (2002); doi:10.4271/2002-01-1350
- [3] Ding, H., Lu, X. J., Jiang, B.: A CFD model for orbital gerotor motor; IOP Conference Series: Earth and Environmental Science (2012), Nr.6 (15)
- [4] Mishev, A., Stehle, T.: CFD-Analyse zur Leistungssteigerung eines Orbit-Motors, Untersuchung des Einflusses von Rotorzähnezahl und Exzentrizität auf die Performance des Motors (2015)
- [5] Conrad, F., Trostmann, E., Zhang, M.: Experimental identification and modelling of flow and torque losses in gerotor hydraulic motors; Proceedings of the JFPS International Symposium on Fluid Power (1993), Nr.2; page 677-682
- [6] Garcia, J. M.: Surface effects on start-up friction and their application to compact gerotor motor design (2011); <http://search.proquest.com/docview/900865878?accountid=16468>. (29.11.2016)
- [7] Furustig, J., Almqvist, A., Pelcastre, L., Bates, C. A., Ennemark, P., Larsson, R.: A strategy for wear analysis using numerical and experimental tools, applied to orbital type hydraulic motors; <http://pic.sagepub.com/content/early/2015/06ogled/10/0954406215590168>. (29.11.2016)
- [8] Ranganathan, G., Hillson Samuel Raj, T., Mohan Ram, P.V.: Wear characterisation of small PM rotors and oil pump bearings; Tribology International (2004), Nr.1(37); page 1-9
- [9] Ivantysyn, J., Ivantysynova M.: Hydrostatic Pumps and Motors, First English Edition, Akademia Books International, 2000
- [10] Schlösser, W. M. J., Hildbrands, J.W.: Das theoretische Hubvolumen von Verdrängermaschinen; Ölhydraulik und Pneumatik (1963), Nr.4 (7)
- [11] Standard ISO 8426; Hydraulic fluid power – Positive displacement pumps and motors, Determination of derived capacity, 2008
- [12] Evaluation of measurement data – Guide to the expression of uncertainty in measurement, JCGM 100:2008, GUM 1995 with minor correction, 2008

Tribological research of different material pairs for water hydraulic seat type of valve

ANDREJA POLJŠAK, FRANC MAJDIČ & MITJAN KALIN

Abstract Development of water hydraulic components are defaulting since differences between water and oil makes oil hydraulic components unsuitable for water applications. One of the fields in a need for development is controlling of hydraulic actuators where a new trend represents digital valves that can substitute sensitive and expensive servo and proportional valves.

Main components of digital valves are seat type on-off valves with fast and stable switching response which is hard to achieve. High friction coefficient with fast switching causes additional wear and possible failure. To reduce friction and wear the implementation of new materials make sense.

Paper presents the results of preliminary tribological measurements of suggested composites based on contact tailored to meet the environmental conditions between poppet and sleeve in water hydraulic seat on-off valves. Friction coefficient and wear of softer polymeric composites will be presented with suggestions for further work.

Keywords: • water hydraulic • set type valve • materials • tribological problems • findings •

CORRESPONDENCE ADDRESS: Andreja Poljšak, MS, University of Ljubljana, Faculty of Mechanical Engineering, Aškerčeva cesta 6, 1000 Ljubljana, Slovenia, e-mail: andreja@pmit.si. Franc Majdič, Ph.D., Assistant Professor, Aškerčeva cesta 6, 1000 Ljubljana, Slovenia, e-mail: franc.majdic@fs.uni-lj.si. Mitjan Kalin, Ph.D., Full Professor, Aškerčeva cesta 6, 1000 Ljubljana, Slovenia, e-mail: mitjan.kalin@fs.uni-lj.si.

1 Introduction

Water hydraulic has a lot of advantages over traditional hydraulics based on mineral oil. It is fire resistant, environmentally friendly, clean and low cost working medium that is suitable for applications in under water tool system, etc. [1]. Reasons, why water hydraulic popularity does not reach oil hydraulic, lies in its properties. Water's kinematic viscosity is around 100 times lower what makes it easier to flow through small gaps and to create turbulences. Vapour pressure is a lot higher thus ensuring steady pressure is important. It is also aggressive medium that causes corrosion and its working temperature is limited to 50 °C [2]. Listed above effects the construction process and costs of water hydraulic components. In terms of material selection, new solutions are researched in order to achieve lower friction, lower weight and, if possible, lower costs of production and costs of raw materials.

In literature several material groups are presented as a solution for different water hydraulic components, stainless steels, as most common ones, engineering ceramics, ceramic coatings, carbon coatings like DLC (diamond like carbon), nitride coatings, polymers and polymer composites.

Our application is water hydraulic is seat on-off valve where two types of contact occur, impact seat contact and sliding contact. First requires a material that is not fragile and has good impact strength and the second requires low friction coefficient. Ceramics and coatings have good wear resistance, high hardness, good chemical stability and low adhesion but, low impact strength in combination with water causes cracking and creating damaging debris [3] to [18]. Material groups that are not so friable are polymers and polymer composites. Literature suggests different polymers which shows low friction coefficient when sliding against harder material. Most common are PEEK, POM, PTFE, PPS, PI, PA, and their composites with graphite fibers, glass fibers, carbon fibers, graphite nanotubes, etc. [19] to [23]. Polymers have different mechanical properties since they are viscoelastic materials. Thus different problems as water absorption and creep arises that need to be tested and evaluated.

In this paper preliminary results of PEEK, POM, PA6 and PA66 + 30% GF materials friction coefficient and wear rate will be presented based on water absorption. The paper structure will be as follows, in chapter 2 factors affecting friction and wear in a seat on-off valves will be presented, chapter 3 covers experimental work structure and specimen preparation, in chapter 4 results are discussed and in the last chapter, further work is introduced.

2 Factors affecting friction and wear of polymers in a seat on-off valves

2.1 Seat on off valves construction

One stage seat on-off valve has a simple construction where moving part is a poppet (Figure 0.81). Electromagnetic actuator uses a coil to induce magnetic field which creates a magnetic force that pushes the armature and consequently the poppet. With the loss of a current, coil loses its force and poppet moves back with a help of a return spring. While the poppet is pressed on its seat, the valve is off and no fluid flow is present, when the poppet is pushed down with the help of a magnetic force and flow pressure, the valve opens and allows fluid to pass.

First problem arises between poppet and housing. In theory, the poppet floats in the housing, but with a high water pressure poppet is coincidentally pushed towards housing in all directions what causes friction and the loss of energy. Second, wear occurs on a valve poppet which hits the seat

every time valve is turned off. Impacts damage poppet's conical surface that causes leakage and increases pressure loss.

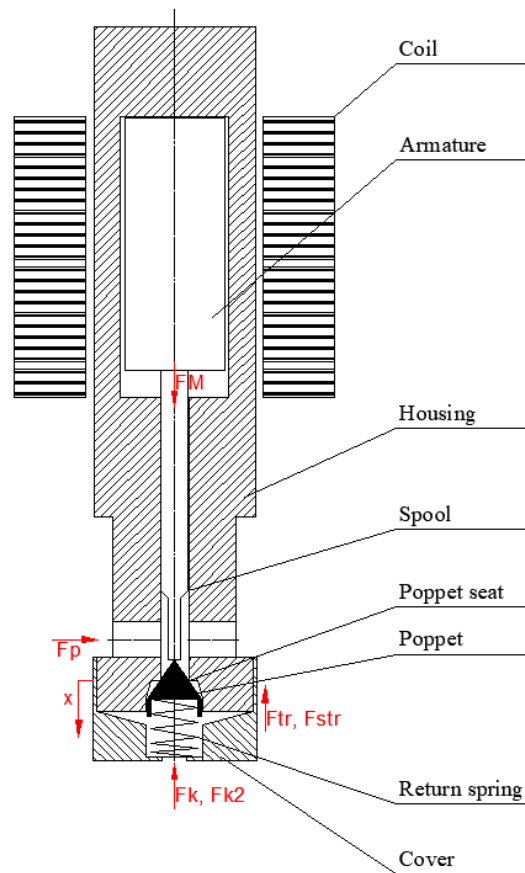


Figure 0.81: Scheme of a simple hydraulic seat on-off valve

2.2 Friction and wear of polymers

In order to introduce polymers to construction of a poppet some differences in behavior of materials needs to be considered. Polymers behave differently and the discrepancy between metallic and polymeric friction is due to the differences in the elastic-plastic behavior of metals and the viscoelastic behavior of polymers. Factors that affects friction and wear of polymers are sliding speed, temperature, counter face roughness, applied load and contact pressure, material properties, lubrication and fatigue of polymers [24].

Dependence of friction coefficient to the **sliding speed** its complex and hard to define. With speed, wear increases due to increase in the contact surface temperature. Thermoplastics have a critical sliding speed over which wear rate slightly reduces due to melting and thermal softening. This critical point is a consequence of adhesive friction at the instantaneous contact interface and thus cannot be measured. [24]

Temperature, as explained, changes during sliding thus mechanical properties of polymers shows transition from glassy to rubbery state. Some analytical and experimental models were obtained by various researchers. Models take into account different correlations between temperature, friction coefficient, sliding speed, contact pressure, semi contact length and width, environmental and/or contact temperatures and normal load, from which some are difficult to define. [24]

Counterface roughness has a strong correlation with tribology of polymeric materials in case counterface is metal with higher hardness. During sliding, as the metal surface roughness decreases, friction coefficient decreases till minimum roughness value is reached, further, decrease in roughness causes high friction. Turning point arises when adhesion forces prevail abrasive wear. Some materials shows vice versa trends where with increasing of counterface roughness friction decreases, but wear increases. [24]

With increasing **contact pressure and load**, it is well known that increase in contact temperature, softening and plastic deformation of polymers occur since plastic deformations change real area of contact thus friction and wear are increased. For many thermoplastics experiments have shown that for high loads 10-100 N, friction coefficient is constant. For lower loads from 0,2 to 1 N plastic deformation governs the sliding process with increase of friction coefficient. Thus transition from elastic to plastic contact plays a big role in friction and wear. Relation between friction force F and applied normal load L can be expressed with equation (1).

$$F = \mu L^n \quad (1)$$

Where μ is friction coefficient and n is exponential constant that is different for different polymers [24].

As already understood **material properties** are crucial in material behavior. Why polymers are so difficult to track and model is due to constant mechanical and physical property change. Mechanical properties as yield strength, hardness, elastic modulus and impact strength have a big effect at glass transition properties. They decrease with increasing temperature thus wear increases. Physical properties of thermoplastics on the other hand, govern chemical composition and interfacial energy. Both determine the rate of adhesion. Polymers with lower surface energy tends to transfer to that of high surface energy. Transferred film thus depends also on physical properties [24].

Another problem to be considered when applying polymers in water hydraulics is **humidity or water lubrication**. The amount of atmospheric humidity has a pronounced effect on the wear and friction of polymers and on creating a film on the counterface. The wear rate under water lubrication was always higher [19] to [24]. This is due to a couple of reasons. One is diffusion of water molecules into free volume of the amorphous phase of polymers what leads to plasticization, swelling and softening. It also reduces the attractive forces between polymer chains. Second is washing action of countersurface, thus transfer film fails to form. And the third, water is a corrosive medium which will modify the countersurface that can cause a debris within the contact [24].

No matter the conditions, wear of polymers is with time increasing due to fatigue of the material. During working cycles materials are affected by cycle frequency, loading wave form, stress ratio, molecular weight of polymer, etc. Rate of fatigue can be improved with higher rate of crystallinity but it can also be exacerbate under harsh operating conditions [24].

In seat on-off valve it is impossible to measure working parameters as contact surface temperature and normal load to the friction surface since small gap tolerances, analytical models are therefore difficult to apply [25].

In order to measure friction coefficient and wear rate of material pairs that interests us, we chose standard tribological test which parameters are closest to working parameters in seat on-off valves. The apparatus and working parameters are presented in following chapter.

3 Experimental work

Tribological behavior of several unfilled and one filled polymer material sliding against 316 L stainless steel in water is studied. Coincidental touching is hard to measure and impossible to repeat therefore we chose standard tribological apparatus (TE 77) with a reciprocal movement to simulate the movement of a poppet in a housing.

3.1 Materials

Preliminary selected polymers are well known in engineering applications due to their regular usage in pumps, bearings, etc.

POM is a semi-crystalline polymer with high crystallinity (70–100 %), good friction and wear properties, high strength, and good chemical stability. It is widely used to replace the traditional metals and ceramics in microelectronic packaging, aerospace, automotive, and biomedical applications. Its low water absorption makes it suitable also for water applications.

PEEK as a typical high performance semi-crystalline thermoplastic polymer, has received significant attention. This is due to its high mechanical strength and elastic modulus, high melting temperature, chemical inertness, high toughness, easy processing and wear resistance. On the other hand, in tribological applications, because of the corrosive problems of the metals in water applications, polyetheretherketone (PEEK) and polyetheretherketone composites are preferred as rubbing materials. So, PEEK polymer material plays more important role as a bearing and slider material especially under water environment [22].

Polyamides (PA6 and PA66) are semi-crystalline polymers used for many engineering parts undergoing friction and wear (bearings and gears) [26]. These properties are attributed to the presence of hydrogen bonds in polyamide molecular chains [27]. Even though they absorb more water than other chosen polymers they are low cost and thus approachable.

Last polymer composite in preliminary measurements is **PA66 + 30 % glass fibers**. PA66 is the hardest and toughest among Polyamides. It absorbs slightly less water than PA6 and it has better wear resistance. With addition of glass fibers composite shows increased strength, rigidity and service temperature.

The counter surface in all experiments was AISI 316L, also known as marine grade stainless steel. Table 0.3 presents characteristics of selected materials.

Table 0.3: Characteristics of polymer materials from material technical data.

Material	Water absorption % ISO 62	Friction coefficient / DIN 53375	Mean thermal expansion 1/K ISO 11359-1;2	Impact strength kJ/m ² ISO 179	Modulus of elasticity MPa ISO 527
POM (Polyoxymethylene)	0,1	0,35	$14 \cdot 10^{-5}$	8 (notch)	2800
PEEK (Polyetheretherketon)	0,1	0,34	$0,5 \cdot 10^{-4}$	No break	3000
PA6 (Polyamide 6)	9,5	-	$1,1 \cdot 10^{-4}$	7 (notch)	3330

PA66 + 30 GF (Polyamide 66 + 30 % Glass fibers)	5,5	0,5	$50 \cdot 10^{-6}$	50	10000
---	-----	-----	--------------------	----	-------

Materials were bought in a company EX-MEGA d.o.o. already shaped in 1 m long bars of diameter 10 mm. Material technical data holds no information about production process and storing conditions.

3.2 Test machine and specimens

Measuring apparatus is high frequency friction machine TE 77 (Figure 0.82, left). It has a water container inside which counterface stainless steel 316L specimen was mounted. Polymer specimen was mounter into a holder presented on a Figure 0.82 right.

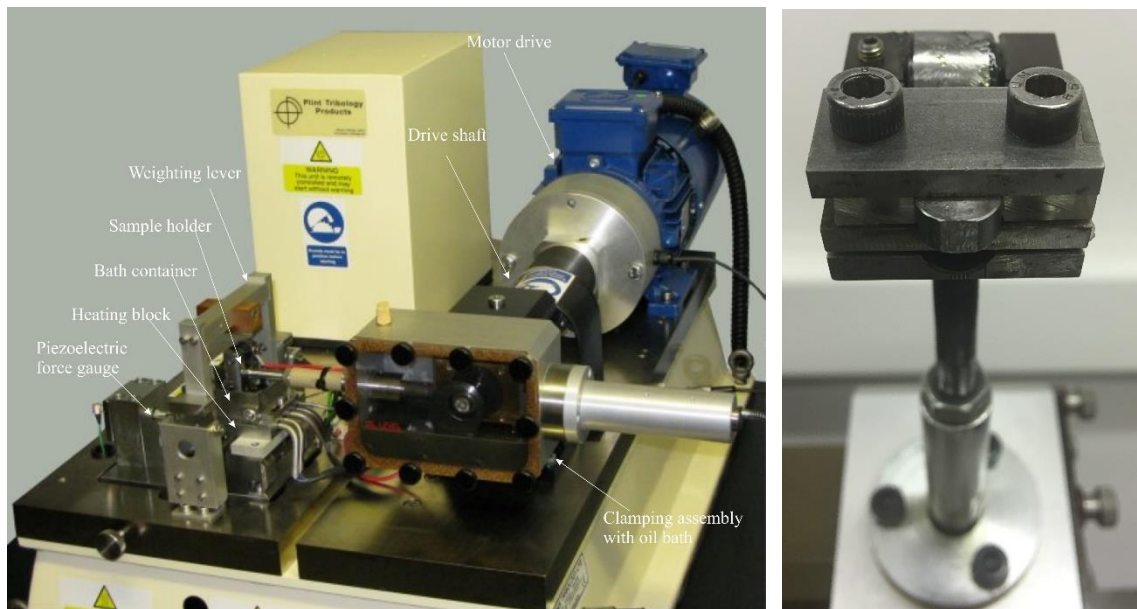


Figure 0.82: Measuring apparatus TE 77 (left) and clamping of specimen (right)

Polymer specimens were 5 mm long cut-outs of a bar with diameter of 10 mm. Bars were first polished to a roughness $Ra = 0,1 \mu\text{m}$.

Counterface stainless steel 316 L was a disc with diameter of 30 mm and 2 mm thickness. Surface of stainless steel was also polished to a roughness $Ra = 0,1 \mu\text{m}$.

Polymer specimens were cleaned with acetone and ethanol before put in a bath. Specimens were immersed in water for different periods of time, from 7 to 28 days. Four different specimens of the same material were immersed in 4 different baths as seen on Figure 0.83: Specimens in water baths Figure 0.83.

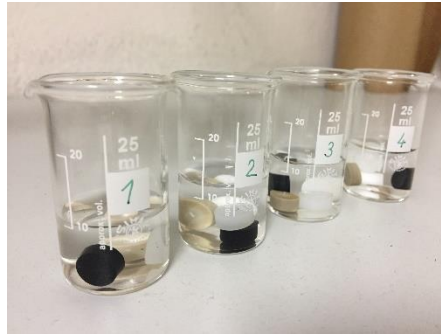


Figure 0.83: Specimens in water baths

3.3 Experimental procedure

As described, wear and friction coefficient of polymers is a function of variety of contact and environmental factors, parameters of our measurements are presented in a Table 0.4. Frequencies of water hydraulic seat on-off valves are currently up to 10 Hz what is low for digital hydraulics where frequencies evolve around 100 Hz and more. Measurements were carried out at a constant frequency of 40 Hz for a 36 000 cycles due to friction coefficient stabilization. Normal force is unmeasurable therefore we used similar pressures and suggested in a literature [19] to [23]. Via Hertzian contact pressure we applied around 15 MPa. Force of 5 N was applied via weighting lever and was kept constant. Polymer specimen holder was moving in a reciprocal direction with a maximum distance of 2,4 mm what is the shortest distance possible with chosen apparatus. Fluid for water bath and irrigation was demineralized water with room temperature to eliminate any effect on the measurements and to ensure repeatability.

Table 0.4: Experimental conditions.

Repetitions per material	3x
Frequency	40 Hz
Number of cycles	36 000
Approximate time	15 min
Normal force	5 N
Max. displacement	2,4 mm
Total distance	172800 mm
Medium	Demineralized water
Water temperature	21 °C
Irrigation	0, 7, 14, 24, 31 days

Every sample, when taken out of a bath, was dried with paper and weighted right after removing it from water and before it was used in tribological tests. Three repetitions were done with every sample and between every repetition sample was again weighted due to wear. Friction force was measured by a piezoelectric force gauge mounted under the water container.

4 Results and discussion

As a follow up, tracking of water absorption was observed due to easier understanding of polymers chemical composition. As expected, PA6 absorption percentage was the highest followed by PA66. For PEEK and POM the line almost become constant and from all, PEEK absorbed the smallest amount of water during our measurements nevertheless it has the same water absorption % as POM in technical data (Table 0.3).

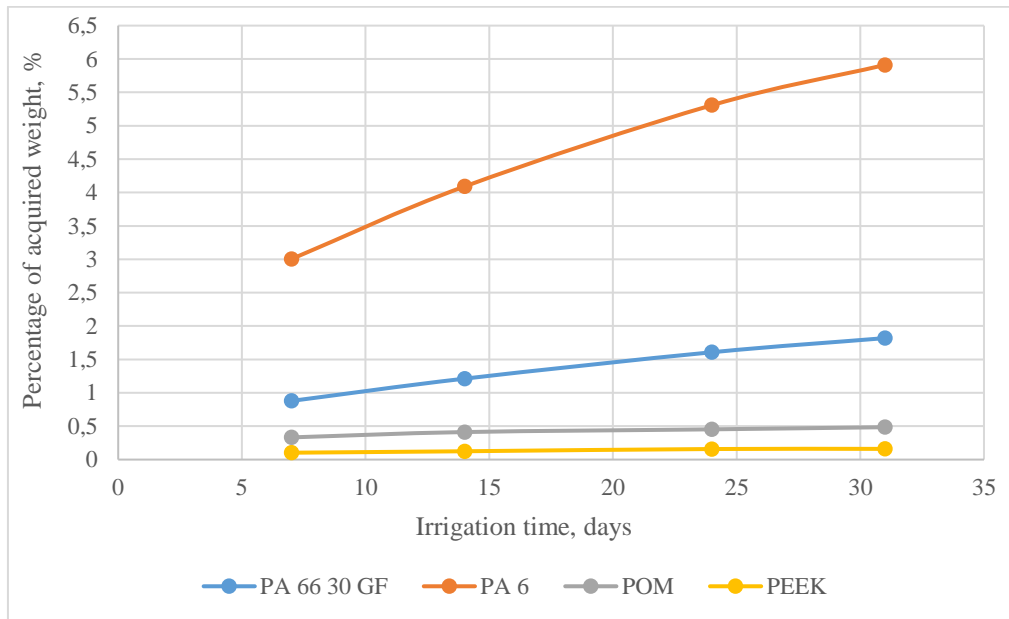


Figure 0.84: Percentage of acquired weight depending on an immersed time

4.1 Friction

Friction was measured after every irrigation time under the same conditions. Figure 0.85 and Figure 0.86 represents friction coefficient during measuring cycles for 14 and 31 days of water absorption.

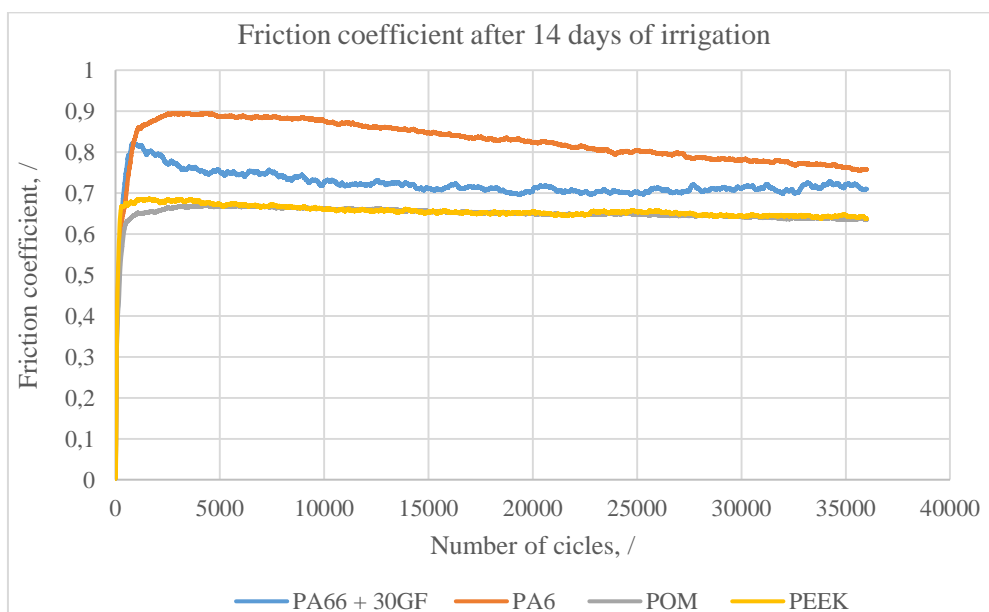


Figure 0.85: Friction coefficient measurements after 14 days of irrigation

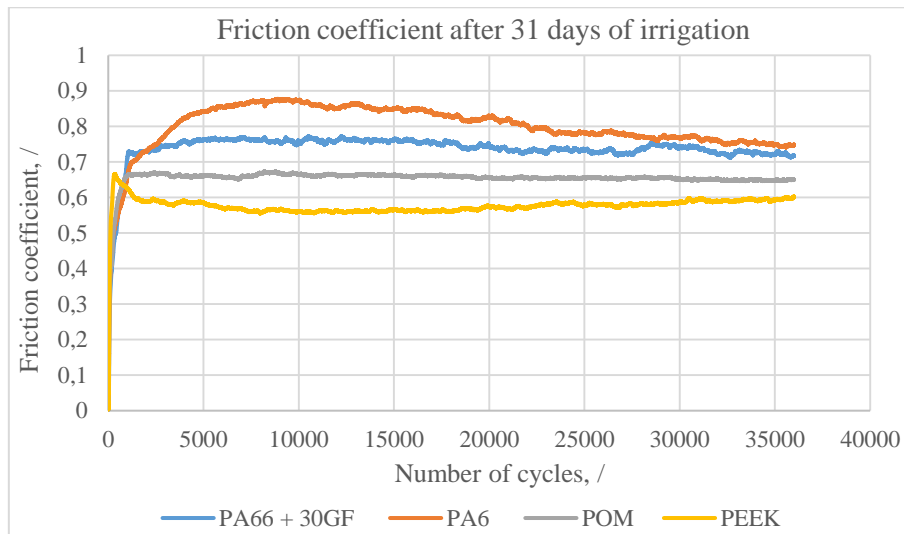


Figure 0.86: Friction coefficient measurements after 31 days of irrigation

Stabilization of friction coefficient was achieved for all polymers and composite except for PA6 whose value was still dropping after 15 min. With higher water percentage this effect was even bigger and coefficient value was dropping even slower. This can be identification of continuous adhesion and abrasion.

PEEK and POM have almost the same friction coefficient at lower water absorption percentage what can also be seen in material technical data but the values in reciprocal movement are almost double 0,66.

PA 66 + 30 GF friction coefficient has more steady curve and reaches lower values as a unfilled PA6 but it can be seen that PA 6 is approaching the same values with time, thus we can question of benefits of glass fibers when polymers are saturated.

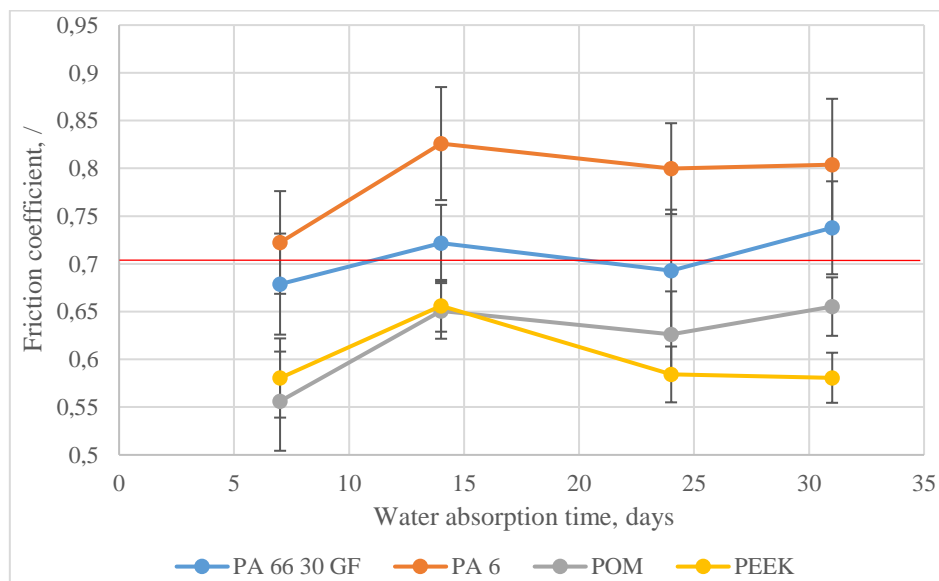


Figure 0.87: Friction coefficient in dependence of water absorption time

Figure 0.87 represents average friction coefficient in dependence of water absorption time with standard deviation. The red line on a graph represents friction coefficient of a stainless steel 316 L and serves as a guideline since this material is already used in water hydraulic seat on-off valves.

In general, all materials have higher friction coefficient than presented in technical data but POM and PEEK are still lower than stainless steel.

With longer immersion POM exhibits growth of friction coefficient when PEEK's after 14 days start to reduce and achieves lower values as at the beginning.

4.2 Wear

Wear was measured with weighting after every measurement. As presented by Figure 0.88, PA6 has the highest wear what was expected due to high and constantly changing friction coefficient. This can be a consequence of constant presence of wear mechanisms till the end of measurement. The lowest wear was achieved by PA 66 + 30 GF therefore fibers do protect softer polymeric matrix but in this case do not contribute to lower friction. As for POM wear starts to increase with higher water absorption percentage, PEEK is showing a big decrease what makes PEEK the most appropriate material based on preliminary measurements.

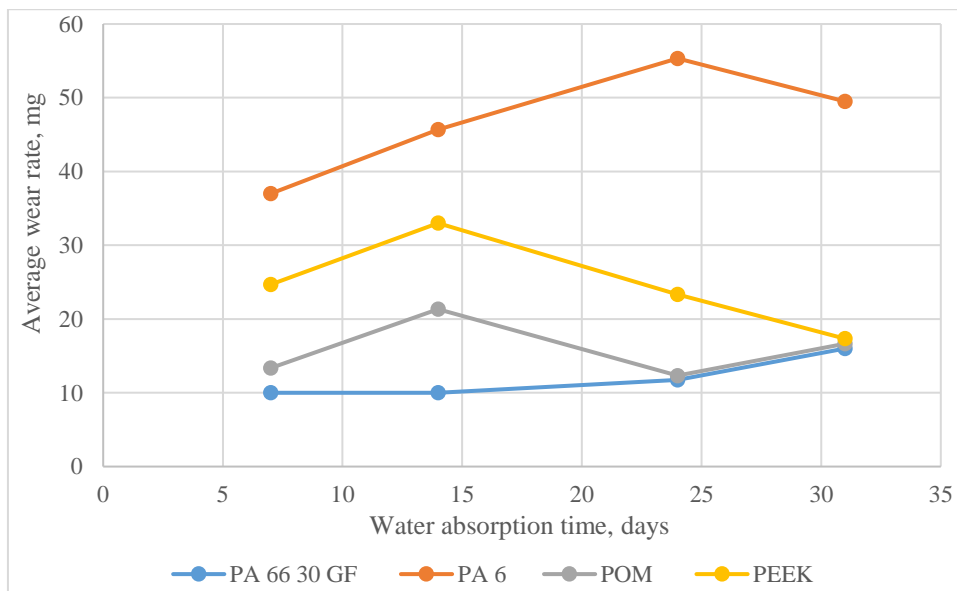


Figure 0.88: Average wear rate in dependence of water absorption time.

5 Conclusion and further work

In the present study, the tribological behaviour of polymers POM, PEEK, PA6 and a composite PA66 + 30 GF was investigated in water lubricated sliding contacts with pre-immersed specimens for different periods of time.

The results of this study first of all shows that sliding direction have a big influence on friction coefficient and consequently on wear rate of polymers and composites therefore standard rotational pin-on-disc tribological measuring process cannot be a measure for tribological parameters in applications with reciprocal movement as present in our water hydraulic seat on-off valve.

Second, as expected due to polymeric visco-elastic behavior and ability of water absorption, the time of immersion have significant influence on tribological properties thus full saturation has to be considered when choosing polymeric material for water applications.

Third, for lower water absorption and lower wear, glass fibers do have positive contribution since they protect polymer matrix from counterface but they are not optimal for reducing friction coefficient in water.

Preliminary results give us guidelines for our work to follow. For further tribological measurements we will exclude all engineering polymers with high water absorption percentage even their low cost benefits. Tribological properties of unfilled polymers and some composites with carbon fibers will be measured at full saturations based on ISO 62. For carbon composites, debris due to wear can cause contamination therefore it will be monitored and evaluated after the measurements.

Before approaching implementation in final application we will also test the most suitable polymers and composites to impact stresses that occurs in water hydraulic seat on-off valve.

References

- [1] Yinshui, L., Wu, D., He, X., & Zhuangyun, L.: Materials screening of matching pairs in a water hydraulic piston pump. *Industrial Lubrication and Tribology* (2009), 61(3), 173-178.
- [2] Trostmann, E.: *Water hydraulics control technology*. CRC Press, 1995.
- [3] Li, Zhuang Yun, et al.: The development and perspective of water hydraulics. In: *Proceedings of the JFPS International Symposium on Fluid Power*. The Japan Fluid Power System Society, 1999. p. 335-342.
- [4] Wang, Qing Hui, et al.: The Properties of Water Hydraulic High-Speed On/Off Valve Ceramic-Based. In: *Advanced Materials Research*. Trans Tech Publications, 2012. p. 340-344.
- [5] Koskinen, Kari T.; vilenius, Matti J. Steady state and dynamic characteristics of water hydraulic proportional ceramic spool valve. *International Journal of Fluid Power*, 2000, 1.1: 5-15.
- [6] Chen, Wei, et al.: Tribochemical behavior of Si₃N₄-hBN ceramic materials with water lubrication. *Tribology letters*, 2010, 37.2: 229-238.
- [7] Saito, Toshiyuki; hosoe, Takeshi; honda, Fumihito. Chemical wear of sintered Si₃N₄, hBN and Si₃N₄-hBN composites by water lubrication. *Wear*, 2001, 247.2: 223-230.
- [8] Lu, Jinjun; zum gahr, Karl-Heinz; schneider, Johannes. Microstructural effects on the resistance to cavitation erosion of ZrO₂ ceramics in water. *Wear*, 2008, 265.11: 1680-1686.
- [9] Wu, Defa, et al. The Tribological Behaviors of Different Mass Ratio Al₂O₃-TiO₂ Coatings in Water Lubrication Sliding against Si₃N₄. *Tribology Transactions*, 2016, 59.2: 352-362.
- [10] Huayong, Yang; jian, Yang; hua, Zhou. Research on materials of piston and cylinder of water hydraulic pump. *Industrial Lubrication and Tribology*, 2003, 55.1: 38-43.
- [11] Takahashi, Tamami; yamashina, Chishiro; miyakawa, Simpei. Development of water hydraulic proportional control valve. In: *Proceedings of the JFPS International Symposium on Fluid Power*. The Japan Fluid Power System Society, 1999. p. 549-554.
- [12] Rämö, Jari; hyvönen, M.; mäntylä, T.; koskinen, K.T.; vilenius, M. Wear resistance of materials in water hydraulics, Institute of Material Science, Finland,
- [13] Basu, Bikramjit; KALIN, Mitjan. *Tribology of ceramics and composites: materials science perspective*. John Wiley & Sons, 2011.
- [14] Mayrhofer, Paul H., et al. Microstructural design of hard coatings. *Progress in materials science*, 2006, 51.8: 1032-1114.
- [15] Wang, Qianzhi, et al. Comparison of tribological properties of CrN, TiCN and TiAlN coatings sliding against SiC balls in water. *Applied Surface Science*, 2011, 257.17: 7813-7820.
- [16] Erdemir, Ali; donnet, Christophe. Tribology of diamond-like carbon films: recent progress and future prospects. *Journal of Physics D: Applied Physics*, 2006, 39.18: R311.
- [17] Uchidate, M., et al. Effects of hard water on tribological properties of DLC rubbed against stainless steel and brass. *Wear*, 2013, 308.1: 79-85.

A. Poljšak, F. Majdič & M. Kalin: Tribological research of different material pairs for water hydraulic seat type of valve

- [18] Niiyama, Yasunori, et al. Friction and Delamination Properties of Self-Mating Diamond-Like Carbon Coatings in Water. *Tribology Letters*, 2016, 62.2: 1-7.
- [19] Dong, Wutao; nie, Songlin; zhang, Anqing. Tribological behavior of PEEK filled with CF/PTFE/graphite sliding against stainless steel surface under water lubrication. *Proceedings of the Institution of Mechanical Engineers, Part J: Journal of Engineering Tribology*, 2013, 227.10: 1129-1137.
- [20] Zhang, Anqing; nie, Songlin; yang, Lijie. Evaluation of tribological properties on PEEK+CA30 sliding against 17-4PH for water hydraulic axial piston motor. *Proceedings of the Institution of Mechanical Engineers, Part C: Journal of Mechanical Engineering Science*, 2014, 228.13: 2253-2265.
- [21] Jia, Junhong, et al. Comparative investigation on the wear and transfer behaviors of carbon fiber reinforced polymer composites under dry sliding and water lubrication. *Composites Science and Technology*, 2005, 65.7: 1139-1147.
- [22] Sumer, M.; unal, H.; mimaroglu, A. Evaluation of tribological behaviour of PEEK and glass fibre reinforced PEEK composite under dry sliding and water lubricated conditions. *Wear*, 2008, 265.7: 1061-1065.
- [23] Golchin, Arash, et al. Tribological behavior of carbon-filled PPS composites in water lubricated contacts. *Wear*, 2015, 328: 456-463.
- [24] Abdelbary, Ahmed. *Wear of polymers and composites*. Woodhead Publishing, 2015.
- [25] Majdič, Franc. *Voda kot kapljevina v pogonsko-krmilni hidravliki*, doktorska disertacija. FS, Ljubljana, 2010.
- [26] Yang, Zhugen, et al. Effects of polyamide 6 on the crystallization and melting behavior of β -nucleated polypropylene. *European Polymer Journal*, 2008, 44.11: 3754-3763.
- [27] De Baets, Patrick, et al. The friction and wear of different polymers under high-load conditions. *Lubrication Science*, 2002, 19.2: 109-118.
- [28] Golchin, Arash, et al. Tribological behaviour of polymeric materials in water-lubricated contacts. *Proceedings of the Institution of Mechanical Engineers, Part J: Journal of Engineering Tribology*, 2013, 227.8: 811-825.

Test stand for determining the performance characteristics of hydraulic directional control valves

ROK PAHIČ, VITO TIČ & DARKO LOVREC

Abstract For the control of a hydraulic system, it is necessary to be familiar with the dynamic characteristics of the hydraulic valves, which vary according to operating conditions. It is possible to evaluate the effect of operating conditions by an appropriate measuring track for dynamic characteristics, which should ensure the comparability of measurements among themselves and with measurements of other measuring tracks as well, taking into account the standard procedure.

The paper describe design of a measurement track for testing the dynamic characteristics of hydraulic valves in accordance with ISO 10770-1: 1998.

In introduction is presented the motivation for the work and the basics of dynamic characteristics in accordance to Standard. Further on, design of the measurement track`s hydraulic part, electrical part and program part are represented and at the end the testing procedure and the results of testing of two different continuously operating valves.

Keywords: • hydraulic valves • dynamic characteristic • test bench • control system • automated measuring procedure •

CORRESPONDENCE ADDRESS: Rok Pahič, Ph.D. Student, IJS-Institute Jožef Stefan, Jamova cesta 39, 1000 Ljubljana, Slovenia, e-mail: rok.pahic@ijs.si. Vito Tič, Ph.D., Assistant Professor, University of Maribor, Faculty of Mechanical Engineering, Smetanova ulica 17, 2000 Maribor, Slovenia, e-mail: vito.tic@um.si. Darko Lovrec, Ph.D., Chairperson of the Fluid Power 2017 organising committee, Associate Professor, University of Maribor, Faculty of Mechanical Engineering, Smetanova ulica 17, 2000 Maribor, Slovenia, e-mail: darko.lovrec@um.si.

1. Introduction

The search for better performance of a hydraulic system has also gone in the direction of improving one of the most crucial elements of the hydraulic system, which is hydraulic fluid. With measurements of their physical and tribological characteristics, we can predict some influences on a valve's working characteristics and on the lifetime wear of hydraulic elements, but the most certain results can be produced with direct testing of the hydraulic element with a certain hydraulic fluid.

Hydraulic control valves are hydraulic elements for controlling the direction and flow of hydraulic fluids in a hydraulic system. With their properties and characteristics, they influence heavily the behavior of the whole hydraulic system and its control. The working characteristics of valves are dependent mostly on their design, however, the influence of the properties of the used hydraulic fluid and lifetime wear are not negligible.

Evaluation of suitability for new hydraulic fluid should, therefore, test the influence of hydraulic fluid on valve characteristics and, consequently, on the whole hydraulic system. The proper measuring track is thus needed for measuring the direct influence of hydraulic fluid on valve characteristics and measuring their change through its lifetime.

1.1 Dynamic characteristics

Characteristics of valves can be separated into static characteristics, like signal-flow characteristics, and dynamical characteristics, such as step response and frequency characteristics. For continuous working valves, dynamical characteristics are essential, because they represent time dependent behaviour of hydraulic valves. There are two different typical representations of dynamical characteristics. The first representation is a step response graph, which represents the time response of an output signal when the input signal changes with a step function. In the case of hydraulic valves, the input signal is usually a control signal for the valve and the output signal hydraulic flow through it. Response time and settling time could be used for quantifying step response characteristics.

The second important representation of dynamical behaviour is frequency characteristics, which is usually represented in frequency space with a Bode diagram. For the construction of frequency characteristics, the input of the system is excited with constant amplitude sinus signal, then the output signal amplitude gain and phase delay is measured in correspondence with the input signal frequency. Amplitude gain is the ratio between the reference amplitude of the output signal for the constant input signal, and amplitude measured in dependencies of different input signal frequencies. The phase delay is an angle of delay between sinus signals on input and on output. A Bode diagram is composed of two parts, amplitude characteristics, and phase characteristics. Amplitude characteristics represent in a logarithmic scale the amplitude gain for different frequencies, and phase characteristics represent the function of the delay angle in correspondence with the input signal frequency. For quantifying frequency characteristics critical frequency is defined, which refers to amplitude gain -3 dB in amplitude characteristics or phase delay -90° in phase characteristics. As for step response, an input signal for the hydraulic valve is usually a control signal and output hydraulic flow through the valve.

1.2 Standard

For comparing characteristics of hydraulic elements from a different producer and evaluating the change of characteristic through the lifetime of an element, they should be obtained with the same standardized test. The standardized form should also apply for result representation.

ISO 10770 [1] is a Standard that regulates all this for electric modulated hydraulic control valves. It is composed of three parts, for testing way valves with four ports, three ports and testing pressure control valves. The Standard divides the test into four sections, for electrical testing, characteristic testing with subdivision on static tests, dynamical tests, and impulse testing. For our work, the relevant part was about dynamical tests of four-way valves. The Standard specifies testing conditions for fluid type, fluid temperature, pressure fluctuation on the measuring cylinder and in the pressure supply. The measurements are divided into three classes corresponding with the precision of measurement.

2 Measuring track

2.1 Hydraulic part of measuring track

The hydraulic part of a measuring track is made of five segments (Figure 1): Hydraulic power supply, hydraulic accumulator, hydraulic fluid, measuring cylinder and testing valve.

The first segment is the hydraulic power supply, which is composed of a hydraulic supply unit. The measuring track is plugged into the network through a pressure control valve set on 100 bar. In the network, parallel from the measuring track, is another branch with a hydraulic resistor for pump cooling.

The second segment are hydraulic accumulators, which minimize pressure fluctuations and are set on the intake of the measuring cylinder. Hydraulic fluid in the hydraulic system is mineral based hydraulic oil, Hydrolubric VG 46 (producer OLMA), which is not of the viscosity grade recommended by the Standard, but is valid for use if its viscosity grade is listed with results.

The measuring cylinder is used for measuring the hydraulic flow through piston displacement. For measuring hydraulic flow in dynamical characteristics, flow turbines and gear motors are not suitable. The first one is not very precise in the area of small flows, and the second one has a very high pressure drop in this area. The measuring cylinder is, as recommended, constructed with a very light piston, low inner friction, and high natural frequency, so that the influence of cylinder dynamics on measurement is minimized. When hydraulic fluid flows into the cylinder, it moves the piston. While the cylinder is the finite length, just a certain amount of fluid can flow into the cylinder before the piston hits the wall and makes measurement impossible, because of the periodical sinus control signal, where, in every period, fluid flows in and out of one and the other sides of the cylinder. If we want that the piston wouldn't hit the wall, the volume of fluid flowing inside the cylinder in one period should be less than the cylinder volume. With mathematical derivates, then can we obtain an equation that connects the geometrical properties of the measuring cylinder with maximal peak fluid flow and testing frequency for undisturbed testing (Equation 1).

$$\frac{\Delta x \cdot d^2 \cdot \pi^2}{4} \cdot f = \dot{V}_{max} \quad (1)$$

Δx piston maximal displacement [m]

d cylinder diameter [m]

f frequency [1/s]

\dot{V}_{max} peak volume flow [m³/s]

For testing of the measuring track, we used two different continuous-working directional valves; a classical proportional valve with a small positive overlap, and a control proportional valve type 4WRPH6 from Bosch Rexroth. The classical proportional valve was driven directly with a PWM signal from a PLC PWM module. The control proportional valve has its own control card for valve position control, which takes as a reference the voltage signal from the PLC output.



Figure 1: Physical construction of measuring track together with control device

2.2 Sensors and PLC

Test results are valid if the pressure fluctuation and fluid temperature are under certain limits, so we have used one temperature sensor and two pressure sensors for controlling the test conditions. The most important measurement for the test is measuring piston displacement, for which we have used an LVDT position sensor with a proper amplifier.

For test valve driving and measuring sensor reading, we used a controller with proper input and output modules from the producer Beckhoff. We used the possibility provided by Beckhoff PLC to configure the personal computer to reserve and use some cores for PLC operations. Communication between input-output modules and personal computer in PLC mode of operation is then through EtherCAT.

An EK1100 EtherCAT interface is used to access the input / output modules. The interface is connected to the PCBs of the PC via Ethernet 100BASE-TX communication, and transmits messages via the E-bus signal EtherCAT to the I / O terminal (Figure 1, right). Module EL3014 is an analogue four channel differential current input module. The data is in the range from 0 to 20 mA and with digital resolution of 12 bit. It measures data from both pressure sensors and a possible temperature sensor on the measuring line.

The EL3104 module is an analogue four-channel differential voltage input module. The measuring range is from -10 to 10 V, and the digital resolution is 16 bit. It covers the voltage signal transmitted

by the electronic position sensor. Module EL4008 is an eight-channel analogue voltage output. It operates in the range between 0 and 10 V with a digital resolution of 12 bits. The module is used in the case of testing the valve with its own amplification card, where the module sends the control voltage signal to the card.

The KL2545 module is a two-channel current power output module with pulse width modulation. It works in the range of ± 3.5 A with a digital resolution of 16 bit. When using a module, it is also necessary to access its control registers, as the power outputs are essentially disabled and must be programmed before use. In the measurement, the module is used to power the coils that move the slider in the valve. Because the KL2545 module operates via standard K-bus communication, and other modules used via the E-bus signal EtherCAT, the BK1250 interface must be used, connecting the K-bus and the E-bus terminal to the KL2545 module.

The control card of the tested hydraulic proportional valve receives an analogue bipolar signal between -10 V and 10 V. The EL4008 output card outputs an analogue voltage signal from 0 to 10 V, and therefore the signal must be adjusted. To adjust the signal, the Wago Jumper 857 bipolar isolation amplifier is used with the option of different configurations.

2.3 Control and measuring part

The program part of the measuring track is designed in two parts. A real-time program on a PLC takes care of all time critical tasks like measurements and control. The Windows application on the computer determines PLC state mode, and enables human interaction with the test through a graphical user interface.

The real-time code on the PLC is using more different program tasks. The “Main task” takes care of initialization and starting-stopping other tasks. It’s made as a state machine, and it changes its states in accordance with the chosen module in the Windows application. The task “Measuring velocity” activates for dynamical testing. With differentiation, the block calculates velocity from piston displacement and, further, with known cylinder geometrical data, calculates flow. The differentiation operation amplifies noise, so the differentiation block has an additional damping coefficient (Eq. 2) for high-frequency signal damping. The bad side of using a damping coefficient is its influence on the transfer function of the differentiation block so that the block output no longer represents correct physical representation of piston velocity. The output signal is, because of the damping coefficient, phase shifted, and with weakened amplitude in comparison to the real signal. In the transfer function, the damping coefficient represents an approximate period of frequency by which an amplitude gain characteristic breaks in the Bode diagram. This means that when the damping coefficient is chosen and changed with linear term to the input frequency, the signal will always be phase shifted with the same angle and weak end with the same constant for all frequencies. That can be compensated independently from the input frequency with addition and multiplication with constant gain from comparing ideal and damped transfer functions of the differentiation block. The task “Measuring velocity” also takes care of calculating the average piston position used in the regulation of piston central position.

$$G(s) = \frac{T_S \cdot s}{1 + T_D \cdot s} \quad (2)$$

$$G(s) = \frac{1 \cdot s}{1 + \frac{1885 [\text{ms}]}{2 \cdot \pi \cdot f} \cdot s} \quad (3)$$

Valve control is done with the task “Valve control”, which generates sinus function with chosen amplitude and frequency, translates chosen values to output modules, and takes care of the central piston position control. Because of asymmetry in measuring a track hydraulic system and transition between different measuring frequencies, the volume of fluid flows on both sides of the measuring cylinder not perfectly equally, that consequently causes the piston to drift to one side.

Although the drift can be compensated for in the measured results, the piston will eventually drift to the side of the cylinder and hit the wall, which will prevent further testing. That’s why there is a need for maintaining the center position of the piston in the cylinder with control. Direct control of piston position is impossible, because it’s the quantity that we wish to measure. Piston sinusoidal movement central position can be only maintained with indirectly controlling the average piston position through shifting the sinus input control signal. Average piston position is calculated from output data for at least ten periods of the input signal, and with a PID controller used for shifting the input signal.

The graphical user interface is made from different program windows for different modules. The user must first set proper drive settings for the tested valve. Then, in another window, it can control valve opening manually. The main parts of the graphical user interface are windows for step response and frequency characteristic measurement. The step response module enables the user to set the percentage of step input signal and capture a real time graph of the step response. The frequency characteristic module (Figure 2) enables the user to test every chosen frequency manually, or automatically to the specified maximal frequency. The user can monitor in real-time the input signal, the output signal, and average piston position. Both amplitude gain and phase characteristics are plotted on a graph and can be exported later.

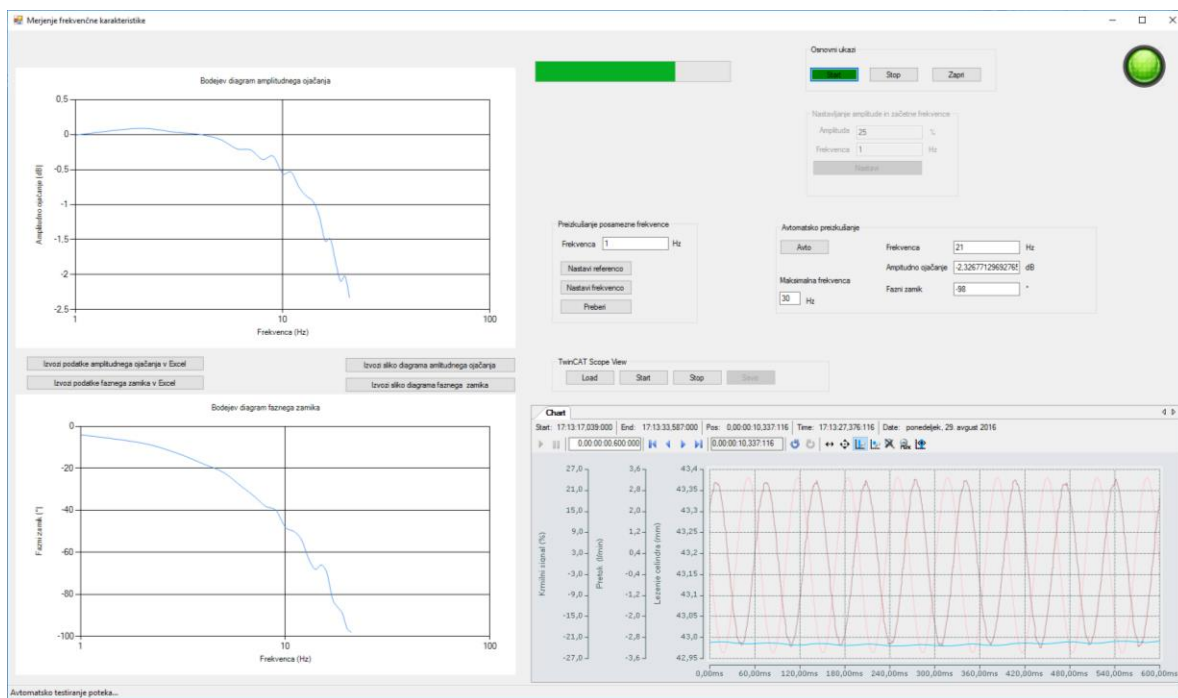


Figure 2: Frequency characteristic module

3 Results

3.1 Measuring procedure

The designed measuring track allows testing of frequency characteristics and step response with the following procedure. The user must first install a valve on the testing track correctly. Then he must connect electrical coils or control card inputs to the output module of PLC properly. In the program, the user must then choose the voltage or current control and set proper limits. The hydraulic supply unit should be set on proper parameters, so that pressure on the pressure regulator doesn't fall below demand. In accordance with the Standard, before testing, the valve should be moved a couple of times with the program manual mode, to avoid the valve sticking at the beginning of the test. In the next step, the user chooses the step response test or frequency characteristics test, and measurement points according to the Standard and collect the required data.

3.2 Hydraulic accumulator influence

The Standard predicts use of a hydraulic accumulator for minimization of fluctuation in the hydraulic power supply, but it does not recommend directly the size of the accumulator. In the Standard is just the demand that, for valid measurement supply, pressure shouldn't fluctuate more than $\pm 2,5\%$. For our measurement track, we tested the use of a hydraulic accumulator with volume 0,75 L, 2 L and measuring without a hydraulic accumulator.

The hydraulic accumulators were fitted with a recommendation for shock absorption on 80 % of supply pressure. Without a hydraulic accumulator, pressure can fluctuate out of the permissible limits. With both accumulators pressure fluctuation did not violate limits, but a bigger accumulator was, as expected, better, so it was chosen for our measuring track. The bigger accumulator will also allow testing of valves with greater flows.

The difference between measured amplitude and phase characteristic with different sizes of accumulators is not noticeable, or is smaller than the precision of the measurement track. A small difference was only observed in characteristics` measurement without an accumulator in a low-frequency area.

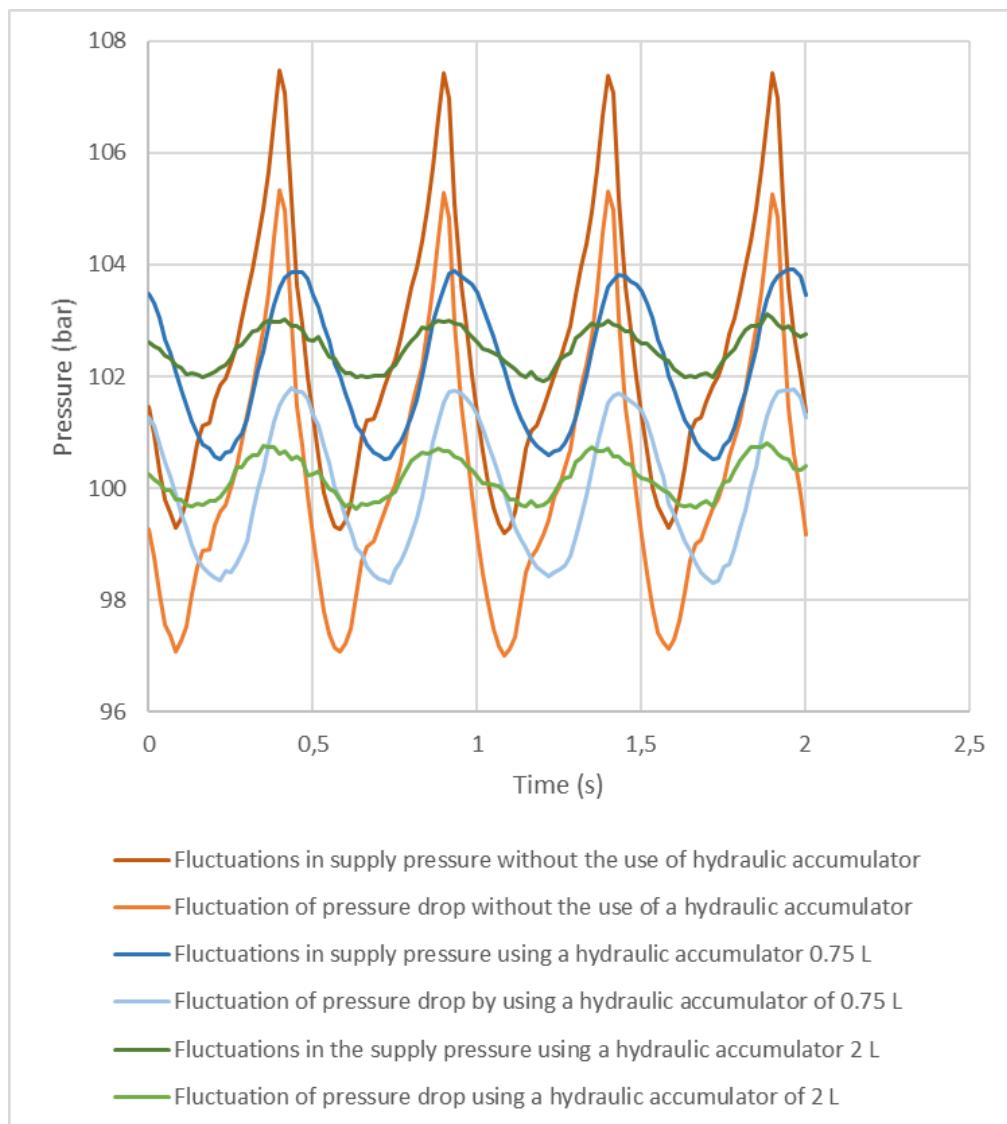


Figure 3: Hydraulic accumulator influence

3.3 Frequency characteristics

For testing of the measuring track, we have measured frequency characteristics for both proportional valves. For the control valve, we used all five measuring points control signal amplitudes defined by the Standard. Problems were in high frequency's and low amplitude control signals amplitudes. Because of small amplitudes in the measured displacement of the piston, the measured characteristic has some fluctuation in that area. Otherwise, the measurement repeatability is good, which we proved with more measurements. Fluctuation of phase characteristics disables the comparison between phase characteristics of the same valve for different input signal amplitudes, but the comparison between phase characteristics of different valves is still possible.

When testing the proportional current driven valve some problems occurred due to its positive overlap and, consequently, nonlinear characteristics. Valves with positive overlap should be, in accordance with the Standard, tested with shifted control signal, which disables use of a measurement cylinder. For using this valve type for our measurement track testing, we lowered the influence of positive overlap with zero zone elimination, so that the control signal doesn't change linearly through zero value, but in the zero zone area change in the step from the value that

has still open valve in one direction to the value that the already open valve has in the other direction.

Despite zero zone elimination, due to valve nonlinearity, the output signal is still not perfectly sinusoidal, but its periodic and smooth zero crossing allows good measuring for amplitudes of input signal amplitudes higher than 10 %. For lower amplitudes` measurement, the zero zone elimination should be more precise for valid results. So, results for these values are not plotted in the graph.

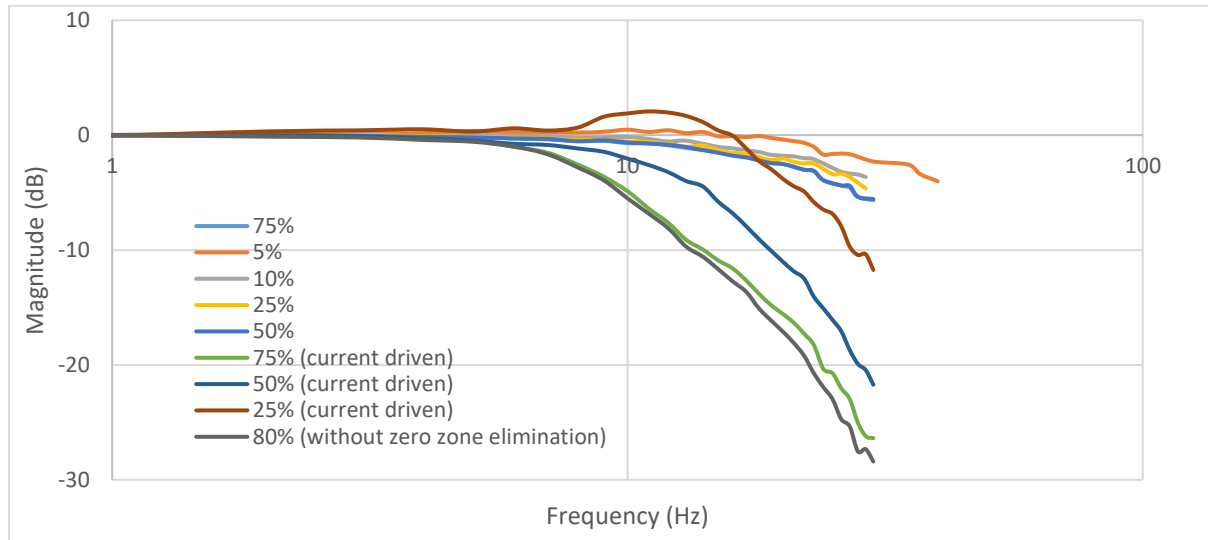


Figure 4: Amplitude characteristics

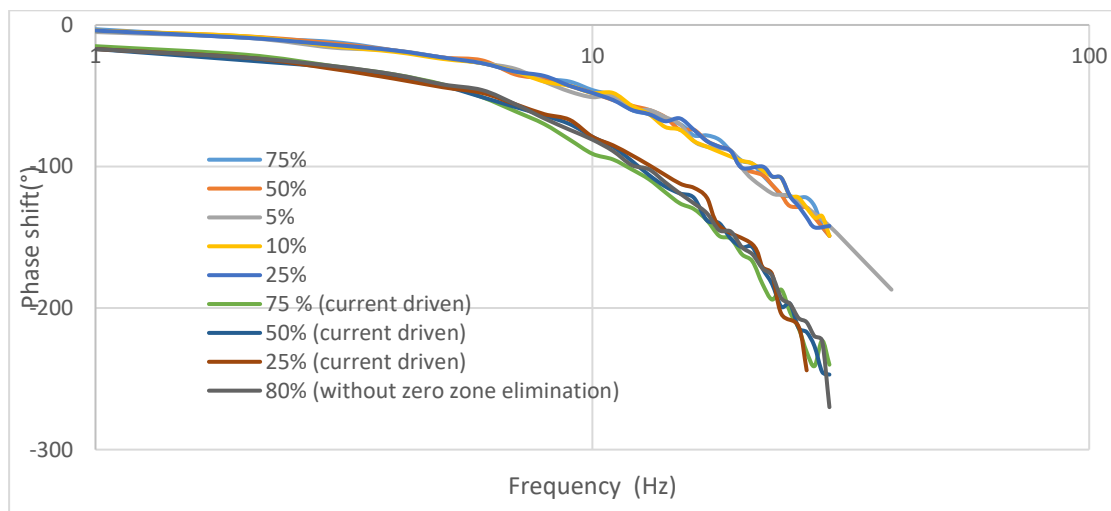


Figure 5: Phase characteristics

4 Step response

With step response measurement, a problem appears with choosing the right damping coefficient for the differentiation block. A damping coefficient in the amount of 100 ms ensures a flow function without noisy signal, but also results in a longer response time, which is the consequence of damping and not a valve response. A damping coefficient in the amount of 10 ms provides a very noisy signal, which makes reading from the plot difficult, but the response is faster – Figure 6. So, it is very difficult to measure the exact response time of just the valve. But, with the use of

the same damping constant, we can still compare two different valves very well, or evaluate the impact of fluid parameters on step response.

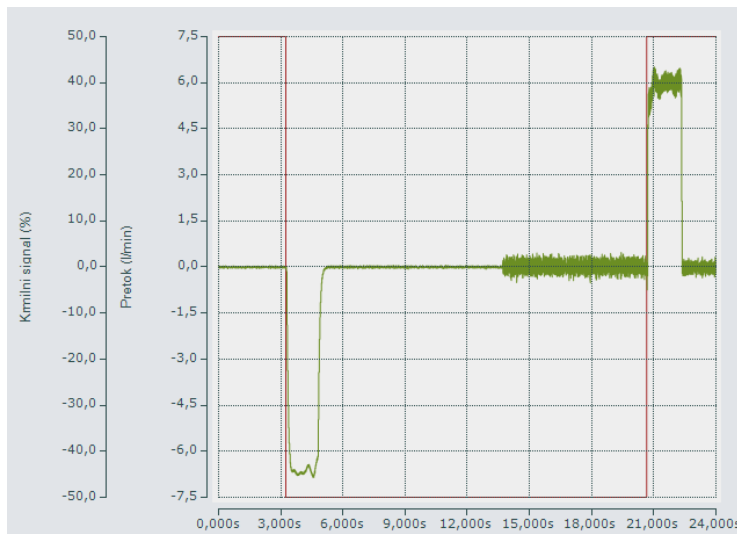


Figure 6: Step response with 100 ms damping coefficient and 10 ms damping coefficient
4. Conclusion

The constructed measuring track allows testing of all dynamical tests listed in the Standard, of course with limitation in amplitude, frequency, and precision of measurement. Physical construction satisfies all the Standard's demands, except the recommended viscosity grade for the used hydraulic fluid. But, the latter does not represent a major problem, since, in the forefront of the measurement, is the comparative measurement of the characteristics of different valves with the same medium. Measured data are still consistent with the Standard if the used fluid viscosity grade is listed by results. For testing valve characteristics with other types of hydraulic fluids, this Standard demand becomes irrelevant.

The program part of measuring track work is good, only in the high-frequency range with some scatter in the phase characteristics. The future development of the measuring track should go in the direction of test process simplification for the user, and explore the possibilities of providing the highest accuracy of measurements. The precision of measurement should also be evaluated so that results can be classified in one of the Standard measurement classes.

References

- [1] ISO 10770-1, "Hydraulic fluid power-Electrically modulated hydraulic control valves- Part 1: test methods for four-port directional flow-control valves", ISO, 1998.
- [2] Jelali, M., Agazarian, Y. M., Kroll, A.: Hydraulic Servo-Systems: Modelling, Identification and Control, Springer, London, 2nd edition, 2002
- [3] Reichert, M.: Development of high-Response Piezo-Servo-Valves for Improved Performance of Electrohydraulic cylinder Drive, Doctoral Thesis, RWTH Aachen, Germany, 2010
- [4] Merkle, D., Schrader, B., Thomes, M.: Hydraulics Basic Level. Festo Didactic KG, 2003
- [5] Scholz, D.: Proportional hydraulics. Esslingen: Festo Didactic KG, 1996
- [6] Pahič, R.: Methods for determining the performance characteristics of hydraulic directional control valves, University of Maribor, Faculty of mechanical engineering, Master thesis, 2016

Problems of testing new hydraulic fluids

MILAN KAMBIČ & DARKO LOVREC

Abstract One of the more important tasks to be performed by any hydraulic fluid is to prevent direct contact of two metal parts. Producers of hydraulic components take this task very seriously and pay significant attention to it. Therefore, a large number of standardized tests have been developed and used in order to establish the relation between the fluid condition and the lubricating properties, and its effect on the component wear.

When it comes to a known type of hydraulic fluid, this does not represent a major problem. In the case of completely new types of fluid, it is a very different situation. So, we cannot rely directly on most of the known standards and known testing procedures.

This paper discusses the usability of different tests for testing of hydraulic fluids, with respect to a variety of tested hydraulic components, test loading profile, energy consumption, and the cost-effectiveness of the test.

Keywords: • hydraulic fluid • mechanical tests • pump tests • hydraulic components • durability • cost effective testing •

CORRESPONDENCE ADDRESS: Milan Kambič, OLMA d.o.o., Poljska pot 2, 1000 Ljubljana, Slovenia, e-mail: milan.kambic@olma.si. Darko Lovrec, Ph.D., Chairperson of the Fluid Power 2017 organising committee, Associate Professor, University of Maribor, Faculty of Mechanical Engineering, Smetanova ulica 17, 2000 Maribor, Slovenia, e-mail: darko.lovrec@um.si.

<https://doi.org/978-961-286-086-8.27>

ISBN 978-961-286-086-8

© 2017 University of Maribor Press

Available at: <http://press.um.si>.

1 Introduction

The tests concerned with lubricating properties and the service-lives of hydraulic components usually use techniques and procedures similar to those occurring during the actual component usages. Testing is performed in approximately identical environmental conditions as during actual use: The temperature conditions, presence of contamination, water, metals, alternating pressure ... but, in most cases, the operating conditions are tightened up (higher lubricant temperature, higher circulation number ...).

Usually the time necessary for testing a new hydraulic fluid under actual, real operating conditions is not available. Such testing would last too long (even several years). The results are wanted sooner than by testing in real and at normal component use conditions, so various different procedures of faster component degradation are used under harsher conditions of use. The results can be gained in a reasonable time by retaining all the characteristics of functioning conditions since matters are only accelerated. The solution to the problem is the use of various methods of accelerated testing on purpose-made test stands.

For these purposes, we generally use two types of tests: Mechanical tests and thermal tests. When the wear of the hydraulic components is at the forefront, the mechanical tests are preferred.

2 Mechanical testing of hydraulic fluid

Hydraulic fluid specifications themselves are not enough to assure that the hydraulic fluid used at normal operating conditions will provide adequate protection over the desired timeframe. Specifications provide a basis for performance, but the reality in today's environment is that equipment demands have increased, which has, in turn, increased the need for the fluid to perform properly in much harsher conditions.

So how does the lubrication industry measure or evaluate a hydraulic fluid's ability to perform under harsher conditions if the specifications haven't changed? There are a number of industry tests to answer this question [1]. Some of them are standardized, the others for targeted testing (tailored testing) or are adapted.

In addition to pump testing, mechanical testing of hydraulic fluids using laboratory testing devices, such as four-ball, pin-on V-block, Timken anti wear test ... are run for determination of anti-wear properties. When a standard vane test is performed, the criterion of failure is the total weight loss on both the cam rings and vanes. When testing is conducted using a standard gear testing rig such as the FZG gear test, the testing criterion is the number of load increases to failure, or failure stage. In both cases, pump tests or bench tests, the performance is compared to the minimum standard specification.

Simple pump tests are desired to determine particular properties of hydraulic fluids under increased load. Recently, it has been necessary to develop a pump testing protocol to evaluate the changing properties of rapidly biodegradable hydraulic fluids. The objective is to develop fluids with longer lifetime and to improve the performance of these, or to check the usability the new type of fluids (as in our case). Such type tests are presented briefly below.

2.1 Testing for durability of components – standard pump test

The **FZG – ASTM D5182 test** (Figure 1) is commonly used for gearing power transmission, used on many automobile and industrial applications. The test is also reliable with respect to predicting steel-steel contact wear, when using hydraulic oils.

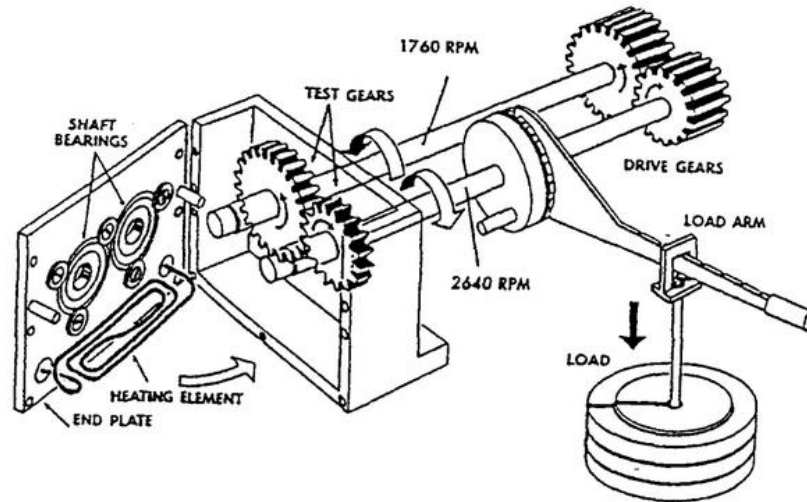


Figure 1: Schematic illustration of the FZG gear test machine [1]

The most direct way to assess durability is to extend the duration of the current standard pump tests and run the tests at higher temperatures. Standard industry pump tests, using Denison's vane pump, the Eaton-Vickers vane pump, and the Sundstrand piston pump, provide the use of mineral based hydraulic oil. Features with test data are summarized hereinafter.

To determine retention of performance, the test fluids were saved and re-evaluated in the standard ASTM bench tests typically used to evaluate hydraulic fluids. The **Denison HF-O specification/test** (Table 1) was chosen because of its comprehensive nature, in that it evaluates all aspects of a hydraulic fluid. The Sundstrand and Eaton/Vickers pump tests were designed to measure durability of the hydraulic fluid.

Table 1: Denison Vane Pump Test – operational conditions [2]

Fluid volume	189 L
Test temperature	71 °C for 60 hours 99 °C for 40 hours
Test duration	100 hours (4 days)
Pressure	cca. 172 bar
Pump speed	cca. 2400 rev/min
Flow rate	265 L/min
Power	90 kW

The layout of the test rig using the Denison HF-O is shown in Figure 2.

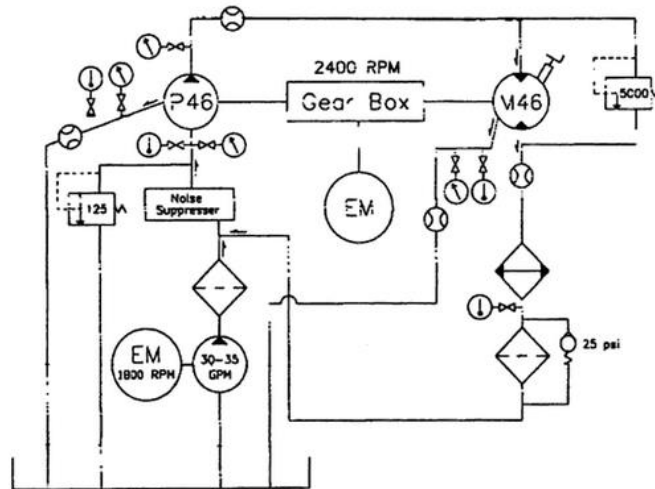


Figure 2: Schematic of the Denison P46 piston pump test according HF-O protocol [2]

The **Sundstrand piston pump test** was run initially under standard conditions with hydraulic (mineral oil based) fluid formulated with anti-wear additives, and it passed all the criteria established for the test. A **second Sundstrand pump test** was run under the same conditions, extended to 450 hours, or double the length of the standard test, and it also passed (Table 2).

All components are assessed visually for signs of wear and discoloration at the end of test.

Table 2: Sundstrand Piston Pump – Series 22 [2]

Fluid volume	45 L
Test temperature standard elevated	82 °C (1 % water content) Heat stressed 120 °C (no water)
Test duration – standard Test duration – extended	225 hours (9 days) 450 hours (19 days)
Pressure	cca. 345 bar
Pump speed	cca. 3100 rev/min
Flow rate	95 L/min
Power	64 kW

The Sundstrand pump test included 1 % water contamination to stress the fluid further. Even with the added water, there was no evidence of any hydrolytic reactions that could cause the formation of precipitates. Contamination from precipitates leads to blocked valves and filter-plugging problems [2].

Another round of Sundstrand pump tests was run at an elevated temperature of 120 °C. Due to the higher temperature, no water was added to this test, and all other conditions remained the same. This round of tests showed that the hydraulic fluid with the premium hydraulic additive package had the endurance to exceed the performance parameters of the Sundstrand piston pump without difficulty, despite the higher temperature and the extended length of the test.

The next phase of testing involved the Eaton-Vickers vane pump **35VQ-25** (Table 3), which ran for extended hours to determine the durability of the hydraulic fluid containing an anti-wear additive package. After 1,000 hours the pump was still below the weight loss limit for total ring and vane wear. [2]

Table 3: Eaton/Vickers 35VQ-25 – ASTM D6973 vane pump test

Fluid volume	196 L
Test temperature	93 °C
Test duration – standard	50 hours (2 days)
Test duration – extended	1,000 hours (42 days) with inspections at 300 hours)
Pressure	cca. 207 bar
Pump speed	cca. 2400 rev/min
Flow rate	144 L/min
Power	58 kW

Figure 3 illustrates, as an example, how the hydraulic fluid was robust enough to exceed the parameters of the test by a large margin. Criterion for wear is the size of weight loss and known performance reserve – at known values for a known pump. [4]

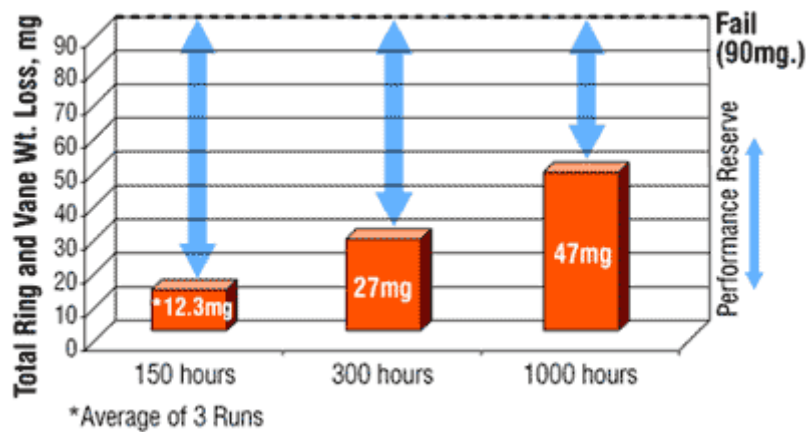


Figure 3: Loss of weight Eaton/Vickers 35VQ-25 – ASTM D6973; standard vs. extended length test

For the Eaton/Vickers 35VQ-25 – ASTM D6973 test a precisely determined type of Vickers vane pump is used built to a 196 L tank. A piston pump is used for the similar **Komatsu 500 hour test**.

In distinction to other tests based on pump wear at constant loading and presence of increased temperature and pressure, the profile of applying pressure to the pump is constant, or is alternating within the test. After the test's completion, the pump is disassembled and all internal parts are measured. Simultaneously, the oil analysis is executed for the presence and concentration of wear metals.

2.2 Low volume mechanical tests

The presented pump test procedures for determining the anti-wear properties of hydraulic fluids are expensive to undertake, have long test duration, require a large quantity of test fluid, and are costly in respect to the energy consumption.

The alternative vane pump test is the Lapotko s.c. "MP-1 test" – schematic is shown in Figure 4. Although the MP-1 may be run at pressures up to 10 MPa the reported pressure is 7 MPa, with a total fluid volume of 0,7 L. In addition to lower volume, the MP-1 test is conducted for only 50 h (and in some cases only 10 hours). The wear rate is based on the weight loss of the vanes only

after the test is completed. In view of the relatively same size, this test comes close to a “bench hydraulic pump test”. [2]

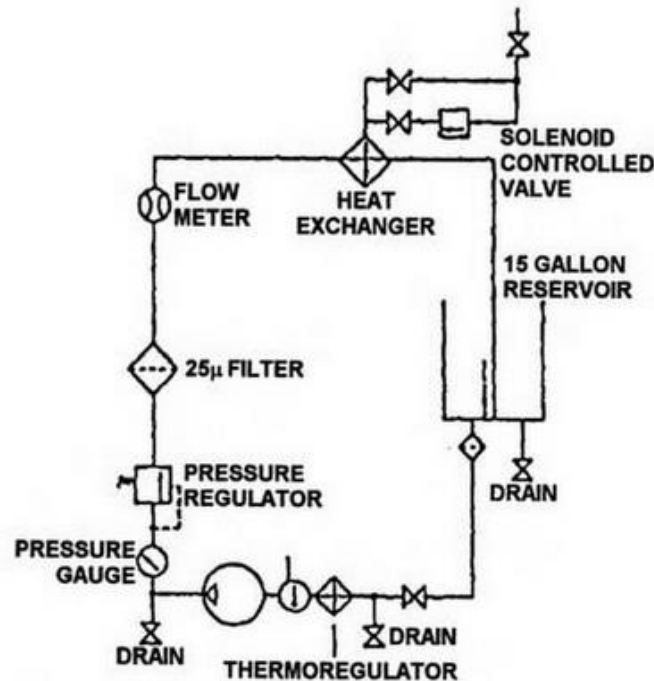


Figure 6: Test circuits for the Vickers V-104 vane pump test

Bosch (Racine fluid power) utilized a cycle pressure vane pump test. The pressure time sequence and the test circuits are illustrated in Figure 5.

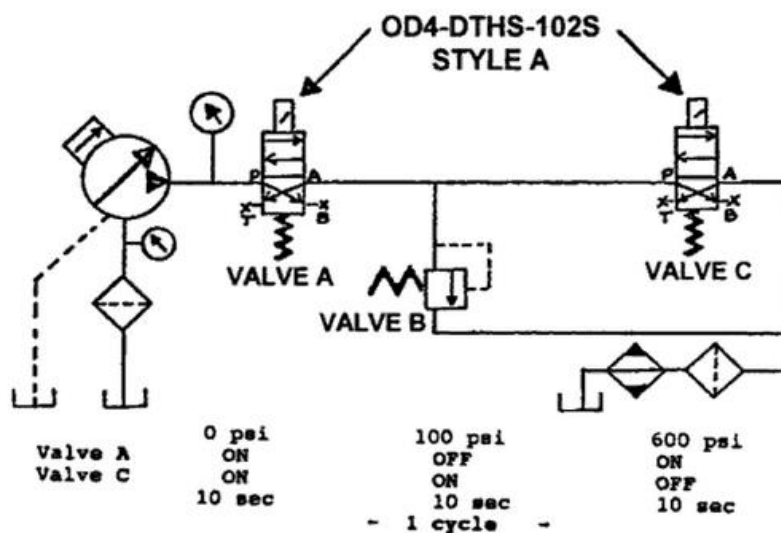


Figure 5: Test circuit for Racine cycled pressure, vane pump test utilizing 5.5 kW electric motor, SV-10 vane pump and a 70 L reservoir

This is reported to be a more representative test as it incorporates pressure spikes that will invariably occur in a hydraulic system during circuit activation and deactivation better. At the conclusion of the test, the weight losses of the ring, vanes, ports and cover plate and body and cover bearings were measured. The ring and bearing were inspected for unusual wear patterns and for evidence of corrosion, rusting and pitting.

The Vickers V-100 vane pump and the test circuit in Figure 6 continue to be the most commonly utilized hydraulic pump test. There are at least three national Standards based on the use of this pump: ASTM D-2882, DIN 51389, and BS 5096. The total loss of the vanes plus ring at the conclusion of the test is the quantitative value of wear. [2]

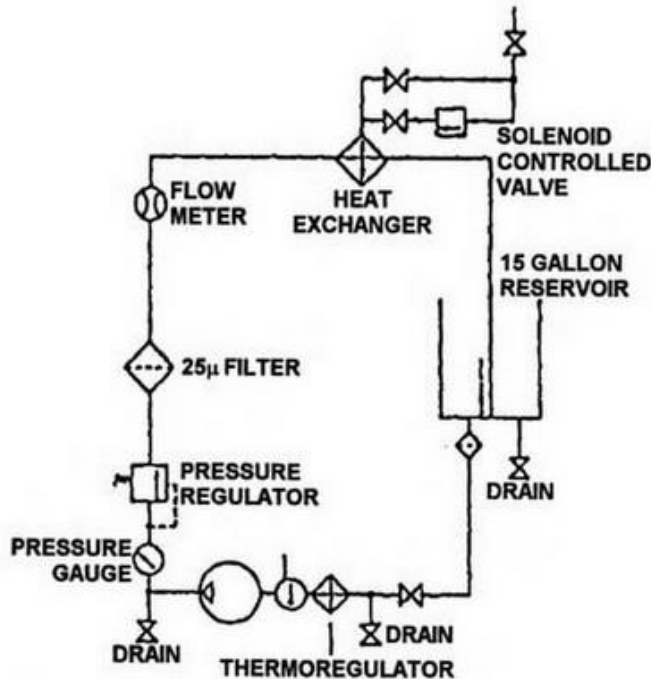


Figure 6: Test circuits for the Vickers V-104 vane pump test

Additionally, such test is a 100-hour low volume hydraulic pump test that utilizes only 1,3 L of fluid (Glancey) This test utilizes a Vickers V10-1P3P1A20 vane pump with a 9,84 cm³/rev displacement. The hydraulic circuit is shown in Figure 9. [2]

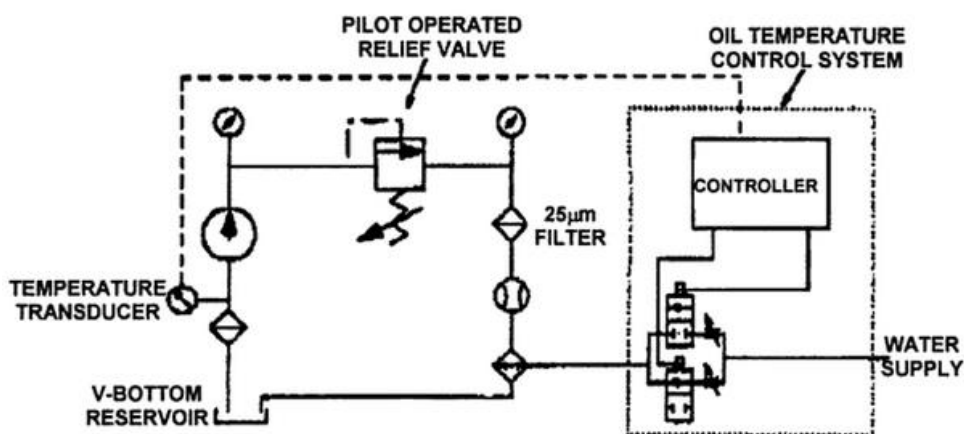


Figure 7: Low-volume hydraulic and temperature control schematic

3 Test features review

Conclusion regarding some presented tests: In the case of testing a completely new hydraulic liquid, we tend to prefer an alternative low-cost bench screening procedure, of short duration, requiring a small quantity of test liquid, using real diverse hydraulic components, not only a pump.

The main characteristics of the presented and similar mechanical tests:

- a) Mainly with the use of different types of mineral based hydraulic oils.
- b) Wear/impact on the component – pump: Just observing the changes in wear or weighting the loss of mass, or any observation the effect on components – only the changes of physical-chemical parameters of lubricant.
- c) Operating pressure while testing: Constant operating pressure during the test or, in some cases, alternating pressure.
- d) Fluid volume: Standard test (45 L to 200 L), small volume test up to 20 L.
- e) Circulation number $Q_{\text{Tank}}/Q_{\text{Pump}}$:
 - Denison: 1: 1,4
 - Sundstrand: 1:2,11
 - Eaton/Vickers: 1:1,36
- f) Energy consumption during the test. Energy to power the system and the cooling energy
Standard test: Up to 90 kW, small volume test: Up to 7 kW.
- g) There are no conclusions in regard to the other components e.g. valves, cylinders, filtering, seals... The suitability of the test for testing a completely new type of fluid is a great unknown.

The results presented here show that there is little, if any, direct correlation between the wear obtained by the ASTM D-2882 using the Sperry Vickers V-104 vane pump and the other proposed testing procedures using e.g. a 20VQ5 pump. These differences are most likely due to the differences in the vane design of the two pumps, and to the expected differences in lubrication requirements resulting from differences in vane loading and pump speed. It is recommended that these problems be examined systematically in order to model better at least nearly equivalent tribological testing conditions with both pumps and, perhaps more importantly, to create realistic testing regimes that model better unavoidable fatigue failure of the pump components. This concern or deficit is minimized when using up-to-date pump design,.

In addition, it is recommended that the pump testing protocol utilize currently available technology better to optimize the quality of data being obtained from the test. Some possibilities include:

1. Measurement of pump leakage and torque over the duration of the test in order to obtain a better measure of the break-in properties of the fluid in the pump, and to determine if wear stabilization has been achieved at the conclusion of the test.
2. Pump wear performance should be monitored continuously and a written record of any changes in the pump performance, and other events, such as unexpected shut-downs, should be reported at the conclusion of the test.
3. Wear measurement should not, indeed must not, be limited to the vanes and the rig. Measurement, or at least visual analysis must be made of other components such as bushings and bearings, metal compatibility, and failure modes. These should be photographed and be required as part of the final report.

If the pump is to be operated in excess of its design limits, some assurance must be made that the wear data obtained is actually due to the lubrication properties of the hydraulic components. That is, the data obtained should make tribological sense.

4 Valve testing methods

For all the methods mentioned above, the conclusions were related only to the pump. Other, also heavily loaded components of the hydraulic system, e.g. valves, were not even mentioned at all.

The test method suitable for valves should allow testing under variable conditions ranging from real to extreme. Therefore, an appropriate test rig should be used, to determine the correlations between operating conditions as input variables and valve performance criteria as output variables during a preliminary test series.

4.1 Wear types inside hydraulic valves

Tribological systems in general are subject to different types of wear. Three of these types of wear are dominant in hydraulic valves (see Figure 8): Erosion, three-body abrasion, and impact wear. The characteristics of these wear types and the factors governing wear behavior are discussed as follows.

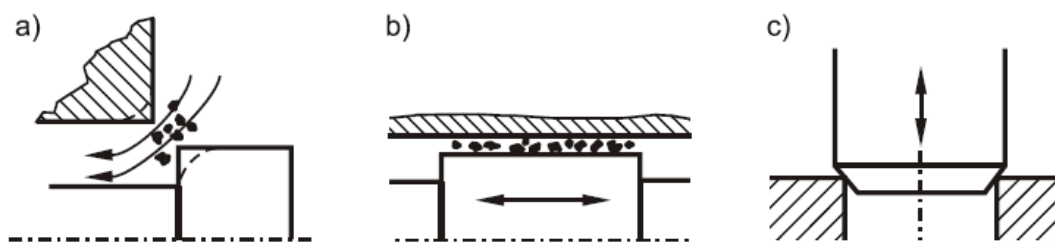


Figure 8: Valve wear mechanisms: a) Erosion, b) Three-body abrasion, c) Impact wear

4.1.1 Erosion

In spite of any filtering measures, fluid power circuits are invariably subject to contamination with solid particles. When passing component walls and edges with high velocity, suspended particles affect erosive wear on the component material by washing it off subtly. This type of wear affects both spool and poppet valves, particularly at small valve openings with narrow flow channels, and all kinds of valve components – spool, sleeve, housing, poppet, and seat –, when they are paired tribologically with solid contaminants. Depending on the valve type, erosive wear phenomena are perceptible in the rounding of metering geometry, such as spool edges, spool notches, and sleeve orifices, or sealing geometry, such as poppet or seat edges.

4.1.2 Three-body abrasion

When relative motion is imposed on the valve components in the presence of solid contaminants, abrasive wear occurs. This type of wear affects mainly spool valves during operation of the spool. The tribological pairing, in effect, consists of the spool, any solid particles, and the housing or sleeve. Component material is sheared off by the particles entering the valve gap when the components are moved. The results of three-body abrasion can be observed in gap widening and deformation of the housing.

4.1.3 Impact wear

In poppet valves, the poppet is frequently pressed into the seat with high velocity and energy when the valve is closed. Especially in pilot-operated valves, this implicates wear due to the impact of the components of the tribological pairing comprising poppet and valve seat. During continuous operation, material can be cracked out of the geometry under stress, resulting in fractures or pitting at the sealing edge or the seat. ([5] – [9])

4.1.4 Wear parameters

The tribological parameters governing the wear process inside hydraulic valves have been the subject of various investigations. Wear has been found to be aggravated mainly by the conditions (Figure 9), of which only those marked in italics are examined at the wear test rig.

Category	Parameter
Fluid contamination	<i>High particle concentration</i>
	Distribution of particle sizes centred around gap height
	Abrasive particle type (protrusive shape, high hardness)
Flow conditions	<i>Low fluid viscosity/high temperatures</i>
	<i>High flow velocities</i>
	<i>Large pressure drops</i>
Duty cycle	<i>Large valve command amplitudes</i>
	<i>Large valve command gradients/high spool velocities</i>
	<i>High impact energy when closing poppet</i>
Geometry	Small gap length/gap height ratio
	Small effective wear area
Material	Low component hardness

Figure 9: Wear influencing factors according IFAS test [8]

4.2 IFAS-accelerated valve wear test

An IFAS test rig is designed for the examination of three-body abrasion, erosion, and impact wear in hydraulic directional spool and seat valves. Certain influence parameters from the fields of fluid contamination, flow conditions, and duty cycle, are investigated experimentally. The focus is set on fluid contamination with ISO MTD (A3) test dust, as this is anticipated to accelerate the wear process significantly. The following Table summarizes the boundary conditions for the accelerated aging test – Figure 10.

	Spool valve	Poppet valve
Size	NG 6, 24 l/min	NG 10, 80 l/min
Operation type	direct-operated	pilot-operated
Geometry	Spool/sleeve	Conical poppet/cylindrical seat
Contaminant	ISO 12103-1 Medium Test Dust (A3), particle size < 120 µm, hardness 1100 HV	
Max. flow rate	min. 70 l/min	
Max. pressure	min. 300 bar	

Figure 10: IFAS test parameters and test conditions [8]

The cycle depending wear of the 4/3-way proportional valves has to be measured under different load conditions. Thus, a resistor is required to simulate different loads on the working ports of the valve. Conventional pressure relief valves and orifices underlie the same wear mechanisms as the tested valves and affect particle concentration, material and size distribution in the test fluid, leading to non-stationary testing conditions.

Replacing the resistor by a second valve of the same type as the test valve avoids further influences on the particles in the test fluid. Moreover, a gradient adaption algorithm affecting the load valve's input signal is able to compensate wear effects on both valves, maintaining the required stationary testing conditions.

This test has some limitations:

- Using the test dust is not equal to the reality,
- Two proportional valves are “spent”,
- Information is obtained only for the valves,
- No information regarding other components e.g., cylinder seals, and, in the case of other liquids, the compatibility with different materials used within hydraulic components.

5 Proposal for a combined test facility

On the basis of the presented important tests, which are limited to only one component in the hydraulic system, it is reasonable to design a different concept of testing for a comprehensive insight. The starting points for the new test rig design:

- To determine the suitability of new fluid under real operating conditions,
- Using the variety of hydraulic components, of industrial quality, commonly used within hydraulic systems,
- Take into account the aspect of energy consumption,
- Take into account the scale of the test rig,
- Take into account the duration of the test,
- Take into account the cost of testing,
- The possibility of on-line monitoring of all important data,
- At certain intervals, to check the changes in the characteristics of the tested components,
- To use the standard test procedures, where possible,
- The possibility of cost-optimal repetition of the test,
- ...

In accordance with the above mentioned requirements, a test rig for the integrated testing of the impact of a new hydraulic fluid on all components of the hydraulic system was designed – Figure 11.

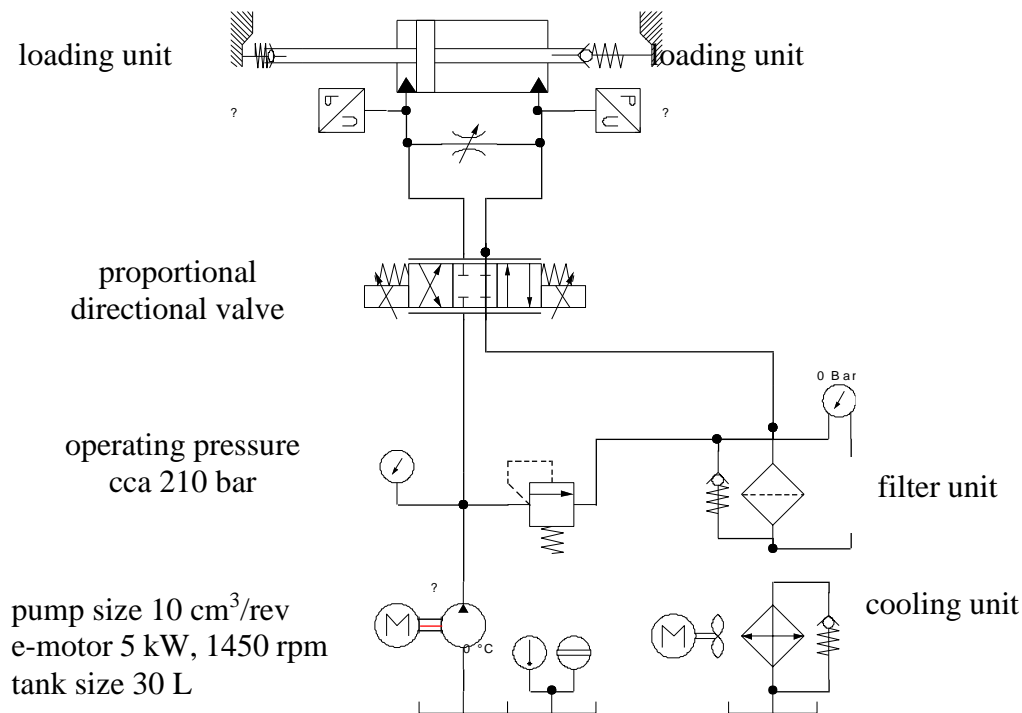


Figure 11: Layout of test rig for integrated testing; Fluid - components

The test rig allows insight into the pump wear, investigation of wear on vital parts of different valve types (control spool valve, poppet valve), the impact of the new liquid on a variety of materials used within other hydraulic system components (filter material, paint coat ...), as well as the on-line and off-line monitoring of the degradation process the components.

6 Conclusion

A number of methods are available to test the wear resistance of individual components, along with the known hydraulic fluid. Some have become standardized; others are dedicated and of internal nature, linked to a single manufacturer, either components or liquids. But, none of the represented methods allows a comprehensive insight into developments in all components of the hydraulic system when completely new hydraulic fluids are tested.

In addition, an additional problem of testing, especially those with pumps, is usually the very high cost of energy consumption (90 kW, several weeks), and testing under unrealistic conditions. For the purpose of testing new hydraulic fluids, a new test device concept has been designed and constructed, appropriate for the combined testing of as many hydraulic components as possible, in market quality. The testing is carried out under demanding, but still normal operating conditions, and with low energy consumption.

References

- [1] Totten, G. E.: Handbook of Hydraulic Fluid Technology, Second edition, CRC Press, Taylor & Francis Group, 2012
- [2] Totten, G. E., Kling, G. H., Smolenski, D. J.: Tribology of Hydraulic Pump Testing, Technology & Engineering, ASTM STP 1310, 1997

- [3] Totten, G.E., Bishop, R. J., Gent, G. M.: Evaluation of Hydraulic Fluid Lubrication by Vickers Vane Pump Testing: Effect of Testing Conditions, NFPA, Presented at the International Exposition for Power Transmission and Technical Conference 4-6 April 2000, Technical paper series I00-9.7
- [4] Light, D.: Hydraulic Fluids Meet Increasing Operating Demands, Machinery lubrication, 5/2005
- [5] Lawrence, M., Experimentelle und analytische Untersuchung der Verschmutzungsempfindlichkeit hydraulischer Komponenten, Dissertation, RWTH Aachen, Germany, 1989
- [6] Lehner, S., Verschleißwechselwirkungen in hydraulischen Komponenten durch Feststoffverschmutzung des Druckmediums, Dissertation, RWTH, Aachen, Germany, 1996
- [7] Zhang, K., Yao, J., Jiang, T., Yin, X., Yu, X.: Degradation Behavior Analysis of Electro-Hydraulic Servo Valve under Erosion Wear, 978-1-4673-5723-4/13/ ©2013 IEEE
- [8] Reinertz, O., Schlemmer, K., Schumacher, J., Murrenhoff, H.: Development of an Accelerated Ageing Test for Hydraulic Spool and Poppet Valves, 7th International Fluid Power Conference, Aachen 2010, 1 – 13
- [9] Weber, P., Schumacher, J., Murrenhoff, H.: Wear Characterization of Hydraulic Spool Valves by Means of Short Time Ageing Tests O+P Journal 1/2015
- [10] Amini, S., Abbaszadeh, S., Lotfi, M.: Measuring wear-resistance of AISI 1.7225 steel under various heat treatments: Hydraulic spool valve, Measurement 98 (2017) 179–185
- [11] Majdič, F., Pezdirnik, J., Kalin, M.: Comparative tribological investigations of continuous control valves for water hydraulics, The Tenth Scandinavian International Conference on Fluid Power, SICFP'07, May 21-23, 2007, Tampere, Finland, 1-12
- [12] Chenglong, W., Qingliang, Z., Zhihai, L., Hongxi, K.: Design and realization of durability test-bed for new developed hydraulic pump, Advanced Materials Research Online: 2012-12-13, ISSN: 1662-8985, Vol. 619, pp 518-521, doi:10.4028/www.scientific.net/AMR.619.518, © 2013 Trans Tech Publications, Switzerland
- [13] Reichel, J.: Mechanical Testing of Hydraulic Fluids, DMT-Gesellschaft für Forschung und Prüfung, Essen, Germany, Tribotest journal, 6-3, 2000 (6), 301 ISSN 1354-4063
- [14] Tkáč, Z., Drabant, Š., Majdan, Š., Cvičela, P.: Testing stands for laboratory tests of hydrostatic pumps of agricultural machinery, RES. AGR. ENG., 54, 2008 (4): 183–191

Conference sponsors

General sponsor

FESTO d.o.o.

Social event sponsor:

HAWE Hidravlika d.o.o.

Conference organization has been sponsored by:

HYDAC d.o.o.

OLMA d.o.o.

BECKHOFF Avtomatizacija d.o.o.

Maziva+ d.o.o.

POCLAIN Hydraulics d.o.o.

MIEL d.o.o.

HENNLICH d.o.o.

TESNILA BOGADI d.o.o.

PARKER Hannifin Ges.m.b.H.

Media sponsors:

VENTIL

IRT3000

**We would like to thank all the sponsors for their support and contribution
to the organization of the conference!**

FESTO



Vi potrebujete maksimalno fleksibilnost.
Vi iščete inteligentne in intuitivne rešitve.
Mi naredimo pnevmatiko digitalno.

→ **WE ARE THE ENGINEERS
OF PRODUCTIVITY.**

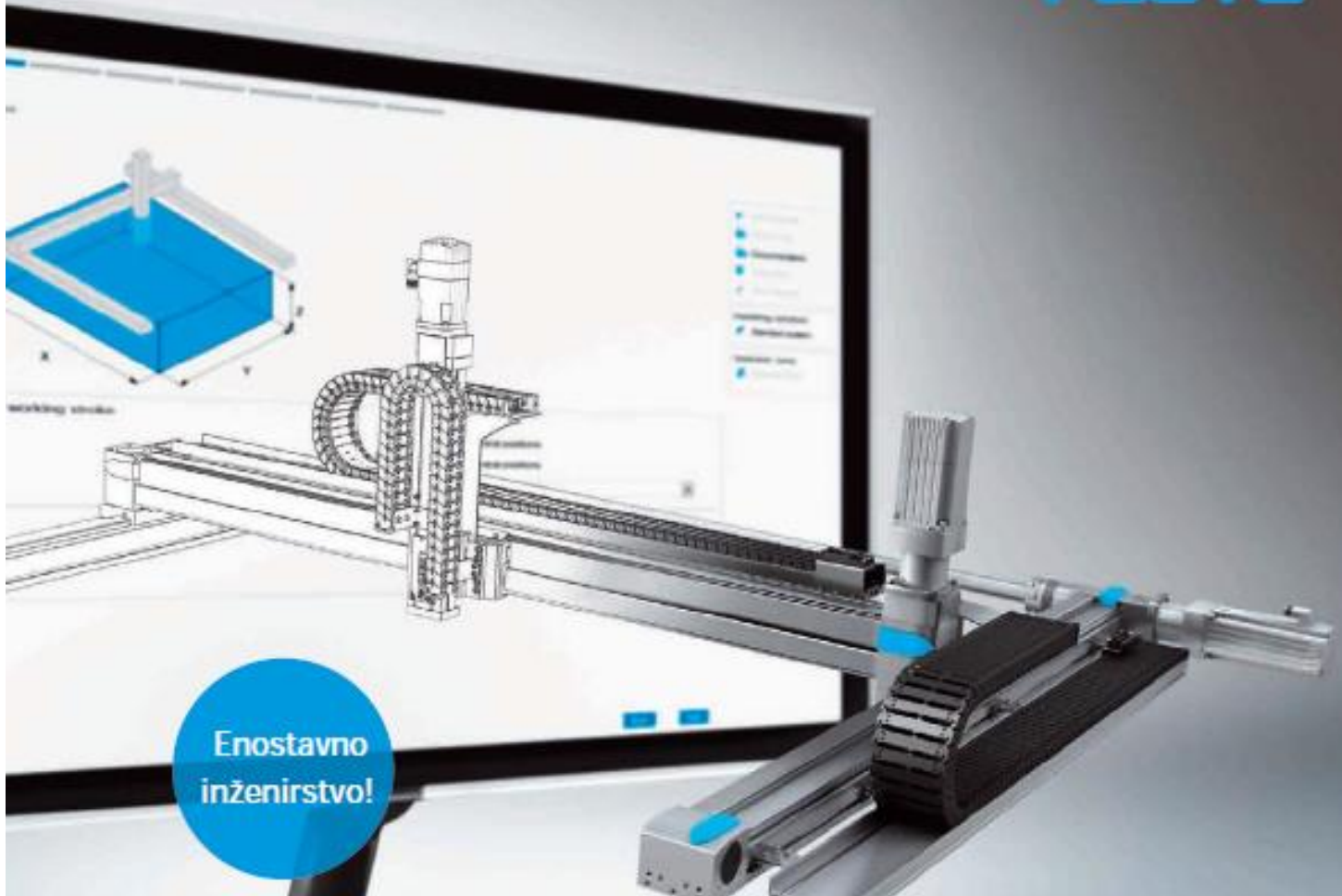
Prvi na svetu v digitalizirani pnevmatiki: Festo Motion Terminal VTEM

Festo Motion Terminal VTEM odpira radikalno nove dimenzije v svetu avtomatizacije. Je prvi ventil na svetu, ki ga upravljamo z aplikacijami. Združuje prednosti električnih in pnevmatičnih tehnologij za številne funkcije, ki trenutno zahtevajo več kakor 50 pozicij.

Festo, d.o.o. Ljubljana
Blatnica 8
SI-1236 Trzin
Telefon: 01/ 530-21-00
Telefax: 01/ 530-21-25
Hot line: 031/766947
sales_si@festo.com
www.festo.si



FESTO



Enostavno
inženirstvo!

Potrebujete kompletne sisteme.
Želite manjšo kompleksnost.
Smo vaš zanesljiv partner za rešitve.

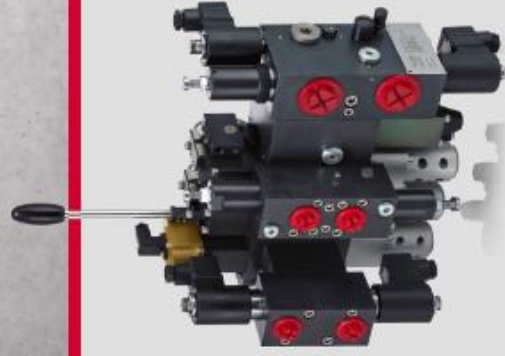
→ WE ARE THE ENGINEERS
OF PRODUCTIVITY.

Najti ustrezen sistem strege ne more biti hitreje in enostavneje:

Oblikujte in naročite vaš standardni strežni sistem v samo treh korakih s spletnim orodjem Handling Guide Online. Izbrani sistem vam bomo dobavili popolnoma preizkušen in sestavljen. Še danes preverite novo programsko orodje!

Festo, d.o.o. Ljubljana
Blatnica 8
SI-1236 Trzin
Telefon: 01/ 530-21-00
Telefax: 01/ 530-21-25
Hot line: 031/766947
sales_si@festo.com
www.festo.si

**The right partner
for compact & efficient
hydraulic solutions.**



HAWE Hidravlika d.o.o.

Petrovče 225 | SI-3301 Petrovče
office@hawe.si | www.hawe.com

Solutions for a World under Pressure

HAWES
HYDRAULIK

HYDAC

INTERNATIONAL

www.hydac.com

HYDAC - že več kot 50 let vaš zanesljiv partner za vse projekte, ki zahtevajo fluidno tehnologijo - hidravliko, elektroniko, inženiring.



HYDAC d.o.o., Tržaška c. 39, 2000 Maribor, tel.: 02 460 15 20, e-mail: info@hydac.si

A man with long brown hair, wearing a light green t-shirt and shorts, is climbing a large, reddish-brown rock face. He is positioned horizontally, with his head to the left and feet to the right. Below him, a waterfall cascades into a pool of dark blue water with white foam. The background is a mix of the rock's texture and the water's movement.

S pravim mazivom

ne spodrsava

OLMA
www.olma.si

Olma d.o.o., Poljska pot 2, 1000 Ljubljana,
tel.: (01) 58 73 600, e-pošta: komerciala@olma.si

Štiri komponente, en sistem: New Automation Technology.

IPC

- Industrijski računalniki
- Embedded računalniki
- Matične plošče



V/I

- EtherCAT komponente
- V/I moduli, IP 20
- V/I moduli, IP 67



Pogonska tehnika

- Servo pogoni
- Servo motorji



Avtomatizacija

- Programska oprema za PLC
- Programska oprema za NC/CNC
- Varnostna tehnologija



www.beckhoff.si

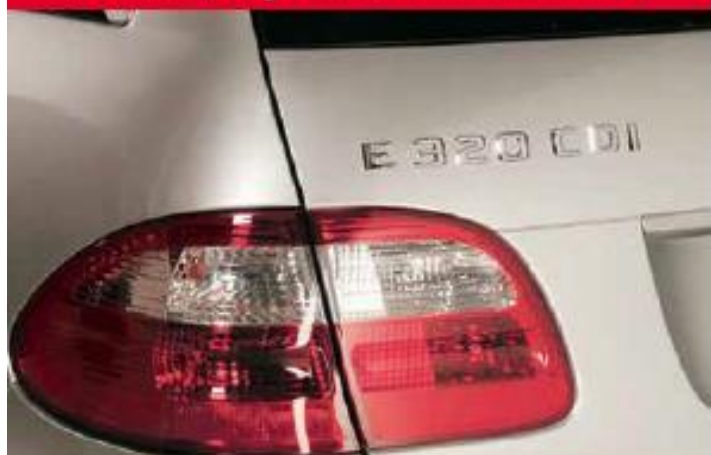
Pod sloganom „New Automation Technology“ podjetje Beckhoff ponuja opremo, ki lahko deluje samostojno ali pa je integrirana v druge sisteme. Industrijski računalniki, PC in „klasični“ krmilniki, modularni V/I sistemi in pogonska tehnika pokrivajo številna področja uporabe. Prisotnost podjetja Beckhoff v več kot 75-ih državah zagotavlja dobro podporo.

New Automation Technology

BECKHOFF



**Maziva za osebna vozila,
tovorni program in delovne stroje**



Maziva + d.o.o.

Mejna ulica 58

2000 Maribor

**Maziva in nega za motocikle,
motorne sani, ATV in kolesa**



PANOLIN[®]

Swiss High-Quality Oil

www.panolin.si



Okolju prijazna maziva



**H1 maziva za prehrambeno
in farmacevtsko industrijo**



HIDRAVLICNE NAPRAVE



Obdelovalni stroj



Hidromehanska oprema



Ladijski vitel

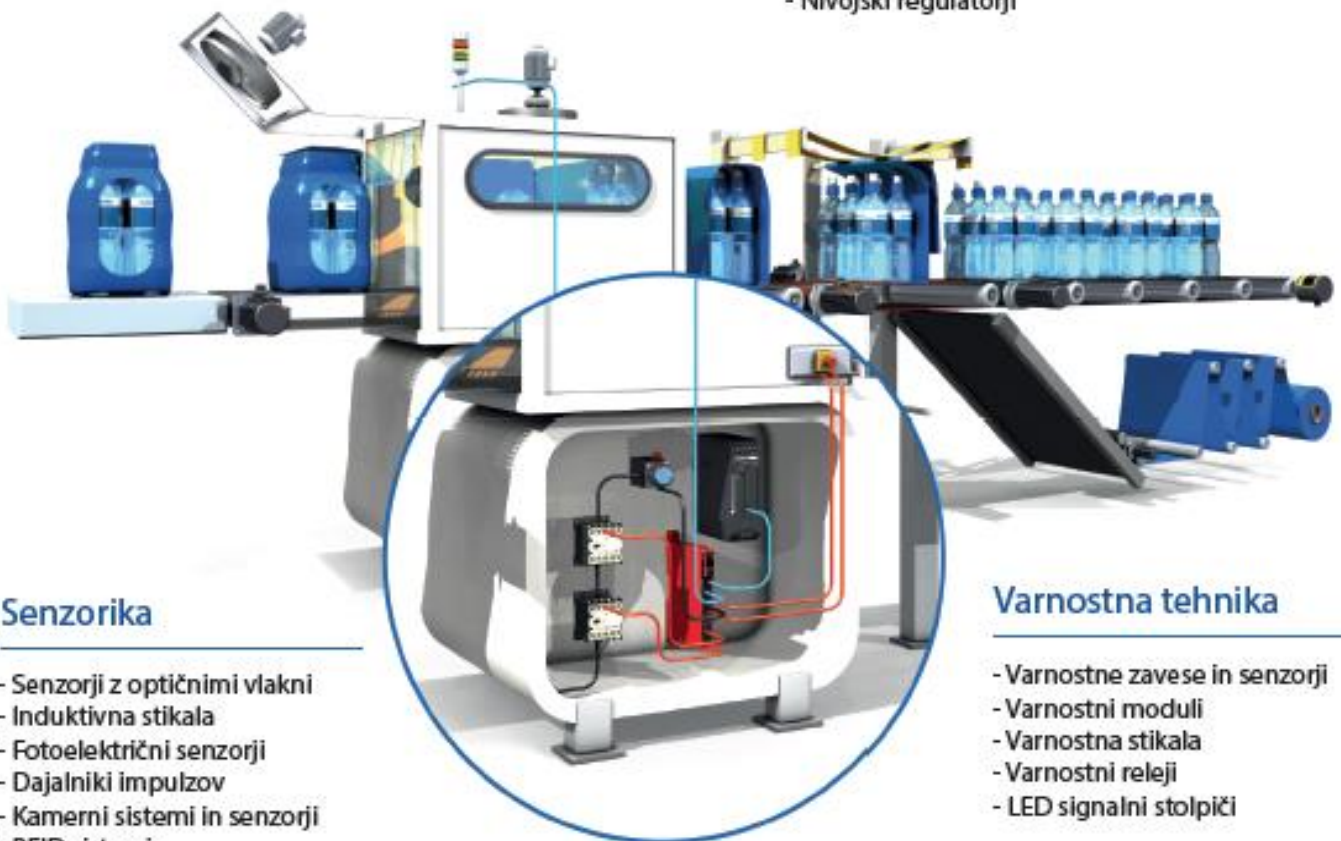
Vse za avtomatizacijo proizvodnje

Avtomatizacija in pogoni

- Industrijski krmilniki
- Krmilniki stroja
- Komunikacijska omrežja
- Operaterski paneli (HMI)
- Frekvenčni pretvorniki
- Servo sistemi
- Industrijski roboti
 - SCARA
 - DELTA
 - Mobilni roboti

Industrijske komponente

- Mehanski in polprevodniški releji
- Časovni releji
- Števci
- Programirljivi releji
- Stikalni napajalniki
- Temperaturni in procesni regulatorji
- Digitalni prikazovalniki
- Nivojski regulatorji



Senzorika

- Senzorji z optičnimi vlakni
- Induktivna stikala
- Fotoelektrični senzorji
- Dajalniki impulzov
- Kamerni sistemi in senzorji
- RFID sistemi

Varnostna tehnika

- Varnostne zavese in senzorji
- Varnostni moduli
- Varnostna stikala
- Varnostni releji
- LED signalni stolpiči

Za višjo produktivnost. ✓



BREZSKRBNOST ALI VROČ PROBLEM?



HENNLICH

Hladilniki hidravličnega olja in
izmenjevalniki toplote ter
akumulatorji

odslej tudi pri **HENNLICHu**.



Nudimo vam:

izdelavo po meri

majhne serije

skoraj neomejene

možnosti kombinacij

kratek rok dobave



www.hennlich.si/hladilniki

HENNLICH d.o.o.,
Ulica Mirka Vadnova 13,
4000 Kranj



TESNILA BOGADI

PROIZVODNJA TESNIL - SERVIS CILINDROV



Tel.: 02 42 60 450/452/453, www.bogadi.si



Vaš rešitelj v primeru okvare

Parker Parkrimp *No-skive* sistem,
gibke cevi, priključki in stiskalnice



it's so easy
to crimp
a hose

Če vaša oprema temelji na hidravličnem sistemu,
ko pride do okvare gibke cevi, veste da se tekma s časom pred zastojem prične.

Parker vam pomaga premagati težave z enostavno,
hitro in varno izdelavo gibke cevi,
kjerkoli in kadarkoli jo potrebujete.

parker.slovenia@parker.com
www.easy-crimping.com

aerospace
climate control
electromechanical
filtration
fluid & gas handling
hydraulics
pneumatics
process control
sealing & shielding



ENGINEERING YOUR SUCCESS.



- Strokovni in znanstveni prispevki
- Iz prakse za prakso
- Ventil na obisku
- Novice - zanimivosti
- Aktualno iz industrije
- Novosti na trgu
- Podjetja predstavljajo
- Ali ste vedeli
- Dogodki

Spoštovani!

Ventil je znanstveno-strokovna revija in objavlja prispevke, ki obravnavajo razvojno in raziskovalno delo na Univerzi, inštitutih in v podjetjih s področja fluidne tehnike, avtomatizacije in mehatronike. Revija želi seznanjati strokovnjake z dosežki slovenskih podjetij, o njihovih izdelkih in dogodkih, ki so povezani z razvojem in s proizvodnjo na področjih, ki jih revija obravnava. Prav tako želi ustvariti povezavo med slovensko industrijo in razvojno in raziskovalno sfero ter med slovenskim in svetovnim proizvodnim, razvojnim in strokovnim prostorom. Naloga revije je tudi popularizacija področij fluidne tehnike, avtomatizacije in mehatronike še posebno med mladimi. Skrbi tudi za strokovno izrazoslovje na omenjenih področjih.

Revija Ventil objavlja prispevke avtorjev iz Slovenije in iz tujine, v slovenskem in angleškem jeziku. Prispevkom v slovenskem jeziku je dodan povzetek v angleščini, prispevki v angleščini pa so objavljeni z daljšim povzetkom v slovenskem jeziku. Člani znanstveno strokovnega sveta so znanstveniki in strokovnjaki iz Slovenije in tujine. Revijo pošiljamo na več naslovov v tujini in imamo izmenjavo z drugimi revijami v Evropi. Revija je vodena v podatkovni bazi INSPEC.

Dvaindvajsetletno izhajanje revije Ventil pomeni, da je v prostoru neprecenljiva za razvoj stroke. Uredništvo si skupaj z znanstveno strokovnim svetom prizadeva za visokokvalitetno raven in relevantnost objav, ki bosta v prihodnosti vse napore usmerila v to, da bo kvalitetna raven še višja. V ta namen vključuje v znanstveno strokovni svet priznane znanstvenike, raziskovalce in strokovnjake, ki s svojim znanjem vspodbujajo vsak na svojem področju objavljanje rezultatov razvojnega in raziskovalnega dela. Uredništvo spremlja razvoj stroke in znanstveno raziskovalno delo doma in vtujini preko konferenc, delavnic in seminarjev ter z izmenjavo tuje periodike.

Revija je priznana v tujini, še posebno na področju fluidne tehnike, kar želimo doseči tudi na področju mehatronike in avtomatizacije. Preko objav v reviji se promovirajo dosežki slovenske znanosti in industrijske proizvodnje. Revija je in bo tudi v prihodnje prostor za predstavljanje kvalitetnih razvojnih in raziskovalnih dosežkov slovenske industrije in raziskovalne sfere na področju fluidne tehnike, avtomatizacije in mehatronike.

Uredništvo



revija Ventil

Univerza v Ljubljani, Fakulteta za strojništvo, Aškerčeva 6, 1000 Ljubljana

Tel.: 01/4771 704, Faks: 01/4771 772

E-pošta: ventil@fs.uni-lj.si, Internet: www.revija-ventil.si

SPLAČA SE BITI NAROČNIK



ZA SAMO 30€ DOBITE:

- celoletno naročnino na revijo IRT3000 (6 številčk)
- strokovne vsebine vsaka dva meseca na več kot 200 straneh
- vsakih 14 dni e-novice IRT3000 na osebni elektronski naslov
- možnost ugodnejšega nakupa strokovne literature

Vsak novi naročnik prejme majico in ovratni trak

NAROČITE SE!

- ☎ 01 5800 884
- ✉ info@irt3000.si
- 🌐 www.irt3000.si/narocam

Od leta 2013 vam je revija IRT3000 še bližje. Berete jo lahko tudi na različnih mobilnih napravah, denimo na pametnih telefonih in tablicah. Poleg spremljanja izbranih vsebin vam ponujamo še nakup posameznih številčk revije in celotnega letnika, hitro in enostavno prek vašega digitalnega spremljevalca.



